

**Use of the toughened hybrid thin-ply laminate concept to
avoid delamination and improve the strength of composite
bonded joints**

Author:

Farin Ramezani Malbizar

Supervisor:

Ricardo João Camilo Carbas

Co-Supervisors:

Lucas Filipe Martins da Silva

Eduardo André de Sousa Marques

Thesis submitted for the degree of Doctor of Philosophy

Doctoral Program in Mechanical Engineering (PRODEM)

Faculty of Engineering of the University of Porto

DEMec, Faculdade de Engenharia da Universidade do Porto, Rua Dr. Roberto Frias,
4200-465 Porto, Portugal
Porto, 2024

© Farin Ramezani Malbizar

Departamento de Engenharia Mecânica

Faculdade de Engenharia da Universidade do Porto

Rua Dr. Roberto Frias, s/n

4200-465 Porto

Portugal

Resumo

O uso de materiais poliméricos reforçados com fibra de carbono (CFRP) tem aumentado em muitas indústrias, tais como na indústria aeronáutica, marítima e automóvel. Nestas aplicações, componentes de compósito são frequentemente ligados a outras peças de compósito ou metal, onde a ligação adesiva desempenha um papel fundamental.

No entanto, o desempenho de uma junta de compósito depende de múltiplos fatores e pode ser melhorada modificando a camada adesiva ou os substratos. Para além disso, a geometria da junta adesiva, a preparação da superfície e os métodos de fabrico utilizados para a produção também são fatores importantes. No entanto, a delaminação de substratos compósitos em juntas adesivas continua a ser uma preocupação importante, pois leva a um desempenho extremamente baixo da junta. Diversos estudos têm proposto técnicas para reduzir a delaminação em compósitos ligados por adesivos. Técnicas que tentam evitar a delaminação através do reforço do substrato, geralmente substituindo camadas de compósito por polímero ou metal (laminados de compósito e metal) na superfície do substrato.

Laminados de folhas finas, que são uma nova geração de materiais compósitos compostos por folhas de espessura inferior a 100 μm , ganharam destaque devido aos desenvolvimentos no processo *spread-tow*. Os laminados de folhas finas oferecem uma maior flexibilidade de design na orientação da disposição e na quantidade de camadas. A redução da espessura da camada e o processo aprimorado da distribuição de resina contribuem para uma distribuição de fibras mais homogênea e regiões mais pequenas que contenham somente resina. O maior número de camadas e interfaces resulta em menores tensões de corte, aumentando a resistência à fratura da matriz.

O objetivo final desta trabalho é investigar o desempenho de um laminado compósito híbrido reforçado por folhas finas usadas como aderentes em juntas de sobreposição simples sob diferentes condições de carga. A componente de tensão principal no laminado, que cria delaminação em juntas adesivas de sobreposição simples (SLJ) com substratos de compósito, é conhecida como sendo a tensão de arrancamento. Como tal, inicialmente, foi estudado o comportamento dos laminados compósitos (configurações de referência com compósito convencional, compósitos de folhas finas e laminados híbridos reforçados por folhas finas) sob solicitações de tração (perpendicular ao plano de orientação das fibras). Os laminados compósitos híbridos foram estudados usando diferentes quantidades de folhas finas, aplicadas através da espessura. Os laminados fabricados, de empilhamento unidirecional, foram testados à tração, transversalmente às fibras, em condições estáticas, a alta taxa de carga e ao impacto.

Posteriormente, uma vez que a orientação das fibras ou o ângulo de folhas é conhecido por ser um dos parâmetros mais importantes no projeto de compósitos, este estudo investiga o efeito de camadas orientadas de folhas finas e compósitos convencionais num laminado híbrido sob solicitação de tração transversal estática. Os resultados experimentais mostram que os compósitos com ângulo de folha apresentam uma força de rotura mais alta quando solicitado a tração perpendicular à fibra, quando comparado com compósitos unidirecionais. Isso pode ser atribuído ao facto de que uma fissura iniciada enfrenta um caminho de fissuração significativamente mais complexo num laminado com ângulo de empilhamento, para avançar pela espessura. Além disso, modelos numéricos de elemento de volume representativo para laminados unidirecionais e com ângulo de folha foram gerados para estudar as configurações em microescala.

Ao intercalar camadas de folhas finas por compósitos convencionais (criando então um laminado híbrido), a delaminação no laminado compósito diminui e a resistência à tração transversal aumenta. Por conseguinte, os laminados compósitos híbridos reforçados por camadas finas podem utilizados como substratos em juntas de sobreposição simples. Juntas de sobreposição simples de referência com um compósito convencional ou com compósito de folhas finas, usados como substratos, também foram consideradas como referências. As juntas foram solicitadas a condições quase estáticas, de alta taxa de carga e de impacto e foi registrado com uma câmara de alta velocidade, permitindo a determinação dos locais de iniciação de dano. Modelos numéricos das juntas também foram criados, permitindo uma melhor compreensão dos mecanismos de falha subjacentes e a identificação dos locais de iniciação de dano.

Keywords: Material compósito; junta adesiva; polímero reforçado com fibra de carbono; folha fina; junta híbrida; junta compósita.

Abstract

The use of carbon fibre reinforced polymer (CFRP) materials is increasing in many industries, such as those operating in the aviation, marine, and automotive sectors. In these applications, composite parts are often joined with other composite or metallic parts, where adhesive bonding plays a key role.

However, the performance of a composite joint is dependent on multiple factors and can be improved by modifying the adhesive layer or the adherends. Moreover, joint geometry, surface preparation, and the manufacturing methods used for production are also important factors. However, delamination of the composite adherends in adhesively bonded composite joints is still a major concern as it leads to extremely low joint performance. Diverse studies have proposed techniques to reduce delamination in adhesively bonded composite joints. A subset of techniques attempts to avoid delamination via reinforcement of the adherend, usually by replacing layers of composite with polymer or metal (composite metal laminates) in the surface of the adherend.

Thin-ply laminates, which are a new generation of composite materials composed of plies with a thickness of less than 100 μm , have gained prominence due to developments in the spread-tow process. Thin-ply laminates offer greater design flexibility in layup orientation and layer quantity. The reduced layer thickness and improved resin spreading process contribute to a more homogeneous fiber distribution and smaller resin-rich regions. The higher number of layers and interfaces results in lower shear stresses, enhancing resistance against matrix cracking.

The final aim of this research is to investigate the performance of a hybrid composite laminate reinforced by thin-ply used as adherends in bonded single lap joints under different loading conditions. The main stress component in the laminate, which creates delamination in bonded Single Lap Joints (SLJs) with composite adherends, is known to be the transverse tensile stress. Therefore, initially, the behavior of the composite laminates (reference configuration of conventional composites, thin-ply composite and hybrid laminates reinforced by thin-ply) under transverse tensile loading were studied. Hybrid composite laminates were studied using different amounts of thin-ply, applied through the thickness. The unidirectionally stacked laminates, were tested under static, high-rate, and impact transverse tensile loading.

Afterward, since fibre orientation or ply angle is known to be one of the most important parameters in composite laminate design, this study investigates the effect of oriented layers of thin-ply and conventional composite in a hybrid laminate under

static transverse tensile loading. Experimental results show that angle-ply composite laminates present higher failure load under out-of-plane tensile loading, when compared with unidirectional composites. This can be attributed to the fact that an initiated crack is faced with a significantly more complex crack path in an angle-ply laminate, to advance through the thickness. Also, numerical Representative Volume Element (RVE) models for unidirectional and angle-ply laminates were generated to study the configurations in micro-scale.

By interlaying layers of thin-ply with conventional composites (thus creating a hybrid laminate), delamination in the composite laminate decreases and transverse tensile strength increases. Therefore, hybrid composite laminates reinforced by thin-ply can be used as substrates in adhesive joints. Two reference single lap joints with a conventional or thin-ply composite used as the adherends were also considered as benchmarks. The joints were loaded under quasi-static, high-rate, and impact loading conditions and were recorded with a high-speed camera, allowing for the determination of damage initiation sites. Numerical models of the joints were also created, allowing for a better understanding of the underlying failure mechanisms and the identification of the damage initiation sites.

Keywords: Composite material; adhesive joint; carbon fibre reinforced polymer; thin-ply; hybrid joint; composite joint.

Acknowledgments

First, I would like to express my sincere gratitude to Doctor Ricardo Carbas, Professor Lucas da Silva, and Professor Eduardo Marques for the opportunity to participate in this project and the technical and academic insights, as well as support throughout this work. I would also like to express my gratitude for the help and availability to discuss the problems faced along the way and find solutions.

This research would also not have been possible without the financial support provided by Fundacao para a Ciencia e a Tecnologia (FCT) through the 2021.07943.BD Ph.D. Grant.

I want to extend my sincere thanks to the members of the Advanced Joining Processes Unit for their constant support, collaborative teamwork, and information sharing that have enabled us to achieve better results in our respective projects. Your friendship, encouragement, and the time we spent together inside and outside of this working group are truly appreciated. I am forever grateful for the experiences we shared.

I would like to express my deepest gratitude to my family, especially my beloved mother and father, for their unwavering support, constant encouragement, and love throughout my journey. Their endless sacrifices, understanding, and motivation have been my driving force, enabling me to pursue my studies abroad and complete this challenging Ph.D. program. I am profoundly grateful for your guidance, love, and belief in my abilities.

Content

Resumo	i
Abstract	iii
Acknowledgments	vi
List of Figures	ix
List of Tables	x
List of Acronyms	xi
List of Symbols	xii
List of Publications	xiii
1 Introduction	1
1.1 Background and motivation.....	1
1.2 Objectives.....	2
1.3 Research methodology.....	2
1.4 Outline of the thesis.....	5
2 Literature review	11
2.1 Introduction.....	11
2.2 Joint configuration and manufacturing.....	12
2.2.1 Joint geometry.....	12
2.2.2 Effect of surface preparation.....	13
2.2.3 Effect of manufacturing process.....	14
2.3 Adhesive layer modifications.....	15
2.3.1 Mixed and functionally graded adhesive layer.....	15
2.3.2 Nano-reinforced adhesive layers.....	16
2.4 Substrate modifications.....	17
2.4.1 Effect of stacking sequence.....	17
2.4.2 Thin-ply laminates.....	18

2.4.3	Composite metal laminates.....	19
2.4.4	Toughened surface layers.....	20
3	Material and experimental methods	22
3.1	Experimental details.....	22
3.1.1	Adhesive.....	22
3.1.2	Conventional composite.....	23
3.1.3	Thin-ply.....	23
3.2	Manufacturing procedures.....	24
3.2.1	Laminate manufacturing.....	24
3.2.2	Single lap joint manufacturing.....	26
3.3	Testing conditions.....	27
3.4	Unidirectional laminates.....	27
3.5	Angle-ply laminates.....	29
3.6	Single lap joints.....	29
4	Numerical Studies	31
4.1	Unidirectional laminates.....	31
4.2	Angle-ply laminates.....	32
4.3	Single lap joints.....	34
5	Conclusions	36
6	Future work	39
	References	40
A	Paper A	50
B	Paper B	77
C	Paper C	90
D	Paper D	111
E	Paper E	126
F	Paper F	142
G	Paper G	155

List of Figures

1.1	Schematic representation of the workflow of the tasks performed.....	3
1.2	Correspondence between tasks proposed and papers published.....	6
2.1	Effect of load level on the deformation and interlaminar failure of the composite adherends.....	12
2.2	Schematic design of a single lap joint.....	13
2.3	Schematic design of composite after (a) grit blasting and (b) sanding.....	14
2.4	(a) Co-bonding, (b) Co-curing, and (c) Secondary bonding.....	15
2.5	Mixed adhesive joint.....	16
2.6	Effect of 0° layer distance from surface in quasi-isotropic laminate.....	18
2.7	CML configurations.....	19
2.8	Configurations for CML and CMLs with additional adhesive layers.....	20
2.9	Schematic design of (a) CFRP, (b) single external adhesive layer, (c) a single interlaminar adhesive layer, and (d) three interlaminar adhesive layers.....	20
3.1	Schematic design for unidirectional conventional composite, thin-ply, and hybrid laminates.....	25
3.2	Schematic design of angle-ply hybrid laminates	26
3.3	Schematic design of reference (a) conventional composite, (b) thin-ply, and (c) hybrid (25% thin-ply) single lap joints.....	27
3.4	Experimentally obtained failure load for the reference and hybrid laminats reinforced using thin-plyes under static traseverse tensile loading.....	28
3.5	Experimentally obtained failure load for the unidirectional and angle-ply hybrid laminates for reference and hybrid configurations reinforced using thin-plyes under static traseverse tensile loading.....	29
3.6	Experimentally obtained failure load for the reference and hybrid single lap joints reinforced using thin-plyes different loading rates.....	30
4.1	Initial RVE for (a) conventional composite and (b) thin-ply under static loading.....	31
4.2	Modified initial RVE for (a) conventional composite and (b) thin-ply under dynamic loading.....	32
4.3	RVE models for (a) unidirectional [0] and angle-ply (b) [45/-45] and (c) [0/90] conventional composite.....	33
4.4	RVE models for (a) unidirectional [0] and angle-ply (b) [45/-45] and (c) [0/90] thin-ply ...	33
4.5	Boundary condition of simulated single lap joint.....	34

4.6	Assigned mechanical properties for (a) conventional composite, (b) thin-ply, and (c) hybrid (25% thin-ply)	35
4.7	Numerically obtained failure load for reference and hybrid single lap joints reinforced using thin-ply under different loading rates.....	35

List of Tables

4.1	Main mechanical properties of "AF 163-2k"	22
4.2	Conventional composite mechanical properties.....	23
4.3	Cohesive properties of the conventional composite.....	23
4.4	Thin-ply mechanical properties.....	23
4.5	Cohesive properties of thin-ply.....	24

List of Acronyms

CFRP	Carbon Fibre Reinforced Polymer
SLJ	Single Lap Joint
DIC	Digital Image Correlation
CNT	Carbon Nano Tube
MWCNT	Multi-Walled Carbon Nanotube
QIQH	Quasi-Isotropic Quasi-Homogeneous
CML	Composite Metal Laminate
ALR	Adhesive Layer Reinforcement
CZM	Cohesive Zone Model
DCB	Double Cantilever Beam
ENF	End Notched Flexure
RVE	Representative Volume Element
SEM	Scanning Electron Microscope
FEA	Finite Element Analysis
XFEM	Extended Finite Element Method

List of Symbols

E	Young's modulus
G	Shear modulus
G_{IC}	Mode I fracture energy
G_{IIC}	Mode II Fracture Energy
P	Load
l	Overlap length
T	Adherend thickness
t	Adhesive thickness
T_g	Glass transition temperature
ν	Poisson's ratio

List of Publications

In the scope of this thesis

- **Ramezani, F.**, Simões, B. D., Carbas, R. J. C., Marques, E. A. S., & da Silva, L. F. M. (2023). Developments in laminate modification of adhesively bonded composite joints. *Materials*.
DOI: 10.3390/ma16020568.
- **Ramezani, F.**, Carbas, R. J. C., Marques, E. A. S., Ferreira, A. M., & da Silva, L. F. M. (2023). A study of the fracture mechanisms of hybrid carbon fiber reinforced polymer laminates reinforced by thin-ply. *Polymer Composites*.
DOI: 10.1002/pc.27196.
- **Ramezani, F.**, Carbas, R. J. C., Marques, E. A. S., & da Silva, L. F. M., Out-of-plane tensile strength of CFRP laminates reinforced by thin-ply under different loading rates. *Steel and Composite Structures*. *Submitted*.
- **Ramezani, F.**, Carbas, R. J. C., Marques, E. A. S., Ferreira, A. M., & da Silva, L. F. M. (2023). Study on out-of-plane tensile strength of angle-ply reinforced hybrid CFRP laminates using thin-ply. *Mechanics of Advanced Materials and Structures*.
DOI: 14.10.1080/15376494.2023.2165742.
- **Ramezani, F.**, Carbas, R. J. C., Marques, E. A. S., & da Silva, L. F. M. (2023). Study of hybrid composite joints with thin-ply-reinforced adherends. *Materials*.
DOI: 10.3390/ma16114002.
- **Ramezani, F.**, Carbas, R. J. C., Marques, E. A. S., & da Silva, L. F. M. (2023). Study of hybrid composite joints with thin-ply-reinforced adherends under high-rate and impact loadings. *Applied and Computational Mechanics*.
DOI: 10.22055/jacm.2023.44216.4181.
- **Ramezani, F.**, Salazar, J. C., Carbas, R. J. C., Marques, E. A. S., & da Silva, L. F. M. (2023). Investigation of adherend thickness in thin-ply hybrid laminates. In

International Conference on Adhesive Bonding. Cham: Springer Nature Switzerland.

Publication regarding adhesive joints research

- **Ramezani, F.**, Nunes, P. D. P., Carbas, R. J. C., Marques, E. A. S., & da Silva, L. F. M., (2022). The joint strength of hybrid composite joints reinforced with different laminates materials. *Advanced Joining*.

DOI: 10.1016/j.jajp.2022.100103.

- Simões, B. D., Nunes, P. D. P., **Ramezani, F.**, Carbas, R. J. C., Marques, E. A. S., & da Silva, L. F. M. (2022). Experimental and numerical study of thermal residual stresses on multimaterial adherends in single-lap joints. *Materials*.

DOI: 10.3390/ma15238541.

- Akhavan-Safar, A., **Ramezani, F.**, Delzendehrooy, F., Ayatollahi, M. R., & da Silva, L. F. M. (2022). A review on bi-adhesive joints: Benefits and challenges. *Adhesion and Adhesives*.

DOI: 10.1016/j.ijadhadh.2022.103098.

Introduction

1.1 Background and motivation

The use of composite materials is increasing substantially in different industries e.g., aviation, marine, and automotive. However, composite components often need to be joined with other composites or metal components in a structure, requiring the use of adequate joining methods. Compared to traditional joining methods, adhesive bonding has been growing in importance, offering unique benefits such as allowing to easily join dissimilar materials and avoiding weight increase or drilling holes, which is a source of stress concentration itself. Therefore, composite structures usually rely on adhesives for assembly as they enable a more uniform stress distribution along the bond line. However, some particular joint geometries can still induce significant peel loads on substrates, which cause premature failure of a composite substrate. This is due to the fact that the behavior of composites is highly anisotropic with respect to both stiffness and strength. In the fibre direction, composites can be very strong and stiff whereas in the transverse and shear directions, their properties are much lower. Compared to isotropic structural materials, such as the most commonly used metal alloys, composite materials present significantly weaker properties in the transverse direction. Therefore, delamination is one of the most common failure modes in the case of composite joints. To address this issue, different methods have been introduced to increase the shear strength in the composite joint which can be divided into the main categories: modification of configuration and geometry, adhesive layer modification, and adherend modification.

1.2 Objectives

Experimental studies reveal that, although the composite laminates which are used as an adherend in a composite joint show high stiffness and strength, the structural performance of these materials is highly susceptible to the loading mode and an improper adherend design can lead to catastrophic failure in a composite joint.

This project has three main goals: the first is the careful and in-depth study of different available methods for the adherend modification of composite bonded joints.

The second is to study the performance of hybrid laminates toughened by thin-ply under different strain rates. For the second part, the effect of hybrid composite laminate was studied for unidirectional and angle-ply laminates. The numerical simulation of the cases studied experimentally was conducted in order to fully understand the phenomena involved.

Afterward, the studied laminates were used as adherend in single lap joints and the effect of hybrid composite single lap joint toughened by thin-ply was investigated.

1.3 Research methodology

This section details the main research activities of this thesis, divided in five tasks. The effect of hybrid composite laminate reinforced by thin-ply was studied for unidirectional and angle-ply laminates. The numerical simulation of the cases studied experimentally was performed in order to allow for a more complete understanding of the phenomena involved. The main goal of this work is to increase the transverse strength of composite laminates and to prevent the delamination or crack propagation of new toughened hybrid composite laminates. Afterward, the studied laminates were used as adherends in single lap joints, and hybrid composite single lap joints reinforced by thin-ply was investigated. Thus, to fully ensure its suitability for being used in adhesively bonded structures, joint specimens were tested at different strain rates to validate the suitability of this novel approach under service conditions. Modeling of the static and dynamic loads were carried out by a finite element analysis using damage mechanics. A general scheme of the tasks can be found in Figure 1.1.

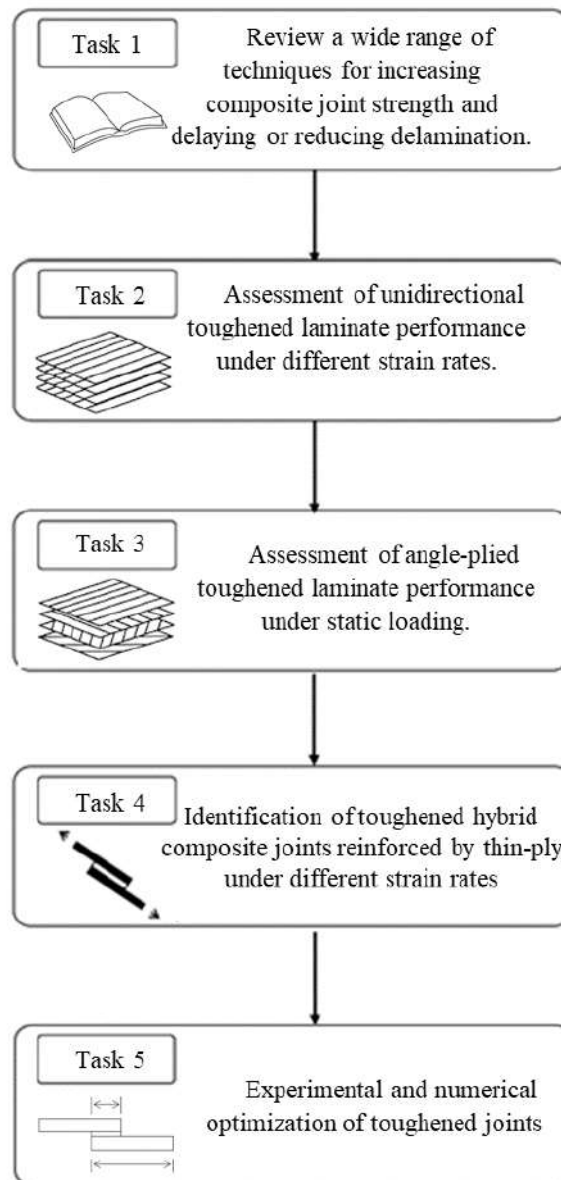


Figure 1.1: Schematic representation of the workflow of the tasks performed.

Task 1: Review a wide range of techniques for increasing composite joint strength and delaying or reducing delamination.

This task consists of a comprehensive review on the published results to illuminate the road of the research. In this part, the already published numerical and experimental results were analyzed. This task covered the already considered experimental efforts for increasing joint strength by reducing stress concentrations at the ends of the overlap, all particularly useful for adhesive joints with composite substrates due to the low transverse strength of these materials.

Task 2: Assessment of unidirectional toughened laminate performance under different strain rates.

The objective of this task is to manufacture different configurations of toughened hybrid laminates reinforced by thin-ply modified in the thickness direction. A conventional and a thin-ply composite material were used in Task 2. The main purpose is to extract the best mechanical performance of the considered materials to achieve a toughened hybrid laminate with the highest transverse tensile strength. The toughened hybrid laminate is a locally toughened through the thickness composite laminate. The use of thin-ply laminates provides a higher toughness (as these laminates suppress or delay crack initiation), therefore, it makes it possible to control the local toughness in the adherends, by allowing for a refined layup design through the thickness direction. In Task 2, different configurations (varying materials and lay-up stacking) of toughened hybrid laminate material were manufactured. Experimental tests were carried out under static, high-rate, and impact loading, in order to evaluate the performance of toughened hybrid laminate under different loading conditions. Experimental tests were conducted on a servo-hydraulic machine for quasi-static and high-rate loading conditions and a drop weight machine was used to evaluate the performance under impact loading. A high-speed camera was used to identify the crack initiation sites and propagation process. Images were captured from the reference conventional composite and hybrid laminates reinforced by thin-ply and an associated Digital Image Correlation (DIC) software was used to identify the effect of the thin-ply on the behavior of the composite laminate. Also, numerical representative volume element models were generated to study the configurations in microscale.

Task 3: Assessment of angle-ply toughened laminate performance under static loading.

As the fibre orientation or ply angle is known to be one of the most important parameters in composite laminate design, this study investigates the effect of oriented layers of thin-ply or both thin-ply and conventional composite in a hybrid laminate under static transverse tensile loading. Two references, conventional and thin-ply composite, and the optimized hybrid laminate in Task 2 were considered. Also, numerical representative volume element models for angle-ply conventional composite and thin-ply were generated to study the configurations in microscale, in order to better understand the effect of angle-ply hybrid composite laminates.

Task 4: Identification of toughened hybrid composite joints reinforced by thin-ply under different strain rates.

The objective of this task is to study the hybrid composite laminate configurations investigated in Task 2 used as an adherend in adhesively bonded composite joints for static, high-rate, and impact loading conditions. Experimental tests were conducted in a servo-hydraulic machine under quasi-static and high-rate conditions and a drop-weight machine to evaluate the performance under impact loading. An adhesive joint with unreinforced composite adherends was used as a reference. Joint manufacturing was carried out in a hot press to reduce the number of possible defects in joints. A high-speed camera was used to determine the locations of delamination that could occur in real components. In parallel, a numerical model of the component was created, using Cohesive Zone Modeling (CZM) to model both the delamination in the composite substrates and the failure in the adhesive layer. Fracture material characterization tests

were also performed in order to determine the fracture properties in mode I, and mode II of the novel thin-ply composite used in the hybrid joints. For mode I and mode II tests, the Double Cantilever Beam (DCB) and End Notch Flexure (ENF) specimen were used respectively.

Task 5: Experimental and numerical optimization of toughened joints

The objective of this task is to optimize the hybrid joints developed and tested in Task 4 numerically and experimentally.

1.4 Outline of the thesis

In its final form, the Ph.D. thesis consist of seven peer-reviewed papers. The list of papers is presented in Figure 1.2, including the indication of those which have already been published, and those under preparation summary.

The summary is divided into six main parts. This introductory chapter contains a brief description of the background and motivation of this work and its objectives. Additionally, it displays a summary of each paper presented. Chapter 2 provides a comprehensive literature review of the work previously developed on this topic and recent developments in the composite bonded joint are presented. The main approach followed in this review was to introduce the available methods which increase the joint strength and delay or eliminate delamination in the composite adherend. Chapter 3 clarifies the experimental procedures used throughout this work, the material used in this study, and the experimental tests performed in order to characterize the thin-ply material. Additionally, the experimental methodology used in the entire study was explained. Chapter 4 presents a succinct description of the numerical models used in this work. Chapter 5 presents the main conclusions about the topics of research and Chapter 6 presents suggestions for further work on these topics. The appendices comprehend the publications developed in the scope of this thesis that represent the research developed, in detail.

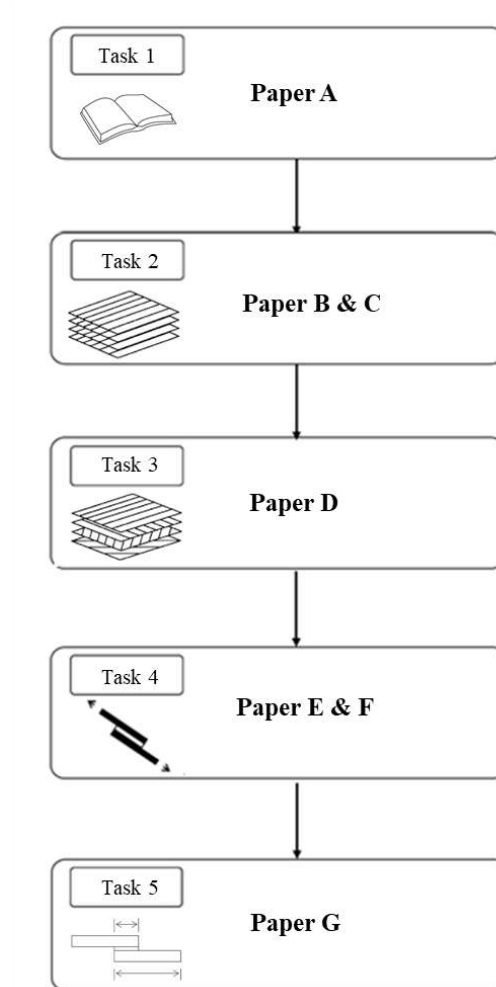


Figure 1.2: Correspondence between tasks proposed and papers published.

Paper A: Developments in laminate modification of adhesively bonded composite joints

Ramezani, F., Simões, B. D., Carbas, R. J. C., Marques, E. A. S., & da Silva, L. F. M. (2023). Developments in Laminate Modification of Adhesively Bonded Composite Joints. *Journal of Materials*.

The use of carbon fibre reinforced polymer (CFRP) materials is increasing in many different industries, such as those operating in the aviation, marine, and automotive sectors. In these applications, composite parts are often joined with other composite or metallic parts, where adhesive bonding plays a key role. Unlike conventional joining methods, adhesive bonding does not add weight nor requires drilling holes, which are both major sources of stress concentration. The performance of a composite joint is dependent on multiple factors and can be improved by modifying the adhesive layer or the composite layup of the adherend. Moreover, joint geometry, surface preparation, and the manufacturing methods used for production are also important factors. The present work reviews recent developments on the design and manufacture of adhesively bonded joints with composite substrates, with particular interest on adherend

modification techniques. The effects of stacking sequence, use of thin-ply, composite metal laminates and its specific surface preparations, and the use of toughened surface layers in the composite adherends are described for adhesively bonded CFRP structures.

Paper B: A study of the fracture mechanisms of hybrid CFRP laminates reinforced by thin-ply

Ramezani, F., Carbas, R. J. C., Marques, E. A. S., Ferreira, A. M., & da Silva, L. F. M. (2023). A study of the fracture mechanisms of hybrid carbon fiber reinforced polymer laminates reinforced by thin-ply. *Journal of Polymer Composites*.

The main stress component which creates delamination in bonded single lap joints with composite adherends is the transverse tensile stress. Therefore, the following study investigates the behavior of composite laminates (reference and hybrid laminates reinforced by thin-ply) under transverse tensile loading. Texipreg HS 160 T700 and NTPT-TP415 were used as the conventional CFRP and thin-ply respectively. Hybrid composite laminates were studied using different amounts of thin-ply, applied through the thickness. The manufactured laminates, of unidirectionally stacked construction, were tested under transverse tensile loading. Digital image correlation was performed to investigate the average peel strain distribution for the composite and to better understand the phenomena associated to the use of hybrid laminates.

Experimental results show that the reinforced hybrid composite laminates, created using thin-ply, present higher failure load compared to the reference conventional CFRP or thin-ply laminates. This was found to be due to the higher ductility enabled by the presence of thin-ply. Distributing a constant amount of thin-ply through the thickness was found to increase the laminate transverse strength, as the thin-ply laminates act as a barrier against crack propagation. A representative volume element was studied for each configuration since this numerical method brings the opportunity to investigate the studied configurations in microscale.

Paper C: Out-of-plane tensile strength of CFRP laminates reinforced by thin-ply under different loading rates

Ramezani, F., Carbas, R. J. C., Marques, E. A. S., & da Silva, L. F. M. (2024). Out-of-plane tensile strength of CFRP laminates reinforced by thin-ply under different loading rates. *Steel and composite structures*.

Delamination in composite laminates is primarily caused by transverse tensile stress. However, experimental and numerical studies have consistently shown that hybrid

composite laminates, reinforced with thin-ply, exhibit greater strength under static transverse tensile loads in comparison to reference conventional composite laminates. This study focuses on analyzing the behavior of composite laminates reinforced by thin-ply, subjected to high-rate and impact transverse tensile loading. A conventional composite, Texipreg HS 160 T700, and a thin-ply, NTPT-TP415, were selected for this investigation. Hybrid laminates were created by integrating 25% thin-ply throughout the laminate's thickness. Subsequently, unidirectionally stacked laminates were subjected to high-rate and impact transverse tensile loading.

The experimental results showed a slight increase in the transverse tensile strength of the hybrid laminate compared to the reference conventional composite under both high-rate and impact-loading conditions. To delve into the microscale behavior of these configurations, a representative volume element was analyzed using numerical methods, providing valuable insights into the studied setups.

Paper D: Study on out-of-plane tensile strength of angle-ply reinforced hybrid CFRP laminates using thin-ply

Ramezani, F., Carbas, R. J. C., Marques, E. A. S., Ferreira, A. M. & da Silva, L. F. M. (2023). Study on out-of-plane tensile strength of angle-ply reinforced hybrid CFRP laminates using thin-ply. *Mechanics of Advanced Materials and Structures*.

Thin-ply are generally defined as composites with ply thicknesses below 100 μm . These materials are rapidly gaining interest for high-performance applications e.g., the aerospace sector. Many practical techniques have been proposed to prevent delamination and improve the strength of composite laminates. A recent study has shown that the delamination could be postponed by replacing layers of CFRP with thin-ply in a unidirectional composite laminate, a configuration known as hybrid laminates reinforced with thin-ply.

Since fibre orientation is known to be one of the most important parameters in composite laminate design, this study investigates the effect of oriented layers of thin-ply or both thin-ply and conventional CFRP in a hybrid laminate under out-of-plane tensile loading. A numerical Representative Volume Element (RVE) model for CFRP and thin-ply was generated, considering the unidirectional [0], cross-ply [45/-45], and [0/90] in order to better understand the effect of angle-ply hybrid composite laminates. Experimental results show that angle-ply composite laminates present higher failure load under out-of-plane tensile loading compared to the unidirectional ones. This can be attributed to the fact that an initiated crack is faced with a significantly more complex crack path in an angle-ply laminate to advance in the through-the-thickness direction.

Paper E: Study of Hybrid Composite Joints with Thin-Ply-Reinforced Adherends

Ramezani, F., Carbas, R. J. C., Marques, E. A. S., & da Silva, L. F. M. (2023). Study of Hybrid Composite Joints with Thin-Ply-Reinforced Adherends. *Journal of Materials*.

It has been demonstrated that a possible solution to reducing delamination in a unidirectional composite laminate lies in the replacement of conventional carbon-fibre-reinforced polymer layers with optimized thin-ply layers, thus creating hybrid laminates. This leads to an increase in the transverse tensile strength of the hybrid composite laminate. This study investigates the performance of a hybrid composite laminate reinforced by thin plies used as adherends in bonded single lap joints. Two different composites with the commercial references Texipreg HS 160 T700 and NTPT-TP415 were used as the conventional composite and thin-ply material, respectively. Three configurations were considered in this study: two reference single lap joints with a conventional composite or thin-ply used as the adherends and a hybrid single lap. The joints were quasi-statically loaded and recorded with a high-speed camera, allowing for the determination of damage initiation sites. Numerical models of the joints were also created, allowing for a better understanding of the underlying failure mechanisms and the identification of the damage initiation sites. The results show a significant increase in tensile strength for the hybrid joints compared to the conventional ones as a result of changes in the damage initiation sites and the level of delamination present in the joint.

Paper F: Study of Hybrid Composite Joints with Thin-ply-reinforced Adherends under High-rate and Impact Loadings

Ramezani, F., Carbas, R. J. C., Marques, E. A. S., & da Silva, L. F. M. (2023). Study of Hybrid Composite Joints with Thin-ply-reinforced Adherends under High-rate and Impact Loadings. *Journal of Applied and Computational Mechanics*.

This research aims to examine the tensile strength of a hybrid composite laminate reinforced by thin-ply when used as an adherend in bonded single lap joints subjected to high-rate and impact loading. Two different composites, namely Texipreg HS 160 T700 and NTPT-TP415, are employed as the conventional and thin-ply composites, respectively. The study considers three configurations: a conventional composite, a thin-ply, and a hybrid single lap joint. Numerical models of the configurations are developed to provide insight into failure mechanisms and the initiation of damage. The results indicate a significant increase in tensile strength for the hybrid joints over the conventional and thin-ply joints, due to the mitigation of stress concentrations. Overall, this study demonstrates the potential of hybrid laminates for improving the performance of composite joints under high-rate loading and impact conditions.

Paper G: Investigation of Adherend Thickness in Thin-Ply Hybrid Laminates

Ramezani, F., Salazar, J. C., Carbas, R. J. C., Marques, E. A. S., & da Silva, L. F. M. (2023). Investigation of Adherend Thickness in Thin-Ply Hybrid Laminates. In *International Conference on Adhesive Bonding Cham: Springer Nature Switzerland*.

The use of composite materials has been continuously increasing, hinged on its multiple advantages such as their high strength-to-weight ratio. However, this type of material is known for its anisotropic properties that may lead to premature failure of the composite laminate, stemming from the delamination of the adherend in an adhesively bonded composite joint. This study aims to study the effect of adherend thickness in uni-directional (UD) hybrid composite single lap joints reinforced by thin-ply and investigate the joint strength and failure mode. Tensile tests were carried out to evaluate the parameters mentioned experimentally, and numerical models were developed to reproduce the joint behavior. Experimental results show that adherend thickness has a minor effect on the joint strength in hybrid composite joints reinforced by thin-ply. However, a considerable change in the failure mode was observed.

Literature review

As mentioned above, the first step of this work was to compile carefully what has already been done by other researchers. This review was published and can be found in **Paper A**. Following the conclusion of this review, experimental and numerical work has already been performed. The key procedures and findings related to this experimental and numerical work are presented in this section.

2.1 Introduction

Composites are high-performance and lightweight materials which are hard to manufacture in large dimensions or in complex configurations [1]. From an industrial point of view, composite structures are often manufactured in multiple parts that will later be connected via different joining methods [2]. Mechanical joining methods such as riveting, fastening [3], or hybrid processes [4, 5] are mostly known to be reliable, although they increase the weight of the structure [6]. However, these methods require drilling holes which cut through the composite fibres and damage the composite laminate during the manufacturing process. This causes stress concentrations, and local damage and leads to an overall degradation of the mechanical performance of the composite structure. In contrast, adhesive joining method provides advantages, such as a lower process cost, high strength-to-weight ratio, low stress concentration, and a higher fatigue resistance [7, 8]. Additionally, adhesive joints distribute the load over a larger area compared to traditional joining methods [9], usually resulting in higher bonding strength.

The strength of an adhesive joint ultimately depends on the stress distribution in the bondline and in the adherend, which is a function of different parameters such as the joint geometry or the material properties of each component (adherend or adhesive) [10-12]. However, it should be noted that many other parameters substantially affect the joint strength such as the service temperature, the humidity level [13], the manufacturing process, and the associated surface treatment.

Importantly, although adhesive bonding provides definite advantages for bonding composites, the low interlaminar strength of composite adherends can lead to important limitations in the performance of joints [14]. The peel stresses generated at the bondline

can overcome the limited transverse strength of the composite and cause failure by delamination. Figure 2.1 provides a schematic representation of how different load levels affect the composite adherends and eventually cause failure by delamination.

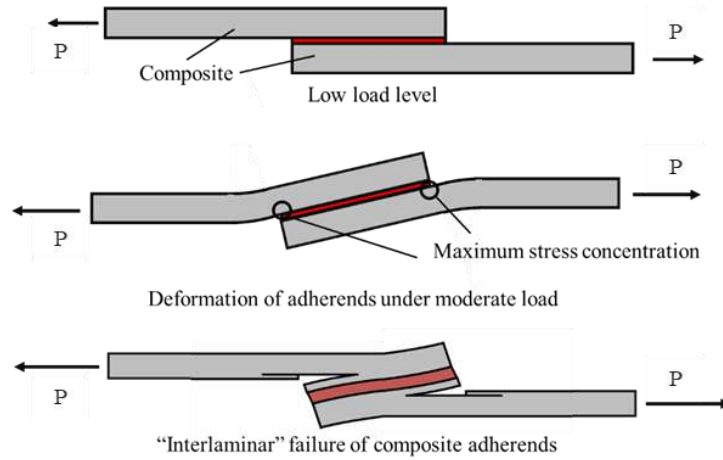


Figure 2.1: Effect of load level on the deformation and interlaminar failure of the composite adherends.

Multiple methods, e.g. the use of mixed adhesive joints (combining two adhesives in a single joint) [15-18], Z-pins [19, 20], 3D weaving [21], stitching [22], braiding [23], and the use of additional thermoplastic inter-ply [24] have been proposed to prevent delamination and improve the strength of composite joints. The use of composite metal laminates [25, 26] or hybrid composites [27] is another method to improve strength of composite materials, which can increase transverse strength on the critical surface region [25] and/or result in a reduction of the shear stresses acting on the adhesive [27].

Multiple review papers have been published on the subject of adhesive bonding of composite substrates [4, 28-31], describing a wide range of methods suitable to improve joint performance under different loading conditions. The current study further contributes to the literature by providing a detailed analysis of the recent developments on adherend modification of adhesively bonded composite joints. The effects of stacking sequence, the use of thin-ply and composite metal laminates, and the use of toughened surface layers on the mechanical performance of adhesively bonded joints (under different loading conditions) have been summarized and analysed in detail.

2.2 Joint configuration and manufacturing

2.2.1 Joint geometry

The mechanical performance of a bonded joint is known to be highly dependent on joint geometry, which includes factors such as the overlap length (l), adherend thickness (T), adhesive thickness (t) and the adherend and adhesive elastic modulus and shear strength [32]. Figure 2.2 presents a schematic design of a single lap joint, illustrating the aforementioned parameters.

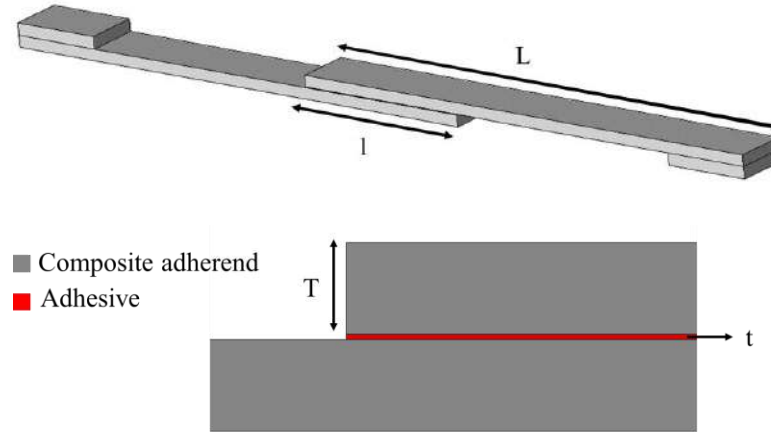


Figure 2.2: Schematic design of a single lap joint.

Multiple research studies have been carried out to understand the effect of the overlap length in composite joints. It could be generally stated that, if the adherend does not fail or yield, an increase in the overlap length will lead to an increase in the failure load of the joint. This is known to occur even under different loading conditions e.g., under quasi-static and impact loads [33-35] and could be explained by the substantial effect that the overlap length has on the peel stress. However, if stiff and brittle adhesives are used, an increase in the overlap length will result in a more modest (or even negligible) increase of the failure load, which is in contrast to that found for joints bonded with a ductile adhesive, where the increase in failure load is found to be almost directly proportional to the overlap length. This can be explained by the fact that severe stress concentrations are generated at the overlap ends by the stiff and brittle adhesive, leading to premature failure. These stress concentrations are present even for very large overlap length values, reducing the effectiveness of increasing this dimensional parameter.

2.2.2 Effect of surface preparation

To ensure maximum joint strength, the bonding surfaces must be thoroughly prepared before adhesive application, which is often a costly and time-consuming process but essential to avoid adhesive failure. Furthermore, bond strength and durability are known to be extremely sensitive to environmental parameters such as the temperature and humidity, both of which can have a deleterious effect on the adhesive/adherend interface and degrade the level of adhesion.

Many different chemical and physical surface treatments are currently available for composites. A proper surface treatment for composite adherends should always seek the removal of all contaminants from the surfaces and ensure a good level of adhesion, which can be achieved through an increase of surface energy and the chemical activation of material surfaces being bonded or increasing the roughness of the surface [36-38]. These employ different methodologies, such as mechanical abrasion [39],

degreasing the surface with solvent [40, 41], laser ablation [42, 43], plasma treatment [44, 45], peel ply technique [45-49], irradiation [50], grit blasting [51, 52] or chemical surface activation [53].

It is important to take into account that the bulk mechanical properties of a composite can be strongly affected by surface treatments. For example, severe abrasive treatments can damage the composite and adversely affect the joint behaviour [54, 55] and bond strength [56, 57]. This is because the fibres closer to the surface can be damaged (see Figure 2.3) by abrasion, reducing composite strength, the adhesion of the fibres to the matrix and may even introduce contamination through loose microparticles [58]. Nonetheless, these microparticles can be removed with the use of suitable power ultrasonic cleaning methods, and, hence, the use of primer coating together with power ultrasonic cleaning leads to a significant increase in strength [59].

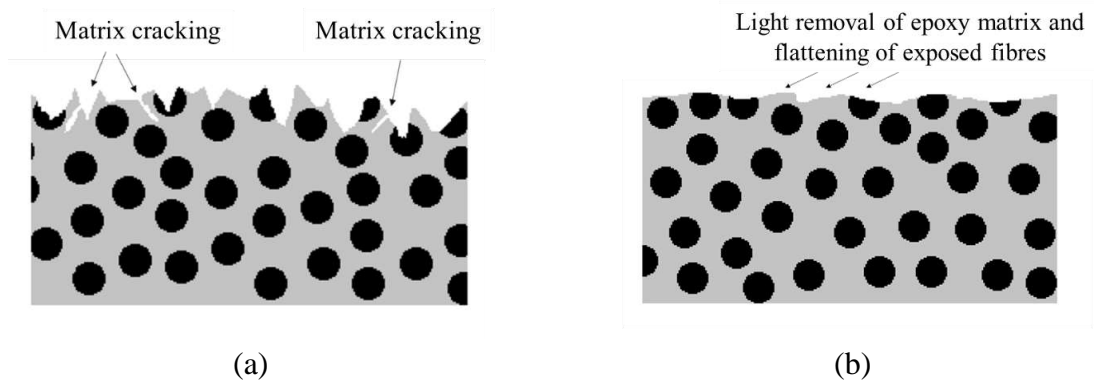


Figure 2.3: Schematic design of composite after (a) grit blasting and (b) sanding. Adapted from [60].

2.2.3 Effect of manufacturing process

The manufacturing process of composite joints can follow three different approaches, the selection of which can be dependent on the curing temperature of the composite and adhesive. These processes are known as co-curing, co-bonding and the secondary bonding method [30]. A co-bonding process is performed when one adherend is cured simultaneously with the adhesive, while in the co-curing process both adherends and the adhesive are simultaneously cured. Secondary bonding is when the adhesive layer is cured between two pre-cured composite substrates [30, 61, 62]. Figure 2.4 shows a schematic design of the mentioned manufacturing methods.

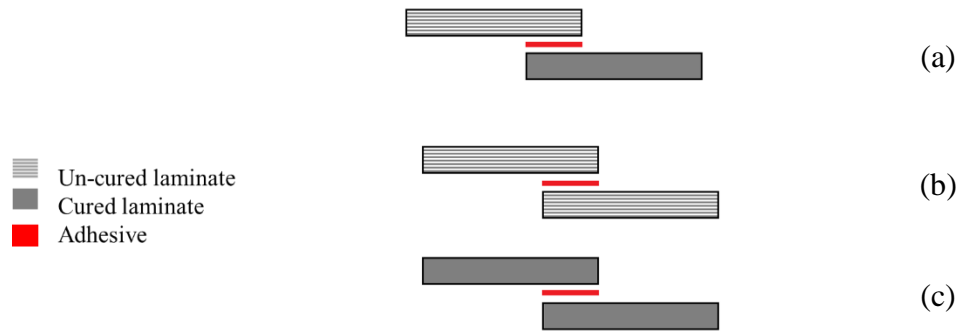


Figure 2.4: (a) Co-bonding, (b) Co-curing, and (c) Secondary bonding. Adapted from [30].

Each of these manufacturing methods is known to have its own specific advantages and disadvantages [63]. For secondary bonded joints, failure it is known to occur in the composite [64] and edge effects are not so predominant [22]. On the other hand, in co-bonded joints, failure typically occurs in the adhesive since greater resistance to crack initiation and propagation has been observed [64] and significant edge effects are known to exist [22]. However, co-bonded joints have been shown to have a lower strength than the secondary bonded joints under a wide range of loading conditions [65-68]. In some cases, the moisture present in the prepreg was found to be released during curing and migrate to the adhesive layer, which leads to a weakening of the interface and lower strength of the co-cured joints [67, 69]. Notwithstanding, co-curing or co-bonding methods are usually preferred over the secondary bonding methods, because the number of parts and curing cycles needed are reduced. Hence, secondary bonding is mostly used for the repair of composite structures while for large and complex structures the secondary bonding process is more suitable [30, 70].

2.3 Adhesive layer modifications

2.3.1 Mixed and functionally graded adhesive layer

Low joint performance is usually the result of a non-uniform distribution of stresses in the bond line in adhesive joints [71]. A non-uniform stress distribution is even more obvious in joints with dissimilar adherends and joints operating in an extreme temperature range [72]. In composite joints, the stiffness of the adhesive used for bonding composites is known to be one of the key parameters controlling the onset of delamination, with several authors demonstrating that the use of low strength yet flexible adhesives through the bondline is able to outperform stronger joints [73].

Mixed adhesive joints in which two different adhesives (one ductile and one brittle adhesive) are used along the bondline, are known to be a valid method to avoid the formation of non-uniform stress distribution in a bondline. In this approach, the brittle adhesive is utilized in the middle part of the bondline and the ductile adhesive is used at the overlap ends, where higher stress concentrations occur (see Figure 2.5) [74, 75].

The mixed adhesive concept is also a viable alternative for joints with dissimilar adherends or operating under demanding environmental conditions [76].

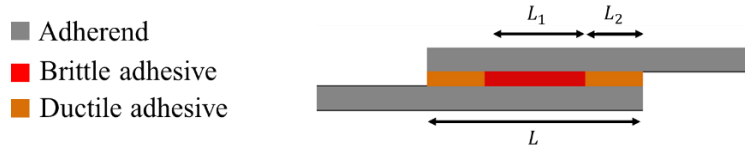


Figure 2.5: Mixed adhesive joint.

Generally, studies on structural adhesive joints for bonding aluminium with composite materials have led to the conclusion that the most suitable adhesives for use in these configurations are toughened epoxies (where stiffness is indispensable) and polyurethanes (for dynamic mechanical requirements that call for flexibility) [77]. These materials are also suitable for combination in a mixed adhesive joint with composite substrates. Nonetheless, it should be mentioned that the performance of a mixed adhesive joint under different loading and testing conditions is highly dependent on the material properties of the both brittle and ductile adhesives used [16]. The work of Machado et al. [78] demonstrated this by studying single lap joints combining of four different adhesives in a mixed adhesive configuration (AV 138 and XNR 6852 as stiff adhesives and DP 8005 and RTV 106 as flexible adhesives). According to the results, for both quasi-static and impact loading conditions, the use of a mixed adhesive joint instead of single adhesive layers does not always guarantee an improvement of the shear strength and this is especially evident when the performance (under different loading conditions) of mixed joints is compared with the use of a brittle and ductile single adhesive joint.

2.3.2 Nano-reinforced adhesive layers

Adhesive layers modified with the use of nanoparticles has been a recent topic of interest [79]. The failure load of a nano-reinforced joint is significantly affected by the ratio and type of the added nanostructure [80]. Further studies have shown that the addition of a small amount of nanoparticles to the adhesive, as low as 1-1.5%, often results in a drastic improvement in mechanical strength [8, 80-83] both in the shear and tensile loading modes [81, 84-87]. This behaviour is the result of a more efficient stress transfer between nanoparticles and the polymer matrix, which improves the cohesive properties of the bond. However, some works report a decrease in the peel strength of the bonded joints [81], attributed to an increase in the glass transition temperature (T_g) and the increased brittleness of the adhesives with larger nanofiller content. The addition of nanoparticles improves the interfacial wettability of the substrates (composite or metal) [81, 88] and it is known to be the reason behind drastic shifts in the failure mode [89], which changes from interfacial failure, with no significant damage on the composite adherends, to cohesive failure in the adhesives, where the load is more effectively transferred to the adherends [8]. It has also been reported that, due to their small dimensions, nanofillers can penetrate into small voids on the adherend

surface, allowing for the joint strength to be enhanced via improved mechanical interlocking [90]. Furthermore, fracture surfaces also seem to be strongly affected by the addition of nanoparticles, often transitioning from a relatively smooth surface to a rougher and grooved morphology [81, 88]. In practice, this suggests that more energy is needed to break the material if an optimal amount of nanoparticles is used [88]. The definition of this optimal value is where the main challenge of using these reinforcements lies, since the addition of particles above a given value will eventually result in a composite joint with reduced static performance [8, 80, 81]. This limit can be attributed to the eventual formation of poorly connected material and agglomerations in specimens with a higher amount of the filler content [8, 81] or incompatibilities between the particles and the adherend surfaces and adhesive [8].

Carbon nanotubes (CNTs) are being widely used as reinforcement nanofillers in polymer nanocomposites and are categorized as single-, double-, or multi-walled, based on the number of concentric graphene sheets rolled together to make up the nanotube. Multi-wall carbon nanotubes (MWCNTs) are often employed as reinforcing nanofillers in composite materials, which results in materials with high strength and stiffness [7, 91]. MWCNTs can also be used to reinforce adhesives [12, 92] and have shown to be an effective alternative for improving mechanical (toughness, strength stiffness, fracture energy), electrical, and thermal properties for multiple applications [91, 93-96]. Improvements in adhesion can also be expected, as reductions in the contact angle have been reported as a result of the inclusion of a low content of MWCNTs in epoxy [94]. Additionally, the presence of MWCNTs in adhesives results in the enhancement of the resistance to crack formation and propagation [7]. These materials can potentiate crack bridging, and act as a barrier in the crack propagation path [91].

2.4 Substrate modifications

Research has been carried out on the modification and adjustment of composite properties, seeking to optimize the joint performance in a holistic manner. Different methods have been found to have a positive influence on strength e.g. by increasing the rigidity of the adherends [34]. This could be achieved by modifying both or at least one of the adherends to minimize the rotation of the joint and promote a more uniform distribution of the stresses acting in the adhesive.

2.4.1 Effect of stacking sequence

In composite joints, the stacking sequence of the adherends is a powerful parameter controlling joint performance and, thus, has been the target of extensive study. It is worth noting that the effect of varying the stacking sequence is highly dependent on the joint configuration and on the material properties. The optimized stacking sequence can be varied by changing these parameters. Ostapiuk and Bienia [97] studied two different stacking sequences, unidirectional and crossply, for the composite part of a composite

metal laminate single lap joint under quasi-static loading. Their results showed that regardless of the composite type and the surface preparation, the crossply presented the highest failure load. This may be due to the more complex crack path expected for an initiated crack in the angle-plyed composite. Ozel et al. [98] studied four different stacking sequences in composite single lap joints ($[0]_{8s}$, $[0/90]_{4s}$, $[45/-45]_{4s}$ and $[0/45/-45/90]_{2s}$). The $[0]_{16}$ stacking sequence was found to present a higher failure load than the angle-plyed configurations, except for the $[0/45/-45/90]_{2s}$ layup. Based on their numerical study, they concluded that this is because of the low peel stresses acting on the overlap edges of the adherends with quasi-isotropic stacking sequence.

Purimpat et al. [99] showed that the strength of the specimens is dependent on both the local orientations and the global properties of the laminates. A vast study was performed on a composite single lap joint with Quasi-Isotropic Quasi-Homogeneous (QIQH) sequences and it was concluded that, since it is more probable for the final failure to occur in the 0° layer (seat of the final break), it could be assumed that as distance from the adhesive layer increases the complexity of the crack path and thus raises the joint strength increases [99]. This can be seen schematically in Figure 2.6. In general, the optimum stacking sequence is highly dependent on the joint configuration. However, stacking sequences with unidirectional fibres parallel to the loading direction and quasi-isotropic stacking sequence tend to perform better for many common joint configurations, such as the single lap joint.

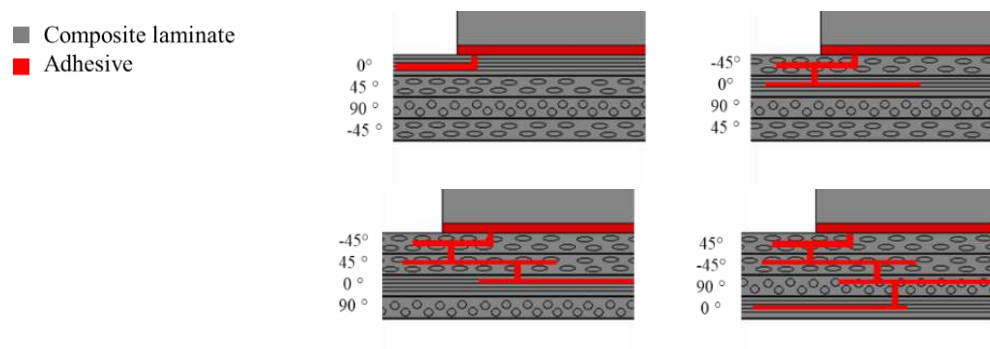


Figure 2.6: Effect of 0° layer distance from surface in quasi isotropic laminate.
Adapted from [99].

2.4.2 Thin-ply laminates

The use of thin-ply laminates is a relatively recent approach for substrate modification. Thin-ply laminates are defined as those composed by plies with a thickness of less than $100\ \mu\text{m}$ [100, 101]. These layer thicknesses became available through recent developments of the spread-tow process [102], which produces flat, straight plies until a dry ply thickness as low as $20\ \mu\text{m}$ is reached [103]. The use of thin-ply laminates brings a higher degree of freedom to layup design (both in orientation and the quantity of the individual layers) [104]. Furthermore, due to the reduced layer thicknesses and the improved resin spreading process, more homogeneous fibre distribution and smaller resin-rich regions can be achieved [105]. The higher number of layers and the associated higher number of interfaces also causes the shear stresses

to be lower [104]. Thinner plies are acknowledged to have higher resistance against matrix cracking [106, 107].

Currently, the use of thin-ply laminates is mainly driven by the search for enhanced static mechanical performance [100] as well as the ability to suppress transverse microcracking [104] and free edge delamination [106-109]. The crack suppression effect may be caused by a decrease in the energy release rate at the crack tip in the thin layer [110]. Additionally, thin-ply has other unique advantages, such as higher in-situ transverse strength. The theory of in-situ strength was proposed by Camanho et al. [111], to demonstrate that a decrease in ply thickness can be correlated to an in-situ effect, characterized by a reduction in the applied stress needed to extend a transverse crack, along the thickness of the ply, when the ply thickness increases.

2.4.3 Composite metal laminates

Generally, metals are known to have better damage tolerance and to fail in a more predictable manner compared to composites. Metals are also generally unaffected by solvents and temperature levels which readily degrade polymers [30]. Therefore, in order to optimize the benefits provided by both types of materials in what regards to the strength, weight and durability of structures, a combination of traditional metals with composite materials has been pursued in recent years [30]. These materials are typically known as Composite Metal Laminates (CMLs) and were initially developed for applications in the aerospace industry. These materials consist of metal and composite layers, as it can be observed in Figure 2.7. Carbas et al. [112] showed that the strength of hybrid joints can be increased when aluminium sheets are placed in the outer layers of the lay-up. The aluminium sheets are able to prevent delamination and serve as a local reinforcement which leads to increased strength over the composite joints. The increase was observed not only under quasi-static loading [113], but also under intermediate [113] and impact [114] testing rates. This can be explained by the minimization of the stress concentrations at the edges of the overlap, as the compliant and tough metal plate is able to redistribute stresses over a much larger area without any failure.

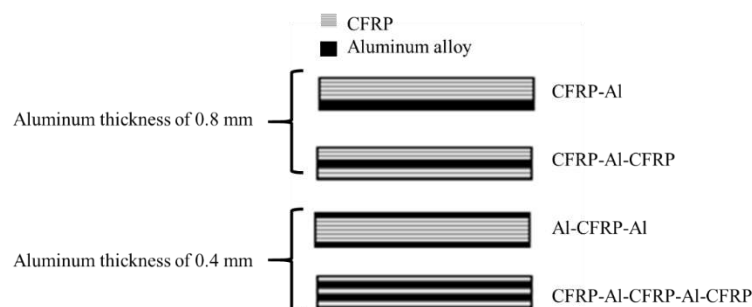


Figure 2.7: CML configurations studied by Carbas et al. [112].

In a related work, Santos et al. [115] studied novel single lap joints of CFRP joints with composite metal laminates and additional adhesive layers (see Figure 2.8). Experimental results showed an increase in the novel single lap joints compared to the ones without an additional adhesive layer.



Figure 2.8: Studied configurations by Santos et al. [115] for CML and CMLs with additional adhesive layers.

2.4.4 Toughened surface layers

The use of toughened, non-metallic, surface layers in composite layups represents another alternative for improving the performance of bonded composite joints under different loading conditions. In this method, a high toughness and compliant layer is applied to both outer surfaces of the composite material which will serve as an adherend in a bonded joint. The toughened layer could take the form of a non-reinforced resin or a more flexible fibre reinforced composite material. The use of toughened adherends is known to delay [113] or even completely eliminate [89] delamination failure in joints with composite substrates. Different possible configurations of composites toughened with polymer layers are schematically presented in Figure 2.9.

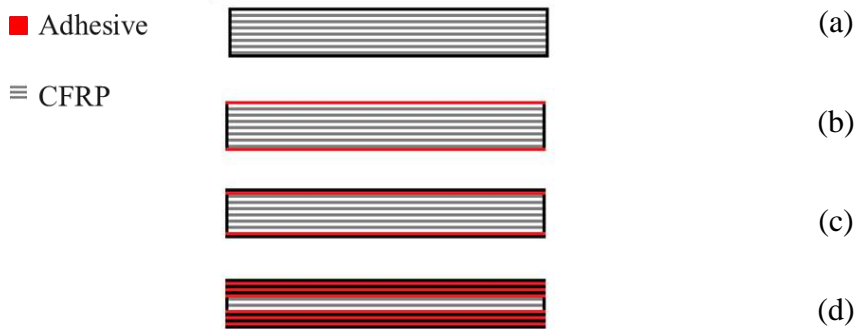


Figure 2.9: Schematic design of (a) CFRP, (b) single external adhesive layer, (c) a single interlaminar adhesive layer and, (d) three interlaminar adhesive layers. Adapted from [113, 116].

The use of a single interlaminar adhesive layer, three interlaminar adhesive layers and a single external adhesive layer, in a concept generally known as Adhesive Layer Reinforcement (ALR), has been shown to perform better than the reference CFRP only joint under quasi-static loads [116]. The configuration with external adhesive layers exhibited the highest strength increase, raising 23% above the failure load of the

reference CFRP only joint. Most importantly, the failure mode changed from delamination to cohesive failure of the adhesive itself, while the reinforcement layer remained fully intact [113, 116]. Experimental studies have demonstrated that the use of toughened adherends results in an enhancement of the shear strength of bonded joints [89] loaded under different testing rates (quasi-static, intermediate rate and impact loading) [113, 116]. However, it has to be mentioned that an optimum thickness of toughened material is dependent on the specific characteristics of the adherend to avoid drastic decreases of the joint strength [113]. In a study from Ramezani et al. [113] toughened hybrid single lap joints and the obtained results clearly show that the use of toughened layers in composite joints leads to an effective increase in joint strength. This increase is the result of two different factors. The first is the increased loadbearing capability provided by yielding of the toughened surface layer before failure occurs [89]. The second factor is associated to the lowered stiffness of the surface toughening material, which is usually substantially below that of the base composite material and thus reduces the presence of stress concentrations at the edges of the overlap length of the bonded joint [113].

Materials and experimental methods

In this chapter, the materials used, as well as the general mechanical test performed to characterize the thin-ply composite are presented. The experimental tests are divided into three sections: first, unidirectional laminates under static, high-rate and impact loading, second, angle-ply laminates under static loading and, and finally, single lap joints under static, high-rate and impact loading.

3.1 Experimental details

3.1.1 Adhesive

The adhesive used in this work was an epoxy structural adhesives in film form with ply thickness of 0.20 mm and commercial reference "Scotch Weld AF 163-2k" (3M, Saint Paul, Minnesota, USA) [117]. The adhesive was cured following manufacturer's recommendations, at 130°C for 1 hour. The mechanical properties of AF 163-2k adhesive are presented in Table 3.1.

It should be noted that an extensive examination of the impact of various adhesives was conducted, and further testing was undertaken to select the most appropriate adhesive for the study. The adhesives investigated included Nagase XNR6852E-3 and Araldite AV 138M-1/HV 998-1 adhesives. However, the aforementioned paste adhesive necessitates a secondary bonding procedure, which is more time-consuming. Furthermore, the film AF 136-2K is well-suited for aeronautical applications and exhibits superior adhesion during manufacturing using the co-curing manufacturing procedure.

Table 3.1: Main mechanical properties of "AF 163-2k" [116].

Mechanical property	Value
Young's Modulus [MPa]	1521.87
Shear Modulus [MPa]	563.67
Tensile strength [MPa]	46.93
Shear strength [MPa]	46.93
G_{IC} [N/mm]	4.05
G_{IIC} [N/mm]	9.77

3.1.2 Conventional composite

The materials used in the studied configurations were chosen to be as representative as possible of a final application in the aerospace sector. Thus, a unidirectional prepreg carbon-epoxy composite with ply thickness of 0.15 mm was selected, with the commercial reference "Texipreg HS 160 T700" (Seal Spa, Legnano, Italy). This is an orthotropic material, whose mechanical properties are presented in Table 3.2. The elastic mechanical properties of the conventional composite correspond to the orientation of a 0° composite ply (1 and 2 are defined as fibre and transverse direction respectively). Moreover, the conventional composite's resin cohesive property is presented in Table 3.3.

Table 3.2: Conventional composite mechanical properties [118].

Mechanical property	Value
E_1 [MPa]	109000
E_2 [MPa]	8819
G_{12} [MPa]	4315
G_{23} [MPa]	3200
ν_{12}	0.34
ν_{23}	0.38

Table 3.3: Cohesive properties of the conventional composite [119].

Property	Value
Tensile strength [MPa]	25
Shear strength [MPa]	13.5
G_{IC} [N/mm]	0.33
G_{IIC} [N/mm]	0.79

3.1.3 Thin-ply

Unidirectional 0° oriented carbon-epoxy prepreg composite with ply thickness of 0.07 mm was selected, with the commercial reference NTPT-TP415. The elastic orthotropic properties for this thin-ply were characterised using a servo-hydraulic testing machine (Instron 8801), with a load cell of 100 kN and following appropriate testing standards. Thin-ply was fully characterised in **Paper D**. Table 3.4 and 3.5 shows a summary of mechanical property characterization for NTPT-TP415 thin-ply.

Table 3.4: Thin-ply mechanical properties.

Mechanical property	Value
E_1 [MPa]	101720
E_2 [MPa]	5680
G_{12} [MPa]	3030
G_{23} [MPa]	3030
ν_{12}	0.38
ν_{23}	0.04

Table 3.5: Cohesive properties of the thin-ply composite.

Property	Value
Tensile strength [MPa]	35
Shear strength [MPa]	32
G_{IC} [N/mm]	0.76
G_{IIC} [N/mm]	0.83

3.2 Manufacturing procedures

3.2.1 Laminate manufacturing

The manufacturing process for both the reference conventional and the thin-ply composite starts with a layer-by-layer stacking of the plies. This process is continued until the desired thickness is reached. Detailed manufacturing process for the composite laminates were presented in **Paper B**, **Paper C** and **Paper D**. Five different configurations for the hybrid laminates, as shown in Figure 3.1, were considered studying the effect of thin-ply thickness and thin-ply distribution in unidirectional composite laminates under static loading (see **Paper B**). In which for instance hybrid (25% thin-ply) contains 25% of thin-ply of the total thickness of the composite laminate placed on the outer surfaces. The study was continued by investigating the configuration presenting the best result under high-rate and impact condition (see **Paper C**).

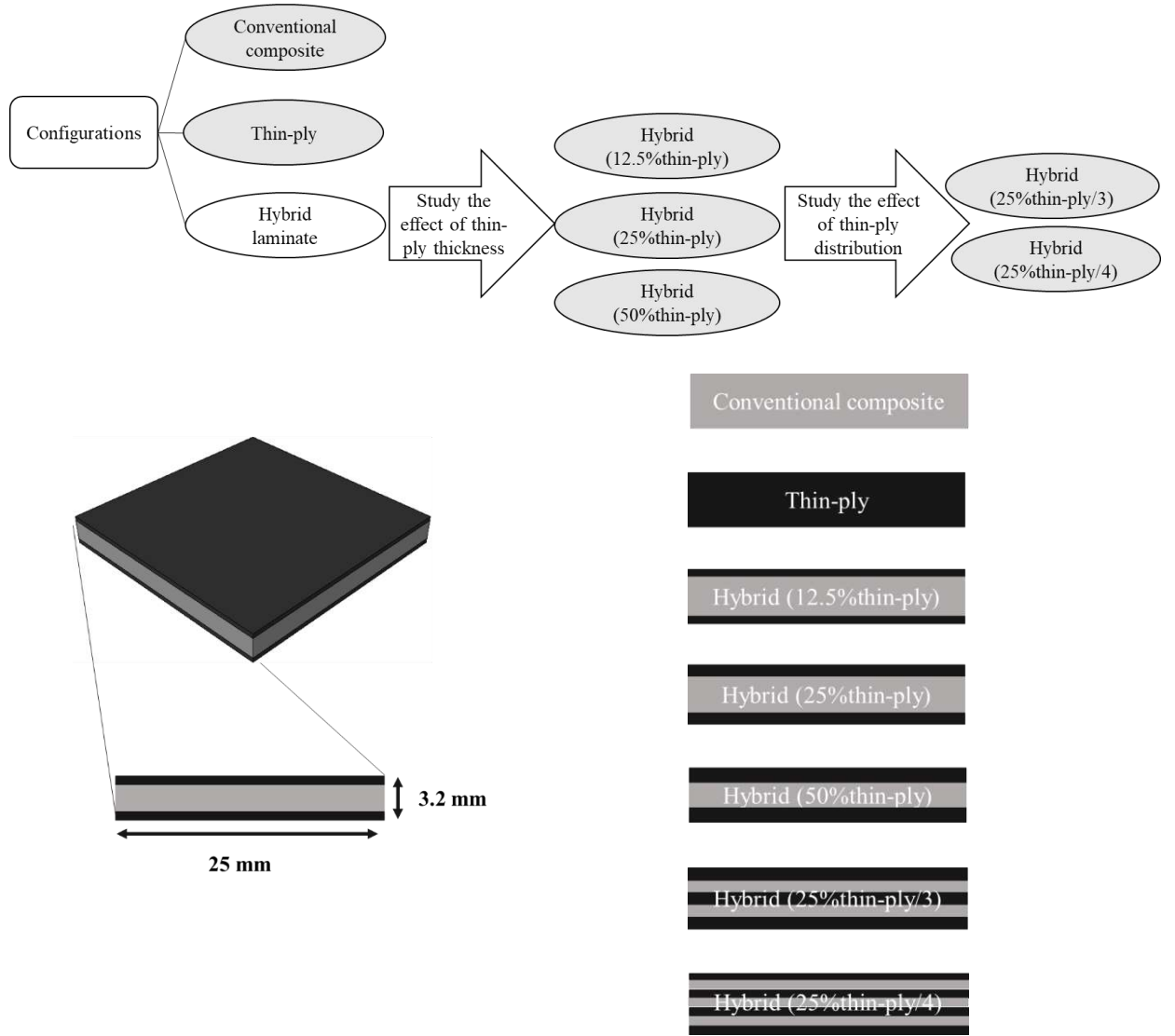


Figure 3.1: Schematic design for unidirectional conventional composite, thin-ply, and hybrid laminates.

Afterwards, in **Paper D**, the hybrid (25%thin-ply/3) configuration was considered and for the first stage, in a hybrid laminates, the conventional composite was kept unidirectional (0°) and thin-ply layers were oriented at $[45/-45]_n$ and $[0/90]_n$ seeking symmetry of the final laminate. Moreover, the reference angle-ply thin-ply laminates ($[0/90]_{ns}$ and $[45/-45]_{ns}$) were also examined.

For the second stage, both the thin-ply and the conventional composite layers were oriented at $[45/-45]_n$ and $[0/90]_n$ seeking symmetry of the final laminate. Moreover, the reference oriented conventional composite laminate ($[0/90]_{ns}$ and $[45/-45]_{ns}$) was also studied. The studied configurations for the angle-ply laminates are presented in Figure 3.2.

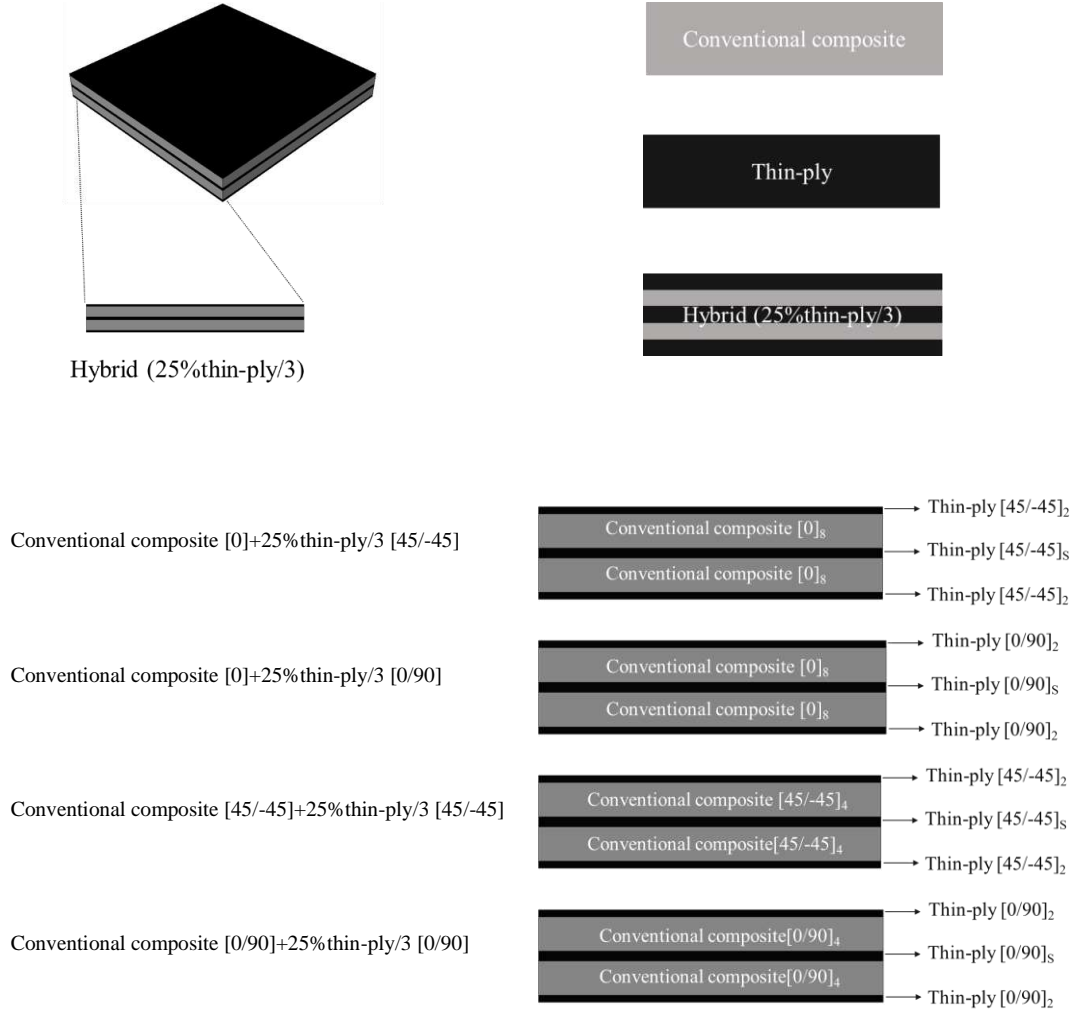


Figure 3.2: Schematic design of the angle-ply hybrid laminates.

3.2.2 Single lap joint manufacturing

The manufactured SLJs were based on the geometry shown in Figure 3.3. The width for all specimens under consideration was set as 15 mm.

The manufacturing process of the reference conventional composite single lap joints starts with the layer-by-layer stacking of the conventional composite adherend, until the desired adherend thickness is attained (3.6 mm). In this case, 24 layers of conventional composite were used. A schematic design of the reference conventional composite, thin-ply and hybrid configurations was presented in Figure 3.3. The manufacturing process of the adhesively bonded composite joints was explained in details in **Paper E**, **Paper F** and **Paper G**.

While the final configuration for the single lap joints incorporated an overlap length of 25 mm, it is important to note that initially, a 50 mm overlap length was considered. However, following experimental and numerical studies, it was discovered that utilizing a 50 mm overlap length resulted in induced stress in the joint during loading approaching the maximum strength of the adherends. Consequently, this limited the

potential for enhancing the joint's behavior. Therefore, the overlap of the joint was decreased to 25 mm to allow for greater scope for improvement.

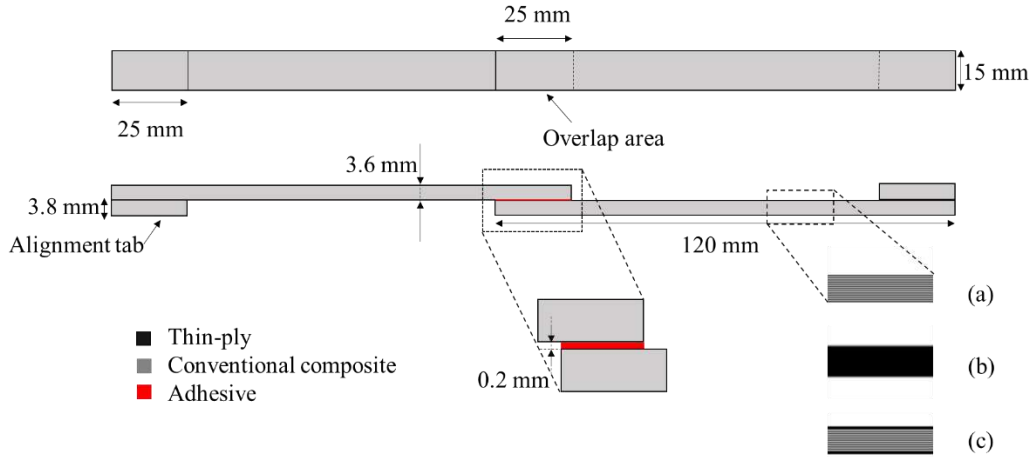


Figure 3.3: Schematic design of reference (a) conventional composite, (b) thin-ply and, (c) hybrid (25% thin-ply) single lap joints.

3.3 Testing conditions

For the static and high-rate loading the specimens (the composite laminates and the single lap joints) were tested using a servo-hydraulic testing machine (Instron 8801), with a load cell of 100 kN at a constant crosshead speed of 1 mm/min and 0.1 m/s respectively. A minimum of three repetitions were performed for each of the configurations tested.

For the dynamic impact loading condition, the composite laminates or the single lap joints were tested at constant crosshead speeds of 2 m/sec. An in-house developed drop-weight testing machine was used to carry out impact tests on the specimens [120]. This machine grips the upper part adherend, leaving the lower portion free. A mass is then dropped from a specific height, causing an impact on the lower part of the grip and loading the specimen in tension-shear. The impact velocity is determined by the drop height, which follows the principle of energy conservation. For the impact tests in this study, a 50 kg mass and an impact velocity of 2 m/s were chosen, resulting in an impact energy of 100 J. Four repetitions were performed for each configuration under analysis. All tests were performed under laboratory ambient conditions (room temperature of 24°C, relative humidity of 55%).

3.4 Unidirectional laminates

The experimentally obtained results including the stress-strain curves obtained using Digital Image Correlation (DIC), load-displacement curves, damage initiation sites, crack propagation and crack path through the thickness for the reference conventional composite, thin-ply, and hybrid laminates under static and dynamic loading is presented in details in **Paper B** and **Paper C** respectively. Under static loading, the highest values and failure load and failure displacement were found for the hybrid (12.5% thin-ply)

and hybrid (25%thin-ply) configuration. With an increase in the thin-ply thickness through the overall thickness of the composite laminate a considerable increase in the transverse strength of the composite laminate was observed. However by further increasing in the thin-ply thickness (up to 50%) a decrease in the transverse strength was observed which was mainly controlled by the thin-ply material (see Figure 3.4). The same trend could be observed for loading the composite laminates under high-rate and impact loading. According to the DIC study the conventional composite could undergo high level of stress with a brittle behaviour. Accordingly a premature failure is expected in the case of conventional composite. However, the thin-ply material could undergo lower level of stress with a ductile behaviour. Therefore, when combining these two materials in the case of hybrid (25%thin-ply), the laminate could undergo higher level of stress retaining a ductile behaviour compared the conventional composite laminate and accordingly preventing premature failure.

Investigating the specimens after failure it could be generally stated that the crack initiation starts on one side of the laminate propagating through the thickness ending on the other side of the composite laminate. However, for the hybrid laminates the crack initiates in the conventional composite and as propagates through the thickness, the interface of the thin-ply and the conventional composite acts as a barrier against the crack propagation. This is known to be due to two main reasons. First, due to the more uniform fibre distribution of the thin-ply composite in the matrix, the crack path through the thickness is expected to be more complicated compared to the conventional composite. Second, this could be also directly attributed to higher fracture toughness of the thin-ply material.

In **Paper B**, Scanning Electron Microscope (SEM) study was preformed to validate the difference between the conventional and thin-ply composite in micro scale. Moreover, the examination of failure surfaces in both the reference conventional composite and the hybrid laminates, featuring a 25% thin-ply content in **Paper C**, to determine the failure mechanism.

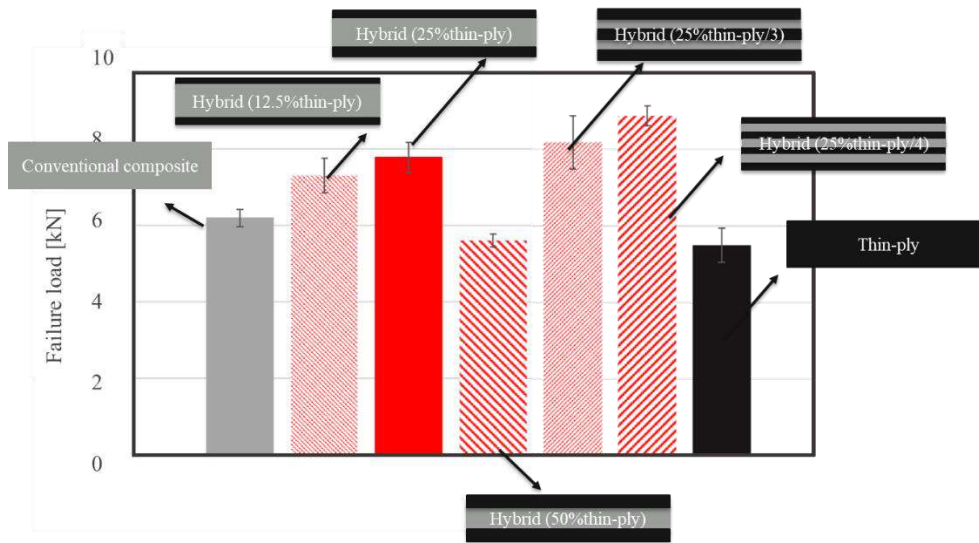


Figure 3.4: Experimentally obtained failure load for the reference and hybrid laminats reinforced using thin-plyes under static trasverse tensile loading.

3.5 Angle-plyed laminates

The experimentally obtained results including the load-displacement curves and crack path through the thickness for the angle-plyed reference conventional composite, thin-ply, and hybrid laminates under static loading is presented in details in **Paper D**. Experimental results confirm that using angle-plyed laminates in the reference or hybrid laminate increases the failure load under out-of-plane tensile loading (see Figure 3.5). This is because the crack path through the thickness is more complex in angle-plyed laminate than unidirectional laminates. This is in line with the literature review.

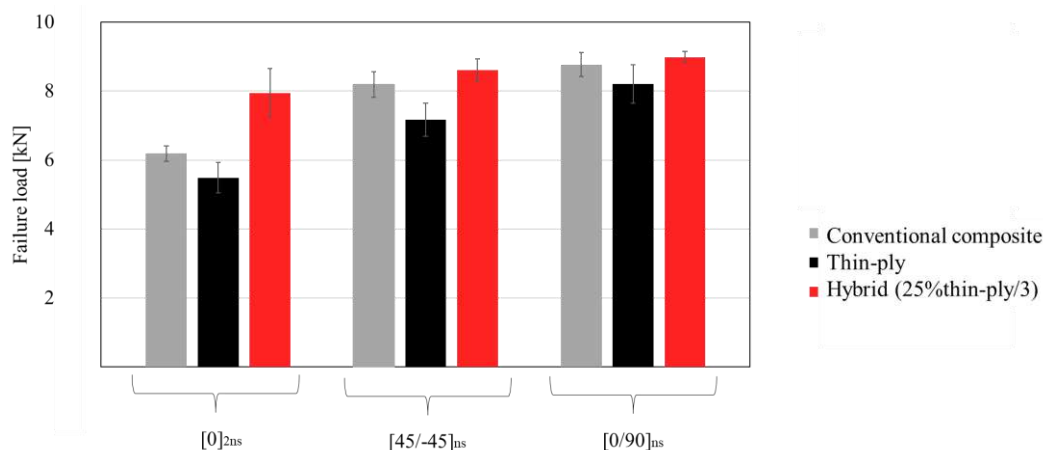


Figure 3.5: Experimentally obtained failure load for the unidirectional and angle-plyed laminates for reference and hybrid configurations reinforced using thin-plyes under static transverse tensile loading.

3.6 Single lap joints

The experimentally obtained results including load-displacement curves, damage initiation sites and final failure surface for the reference conventional composite, thin-ply, and hybrid single lap joints under static and dynamic loading is presented in details in **Paper E** and **Paper F** respectively. According to the experimentally obtained results, the replacement of conventional composite with thin-ply material in a composite laminate used as an adherend in a single lap joint leads to an increase in the strength of the structure for different loading rates (see Figure 3.6). Damage initiation sites were determined in the specimens while testing using a high-speed camera. According to the observation the crack initiation in both references (single lap joints with conventional composite and thin-ply) occurs in the adherend. This is while for the hybrid single lap joint the crack initiation occurs in the adhesive layer. This explained the less amount of delamination observed in the failure surface of the hybrid single lap joint compared to both references. Moreover, the examination of failure surfaces in both the reference conventional composite and the hybrid laminates under static loading, featuring a 25% thin-ply content in **Paper E**, to determine the failure mechanism in composite single lap joints. According to the observations, fibre breakage and fibre matrix debonding has been the predominant in the failure surface of single lap joints with conventional composite compared to hybrid single lap joints. Additionally, the effect of adherend

thickness in the strength of the hybrid (25% thin-ply) single lap joint was investigated under static loading which the results are presented in **Paper G**.

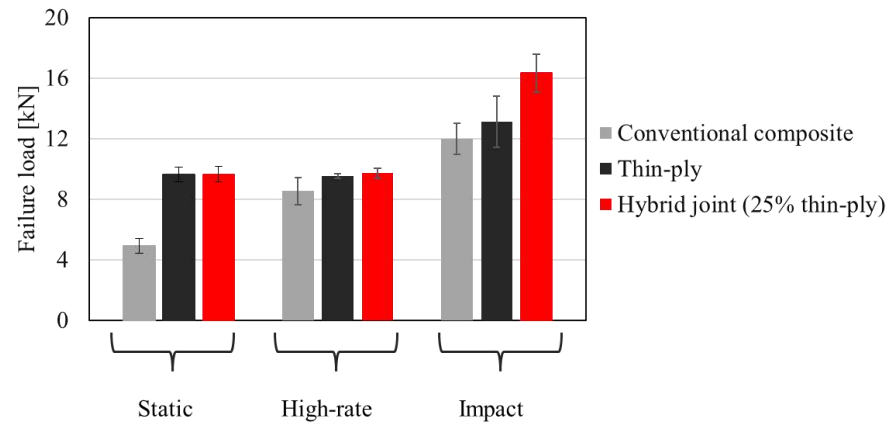


Figure 3.6: Experimentally obtained failure load for the reference and hybrid single lap joints reinforced using thin-ply different loading rates.

Numerical studies

In this chapter, the main characteristics of the numerical models conducted are presented. The simulations are divided in three main groups: unidirectional laminates under static, high-rate and impact loading, angle-ply laminates under static loading and, single lap joints under static, high-rate and impact loading. The Finite Element Analysis (FEA) was performed using the *Abaqus* software.

4.1 Unidirectional laminates

Initially, only a small-scale RVE of conventional composite and thin-ply with the dimension of $0.16 \times 0.2 \text{ (mm)}^2$ was generated for the static loading condition. The main purpose of this initial RVE was to study the distribution of fibres as close as possible to that found through SEM images mentioned in **Paper B**, allowing to represent the presence of resin-rich and fibre-rich areas in the model (see Figure 4.1). Moreover, the number of fibres was calculated using resulting in total of 291 fibres for the initial RVEs. The properties of the fibre and matrix (for the conventional composite and thin-ply) are presented in **Paper B**, **Paper C** and **Paper D**.

A large 2-D elastoplastic RVE model with dimensions of $1.6 \times 1.6 \text{ (mm)}^2$ was studied using the ABAQUS commercial finite element package. These dimensions were selected to permit the analysis of all configurations under study. The detailed information about the boundary condition and mesh of the numerical models is mentioned in **Paper B**.

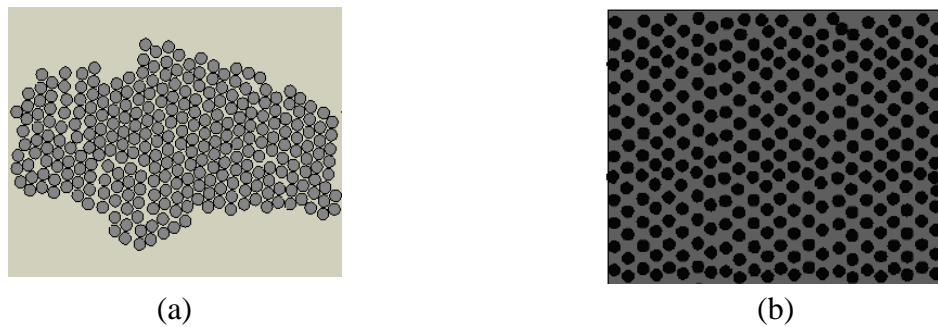


Figure 4.1: Initial RVE for the (a) conventional composite and (b) thin-ply under static loading.

However, to model the reference and hybrid composite laminates under high-rate and impact loading in **Paper C**, the mentioned initial RVEs were modified in order to replicate more realistic resin-rich and fibre-rich area as shown in Figure 4.2. The detailed information about the boundary condition and mesh of the numerical models is mentioned in **Paper C**.

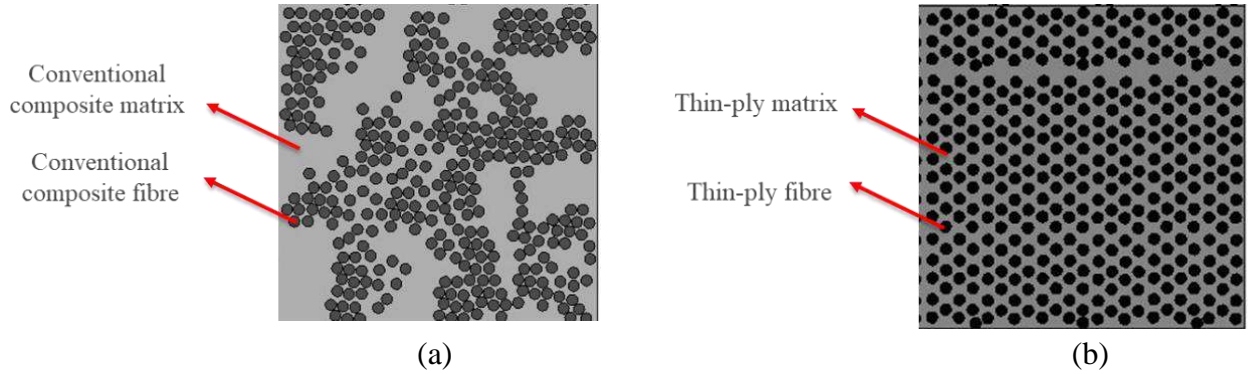


Figure 4.2: Modified initial RVE for the (a) conventional composite and (b) thin-ply under dynamic loading.

As the strength of fibres is much higher than that of the matrix, failure is always expected to occur in the matrix. Therefore, stresses in the fibres were eliminated from the results in **Paper B** and **Paper C** in order to better highlight the behaviour of the matrix. Also, the colour scale was limited to maximum stress within the conventional composite matrix (148 MPa) and any elements with stress values higher than this value are shown in a grey colour in **Paper B** and **Paper C**. Therefore, the elements that exceeded the matrix maximum strength in the RVE models are expected to correspond to the initiation of matrix failure. It has to be mentioned that the area of the failed elements in the RVE models per total area of the RVE was defined as the level of failure. According to the results the level of failure decreases considerably with the replacement conventional composites with thin-ply in the composite laminates in different loading condition which is illustrating higher strength and this is in line with the experimentally obtained results.

4.2 Angle-plyed laminates

A 3D RVE model was employed to better understand the advantages associated with angle-plyed laminates in micro scale under static loading. Following the result of the SEM micrographs presented in **Paper B**, the model was designed to account for the difference in fibre distribution between the conventional and the thin-ply composite (fibre clustering in conventional composite RVE and relatively uniform fibre distribution for the thin-ply).

Therefore, fibre directions of $[0]$, $[45/-45]$ and $[0/90]$ were considered (see Figure 4.3 and Figure 4.4). The detailed information regarding the dimension of the numerical models and boundary condition applied was presented in details in **Paper D**.

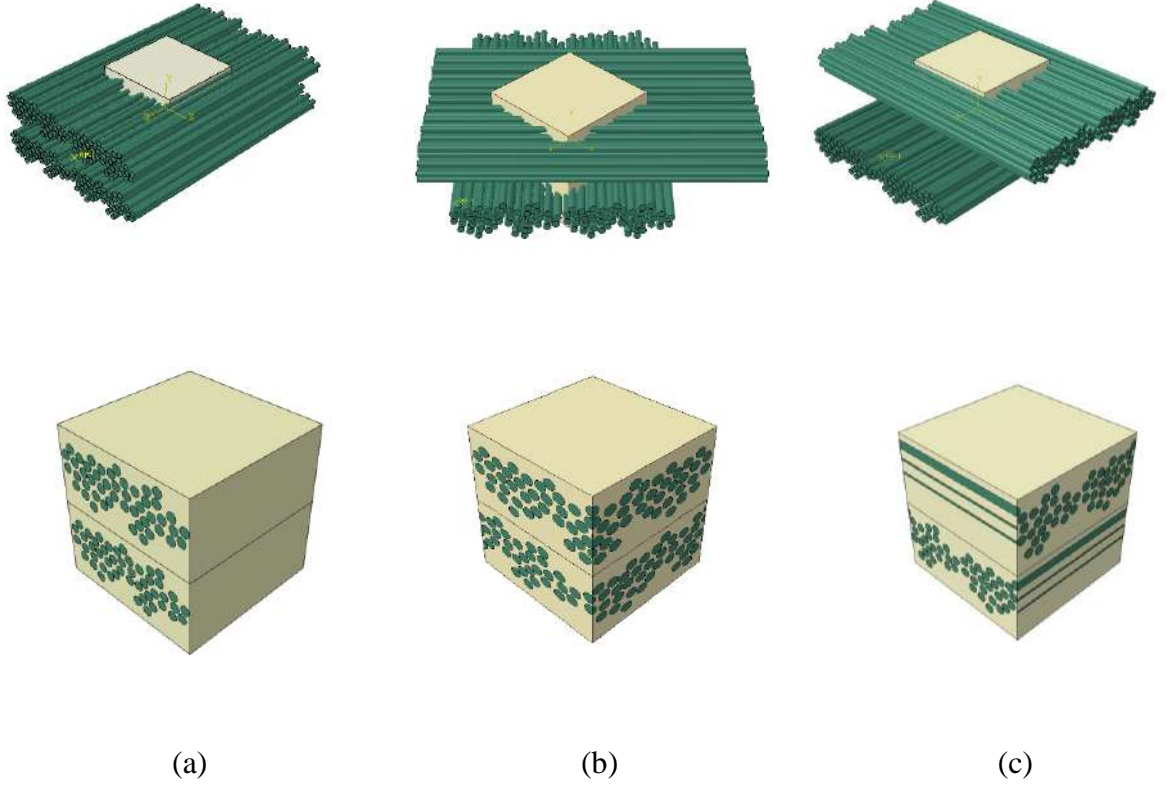


Figure 4.3: RVE models for (a) unidirectional $[0]$ and angle-ply (b) $[45/-45]$ and (c) $[0/90]$ conventional composite.

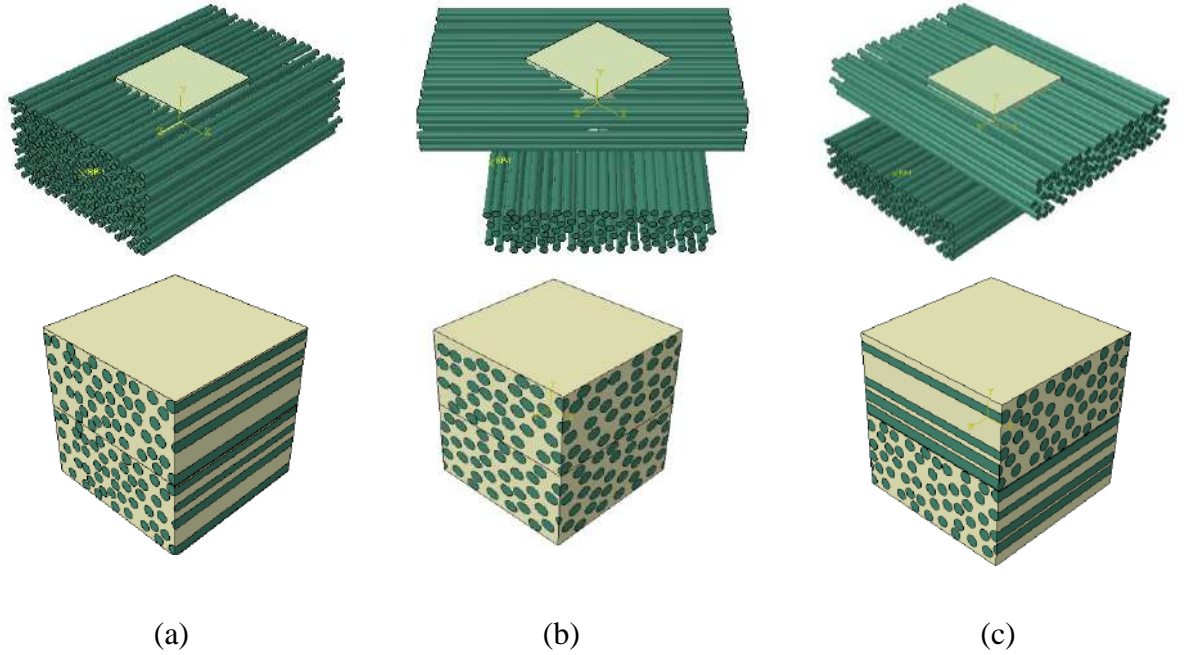


Figure 4.4: RVE models for (a) unidirectional $[0]$ and angle-ply (b) $[45/-45]$ and (c) $[0/90]$ thin-ply.

4.3 Single lap joints

In **Paper E**, **Paper F** and **Paper G** a 2D static, 2D explicit and 3D implicit dynamic loading was used for static, high-rate and impact loading respectively. The boundary conditions were defined as shown in Figure 4.5. A cohesive zone model was used to model the adhesive behaviour, employing 4 node elements cohesive quadrilateral elements. Non-linear geometrical effects were included. Triangular traction separation laws were applied to the adhesive and composite material of the model to simulate damage evolution as the cohesive failure in the adhesive layer or delamination in the composite material respectively. The interlaminar cohesive element layers in the composite material were placed in between elastic homogeneous sections (see Figure 4.6) and effectively simulate the possible debonding between the plies of composite. The thickness of the cohesive layer is considered as the thickness of one equivalent composite ply (0.07 mm for thin-ply and 0.15 mm for conventional composite). The distance of the cohesive layers in the composite material is explained in details in **Paper E**, **Paper F** and **Paper G**. The load-displacement curves, damage initiation sites and final failure mode was investigated for each configuration and presented in details in **Paper E**, **Paper F** and **Paper G**. According to the results the numerical simulation could accurately predict the failure load see Figure 4.7, displacement at failure at different loading rates. Also the crack initiation sites for the configurations under static loading and the final failure mode was precisely comparable with the experimentally obtained results.

It is worth noting that, in addition to CZM numerical modeling, the Extended Finite Element Method (XFEM) approach and Hashin composite failure criteria were employed to simulate the behavior of the configurations under various loading conditions. However, it was ultimately discovered that since delamination emerged as the primary failure mode in the joints, CZM proved to be the most effective damage model for representing the failure in the numerical simulations.

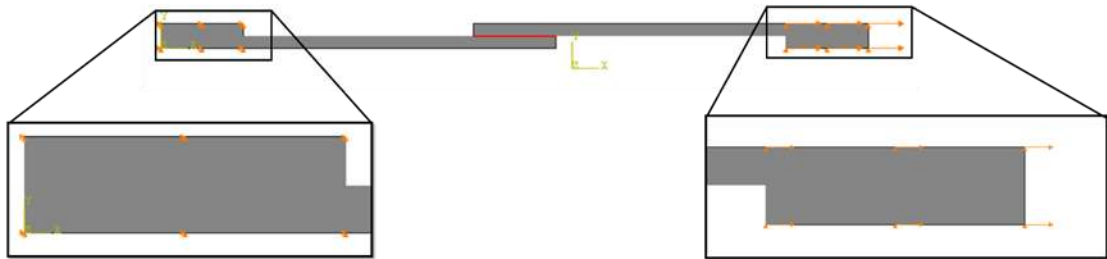


Figure 4.5: Boundary condition of simulated single lap joint

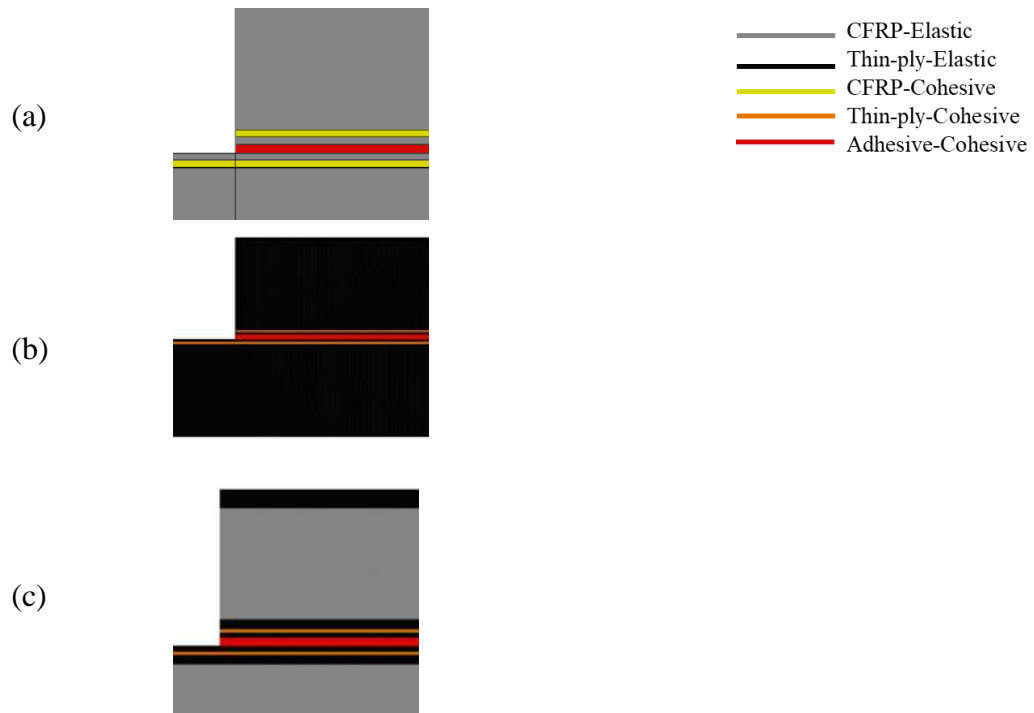


Figure 4.6: Assigned mechanical properties for (a) conventional composite, (b) thin-ply and, (c) hybrid (25% thin-ply) single lap joint.

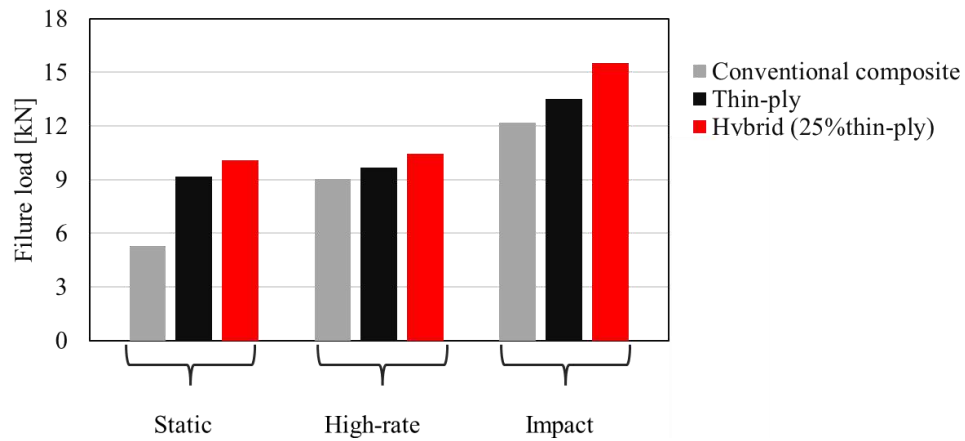


Figure 4.7: Numerically obtained failure load for reference and hybrid single lap joints reinforced using thin-ply under different loading rates.

Conclusion

This work is a combination of tasks and, therefore, the conclusions are going to be divided in three main sections: (i) conclusions from the use of unidirectional hybrid composite laminates under static, high-rate and impact loading; (ii) conclusions from hybrid angle-ply laminates under static loading; (iii) reference and hybrid single lap joints reinforced by thin-ply under static, high-rate and impact loading.

Unidirectional composite laminates

- Experimental results show that the hybrid composite laminates using 25% of thin-ply present considerably higher failure load under different transverse tensile loading conditions when compared to the reference conventional composite laminates. This is mainly due to higher ductility, regularity, and homogeneity conferred to the material by the presence of thin-ply.
- Analysis of the failure mechanism reveals that the thin-ply layers effectively impede crack propagation, primarily due to their more uniform fibre distribution and reduced presence of resin-rich and fibre-rich areas.
- Distributing a constant amount of thin-ply through the thickness increases the failure load.
- Numerical simulations using a 2D representative volume element model indicate that the conventional composite model exhibits a larger number of elements surpassing the maximum strength of the matrix (which have failed) compared to the hybrid (25% thin-ply) model.
- A decrease in level of failure was observed numerically as the loading speed transitions from static to high-rate and from high-rate to impact loading which is consistent with the experimental observations.

Angle-ply composite laminates

- Experimental results confirm that using angle-ply laminates in the reference or hybrid laminate increases the failure load under static out-of-plane tensile loading. This is because the through the thickness crack path is expected to be more complex in angle-ply laminate than unidirectional laminates.
- According to experimental result, hybrid laminates reinforced with thin-ply and with the stacking sequence of $[0/90]_{ns}$ present the highest strength under static out-of-plane tensile loads.
- A numerical analysis indicated that angle-ply conventional composite and thin-ply laminates experience a lower level of failure under static out-of-plane tensile loading, and therefore the matrix failure process is delayed. Accordingly, angle-ply hybrid laminates reinforced with thin-ply are expected to present higher strength compared to the unidirectional ones.
- According to the same numerical study, the stacking sequence of $[0/90]_{ns}$ presents a lower level of failure compared to $[45/-45]_{ns}$ for both conventional composite and thin-ply configurations.

Single lap joints

- The use of hybrid (25% thin-ply) composite joints reinforced with thin-ply exhibit higher tensile strength than conventional composite joints under all loading conditions.
- According to the experimental observation for the single lap joints under static loading, damage initiation occurs in the adherend for the reference conventional composite and thin-ply joint, while for the hybrid (25% thin-ply) joint, damage initiation occurs in the adhesive layer. Damage propagates as a combination of delamination and cohesive failure for all configurations. However, a more limited amount of delamination was obtained for the hybrid joint under static loading.
- Delamination is the dominant failure mode across all configurations for high-rate and impact loads.

- Microscopic images of the bond line allowed for the identification of multiple fibre breakages and fibre pull-outs on the failure surface of the reference conventional composite configuration. In contrast, the fibres were still intact and well-aligned in the failure surface of the hybrid joint.
- The configurations under analysis were modelled numerically, and a good agreement was obtained between the numerical and experimental results, allowing for a precise representation of the damage initiation and failure processes.

Future work

This work can be continued and complemented in the future following different approaches to study in more detail additional topics left unanswered.

Continuing and expanding upon this work offers numerous avenues for in-depth exploration of additional topics that have yet to be fully addressed. Specifically, for the optimized hybrid composite joint reinforced by thin-ply, there's an opportunity to investigate the impact of aging and temperature variations, comparing the results with reference joints made using conventional composite materials and thin-ply reinforcement alone.

Moreover, the study could delve into the effects of cyclic loading on the aforementioned configuration. By subjecting the joints to cyclic loading conditions, researchers can gain insights into their durability, fatigue resistance, and long-term performance, which are crucial considerations for real-world applications.

To ensure the relevance and practicality of these investigations, it's essential to select a real component geometry representative of aeronautical industry applications. This geometry should be characterized by high strain rates and cyclic loads, aligning with the operational conditions typically encountered in aerospace environments. By choosing such a geometry, the study can effectively demonstrate the potential benefits of the tough hybrid laminate concept in addressing the unique challenges faced by the industry.

Through these comprehensive analyses and experiments, researchers can advance our understanding of optimized hybrid composite joints, paving the way for improved design methodologies and enhanced performance of aerospace structures. Ultimately, this research has the potential to drive innovation, optimize manufacturing processes, and contribute to the development of safer and more efficient aircraft systems.

References

1. Wang, C., Huang, Y.D., Xv, H.Y. and Liu, W.B., 2004. The durability of adhesive/carbon–carbon composites joints in salt water. *International journal of adhesion and adhesives*, 24(6), pp.471-477.
2. Seong, M.S., Kim, T.H., Nguyen, K.H., Kweon, J.H. and Choi, J.H., 2008. A parametric study on the failure of bonded single-lap joints of carbon composite and aluminum. *Composite structures*, 86(1-3), pp.135-145.
3. Kelly, G., 2006. Quasi-static strength and fatigue life of hybrid (bonded/bolted) composite single-lap joints. *Composite structures*, 72(1), pp.119-129.
4. Jeevi, G., Nayak, S.K. and Abdul Kader, M., 2019. Review on adhesive joints and their application in hybrid composite structures. *Journal of Adhesion Science and Technology*, 33(14), pp.1497-1520.
5. Marannano, G. and Zuccarello, B., 2015. Numerical experimental analysis of hybrid double lap aluminum-CFRP joints. *Composites Part B: Engineering*, 71, pp.28-39.
6. Choi, J.I., Hasheminia, S.M., Chun, H.J. and Park, J.C., 2017. Experimental study on failure mechanism of hybrid composite joints with different adhesives. *Fibers and Polymers*, 18(3), pp.569-574.
7. Ariaee, S., Tutunchi, A., Kianvash, A. and Entezami, A.A., 2014. Modeling and optimization of mechanical behavior of bonded composite–steel single lap joints by response surface methodology. *International Journal of Adhesion and Adhesives*, 54, pp.30-39.
8. Vietri, U., Guadagno, L., Raimondo, M., Vertuccio, L. and Lafdi, K., 2014. Nanofilled epoxy adhesive for structural aeronautic materials. *Composites Part B: Engineering*, 61, pp.73-83.
9. Kim, C.H., Choi, J.H. and Kweon, J.H., 2015. Defect detection in adhesive joints using the impedance method. *Composite Structures*, 120, pp.183-188.

10. Sancaktar, E. and Kumar, S., 2000. Selective use of rubber toughening to optimize lap-joint strength. *Journal of Adhesion Science and Technology*, 14(10), pp.1265-1296.
11. Dean, G., Crocker, L., Read, B. and Wright, L., 2004. Prediction of deformation and failure of rubber-toughened adhesive joints. *International journal of adhesion and adhesives*, 24(4), pp.295-306.
12. Zhang, J., Luo, R. and Yang, C., 2012. A multi-wall carbon nanotube-reinforced high-temperature resistant adhesive for bonding carbon/carbon composites. *Carbon*, 50(13), pp.4922-4925.
13. Balkova, R., S. Holcnerova, and V. Cech. "Testing of adhesives for bonding of polymer composites." *International Journal of adhesion and adhesives* 22.4 (2002): 291-295.
14. Adams, R.D. and Peppiatt, N.A., 1974. Stress analysis of adhesive-bonded lap joints. *Journal of strain analysis*, 9(3), pp.185-196.
15. Da Silva, L.F. and Adams, R.D., 2007. Techniques to reduce the peel stresses in adhesive joints with composites. *International Journal of Adhesion and Adhesives*, 27(3), pp.227-235.
16. Machado, J.J.M., Gamarra, P.R., Marques, E.A.S. and da Silva, L.F., 2018. Improvement in impact strength of composite joints for the automotive industry. *Composites Part B: Engineering*, 138, pp.243-255.
17. Ganesh, V.K. and Choo, T.S., 2002. Modulus graded composite adherends for single-lap bonded joints. *Journal of composite materials*, 36(14), pp.1757-1767.
18. Boss, J.N., Ganesh, V.K. and Lim, C.T., 2003. Modulus grading versus geometrical grading of composite adherends in single-lap bonded joints. *Composite Structures*, 62(1), pp.113-121.
19. Potter, K.D., Guild, F.J., Harvey, H.J., Wisnom, M.R. and Adams, R.D., 2001. Understanding and control of adhesive crack propagation in bonded joints between carbon fibre composite adherends I. Experimental. *International journal of adhesion and adhesives*, 21(6), pp.435-443.
20. Mouritz, A.P., 2007. Review of z-pinned composite laminates. *Composites Part A: applied science and manufacturing*, 38(12), pp.2383-2397.
21. Ko FK. Three-dimensional fabrics for composites. In: TW Chou and FK Ko (eds) *Textile structural composites*. Amsterdam: Elsevier, 1989, pp.129–171
22. Sawyer, J.W., 1985. Effect of stitching on the strength of bonded composite single lap joints. *AIAA journal*, 23(11), pp.1744-1748.

23. Chan, W.S., 1991. Design approaches for edge delamination resistance in laminated composites. *Journal of Composites, Technology and Research*, 13(2), pp.91-96.
24. Hader-Kregl, L., Wallner, G.M., Kralovec, C. and Eyßell, C., 2019. Effect of inter-ply on the short beam shear delamination of steel/composite hybrid laminates. *The Journal of Adhesion*, 95(12), pp.1088-1100.
25. Vogelesang, L.B. and Vlot, A., 2000. Development of fibre metal laminates for advanced aerospace structures. *Journal of materials processing technology*, 103(1), pp.1-5.
26. Simões, B.D., Nunes, P.D., Ramezani, F., Carbas, R.J., Marques, E.A. and da Silva, L.F., 2022. Experimental and Numerical Study of Thermal Residual Stresses on Multimaterial Adherends in Single-Lap Joints. *Materials*, 15(23), p.8541.
27. Mokhtari, M., Madani, K., Belhouari, M., Touzain, S., Feaugas, X. and Ratwani, M., 2013. Effects of composite adherend properties on stresses in double lap bonded joints. *Materials & Design*, 44, pp.633-639.
28. Pramanik, A., Basak, A.K., Dong, Y., Sarker, P.K., Uddin, M.S., Littlefair, G., Dixit, A.R. and Chattopadhyaya, S., 2017. Joining of carbon fibre reinforced polymer (CFRP) composites and aluminium alloys—A review. *Composites Part A: Applied Science and Manufacturing*, 101, pp.1-29.
29. Dos Reis, M.Q., Marques, E.A.S., Carbas, R.J.C. and Da Silva, L.F.M., 2020. Functionally graded adherends in adhesive joints: an overview. *Journal of Advanced Joining Processes*, 2, p.10003
30. Budhe, S., Banea, M.D., De Barros, S. and Da Silva, L.F.M., 2017. An updated review of adhesively bonded joints in composite materials. *International Journal of Adhesion and Adhesives*, 72, pp.30-42.
31. Shang, X., Marques, E.A.S., Machado, J.J.M., Carbas, R.J.C., Jiang, D. and Da Silva, L.F.M., 2019. Review on techniques to improve the strength of adhesive joints with composite adherends. *Composites Part B: Engineering*, 177, p.107363.
32. Matthews, F.L., Kilty, P.F. and Godwin, E.W., 1982. A review of the strength of joints in fibre-reinforced plastics. Part 2. Adhesively bonded joints. *Composites*, 13(1), pp.29-37.
33. Araújo, H.A.M., Machado, J.J.M., Marques, E.A.S. and Da Silva, L.F.M., 2017. Dynamic behaviour of composite adhesive joints for the automotive industry. *Composite Structures*, 171, pp.549-561.
34. Reis, P.N., Ferreira, J.A.M. and Antunes, F., 2011. Effect of adherend's rigidity on the shear strength of single lap adhesive joints. *International Journal of Adhesion and Adhesives*, 31(4), pp.193-201.

35. Ozel, A., Yazici, B., Akpınar, S., Aydın, M.D. and Temiz, Ş., 2014. A study on the strength of adhesively bonded joints with different adherends. *Composites Part B: Engineering*, 62, pp.167-174.
36. Kanerva, M. and Saarela, O., 2013. The peel ply surface treatment for adhesive bonding of composites: A review. *International journal of adhesion and adhesives*, 43, pp.60-69.
37. Islam, M.S., Tong, L. and Falzon, P.J., 2014. Influence of metal surface preparation on its surface profile, contact angle, surface energy and adhesion with glass fibre prepreg. *International Journal of Adhesion and Adhesives*, 51, pp.32-41.
38. Encinas, N., Oakley, B.R., Belcher, M.A., Blohowiak, K.Y., Dillingham, R.G., Abenojar, J. and Martínez, M.A., 2014. Surface modification of aircraft used composites for adhesive bonding. *International Journal of Adhesion and Adhesives*, 50, pp.157-163.
39. Li, S., Sun, T., Liu, C., Yang, W. and Tang, Q., 2018. A study of laser surface treatment in bonded repair of composite aircraft structures. *Royal Society open science*, 5(3), p.171272.
40. Wingfield, J.R.J., 1993. Treatment of composite surfaces for adhesive bonding. *International journal of adhesion and adhesives*, 13(3), pp.151-156.
41. Baker, A. ed., 1988. *Bonded repair of aircraft structures* (Vol. 7). Springer Science & Business Media.
42. Palmieri, F.L., Belcher, M.A., Wohl, C.J., Blohowiak, K.Y. and Connell, J.W., 2016. Laser ablation surface preparation for adhesive bonding of carbon fiber reinforced epoxy composites. *International Journal of Adhesion and Adhesives*, 68, pp.95-101.
43. Fischer, F., Kreling, S., Gäbler, F. and Delmdahl, R., 2013. Using excimer lasers to clean CFRP prior to adhesive bonding. *Reinforced Plastics*, 57(5), pp.43-46.
44. Mohan, J., Ramamoorthy, A., Ivanković, A., Dowling, D. and Murphy, N., 2014. Effect of an atmospheric pressure plasma treatment on the mode I fracture toughness of a co-cured composite joint. *The Journal of Adhesion*, 90(9), pp.733-754.
45. Holtmannspötter, J., Czarnecki, J.V., Feucht, F., Wetzel, M., Gudladt, H.J., Hofmann, T., Meyer, J.C. and Niedernhuber, M., 2015. On the fabrication and automation of reliable bonded composite repairs. *The Journal of Adhesion*, 91(1-2), pp.39-70.
46. Arenas, J.M., Alía, C., Narbón, J.J., Ocaña, R. and González, C., 2013. Considerations for the industrial application of structural adhesive joints in the aluminium–composite material bonding. *Composites Part B: Engineering*, 44(1), pp.417-423.
47. Kanerva, M., Sarlin, E., Hoikkanen, M., Rämö, K., Saarela, O. and Vuorinen, J., 2015. Interface modification of glass fibre–polyester composite–composite joints using peel plies. *International Journal of Adhesion and Adhesives*, 59, pp.40-52.

48. Buchmann, C., Langer, S., Filsinger, J. and Drechsler, K., 2016. Analysis of the removal of peel ply from CFRP surfaces. *Composites Part B: Engineering*, 89, pp.352-361.
49. Thull, D., Zimmer, F., Hofmann, T., Holtmannspötter, J., Koerwien, T. and Hoffmann, M., 2019. Investigation of fluorine-based release agents for structural adhesive bonding of carbon fibre reinforced plastics. *Applied Adhesion Science*, 7(1), pp.1-19.
50. Rhee, K.Y. and Yang, J.H., 2003. A study on the peel and shear strength of aluminum/CFRP composites surface-treated by plasma and ion assisted reaction method. *Composites science and technology*, 63(1), pp.33-40.
51. Ramaswamy, K., O'Higgins, R.M., Kadiyala, A.K., McCarthy, M.A. and McCarthy, C.T., 2020. Evaluation of grit-blasting as a pre-treatment for carbon-fibre thermoplastic composite to aluminium bonded joints tested at static and dynamic loading rates. *Composites Part B: Engineering*, 185, p.107765.
52. Prolongo, S.G., Gude, M.R., Del Rosario, G. and Ureña, A., 2010. Surface pretreatments for composite joints: study of surface profile by SEM image analysis. *Journal of adhesion science and technology*, 24(11-12), pp.1855-1867.
53. Schmutzler, H., Popp, J., Büchter, E., Wittich, H., Schulte, K. and Fiedler, B., 2014. Improvement of bonding strength of scarf-bonded carbon fibre/epoxy laminates by Nd: YAG laser surface activation. *Composites Part A: Applied Science and Manufacturing*, 67, pp.123-130.
54. De Barros, S., Kenedi, P.P., Ferreira, S.M., Budhe, S., Bernardino, A.J. and Souza, L.F.G., 2017. Influence of mechanical surface treatment on fatigue life of bonded joints. *The Journal of Adhesion*, 93(8), pp.599-612.
55. Brack, N. and Rider, A.N., 2014. The influence of mechanical and chemical treatments on the environmental resistance of epoxy adhesive bonds to titanium. *International Journal of Adhesion and Adhesives*, 48, pp.20-27.
56. Baker, A.A. and Chester, R.J., 1992. Minimum surface treatments for adhesively bonded repairs. *International journal of adhesion and adhesives*, 12(2), pp.73-78.
57. Schubbe, J.J. and Mall, S., 1999. Investigation of a cracked thick aluminum panel repaired with a bonded composite patch. *Engineering Fracture Mechanics*, 63(3), pp.305-323.
58. Oliveira, V., Sharma, S.P., De Moura, M.F.S.F., Moreira, R.D.F. and Vilar, R., 2017. Surface treatment of CFRP composites using femtosecond laser radiation. *Optics and Lasers in Engineering*, 94, pp.37-43.
59. De Freese, J., Holtmannspötter, J., Raschendorfer, S. and Hofmann, T., 2018. End milling of Carbon Fiber Reinforced Plastics as surface pretreatment for adhesive bonding—effect of intralaminar damages and particle residues. *The Journal of Adhesion*.

60. Morano, C., Tao, R., Alfano, M. and Lubineau, G., 2021. Effect of Mechanical Pretreatments on Damage Mechanisms and Fracture Toughness in CFRP/Epoxy Joints. *Materials*, 14(6), p.1512.
61. Leone, C. and Genna, S., 2018. Effects of surface laser treatment on direct co-bonding strength of CFRP laminates. *Composite Structures*, 194, pp.240-251.
62. Ashcroft, I.A., Hughes, D.J. and Shaw, S.J., 2000. Adhesive bonding of fibre reinforced polymer composite materials. *Assembly Automation*.
63. Masmanidis, I.T. and Philippidis, T.P., 2015. Progressive damage modeling of adhesively bonded lap joints. *International Journal of Adhesion and Adhesives*, 59, pp.53-61.
64. Bishop, S.M. and Gilmore, R.B., "Fatigue of bonded CFRP joints: Fracture mechanisms and environmental effects", *Adhesion '90*, Cambridge Sept 1990, Plastics and Rubber Institute.
65. Mohan, J., Ivanković, A. and Murphy, N., 2015. Mixed-mode fracture toughness of co-cured and secondary bonded composite joints. *Engineering Fracture Mechanics*, 134, pp.148-167.
66. Song, M.G., Kweon, J.H., Choi, J.H., Byun, J.H., Song, M.H., Shin, S.J. and Lee, T.J., 2010. Effect of manufacturing methods on the shear strength of composite single-lap bonded joints. *Composite Structures*, 92(9), pp.2194-2202.
67. Mohan, J., Ivanković, A. and Murphy, N., 2014. Mode I fracture toughness of co-cured and secondary bonded composite joints. *International Journal of Adhesion and Adhesives*, 51, pp.13-22.
68. Sebastiani, G., Pfeifer, S., Röber, L., Katoh, J., Yamaguchi, Z. and Takada, S., 2019. Bonding Strength of FRP-Metal Hybrids. *Technologies for Lightweight Structures (TLS)*, 3(1), pp.1-8.
69. Mohan, J., Ivanković, A. and Murphy, N., 2013. Effect of prepreg storage humidity on the mixed-mode fracture toughness of a co-cured composite joint. *Composites Part A: Applied Science and Manufacturing*, 45, pp.23-34.
70. Balzani, C., Wagner, W., Wilckens, D., Degenhardt, R., Büsing, S. and Reimerdes, H.G., 2012. Adhesive joints in composite laminates—A combined numerical/experimental estimate of critical energy release rates. *International journal of adhesion and adhesives*, 32, pp.23-38.
71. Dadian, A. and Rahnama, S., 2021. Experimental and numerical study of optimum functionally graded Aluminum/GFRP adhesive lap shear joints using Epoxy/CTBN. *International Journal of Adhesion and Adhesives*, 107, p.102854.
72. Da Silva, L.F. and Adams, R.D., 2007. Joint strength predictions for adhesive joints to be used over a wide temperature range. *International Journal of Adhesion and Adhesives*, 27(5), pp.362-379.

73. Neto, J.A.B.P., Campilho, R.D. and Da Silva, L.F.M., 2012. Parametric study of adhesive joints with composites. *International Journal of Adhesion and Adhesives*, 37, pp.96-101.
74. Akhavan-Safar, A., Ramezani, F., Delzendehrooy, F., Ayatollahi, M.R. and da Silva, L.F.M., 2022. A review on bi-adhesive joints: Benefits and challenges. *International Journal of Adhesion and Adhesives*, p.103098.
75. Ramezani, F., Ayatollahi, M.R., Akhavan-Safar, A. and Da Silva, L.F.M., 2020., A comprehensive experimental study on bi-adhesive single lap joints using DIC technique. *International Journal of Adhesion and Adhesives*, 102, p.102674.
76. Jairaja, R. and Naik, G.N., 2019. Single and dual adhesive bond strength analysis of single lap joint between dissimilar adherends. *International Journal of Adhesion and Adhesives*, 92, pp.142-153.
77. Arenas, J.M., Alía, C., Narbón, J.J., Ocaña, R. and Recio, M.M., 2012, April. Considerations for application of structural adhesives for joining aluminium with compound materials in the manufacturing of competition motorcycles. In *AIP Conference Proceedings* (Vol. 1431, No. 1, pp. 959-966). American Institute of Physics.
78. Machado, J.J.M., Gamarra, P.R., Marques, E.A.S. and da Silva, L.F., 2018. Numerical study of the behaviour of composite mixed adhesive joints under impact strength for the automotive industry. *Composite Structures*, 185, pp.373-380.
79. Jojibabu, P., Zhang, Y.X. and Prusty, B.G., 2020. A review of research advances in epoxy-based nanocomposites as adhesive materials. *International Journal of Adhesion and Adhesives*, 96, p.102454.
80. Akpinar, I.A., Gültekin, K., Akpinar, S., Akbulut, H. and Ozel, A., 2017. Experimental analysis on the single-lap joints bonded by a nanocomposite adhesives which obtained by adding nanostructures. *Composites Part B: Engineering*, 110, pp.420-428.
81. Tutunchi, A., Kamali, R. and Kianvash, A., 2015. Adhesive strength of steel–epoxy composite joints bonded with structural acrylic adhesives filled with silica nanoparticles. *Journal of Adhesion Science and Technology*, 29(3), pp.195-206.
82. Pavlidou, S. and Papaspyrides, C.D., 2008. A review on polymer–layered silicate nanocomposites. *Progress in polymer science*, 33(12), pp.1119-1198.
83. Feng, L. and Bae, D.H., 2013. Joining STS304l sheets by using nano-adhesives. *Journal of Mechanical Science and Technology*, 27(7), pp.1943-1947.
84. Hsiao, K.T., Alms, J. and Advani, S.G., 2003. Use of epoxy/multiwalled carbon nanotubes as adhesives to join graphite fibre reinforced polymer composites. *Nanotechnology*, 14(7), p.791.

85. Kinloch, A.J., Lee, J.H., Taylor, A.C., Sprenger, S., Eger, C. and Egan, D., 2003. Toughening structural adhesives via nano-and micro-phase inclusions. *The Journal of Adhesion*, 79(8-9), pp.867-873.
86. Patel S, B.A., Ganguly A, Bhowmick AK. Synthesis and properties of nanocomposite and a.J.A.S.T. 2006;20:371–385.
87. Park, S.W. and Lee, D.G., 2009. Strength of double lap joints bonded with carbon black reinforced adhesive under cryogenic environment. *Journal of adhesion science and technology*, 23(4), pp.619-638.
88. Dorigato, A. and Pegoretti, A., 2011. The role of alumina nanoparticles in epoxy adhesives. *Journal of Nanoparticle Research*, 13(6), pp.2429-2441.
89. Shang, X., Marques, E.A.S., Machado, J.J.M., Carbas, R.J.C., Jiang, D. and Da Silva, L.F.M., 2019. A strategy to reduce delamination of adhesive joints with composite substrates. *Proceedings of the Institution of Mechanical Engineers, Part L: Journal of Materials: Design and Applications*, 233(3), pp.521-530.
90. Meguid, S.A. and Sun, Y., 2004. On the tensile and shear strength of nano-reinforced composite interfaces. *Materials & design*, 25(4), pp.289-296.
91. Srivastava, V.K., 2011. Effect of carbon nanotubes on the strength of adhesive lap joints of C/C and C/C–SiC ceramic fibre composites. *International journal of adhesion and adhesives*, 31(6), pp.486-489.
92. Akpınar, I.A., Gültekin, K., Akpınar, S., Akbulut, H. and Ozel, A., 2017. Experimental analysis on the single-lap joints bonded by a nanocomposite adhesives which obtained by adding nanostructures. *Composites Part B: Engineering*, 110, pp.420-428.
93. Faulkner, S.D., Kwon, Y.W., Bartlett, S. and Rasmussen, E.A., 2009. Study of composite joint strength with carbon nanotube reinforcement. *Journal of materials science*, 44(11), pp.2858-2864.
94. Kumar, A., Kumar, K., Ghosh, P.K., Rathi, A. and Yadav, K.L., 2018. MWCNTs toward superior strength of epoxy adhesive joint on mild steel adherent. *Composites Part B: Engineering*, 143, pp.207-216.
95. Gude, M.R., Prolongo, S.G., Gómez-del Río, T. and Ureña, A., 2011. Mode-I adhesive fracture energy of carbon fibre composite joints with nanoreinforced epoxy adhesives. *International Journal of Adhesion and Adhesives*, 31(7), pp.695-703.
96. Khashaba, U.A., Aljinaidi, A.A. and Hamed, M.A., 2015. Analysis of adhesively bonded CFRE composite scarf joints modified with MWCNTs. *Composites Part A: Applied Science and Manufacturing*, 71, pp.59-71.
97. Ostapiuk, M. and Bieniaś, J., 2019. Fracture analysis and shear strength of aluminum/CFRP and GFRP adhesive joint in fiber metal laminates. *Materials*, 13(1), p.7.

98. Ozel, A., Yazici, B., Akpınar, S., Aydın, M.D. and Temiz, Ş., 2014. A study on the strength of adhesively bonded joints with different adherends. *Composites Part B: Engineering*, 62, pp.167-174.
99. Purimpat, S., Jérôme, R. and Shahram, A., 2013. Effect of fiber angle orientation on a laminated composite single-lap adhesive joint. *Advanced Composite Materials*, 22(3), pp.139-149.
100. Arteiro, A., Catalanotti, G., Xavier, J., Linde, P. and Camanho, P.P., 2018. A strategy to improve the structural performance of non-crimp fabric thin-ply laminates. *Composite Structures*, 188, pp.438-449.
101. Ramezani, F., Carbas, R.J., Marques, E.A., Ferreira, A.M. and da Silva, L.F., 2023. A study of the fracture mechanisms of hybrid carbon fiber reinforced polymer laminates reinforced by thin-ply. *Polymer Composites*, 44(3), pp.1672-1683.
102. Sihm, S., Kim, R.Y., Kawabe, K. and Tsai, S.W., 2007. Experimental studies of thin-ply laminated composites. *Composites Science and Technology*, 67(6), pp.996-1008.
103. Roure, Thomas. "C-PLY™, a new structural approach to multiaxials in composites: BI-ANGLE NCF." *JEC composites* 68 (2011): 53-54.
104. Kötter, B., Karsten, J., Körbelin, J. and Fiedler, B., 2020. CFRP thin-ply fibre metal laminates: Influences of ply thickness and metal layers on open hole tension and compression properties. *Materials*, 13(4), p.910.
105. Amacher, R., Cugnoni, J., Botsis, J., Sorensen, L., Smith, W. and Dransfeld, C., 2014. Thin ply composites: Experimental characterization and modeling of size-effects. *Composites Science and Technology*, 101, pp.121-132.
106. Yokozeki, T., Kuroda, A., Yoshimura, A., Ogasawara, T. and Aoki, T., 2010. Damage characterization in thin-ply composite laminates under out-of-plane transverse loadings. *Composite structures*, 93(1), pp.49-57.
107. Mania, R.J. and York, C.B., 2017. Buckling strength improvements for Fibre Metal Laminates using thin-ply tailoring. *Composite Structures*, 159, pp.424-432.
108. Zubillaga, L., Turon, A., Renart, J., Costa, J. and Linde, P., 2015. An experimental study on matrix crack induced delamination in composite laminates. *Composite Structures*, 127, pp.10-17.
109. Wisnom, M.R., Khan, B. and Hallett, S.R., 2008. Size effects in unnotched tensile strength of unidirectional and quasi-isotropic carbon/epoxy composites. *Composite Structures*, 84(1), pp.21-28.
110. Saito, H., Takeuchi, H. and Kimpara, I., 2012. Experimental evaluation of the damage growth restraining in 90 layer of thin-ply CFRP cross-ply laminates. *Advanced Composite Materials*, 21(1), pp.57-66.



111. Camanho, P.P., Dávila, C.G., Pinho, S.T., Iannucci, L. and Robinson, P., 2006. Prediction of in situ strengths and matrix cracking in composites under transverse tension and in-plane shear. *Composites Part A: Applied Science and Manufacturing*, 37(2), pp.165-176.
112. Carbas, R.J., Palmares, M.P. and Da Silva, L.F., 2020. Experimental and FE study of hybrid laminates aluminium carbon-fibre joints with different lay-up configurations. *Manufacturing Review*, 7, p.2.
113. Ramezani, F., Nunes, P.D.P., Carbas, R.J.C., Marques, E.A.S. and da Silva, L.F.M., 2022. The joint strength of hybrid composite joints reinforced with different laminates materials. *Journal of Advanced Joining Processes*, 5, p.100103.
114. Morgado, M.A., Carbas, R.J.C., Marques, E.A.S. and Da Silva, L.F.M., 2019. Reinforcement of CFRP single lap joints using metal laminates. *Composite Structures*, 230, p.111492.
115. Dos Santos, D.G., Carbas, R.J.C., Marques, E.A.S. and da Silva, L.F.M., 2019. Reinforcement of CFRP joints with fibre metal laminates and additional adhesive layers. *Composites Part B: Engineering*, 165, pp.386-396.
116. Morgado, M.A., Carbas, R.J.C., Dos Santos, D.G. and Da Silva, L.F.M., 2020. Strength of CFRP joints reinforced with adhesive layers. *International Journal of Adhesion and Adhesives*, 97, p.102475.
117. 3M. 3m scotch-weld structural adhesive lm af 163-2k technical datasheet. Technical report, 3M, 2009.
118. Campilho, R.D., De Moura, M.F.S.F. and Domingues, J.J.M.S., 2005. Modelling single and double-lap repairs on composite materials. *Composites Science and Technology*, 65(13), pp.1948-1958.
119. Machado, J.J.M., Marques, E.A.S., Campilho, R.D.S.G. and da Silva, L.F., 2017. Mode I fracture toughness of CFRP as a function of temperature and strain rate. *Journal of Composite Materials*, 51(23), pp.3315-3326.
120. Antunes, D.P.C., Lopes, A.M., Moreira da Silva, C.M.S., da Silva, L.F.M., Nunes, P.D.P., Marques, E.A.S. and Carbas, R.J.C., 2019. Development of a Drop Weight Machine for Adhesive Joint Testing. *Journal of Testing and Evaluation*, 49(3), pp.20190147.

Appendix A

Paper A

Developments in Laminate Modification of Adhesively Bonded Composite Joints

Developments in Laminate Modification of Adhesively Bonded Composite Joints

Farin Ramezani ¹, Beatriz D. Simões ¹, Ricardo J. C. Carbas ^{1,*} , Eduardo A. S. Marques ¹
and Lucas F. M. da Silva ² 

¹ Instituto de Ciência e Inovação em Engenharia Mecânica e Engenharia Industrial (INEGI),
Rua Dr. Roberto Frias, 4200-465 Porto, Portugal

² Departamento de Engenharia Mecânica, Faculdade de Engenharia (FEUP), Universidade Do Porto,
Rua Dr. Roberto Frias, 4200-465 Porto, Portugal

* Correspondence: rcarbas@fe.up.pt

Abstract: The use of carbon fibre reinforced polymer (CFRP) materials is increasing in many different industries, such as those operating in the aviation, marine, and automotive sectors. In these applications, composite parts are often joined with other composite or metallic parts, where adhesive bonding plays a key role. Unlike conventional joining methods, adhesive bonding does not add weight or require the drilling of holes, both of which are major sources of stress concentration. The performance of a composite joint is dependent on multiple factors and can be improved by modifying the adhesive layer or the composite layup of the adherend. Moreover, joint geometry, surface preparation, and the manufacturing methods used for production are also important factors. The present work reviews recent developments on the design and manufacture of adhesively bonded joints with composite substrates, with particular interest in adherend modification techniques. The effects of stacking sequence, use of thin-ply, composite metal laminates and its specific surface preparations, and the use of toughened surface layers in the composite adherends are described for adhesively bonded CFRP structures.

Keywords: composite materials; adhesively bonded joints; carbon fibre reinforced polymers



Citation: Ramezani, F.; Simões, B.D.; Carbas, R.J.C.; Marques, E.A.S.; da Silva, L.F.M. Developments in Laminate Modification of Adhesively Bonded Composite Joints. *Materials* **2023**, *16*, 568. <https://doi.org/10.3390/ma16020568>

Academic Editor: Alessandro Pirondi

Received: 2 December 2022

Revised: 31 December 2022

Accepted: 3 January 2023

Published: 6 January 2023



Copyright: © 2023 by the authors. Licensee MDPI, Basel, Switzerland. This article is an open access article distributed under the terms and conditions of the Creative Commons Attribution (CC BY) license (<https://creativecommons.org/licenses/by/4.0/>).

1. Introduction

Composites are high-performance and lightweight materials but ones that are hard to manufacture in large dimensions or in complex configurations [1]. From an industrial point of view, composite structures are often manufactured in multiple parts that will later be connected via different joining methods [2]. Joining of composites may take place during the manufacture of the original structure or during service, when repairing damage or replacing older components [3]. Multiple well-established joining methods are available for joining composites, such as riveting, fastening [4] and fusion bonding/welding [5–7] (in the case of thermoplastic composites). Different joining methods can also be combined in hybrid processes (using rivets, pins, or bolts) [8,9]. Mechanical joining methods are mostly known to be reliable, although they increase the weight of the structure [10]. However, these methods require holes which cut through the composite fibres and damage the composite laminate during the manufacturing process. This causes stress concentrations and local delamination, and leads to an overall degradation of the mechanical performance of the composite structure. In contrast, joining composites using adhesive bonding provides some important advantages, such as a lower process cost, high strength-to-weight ratio, low stress concentration, and a higher fatigue resistance [11,12]. Adhesive joints also distribute the load over a larger area compared to traditional joining methods [13], and therefore usually result in higher bonding strength. Moreover, adhesive bonding can be used for bonding similar and dissimilar materials and different thicknesses, which is an important advantage from an industrial standpoint, as modern structure design hinges on

the combination of multiple materials with vastly different properties to optimize structure performance and cost [14].

The strength of an adhesive joint ultimately depends on the stress distribution in the bond-line and in the adherend, which is a function of different parameters such as the joint geometry and the material properties of each component (adherend or adhesive). However, it should be noted that many other parameters substantially affect the joint strength, such as the service temperature, the humidity level [15], the manufacturing process and the associated surface treatment. The mechanical properties of structural adhesives can also be effectively controlled and modified, for example, through the addition of thermoplastic compounds [16,17] or inorganic particles [18].

Although adhesive bonding provides an important set of advantages for bonding composites, the low interlaminar strength of composite adherends can lead to important limitations in the performance of bonded joints with composite adherends [19]. In poorly designed joints, the peel stresses generated at the bond-line can overcome the limited transverse strength of the composite and cause failure by delamination at load levels well below the strength limits of the adhesive. Figure 1 provides a schematic representation of how different load levels affect the composite adherends and eventually cause delamination.

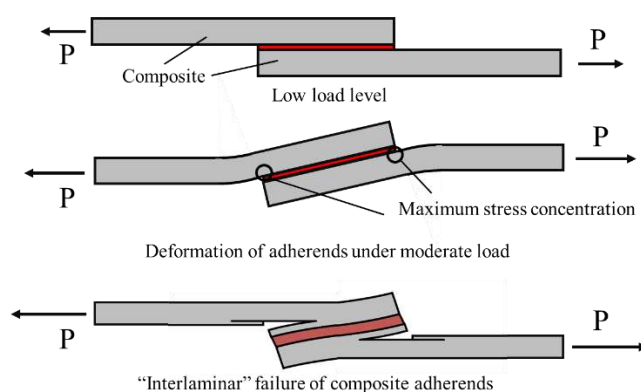


Figure 1. Effect of load level on the deformation and interlaminar failure of the composite adherends.

The stiffness of the adhesive used for bonding composites is also known to be one of the key parameters which increases the likelihood of delamination failure [20–22]. It has been experimentally [23,24] and numerically [25,26] shown that the use of mixed adhesive joints (combining two adhesives in a single joint) reduces the local peel stresses that lead to delamination. Many other practical techniques have been proposed to prevent delamination and improve the strength of composite joints, such as the use of Z-pins [27,28], 3D weaving [29], stitching [30], braiding [31], and the use of additional thermoplastic interplies [32]. It should be noted that the Z-pinning method is known to be most effective, when compared to other methods, but it requires a complex manufacturing process, which increases the cost of the final product. The use of composite metal laminates [33,34] or hybrid composites [35] are other methods to improve strength of composite materials, which can increase transverse strength on the critical surface region [33] and/or result in a reduction of the shear stresses acting on the adhesive [35]. Recently, the use of hybrid bonded/riveted joints has also been found to be effective, since these joints are known to improve static strength and fatigue performance, and present higher energy absorption [9].

Multiple review papers have been published on the subject of adhesive bonding of composite substrates [8,36–39], describing a wide range of methods suitable for improving joint performance under different loading conditions. The current study further contributes to the literature by providing a detailed analysis of the recent developments on adherend modification of adhesive bonded composite joints. The effects of stacking sequence, the use of thin-ply and composite metal laminates, specific surface preparations and the use of toughened surface layers on the mechanical performance (under different loading conditions) of adhesively bonded joints have been summarized and analysed in detail.

2. Joint Configuration and Geometry

2.1. Joint Geometry

The mechanical performance of a bonded joint is known to be highly dependent on joint geometry, which includes factors such as overlap length, adherend and adhesive thickness, etc. Among the most significant of these parameters are the overlap length (l), adherend thickness (T), adhesive thickness (t) and the adherend and adhesive elastic modulus and shear strength [40]. Figure 2 presents a schematic design of a single lap joint, illustrating the aforementioned parameters.

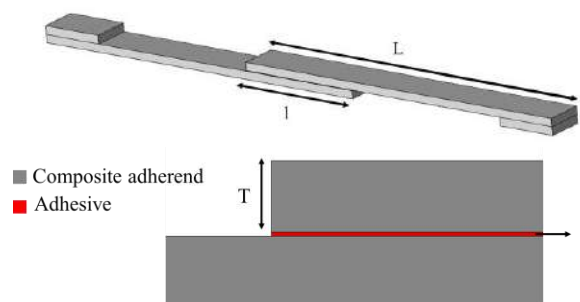


Figure 2. Schematic design of a single lap joint.

Multiple research studies have been carried out to understand the effect of the overlap length in composite joints. It can be generally stated that, if the adherend does not fail or yield, an increase in the overlap length will lead to an increase in the failure load of the joint. This is known to occur even under different loading conditions e.g., under quasi-static and impact loads (see Figure 3) [41–43].

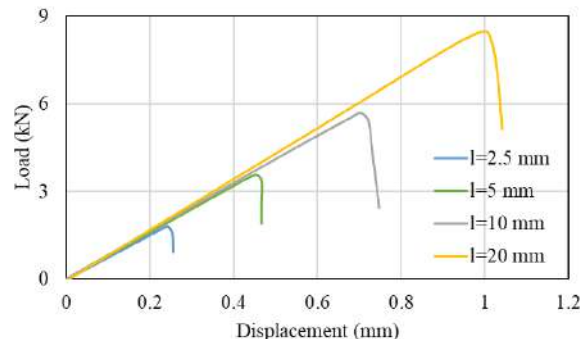


Figure 3. Load-displacement for different overlap length under tensile loading conditions. Adapted from [44].

This increase in the failure load could be explained by the substantial effect that the overlap length has on the peel stress, a fact shown numerically by Demiral and Kadioglu [45,46]. At the same time, the failure load is also highly affected by the applied strain rate in composite joints, a result of the strain rate sensitivity exhibited by the adhesive and the polymeric resin of composites [41,44].

However, if stiff and brittle adhesives are used, an increase in the overlap length will result in a more modest (or even a negligible) increase of the failure load, which is in contrast to that found for joints bonded with a ductile adhesive, where the increase in failure load is found to be almost directly proportional to the increase in overlap length. This can be explained by the fact that severe stress concentrations are generated at the overlap ends by the stiff and brittle adhesive, leading to premature failure. These stress concentrations are present even for very large overlap length values, reducing the effectiveness of increasing this dimensional parameter.

Li et al. [47] presented a thorough experimental study on the effect of adherend thickness for single lap, double lap and scarf composite joints, where a higher failure load

was observed for all the mentioned configurations in larger adherend thicknesses (higher strength for single and double lap joints, but lower strength for scarf joints). In the case of scarf joints, the authors [47] showed that by increasing the scarf angle a higher lap shear strength was obtained.

2.2. Effect of Surface Preparation

To ensure maximum joint strength, the bonding surfaces must be thoroughly prepared before the adhesive application, which is often a costly and time-consuming process, but essential to avoid adhesive failure. Furthermore, bond strength and durability are known to be extremely sensitive to environmental parameters such as the temperature and humidity, both of which can have a deleterious effect on the adhesive/adherend interface and degrade the level of adhesion.

A proper surface treatment for composite adherends should always seek the removal of all contaminants from the surfaces and ensure a good level of adhesion, which can be achieved through an increase of wettability (increasing surface energy and the chemical activation of material surfaces being bonded) or by increasing the roughness of the surface (and increasing the level of mechanical interlocking between the adhesive and the adherend) [48–50]. Many different chemical and physical surface treatments are currently available for composites. These employ different methodologies, such as mechanical abrasion [51], degreasing the surface with solvent [52,53], laser ablation [54,55], plasma treatment [56,57], peel ply technique [57–61], irradiation [62], grit blasting [63,64] and chemical surface activation [65]. It is important to take into account the fact that the bulk mechanical properties of a composite can be strongly affected by surface treatments. For example, severe abrasive treatments can damage the composite and adversely affect joint behaviour [66,67] and bond strength [68,69]. This is because the fibres closer to the surface can be damaged by abrasion, reducing composite strength and the adhesion of the fibres to the matrix, and may even introduce contamination through loose microparticles (see Figure 4) [70]. Nonetheless, microparticles can be removed with the use of suitable high-power ultrasonic cleaning methods, and, hence, the use of primer coating together with high-power ultrasonic cleaning leads to a significant increase in strength [71].

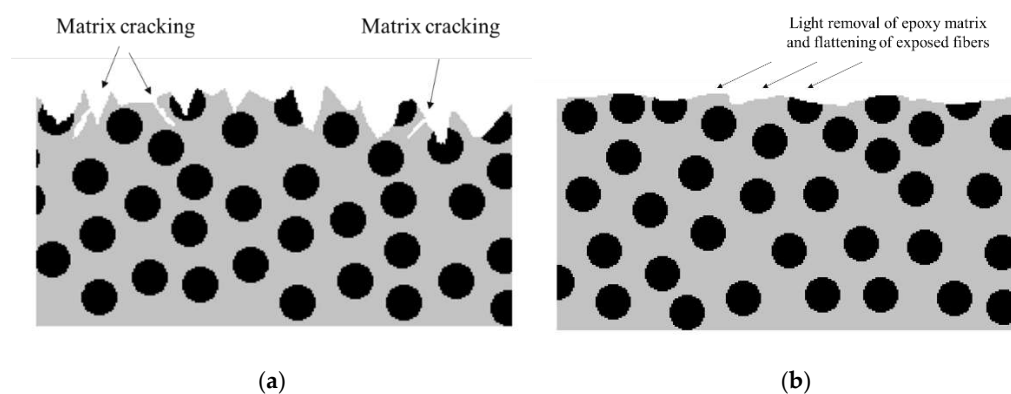


Figure 4. Schematic design of composite after (a) grit blasting and (b) sanding. Adapted from [72].

Laser surface treatment is an eco-friendly and non-contact procedure which dispenses with harmful chemical solutions and does not introduce secondary contaminations. This method can be used to provide greater roughness and wettability, leading to higher shear strength and a cohesive failure mode when compared with conventional mechanical abrasion [51,73]. It has also been shown that aging does not significantly degrade the quality of the laser-treated interface [54]. The use of this approach is well suited for the preparation of composite adherends [74], although there is still some possibility of local fibre damage with high accumulated laser fluence [75].

The use of peel ply is a commonly used technique to protect the surface of composite laminates from contamination, while also creating and maintaining a specific surface

texture [59]. A peel ply layer is used to absorb any residual resin and to create an activated surface for adhesive bonding or coating by peel ply removal. This method is also able to provide a good surface treatment for bonding purposes.

Different methods are available to assess the pre-bond quality of CFRP surfaces. One of these is the optically stimulated electron emission (OSEE) [76], able to detect weak adhesive bonds of CFRP [77], which might have been caused by contamination or poor curing of the adhesive. Other methods can be used to detect defects in the laminate itself, such as the use of electromechanical impedance [78], acoustic emission [79] or ultrasonic emission [80], or the electrical resistance method [13,81–83]. However, interfacial defects in the form of kissing bonds may still go undetected. Attempts using advanced ultrasonic methods such as nonlinear ultrasounds, guided waves or digital image correlation (DIC) [84] inspection to detect kissing bonds have met with limited success. However, some authors report that DIC can be effective when applied in the case of partial or localized kissing bonds [84].

2.3. Effect of Manufacturing Process

The manufacturing process of composite joints can follow three different approaches, the selection of which can be dependent on the nature of the composite and adhesive, and their curing temperatures. These processes are known as co-curing, co-bonding and the secondary bonding method [38]. A co-bonding process is performed when one adherend is cured simultaneously with the adhesive, while in the co-curing process both adherends and the adhesive are simultaneously cured. Secondary bonding is when the adhesive layer is cured between two pre-cured composite substrates [38,73,85]. Figure 5 shows a schematic design of the mentioned manufacturing methods.

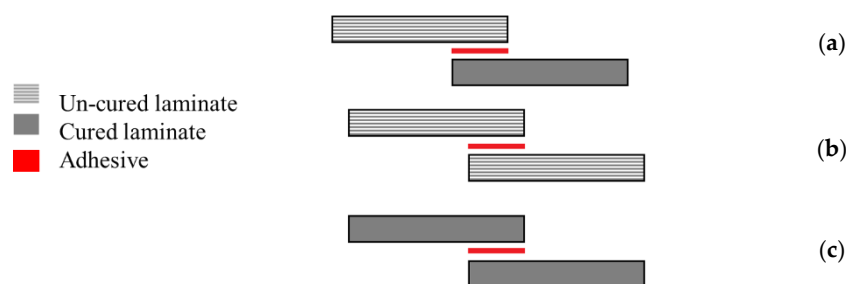


Figure 5. (a) Co-bonding, (b) co-curing, and (c) secondary bonding. Adapted from [38].

Each of these manufacturing methods is known to have its own specific advantages and disadvantages [86]. For secondary bonded joints, failure is known to occur in the composite [87] and edge effects are not so predominant [22]. On the other hand, in co-bonded joints, failure typically occurs in the adhesive, since greater resistance to crack initiation and propagation has been observed [87] and significant edge effects have been observed [22]. However, the co-bonded joints have been shown to have a lower strength than the secondary bonded joints under a wide range of loading conditions [88–91]. In some cases, the moisture present in the prepreg was found to have been released during curing and had migrated to the adhesive layer, which led to a weakening of the interface and lower strength of the co-cured joints [90,92].

Notwithstanding, co-curing or co-bonding methods are usually preferred over the secondary bonding methods, because the number of parts and curing cycles needed are reduced. Hence, secondary bonding is mostly used for the repair of composite structures while for large and complex structures the secondary bonding process is more suitable [38,93].

2.4. Alternative Joint Configurations

As stated above, undesired peel stresses are a main cause of delamination failure in composite adherends [94]. Accordingly, a proper joint design process should seek, as an objective, to reduce the peeling stress concentration in the overlap. Many different

geometrical modifications have been proposed to reduce delamination, whether through reductions of the joint overlap length [20,95], increasing the bonded area width [10] or increasing adherend thickness [2]. As an alternative, the adherend geometry can also be changed by adding tapered sections, reducing adherend thickness [23,96], using internal tapers of adhesive [97], adding a spew fillet [98,99], using adhesively bonded joint with non-flat interfaces [100] or using wavy-lap [101] (see Figure 6a). The flat joggle flat joint (FJF) [102] (seen in Figure 6b) is a relatively complex joint design which is known to reach very high failure loads due to the compressive stress field developed [101] and its ability to overcome the bending effect [102]. However, all of these modifications require cost and time-consuming machining and manufacturing steps [98].

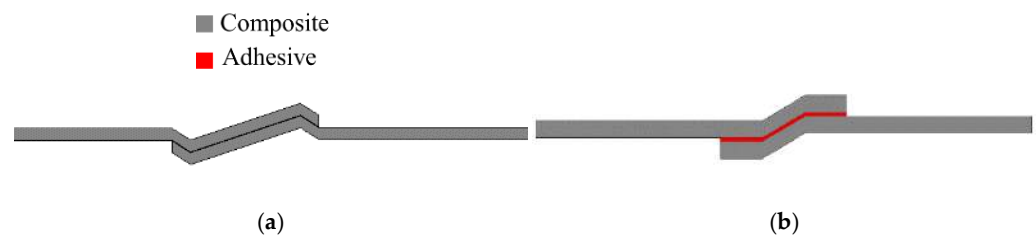


Figure 6. (a) Wavy-lap joint and (b) flat joggle flat joint (FJF).

A study from Teixeira and Sinke [103] showed that peel tests could be performed in bonded composite-to-metal and composite-to-composite joints using a floated rolling peel test (see Figure 7) [103,104], and concluded that using CFRP as the flexible adherend has a considerable effect on the peel load since the peel load gives a direct indication of the failure mode [103].

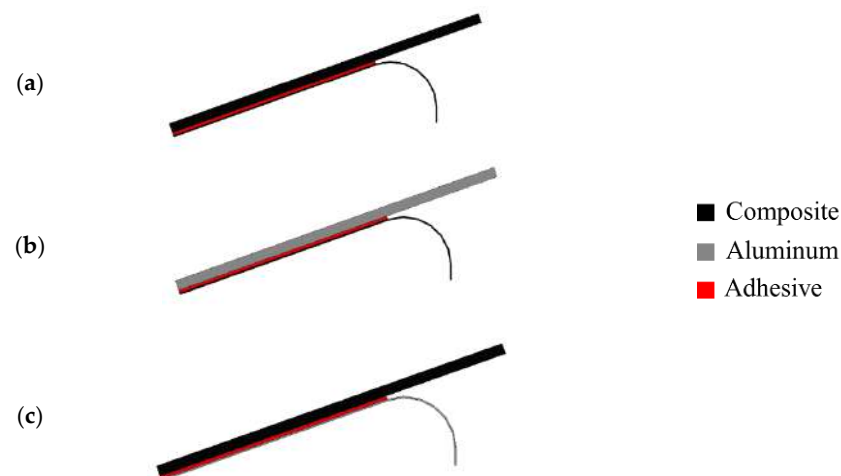


Figure 7. Peel tests for bonded (a) composite-to-composite and (b,c) composite-to-metal. Adapted from [103,104].

In conclusion, the use of modifications in joint configuration has been shown to be a powerful method for overcoming the bending effect typical of unbalanced joints, and it can also be used to develop a compressing stress field in the overlap length. Moreover, the literature demonstrates that delamination can be eliminated or delayed, and joint strength can be improved in a composite joint, by modifying the shape and configuration of the adherend or the adhesive layer. This issue is discussed in further detail in Sections 3 and 4.

3. Adhesive Layer Modifications

3.1. Mixed and Functionally Graded Adhesive Layer

In adhesive joints, failure is usually the result of a non-uniform distribution of stresses in the bond-line [105]. A non-uniform stress distribution is even more obvious in joints with dissimilar adherends and those operating in an extreme temperature range [106]. In

composite joints, whether with similar or dissimilar adherends, the stiffness of the adhesive used for bonding composites is known to be one of the key parameters controlling the onset of delamination, with several authors demonstrating that low strength yet flexible adhesives are able to outperform stronger but stiffer adhesives [20].

Mixed adhesive joints, in which two different adhesives (one ductile and one brittle adhesive) are used along the bond-line, are known to be a valid method for avoiding the formation of non-uniform stress distribution in a bond-line. In this approach, the brittle adhesive is utilized in the middle part of the bond-line and the ductile adhesive is used at overlap ends, where higher stress concentrations occur (see Figure 8) [107,108]. The dual adhesive concept is also a viable alternative for cases where there is a large difference in the properties of two dissimilar adherends and where the joint must operate under demanding environmental conditions [109].

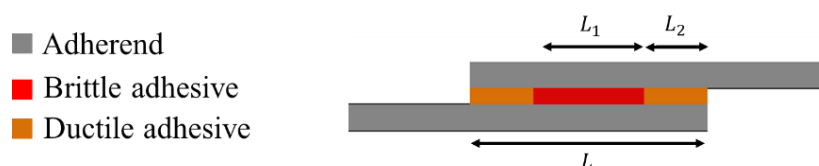


Figure 8. Mixed adhesive joint.

Generally speaking, studies on structural adhesive joints for bonding aluminium with composite materials have led to the conclusion that the most suitable adhesives for use in these configurations are toughened epoxies (where stiffness is indispensable) and polyurethanes (for dynamic mechanical requirements that call for flexibility) [110]. Logically, these materials are also suitable for combination in a mixed adhesive joint with composite substrates. Nonetheless, it is worth mentioning that the performance of a mixed adhesive joint under different loading and testing conditions (quasi-static and impact) is highly dependent on the material properties of the adhesives used [24]. Adhesive selection is crucial for maximizing not only the performance of the bond-line but also that of the adherends. The work of Machado et al. [111] demonstrated this by studying the use of four different adhesives in a mixed-adhesive single lap joint configuration (AV 138 and XNR 6852 were used as stiff adhesives and DP 8005 and RTV 106 as flexible adhesives). According to the results, presented in Figure 9, for both quasi-static and impact loading conditions, the use of a mixed adhesive joint instead of single adhesive layers does not always guarantee an improvement of the shear strength, and this is especially evident when the performance (under different loading conditions) of mixed joints is compared with the use of a brittle and ductile single adhesive joint.

Jairaja and Naik [109] studied two configurations for dual adhesive joints, including 20% and 40% overlap length for the brittle adhesive (L_1/L). They used two different adhesives, AV 138 (as the brittle adhesive) and Araldite 2015 (as the ductile adhesive), in a single lap joint with dissimilar adherends. As shown in Figure 10, experimental results have demonstrated that a length ratio of 0.2 presents the highest failure load over both brittle and ductile reference single lap joints. Furthermore, the configuration with the length ratio of 0.4 presents a lower failure load as compared to the single lap joint with ductile adhesive. A parallel numerical analysis was performed, in which it was observed that the use of dual adhesive layers presented lower stress concentration at the overlap edges (see Figure 11). The mixed adhesive bond-line with 20% of brittle adhesive presented a higher bond strength than single adhesive joints using brittle and ductile adhesives. The mixed adhesive bond-line with 40% of brittle adhesive presented lower strength when compared to the ductile adhesive.

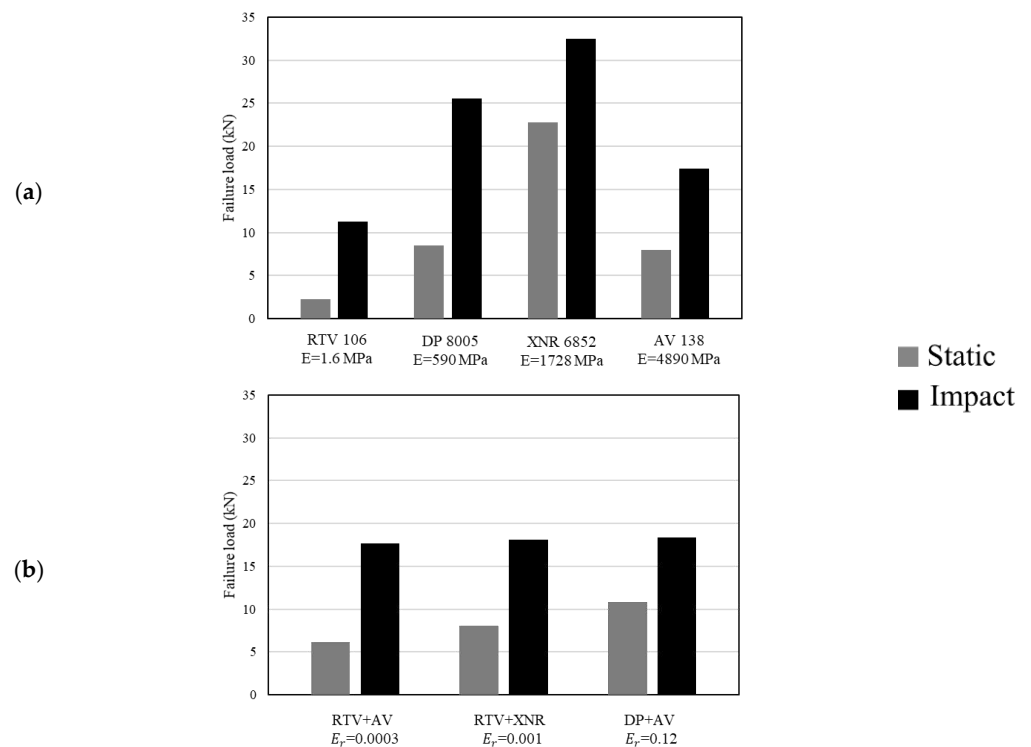


Figure 9. Failure load for single and mixed adhesive joint for (a) single adhesive (E represents the adhesive's Young's modulus) and (b) mixed adhesive joint (E_r represents the ratio of flexible adhesive's Young's modulus to stiff adhesive's Young's modulus). Adapted from [111].

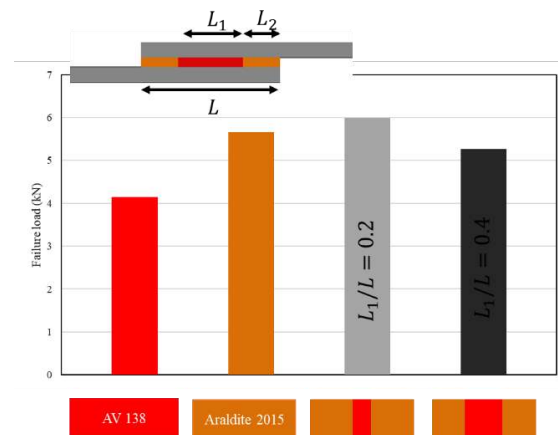


Figure 10. Effect of length ratio on failure load in mixed adhesive joint. Adapted from [109].

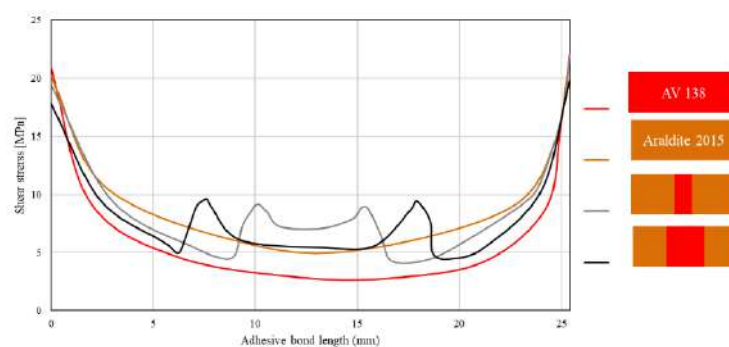


Figure 11. Effect of length ratio on shear stress distribution in mixed adhesive joint. Adapted from [109].

Functionally graded adhesive layers can be seen as a natural evolution of mixed adhesive layers in which the material property of the adhesive changes gradually rather than discretely (see Figure 12). These are considered as highly effective, but hard to implement alternatives to reduce the peel stress concentrations located at bond-line ends [112,113]. Dadian and Rahnema [105] performed an experimental and numerical study on functionally graded joints with dissimilar adherends, where 7075-T6 aluminium and a CFRP adherends were used. This research used a neat adhesive and four other epoxies containing different amounts of additives, namely 5, 10, 15 and 20 phr (parts per hundred rubber), which led to adhesive formulations with increasingly higher ductility.

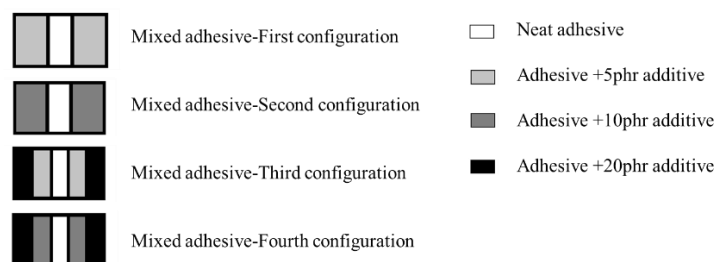


Figure 12. Schematic design of mixed adhesive joint studied by Dadian and Rahnema [105].

Ductile adhesives were used at the edges of the overlap and the number of bands in the overlap was increased by adding adhesives with intermediate properties between two adjacent adhesives. As a result, the stress concentrations at both edges decreased and the inner zones of the adhesive layer were now able to provide a larger contribution to the overall load-bearing capacity of the joint. As seen in Figure 13, shear strength was increased significantly in a mixed adhesive configuration, especially when compared to the related brittle and ductile adhesive [105]. It should be mentioned the failure load increases as the number of bands in the overlap increases.

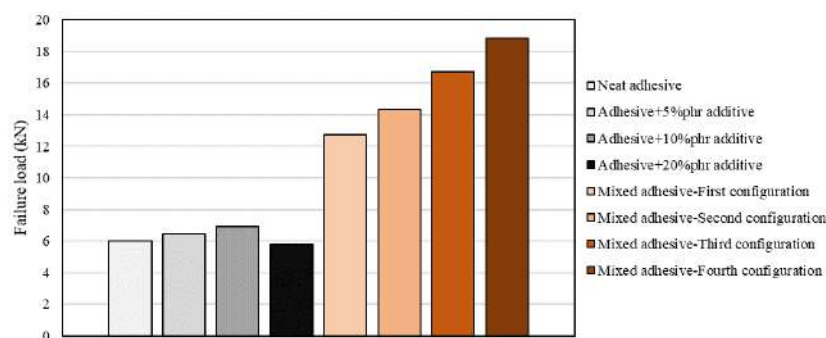


Figure 13. Effect of mixed and functionally graded adhesive layer. Adapted from [105].

Considering the works analysed in this section, one can state that the use of mixed adhesive bonded joints has already a good track record in achieving strength improvement of composite joints. However, this technique hinges on fine balances, as the material properties of the adhesives (brittle and ductile) and their relative dimensions require careful optimization in order to achieve the best results. Moreover, the use of functionally graded adhesive joints is even more advantageous when compared to a mixed adhesive bonded joint, but it is beset with significant manufacturability issues.

3.2. Nano-Reinforced Adhesive Layers

Adhesive layers modified with the use of nanoparticles have been a recent topic of interest [114], being based on research that has shown nanocomposites to exhibit much better mechanical, thermal, and barrier properties than do polymer-based composites [115]. The failure load of a nano-reinforced joint is significantly affected by multiple parameters, such as whether the adhesive is rigid, flexible, or toughened and the ratio and type of

the added nanostructure [116]. Further studies have shown that the addition of a small amount of nanoparticles to the adhesive, at as low a ratio as 1–1.5%, often results in a drastic improvement in its properties [12,116–118], with direct effects on the mechanical strength of structural joints [119] both in the shear and tensile loading modes [117,120–123]. This behaviour is the result of a more efficient stress transfer between nanoparticles and polymer matrix, which improves the cohesive properties of the bond. However, some works report a decrease in the peel strength of the bonded joints [117], attributed to an increase in the glass transition temperature (T_g) and the increased brittleness of the adhesives with higher nanofiller content. The addition of nanoparticles improves the interfacial wettability of the substrates (composite or metal) [117,124], and it is known to be the reason behind drastic shifts in the failure mode [125], which changes from interfacial failure, with no significant damage on the composite adherends, to cohesive failure in the adhesives, where the load is more effectively transferred to the adherends [12]. It has also been reported that, due to their small dimensions, nanofillers can penetrate into small voids on the adherend's surface, allowing for the joint strength to be enhanced via improved mechanical interlocking [126]. Furthermore, fracture surfaces also seem to be strongly affected by the addition of nanoparticles, often transitioning from a relatively smooth surface to a rougher and grooved morphology [117,124]. In practice, this suggests that more energy is needed to break the material if an optimal amount of nanoparticles is used [124]. The definition of this optimal value is where the main challenge of using these reinforcements lies, since the addition of particles above a given value will eventually result in a composite joint with reduced static performance (see Figure 14) [12,116,117]. This limit can be attributed to the eventual formation of poorly connected material agglomerations in specimens with higher amount of the filler content [12,117] or incompatibilities between the particles and the adherend surfaces and adhesives [12].

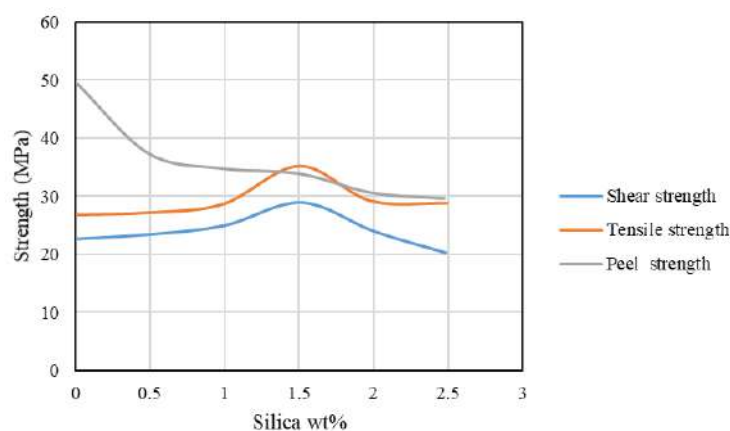


Figure 14. Effect of filler content on joint strength. Adapted from [117].

Carbon nanotubes (CNTs) are being widely used as reinforcement nanofillers in polymer nanocomposites and are categorized as single-, double-, or multi-walled, based on the number of concentric graphene sheets rolled together to make up the nanotube. Multi-wall carbon nanotubes (MWCNTs) are often employed as reinforcing nanofillers in composite materials, which results in materials with high strength and stiffness [11,127]. MWCNTs can also be used to reinforce adhesives [18,116] and have been shown to be an effective alternative for improving mechanical (e.g., toughness, strength stiffness, and fracture energy), electrical, and thermal properties for multiple applications [127–131]. Improvements in adhesion can also be expected, as reductions in the contact angle have been reported as a result of the inclusion of a low content of MWCNTs in epoxy [129]. Additionally, the presence of MWCNTs in adhesives results in the enhancement of the resistance to crack formation and propagation [11]. These materials can also potentiate crack bridging, and act as a barrier in the crack propagation path [127]. This happens because crack initiation and propagation times are generally larger when carbon nanotubes

are dispersed in adhesives [132]. In a similar manner, the use of these materials has also been shown to result in increased fatigue performance [132,133].

A nanotube reinforcement process can have many different characteristics, such as dispersion, structure, and nanotube length and diameter. Research has found that all these characteristics play an important role in the static performance of the reinforced joint [120]. Although this is still an incipient field of research, experimental results obtained so far show that the addition of shorter and thin nanotubes generally results in weaker bonding in the composite–composite joint tests [3]. Some authors further postulate that the optimum nanotube reinforcement should be around 1% [3,120], and that an extra addition of nanotubes leads to a general decrease in the lap shear strength [81]. It has also been shown that the use of CNT opens the door for advanced interfacial damage detection. A highly conductive CNT network will show noticeable changes in electric resistance as the crack grows [133,134].

4. Substrate Modifications

Due to the significant growth in the use of composites, such as CFRP, and the limited number of processes available for joining these materials, adhesive bonding is an integral part of composite design. In light of this, research has been carried out on the modification and adjustment of composite properties, seeking to optimize the joint performance in a holistic manner. Different methods have been found to have positive influence on strength, e.g., by increasing the rigidity of the adherends [42]. This could be achieved by modifying both of the adherends, or at least one, to minimize the rotation of the joint and promote a more uniform distribution of stresses in the adhesive. As shown in Figure 15, by replacing one of the composite adherends with a metallic material (in this case the joints under analysis combined steel/composite (S/C) and aluminium/composite (Al/C), higher strength could be attained than joints with symmetrical composite/composite (C/C) adherends.

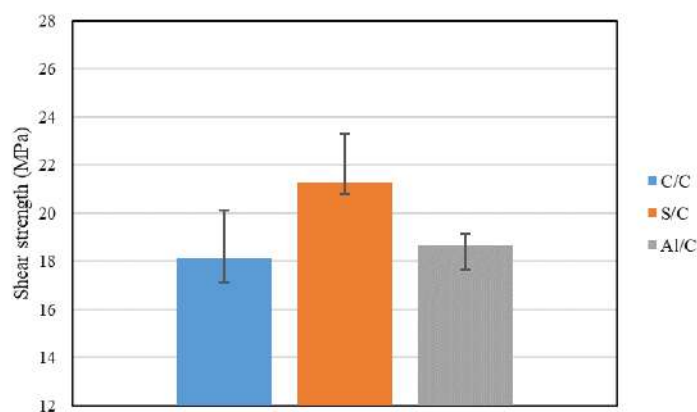


Figure 15. Effect of dissimilar adherend on single lap joint shear strength. Adapted from [42].

Another approach consists of locally recessing the adherends [135] (see Figure 16b), which creates a peak of the peel stress in the adhesive at the point where the recess was made, but one that is lower than the peak peel stress at the edge of the overlap, and, thus allows for a more uniform use of the available overlap length [136]. In this case, the depth of the recess seems to be the most effective parameter and not the length [136]. The effect of chamfering was numerically studied by Moya Sanz [136], including the effect of the chamfer angle upon the adherend, the adhesive or both. Schematic designs of this configuration are shown in Figure 16c–e), respectively. The best-performing configuration had both adherends and the adhesive chamfered at an angle of 15%.

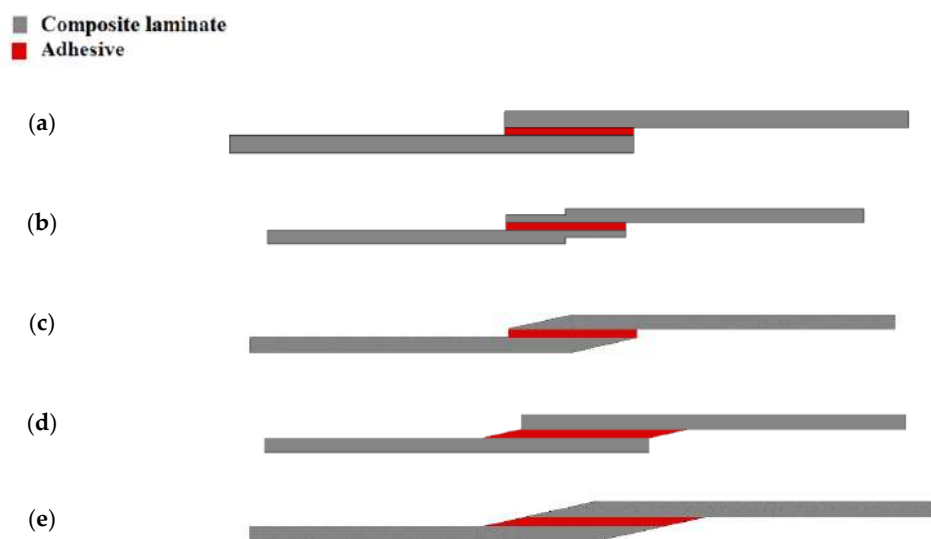


Figure 16. Schematic design for (a) single lap joint, (b) adherend recessing, (c) adherend chamfering, (d) adhesive chamfering and (e) adherend and adhesive chamfering. Adapted from [136].

4.1. Effect of Stacking Sequence

Although there are many different techniques that allow for increased performance (under different loading conditions) of bonded joints, in composite joints, stacking sequence of the adherends is a uniquely effective parameter and, thus, has been the target of extensive study. It is worth noting that the effect of the stacking sequence is highly dependent on the joint configuration and on the material properties and that the optimized stacking sequence can be varied by changing these parameters. Ostapiuk and Bienia [137] used composite material, particularly CFRP or GFRP (glass fibre reinforced plastic), to connect aluminium adherends and consequently studied two different stacking sequences, $[0]$ and $[\pm 45]$ for the composite part of a composite metal laminate single lap joint under quasi-static loading. Their results showed that regardless of the composite type and the surface preparation, the $[\pm 45]$ presented the highest failure load. This may be due to the more complex crack path expected for an initiated crack in the angle-plyed composite. Ozel et al. [43] studied four different stacking sequences in composite single lap joints ($[0]$, $[0/90]$, $[45/-45]$ and $[0/45/-45/90]$) in which both adherends (see Figure 17) were composites. As shown in Figure 18, the $[0]_{16}$ stacking sequence was found to present a higher failure load than the angle-plyed configurations, except for the $[0/45/-45/90]$ layup. A related numerical study determined this to be due to the low peel stresses acting on the overlap edges in the adherends with quasi-isotropic stacking sequence. The same consideration is also applicable here, explaining why, in a quasi-isotropic stacking sequence, the expected crack path for an initiated crack in the addends is more complex. Demiral and Kadioglu [45] have shown that, with the increase of fibre orientation angle, the failure mode changes from interfacial failure towards delamination in the composite adherend.

Akpınar [138] studied the effect of five different orientations ($[0]_{16}$, $[88]_{16}$, $[0/90]_8$, $[45/-45]_8$, $[0/45/-45/90]_4$) in the static performance of composite double strapped joints under tensile loading (see Figure 19), and concluded that joints with composite patches of $[0/45/-45/90]_4$ presented the highest failure load of all configurations under study. Furthermore, angle ply laminates generally presented higher failure load than all unidirectional layups, except for $[88]_{16}$. The same was observed for double lap joints tested under impact loads [139]. The lowest shear strength was recorded for the joints having substrates with fibres oriented perpendicularly to the impact loading direction.



Figure 17. Single lap joint studied by Ozel et al. [43].

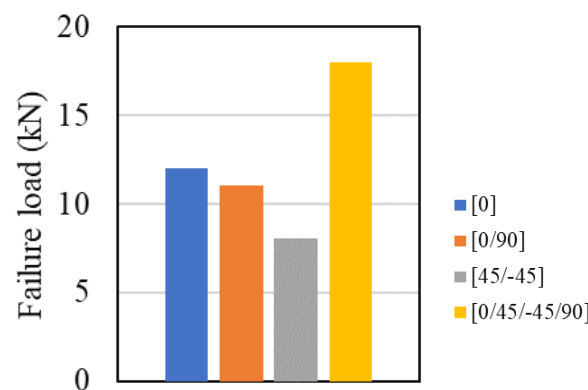


Figure 18. Effect of stacking sequence on failure load composite single lap joint. Adapted from [43].

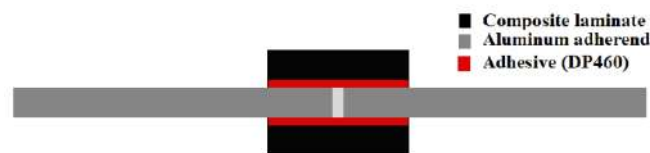


Figure 19. Double strapped composite joint as studied by Akpınar [138].

The maximum shear stress was higher when dissimilar adherends were used (with different stacking sequences), which is due to the loss of homogeneity caused by the imbalance between the two adherends, combined with the edge effects of their discontinuities [139]. Purimpat et al. [140] showed that the strength of the specimens is dependent on both the local orientations and the global properties of the laminates. A vast study was performed on quasi-isotropic quasi-homogeneous (QIQH) sequences and it was concluded that, since it is more probable for the final failure to occur in the 0° layer (seat of the final break), it can be assumed that its distance from the adhesive layer increases the complexity of the crack path and thus raises the joint strength [140]. This can be seen schematically in Figure 20.

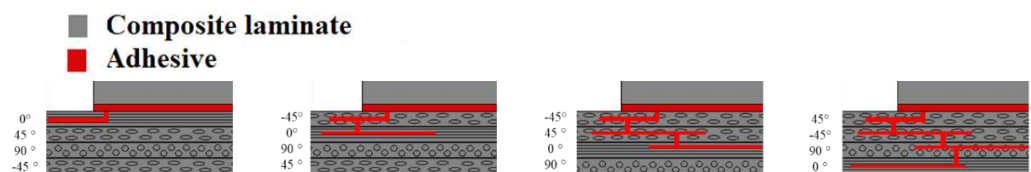


Figure 20. Effect of 0° layer distance from surface in quasi isotropic laminate. Adapted from [140].

In general, the optimum stacking sequence is highly dependent on the joint configuration. However, stacking sequences with unidirectional fibres perpendicular to the loading direction and quasi-isotropic stacking sequence tend to perform better for many common joint configurations, such as the single lap joint.

4.2. Thin-Ply Laminates

The use of thin-ply laminates is a relatively recent approach for substrate modification. Thin-ply laminates are defined as those composed by plies with a thickness of less than $100\ \mu\text{m}$ [141,142]. These layer thicknesses became available through recent developments of the spread-tow process [143], one which produces flat, straight plies until a dry ply thickness as low as $20\ \mu\text{m}$ is reached [144]. Failure strength and ultimate strength of laminates can be greatly improved with a significant decrease of the fibre areal weight [145]. The non-monotonic strength change of thin-ply laminates is ultimately brought on by two competing mechanisms. The decrease of ply thickness increases the specific strength while the decrease of fibre volume fraction leads to some reduction in strength [20].

The use of thin-ply laminates brings a higher degree of freedom to layup design (both in orientation and the quantity of the individual layers) [146]. Furthermore, due to the reduced layer thicknesses and the improved resin spreading process, more homogeneous fibre distribution and smaller resin-rich regions can be achieved [145]. The higher number of layers and the associated higher number of interfaces also causes the shear stresses to be lower [146], and thinner plies are acknowledged to have higher resistance against matrix cracking [147,148]. Currently, the use of thin-ply laminates is mainly driven by the search for enhanced static mechanical performance [141] as well as the ability to suppress transverse microcracking [146] and free edge delamination [147–150]. This last failure mode is a function of ply thickness, as well as the stacking sequence [151]) for quasi-static, fatigue and impact loadings [143] and is typically observed in conventional composite materials [146]. The crack suppression effect may be caused by a decrease in the energy release rate at the crack tip in the thin layer [152]. Additionally, thin-ply plies have other unique advantages, such as higher in-situ transverse strength. The theory of in-situ strength was proposed by Camanho et al. [153], to demonstrate that a decrease in ply thickness can be correlated to an in-situ effect, characterized by a reduction in the applied stress needed to extend a transverse crack, along the thickness of the ply, when the ply thickness increases. Based on Camanho's ply failure criteria, damage onset in the composite is likely to occur at the same load level as in the adhesive in the case of the thick configuration and at 50% higher load level in the case of the thin configuration [154].

Kupski et al. [154] studied three different single lap joint (SLJ) configurations using thin-ply plies, namely: $[45_4/0_4/-45_4/90_4]_S$, $[45_2/0_2/-45_2/90_2]_{2S}$ and $[45/0/-45/90]_{4S}$ by resorting to NTPT-HTS(12K)-5–35% prepreg, which is a thermoplastic-toughened epoxy resin with an unidirectional prepreg system. The thickness of a single ply was 50 μm , and all adherend laminates were manufactured with 32 layers of a single ply adding up to 1.6 mm of total adherend thickness. Experimental results showed that, with decreasing ply thickness, damage initiation was postponed to higher load levels, although it resulted in a more sudden damage progression until the final failure [154]. In the end, an increase in the SLJ shear strength and in the strain energy was obtained [154], and the numerical study indicated that with decreasing ply thickness, the damage onset moves away from the adhesive interface towards the mid-thickness of the adherend [154].

4.3. Composite Metal Laminates

Composites are structurally more efficient than metals, although the latter have better damage tolerance and fail in a more predictable manner. Metals are also generally unaffected by the solvents and temperature levels which readily degrade polymers [38]. Therefore, in order to optimize the benefits provided by both types of materials (in what regards to the strength, weight and durability of structures), a combination of traditional metals with composite materials has been pursued in recent years [38]. These materials are typically known as composite metal laminates (CMLs) and were initially developed for applications in the aerospace industry. These materials consist of metal and composite layers, and different configuration of composite metal laminates can be used as adherend in a single lap joint, as it can be observed in Figure 21. Carbas et al. [155] showed that the strength of hybrid joints can be increased when thin aluminium sheets are placed in the outer layers of the lay-up. The aluminium sheets serve as a local reinforcement, being able to prevent delamination and increased strength over the CFRP-only joints. For overlap lengths of 50 mm, hybrid joints that had aluminium in the middle of the layup exhibited just slightly higher strength values than the reference joints.

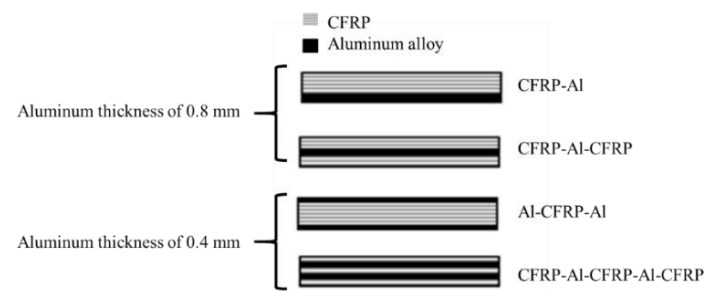


Figure 21. CML configurations studied by Carbas et al. [155].

In a subsequent work, Ramezani et al. [156] replaced layers of prepreg with aluminium plates on the outer surfaces of each adherend (CML) and subsequently studied the effect of the aluminium plate thickness, while maintaining the overall thickness of the adherend constant. The experimental results show that replacing layers of CFRP with metal laminates increases the failure load under quasi-static [156], intermediate [156] and impact testing rates [157]. This can be explained by the minimization of the stress concentrations at the edges of the overlap, as the compliant and tough metal plate is able to redistribute stresses over a much larger area without any failure. In a related work, Santos et al. [158] studied novel single lap joints of CFRP joints with composite metal laminates and additional adhesive layers. As shown in Figure 22, experimental results showed an increase in the novel single lap joints compared to the ones without an additional adhesive layer.

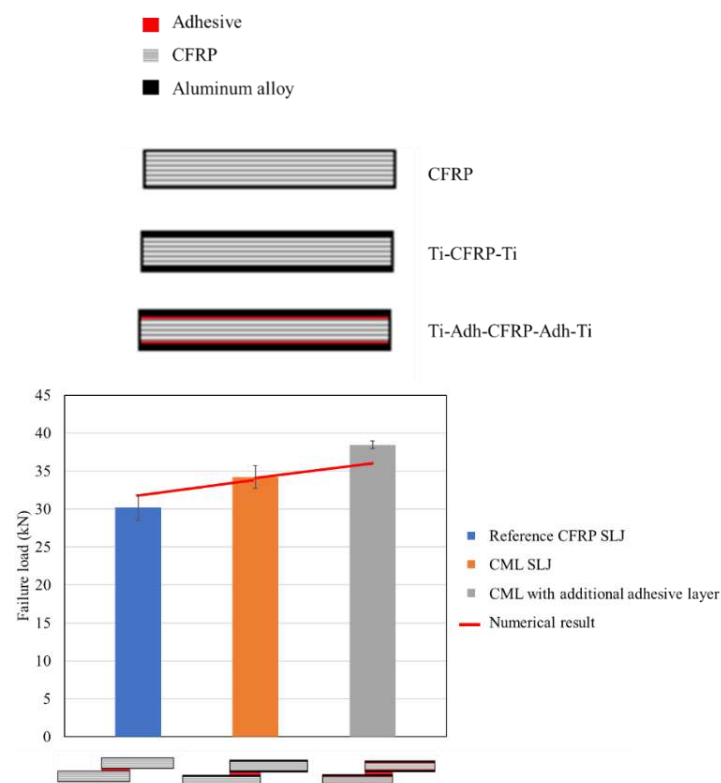


Figure 22. Failure load obtained by Santos et al. [158] for CML and CMLs with additional adhesive layers.

Considering that these materials were initially designed for aerospace applications, one important component of the material selection process was to balance the stresses present on the structures. As seen in Figure 23, for a CML single lap joint, the maximum peel stress induced in the joint is reversely affected by the Young's modulus of the metal laminate. [158].

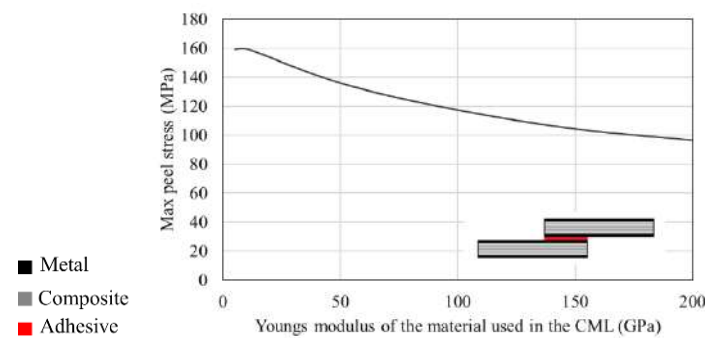


Figure 23. Effect of the Young's modulus of the metal laminate used in CML on maximum peel stress. Adapted from [158].

Morgado et al. [157] showed that the static and impact performance of composite metal laminates is highly dependent on the material property of the adhesive under both quasi-static and impact loads. As seen in Figure 24, the hybrid joint presents higher shear strength while using AF 163-2K adhesive (epoxy-based structural adhesives in film form) in both quasi-static and impact loading, which contrasts with what was observed while using XNR 6852 E-3 adhesive (epoxy-based paste adhesive). The same trend was observed by Carbas et al. [159], where the effect of reinforced hybrid composite single lap joint was also determined to be highly dependent on the adhesive. The authors found that the adhesive with lower stiffness behaved better than stronger and stiffer adhesives in regard to delamination prevention.

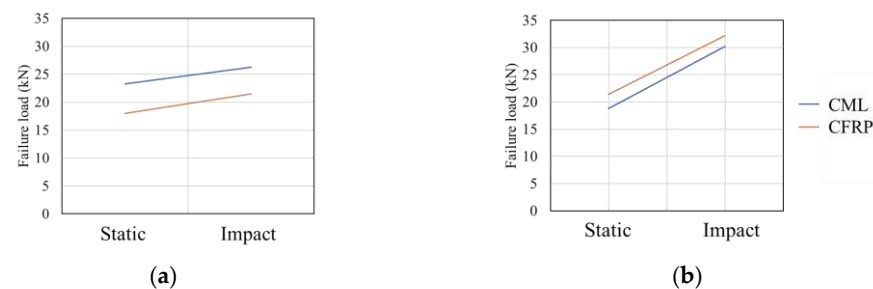


Figure 24. Failure load under quasi-static and impact loading for (a) AF 163-2K and (b) XNR 6852 E-3. Adapted from [157].

In the case of the adhesive with lower stiffness, higher joint strength is found for both quasi-static and fatigue loadings [103,157]. Thus, while adhesives with high tensile strength might appear more attractive for use in the assembly of high performance (static and fatigue) composite structures, this does not always translate into high joint strength [20–22]. In fact, the inherent stiffness of these adhesives often results in higher peel stress at the interface, leading to premature failure by delamination [157].

Overall, CMLs have been experimentally shown to be a good alternative for use with conventional composite laminates, leading to bonded joints which perform well under diverse loading conditions. The material properties of the metal laminate being used significantly impact the stress distribution in the joint and thus directly affect the joint strength. However, selection of the adhesive is ultimately the most critical factor since excessive stiffness might generate high peel stresses which wholly suppress the effect of adding the metal layer.

4.4. Toughened Surface Layers

The use of toughened, non-metallic, surface layers in composite layups represents another alternative for improving the performance of bonded composite joints under different loading conditions. In this method, a high toughness and compliant layer is applied to both outer surfaces of the composite material, one which will serve as an

adherend in a bonded joint. The toughened layer could take the form of a non-reinforced resin or a less stiff fibre reinforced composite material. The use of toughened adherends is known to delay [156] or even completely eliminate [125] delamination failure in joints with composite substrates. Different possible configurations of composites toughened with polymers layers are schematically presented in Figure 25.

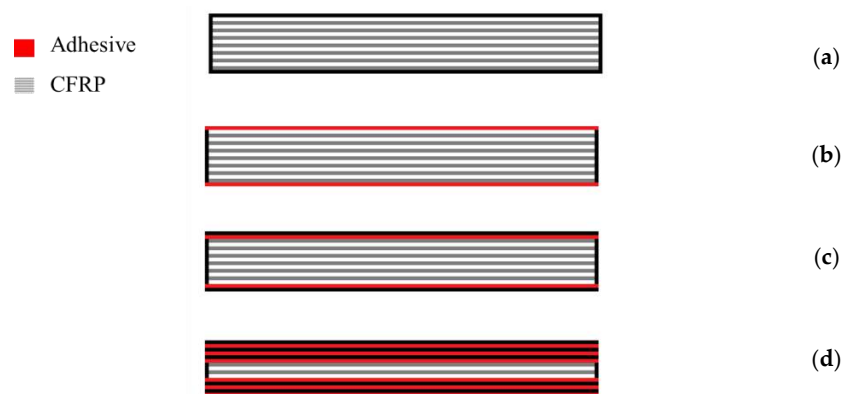


Figure 25. Schematic design of (a) CFRP, (b) a single external adhesive layer, (c) a single interlaminar adhesive layer, and (d) three interlaminar adhesive layers. Adapted from [156,160].

Morgado et al. [160] evaluated the use of a single interlaminar adhesive layer, three interlaminar adhesive layers and a single external adhesive layer, which together is known as adhesive layer reinforcement (ALR). Under quasi-static loads, all the optimized designs under evaluation performed better than the reference CFRP-only joint. The configuration with external adhesive layers exhibited the highest strength increase, raising 23% above the failure load of the reference CFRP-only joint. Most importantly, the failure mode changed from delamination to cohesive failure of the adhesive itself, while the reinforcement layer remained fully intact [156,160].

Experimental studies have demonstrated that the use of toughened adherends results in an enhancement of the shear strength of bonded joints [125] loaded under different testing rates (quasi-static, intermediate rate and impact loading) [156,160]. However, the authors note that an optimum thickness of toughened material is dependent on the specific characteristics of the adherend to avoid drastic decreases of the joint strength [156]. Figure 26 presents the failure load of bonded joints created using a reference CFRP adherend and the toughened hybrid single lap joints obtained by Ramezani et al. [156]. The results clearly show that the use of toughened layers in composite joints leads to an effective increase in joint strength. This increase is the result of two different factors. The first is the increased loadbearing capability provided by yielding of the toughened surface layer before failure occurs [125]. The second factor is associated to the lowered stiffness of the surface toughening material, which is usually much lower than that of the base composite material and thus reduces the presence of stress concentrations at the edges of the overlap length of the bonded joint [156].

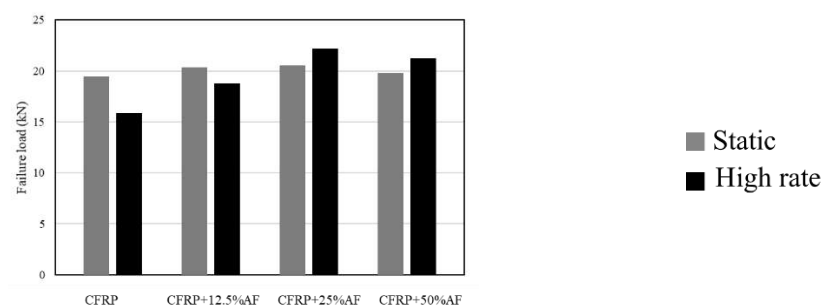


Figure 26. Failure load obtained for composite single lap joints with toughened adherends. Adapted from [156].

Shang et al. [125] studied the use of novel composite material as an adherend, one composed of 0.5 mm thick layers of glass fabric reinforced on both surfaces and a 1 mm thick CFRP core. The novel composite adherend was found out to have 22% higher failure load than that of specimens using CFRP-only adherends. Again, the failure mode was found to change from delamination of the adherends to cohesive failure in the adhesive, which was ultimately the main target of this work.

Schollner et al. [161] studied a novel local adherend surface toughening concept by using a localized thermoplastic layer, as shown in Figure 27. An increase of up to 84% in the failure was observed to be the result of localized surface toughening in joints. The toughened surfaces create less peel and shear stress concentration in the bond-line ends. It should be noted that an optimum length of surface toughening was found to exist, whereupon the use of a reinforcement larger than the optimum surface toughening length results in adherend delamination.



Figure 27. Localised surface toughening concept. Adapted from [161].

In light of these results, while a toughened composite laminate with external adhesive layer (Figure 25b) presents the highest strength among all other comparable configurations, the use of composite adherends with toughened surfaces is now seen as a very promising method to increase joint strength and to delay or eliminate delamination in adhesive joints intended for service under for different loading conditions.

5. Discussion

An analysis and discussion of the results described in the literature allows for a relative comparison of the different revised techniques both in terms of strength improvement and in their failure mechanisms. To this aim, a scheme showing a comparison between the basic characteristics of the different processes is presented in Figure 28. Considering non-modified joints with CFRP adherends as a reference, an ideal reinforcement technique would allow for a substantial increase in failure load, while avoiding delamination (by providing fully cohesive failure in the adhesive layer).

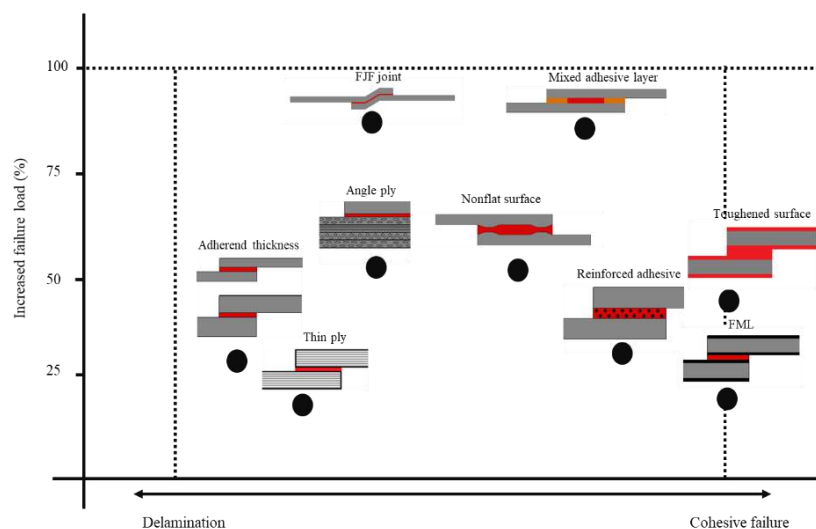


Figure 28. A comparison of different techniques in terms of strength improvement and failure mechanism.

It is known that changes in the joint geometry, specifically the substrate thickness, allow for increases in the failure load above 25%. However, higher improvements are limited by the onset of delamination. A similar phenomenon is also observed when thin-ply is introduced in composite laminates. Even though this technique allows the delay of crack initiation and propagation, delamination failure will almost always eventually occur, precluding the adhesive layer from attaining its maximum potential. However, the use of different fibre orientations-angle plies, does allow the joint to achieve more significant improvements to its performance, both in terms of strength and failure mode. Further improvements can be attained only with more complex joint configurations, such as those using highly shaped adherends and reinforced adhesives. The former possesses geometrical features which are specially designed to overcome the bending effect and to create compression states, all of which serve to reduce the peel stresses that limit the joint's performance. On the other hand, modifications of the adhesive are also possible, such as those which rely on the use of nanoparticles, which improve stress transfer in the adhesive layer. Full cohesive failure has only been demonstrated for the case of two types of adherend modifications: CMLs and the use of toughened surface layers. The metal-composite hybrid approach creates an improved load transfer platform from the adhesive to the metal that although it has to withstand considerable stresses, makes use of the high toughness and compliance of metals to avoid damage. Adherends reinforced with toughened layers, exhibiting a failure mechanism similar to that observed in CMLs, take advantage of the properties of the resin used, creating highly ductile and compliant surface layers that improve stress distributions and avoid delamination in the substrate. From the strength improvement perspective, the two geometries that have been shown to have superior static performance are the FJF joints and joints using mixed adhesive layers. All of the configurations described above, regardless of their failure mode, lead to an increase in strength that varies approximately between 20–60%, but FJF joints can show an increase of almost 100%. FJF joints take advantage of their geometric configuration to guarantee that compression stresses delay joint failure. However, the presence of notches in the composites can also induce localized delamination. In mixed adhesive layers, performance is maximised through a precise control of adhesive stiffness and thus of the peel stress distribution. While these solutions are admittedly technically complex, they have been shown to be able to overcome non-uniform distribution of the adhesive layer, increasing its strength.

Although multiple solutions have been proposed presented and demonstrated to maximize the performance of composite bonded joints, determining an optimal solution for practical applications is still a significant challenge. Nonetheless, a simple conclusion can be extracted from this analysis. Irrespective of the solution chosen, the ideal joint should always be designed to minimise peel stresses at the edge of the overlap, avoiding delamination, but without damaging the substrates through time-consuming and complex geometric alterations, while meeting the practicality demands associated with cost and manufacturability concerns. An efficient load transfer, with a customised distribution of adhesive stiffness, may be the basis of a solution closer to the ideal.

6. Conclusions

The present work reviews recent developments in adhesively bonded composite joints, with particular interest in adherend modification techniques. The effects of stacking sequence, the use of thin-ply, composite metal laminates and its specific surface preparations, and the use of toughened surface layers in the composite adherends were thoroughly analysed in the context of adhesively bonded CFRP joints and structures.

- It has been shown that, optimising the joint geometry, e.g., the substrate thickness, can cause an increase in the failure load, although substrate delamination will still be a concern. Advanced joint configurations were proposed for composite joints, being shown that, among all configurations under analysis, the FJF joints exhibit the highest

static performance, but are still susceptible to delamination due to the modifications that must be made to the composite.

- The adhesive layer can be modified by using a functionally graded or a nano-reinforced adhesive layer. The former overcomes non-uniform distribution of the adhesive layer and allows for the delay of delamination failure. The latter creates efficient stress transfer between nanoparticles and the polymer matrix, which improves the strength of the bond.
- The use of different fibre orientations does allow the joint to improve its performance and strength, forcing the crack to grow through more complex crack paths.
- The use of thin-ply in laminates can cause a delay in crack initiation and propagation due to lowered ply thickness and increased fibre ratios. In addition, the higher degree of design freedom they provide allows for the use of a wider range different fibre orientations and leads to an increase in the static performance of the joint. However, there are very few papers studying the effect of using of thin-ply in composite joints and this technique has now been shown as a viable concept for future research and developments.
- Fully cohesive failure has been obtained for the case of CMLs subjected to different loading conditions. This approach creates a tough and compliant load transfer platform from the adhesive to the metal, which shields the composite core from failure.
- Finally, the use of adherends reinforced with toughened layers follows an approach which is similar to that of CMLs, as it is also able to provide fully cohesive failure. This method allows for the mitigation of the peel stress concentrations in the adhesive layer, virtually eliminating failure by delamination of the substrate.

Funding: The Portuguese Foundation for Science and Technology (FCT) for supporting the work presented here, through individual grants CEECIND/03276/2018 and 2021.07943.BD, and Project No. PTDC/EME-EME/2728/2021 ‘New approaches to improve the joint strength and reduce the delamination of composite adhesive joints’.

Institutional Review Board Statement: Not applicable.

Informed Consent Statement: Not applicable.

Data Availability Statement: Not applicable.

Acknowledgments: The authors gratefully acknowledge the Portuguese Foundation for Science and Technology (FCT) for supporting the work presented here, through individual grants CEECIND/03276/2018 and 2021.07943.BD, and Project No. PTDC/EME-EME/2728/2021 ‘New approaches to improve the joint strength and reduce the delamination of composite adhesive joints’.

Conflicts of Interest: The authors declare no conflict of interest.

References

1. Wang, C.; Huang, Y.D.; Xv, H.Y.; Liu, W.B. The durability of adhesive/carbon–carbon composites joints in salt water. *Int. J. Adhes. Adhes.* **2004**, *24*, 471–477. [[CrossRef](#)]
2. Seong, M.S.; Kim, T.H.; Nguyen, K.H.; Kweon, J.H.; Choi, J.H. A parametric study on the failure of bonded single-lap joints of carbon composite and aluminum. *Compos. Struct.* **2008**, *86*, 135–145. [[CrossRef](#)]
3. Burkholder, G.L.; Kwon, Y.W.; Pollak, R.D. Effect of carbon nanotube reinforcement on fracture strength of composite adhesive joints. *J. Mater. Sci.* **2011**, *46*, 3370–3377. [[CrossRef](#)]
4. Kelly, G. Quasi-static strength and fatigue life of hybrid (bonded/bolted) composite single-lap joints. *Compos. Struct.* **2006**, *72*, 119–129. [[CrossRef](#)]
5. Jongbloed, B.C.; Teuwen, J.J.; Benedictus, R.; Villegas, I.F. A Study on Through-the-Thickness Heating in Continuous Ultrasonic Welding of Thermoplastic Composites. *Materials* **2021**, *14*, 6620. [[CrossRef](#)] [[PubMed](#)]
6. Korycki, A.; Garnier, C.; Bonmatin, M.; Laurent, E.; Chabert, F. Assembling of Carbon Fibre/PEEK Composites: Comparison of Ultrasonic, Induction, and Transmission Laser Welding. *Materials* **2022**, *15*, 6365. [[CrossRef](#)] [[PubMed](#)]
7. Villegas, I.F. Ultrasonic welding of thermoplastic composites. *Front. Mater.* **2019**, *6*, 291. [[CrossRef](#)]
8. Jeevi, G.; Nayak, S.K.; Abdul Kader, M. Review on adhesive joints and their application in hybrid composite structures. *J. Adhes. Sci. Technol.* **2019**, *33*, 1497–1520. [[CrossRef](#)]

9. Marannano, G.; Zuccarello, B. Numerical experimental analysis of hybrid double lap aluminum-CFRP joints. *Compos. Part B Eng.* **2015**, *71*, 28–39. [[CrossRef](#)]
10. Choi, J.I.; Hasheminia, S.M.; Chun, H.J.; Park, J.C. Experimental study on failure mechanism of hybrid composite joints with different adhesives. *Fibers Polym.* **2017**, *18*, 569–574. [[CrossRef](#)]
11. Ariaee, S.; Tutunchi, A.; Kianvash, A.; Entezami, A.A. Modeling and optimization of mechanical behavior of bonded composite–steel single lap joints by response surface methodology. *Int. J. Adhes. Adhes.* **2014**, *54*, 30–39. [[CrossRef](#)]
12. Vietri, U.; Guadagno, L.; Raimondo, M.; Vertuccio, L.; Lafdi, K. Nanofilled epoxy adhesive for structural aeronautic materials. *Compos. Part B Eng.* **2014**, *61*, 73–83. [[CrossRef](#)]
13. Kim, C.H.; Choi, J.H.; Kweon, J.H. Defect detection in adhesive joints using the impedance method. *Compos. Struct.* **2015**, *120*, 183–188. [[CrossRef](#)]
14. Kinloch, A.J. The science of adhesion. *J. Mater. Sci.* **1980**, *15*, 2141–2166. [[CrossRef](#)]
15. Balkova, R.; Holcnerova, S.; Cech, V. Testing of adhesives for bonding of polymer composites. *Int. J. Adhes. Adhes.* **2002**, *22*, 291–295. [[CrossRef](#)]
16. Sancaktar, E.; Kumar, S. Selective use of rubber toughening to optimize lap-joint strength. *J. Adhes. Sci. Technol.* **2000**, *14*, 1265–1296. [[CrossRef](#)]
17. Dean, G.; Crocker, L.; Read, B.; Wright, L. Prediction of deformation and failure of rubber-toughened adhesive joints. *Int. J. Adhes. Adhes.* **2004**, *24*, 295–306. [[CrossRef](#)]
18. Zhang, J.; Luo, R.; Yang, C. A multi-wall carbon nanotube-reinforced high-temperature resistant adhesive for bonding carbon/carbon composites. *Carbon* **2012**, *50*, 4922–4925. [[CrossRef](#)]
19. Adams, R.D.; Peppiatt, N.A. Stress analysis of adhesive-bonded lap joints. *J. Strain Anal.* **1974**, *9*, 185–196. [[CrossRef](#)]
20. Neto, J.A.B.P.; Campilho, R.D.; Da Silva, L.F.M. Parametric study of adhesive joints with composites. *Int. J. Adhes. Adhes.* **2012**, *37*, 96–101. [[CrossRef](#)]
21. Da Silva, L.F.; Rodrigues, T.N.S.S.; Figueiredo, M.A.V.; De Moura, M.F.S.F.; Chousal, J.A.G. Effect of adhesive type and thickness on the lap shear strength. *J. Adhes.* **2006**, *82*, 1091–1115. [[CrossRef](#)]
22. Kang, S.G.; Kim, M.G.; Kim, C.G. Evaluation of cryogenic performance of adhesives using composite–aluminum double-lap joints. *Compos. Struct.* **2007**, *78*, 440–446. [[CrossRef](#)]
23. Da Silva, L.F.; Adams, R.D. Techniques to reduce the peel stresses in adhesive joints with composites. *Int. J. Adhes. Adhes.* **2007**, *27*, 227–235. [[CrossRef](#)]
24. Machado, J.J.M.; Gamarra, R.; Marques, E.A.S.; da Silva, L.F. Improvement in impact strength of composite joints for the automotive industry. *Compos. Part B Eng.* **2018**, *138*, 243–255. [[CrossRef](#)]
25. Ganesh, V.K.; Choo, T.S. Modulus graded composite adherends for single-lap bonded joints. *J. Compos. Mater.* **2002**, *36*, 1757–1767. [[CrossRef](#)]
26. Boss, J.N.; Ganesh, V.K.; Lim, C.T. Modulus grading versus geometrical grading of composite adherends in single-lap bonded joints. *Compos. Struct.* **2003**, *62*, 113–121. [[CrossRef](#)]
27. Potter, K.D.; Guild, F.J.; Harvey, H.J.; Wisnom, M.R.; Adams, R.D. Understanding and control of adhesive crack propagation in bonded joints between carbon fibre composite adherends I. Experimental. *Int. J. Adhes. Adhes.* **2001**, *21*, 435–443. [[CrossRef](#)]
28. Mouritz, A.P. Review of z-pinned composite laminates. *Compos. Part A Appl. Sci. Manuf.* **2007**, *38*, 2383–2397. [[CrossRef](#)]
29. Ko, F.K. Three-dimensional fabrics for composites. In *Textile Structural Composites*; Chou, T.W., Ko, F.K., Eds.; Elsevier: Amsterdam, The Netherlands, 1989; pp. 129–171.
30. Sawyer, J.W. Effect of stitching on the strength of bonded composite single lap joints. *AIAA J.* **1985**, *23*, 1744–1748. [[CrossRef](#)]
31. Chan, W.S. Design approaches for edge delamination resistance in laminated composites. *J. Compos. Technol. Res.* **1991**, *13*, 91–96.
32. Hader-Kregl, L.; Wallner, G.M.; Kralovec, C.; Eyßell, C. Effect of inter-ply on the short beam shear delamination of steel/composite hybrid laminates. *J. Adhes.* **2019**, *95*, 1088–1100. [[CrossRef](#)]
33. Vogelesang, L.B.; Vlot, A. Development of fibre metal laminates for advanced aerospace structures. *J. Mater. Process. Technol.* **2000**, *103*, 1–5. [[CrossRef](#)]
34. Simões, B.D.; Nunes, D.; Ramezani, F.; Carbas, R.J.; Marques, E.A.; da Silva, L.F. Experimental and Numerical Study of Thermal Residual Stresses on Multimaterial Adherends in Single-Lap Joints. *Materials* **2022**, *15*, 8541. [[CrossRef](#)] [[PubMed](#)]
35. Mokhtari, M.; Madani, K.; Belhouari, M.; Touzain, S.; Feaugas, X.; Ratwani, M. Effects of composite adherend properties on stresses in double lap bonded joints. *Mater. Des.* **2013**, *44*, 633–639. [[CrossRef](#)]
36. Pramanik, A.; Basak, A.K.; Dong, Y.; Sarker, K.; Uddin, M.S.; Littlefair, G.; Dixit, A.R.; Chattopadhyaya, S. Joining of carbon fibre reinforced polymer (CFRP) composites and aluminium alloys—A review. *Compos. Part A Appl. Sci. Manuf.* **2017**, *101*, 1–29. [[CrossRef](#)]
37. Dos Reis, M.Q.; Marques, E.A.S.; Carbas, R.J.C.; Da Silva, L.F.M. Functionally graded adherends in adhesive joints: An overview. *J. Adv. Join. Process.* **2020**, *2*, 10003. [[CrossRef](#)]
38. Budhe, S.; Banea, M.D.; De Barros, S.; Da Silva, L.F.M. An updated review of adhesively bonded joints in composite materials. *Int. J. Adhes. Adhes.* **2017**, *72*, 30–42. [[CrossRef](#)]
39. Shang, X.; Marques, E.A.S.; Machado, J.J.M.; Carbas, R.J.C.; Jiang, D.; Da Silva, L.F.M. Review on techniques to improve the strength of adhesive joints with composite adherends. *Compos. Part B Eng.* **2019**, *177*, 107363. [[CrossRef](#)]

40. Matthews, F.L.; Kilty, F.; Godwin, E.W. A review of the strength of joints in fibre-reinforced plastics. Part 2. Adhesively bonded joints. *Composites* **1982**, *13*, 29–37. [\[CrossRef\]](#)
41. Araújo, H.A.M.; Machado, J.J.M.; Marques, E.A.S.; Da Silva, L.F.M. Dynamic behaviour of composite adhesive joints for the automotive industry. *Compos. Struct.* **2017**, *171*, 549–561. [\[CrossRef\]](#)
42. Reis, N.; Ferreira, J.A.M.; Antunes, F. Effect of adherend's rigidity on the shear strength of single lap adhesive joints. *Int. J. Adhes. Adhes.* **2011**, *31*, 193–201. [\[CrossRef\]](#)
43. Ozel, A.; Yazici, B.; Akpınar, S.; Aydin, M.D.; Temiz, Ş. A study on the strength of adhesively bonded joints with different adherends. *Compos. Part B Eng.* **2014**, *62*, 167–174. [\[CrossRef\]](#)
44. Ye, J.; Yan, Y.; Hong, Y.; Guo, F. An integrated constitutive model for tensile failure analysis and overlap design of adhesive-bonded composite joints. *Compos. Struct.* **2019**, *223*, 110986. [\[CrossRef\]](#)
45. Demiral, M.; Kadioglu, F. Failure behaviour of the adhesive layer and angle ply composite adherends in single lap joints: A numerical study. *Int. J. Adhes. Adhes.* **2018**, *87*, 181–190. [\[CrossRef\]](#)
46. da Costa Mattos, H.S.; Monteiro, A.H.; Palazzetti, R. Failure analysis of adhesively bonded joints in composite materials. *Mater. Des.* **2012**, *33*, 242–247. [\[CrossRef\]](#)
47. Li, J.; Yan, Y.; Zhang, T.; Liang, Z. Experimental study of adhesively bonded CFRP joints subjected to tensile loads. *Int. J. Adhes. Adhes.* **2015**, *57*, 95–104. [\[CrossRef\]](#)
48. Kanerva, M.; Saarela, O. The peel ply surface treatment for adhesive bonding of composites: A review. *Int. J. Adhes. Adhes.* **2013**, *43*, 60–69. [\[CrossRef\]](#)
49. Islam, M.S.; Tong, L.; Falzon, J. Influence of metal surface preparation on its surface profile, contact angle, surface energy and adhesion with glass fibre prepreg. *Int. J. Adhes. Adhes.* **2014**, *51*, 32–41. [\[CrossRef\]](#)
50. Encinas, N.; Oakley, B.R.; Belcher, M.A.; Blohowiak, K.Y.; Dillingham, R.G.; Abenojar, J.; Martínez, M.A. Surface modification of aircraft used composites for adhesive bonding. *Int. J. Adhes. Adhes.* **2014**, *50*, 157–163. [\[CrossRef\]](#)
51. Li, S.; Sun, T.; Liu, C.; Yang, W.; Tang, Q. A study of laser surface treatment in bonded repair of composite aircraft structures. *R. Soc. Open Sci.* **2018**, *5*, 171272. [\[CrossRef\]](#) [\[PubMed\]](#)
52. Wingfield, J.R.J. Treatment of composite surfaces for adhesive bonding. *Int. J. Adhes. Adhes.* **1993**, *13*, 151–156. [\[CrossRef\]](#)
53. Baker, A. *Bonded Repair of Aircraft Structures*; Springer Science & Business Media: New York, NY, USA, 1988; Volume 7.
54. Palmieri, F.L.; Belcher, M.A.; Wohl, C.J.; Blohowiak, K.Y.; Connell, J.W. Laser ablation surface preparation for adhesive bonding of carbon fiber reinforced epoxy composites. *Int. J. Adhes. Adhes.* **2016**, *68*, 95–101. [\[CrossRef\]](#)
55. Fischer, F.; Kreling, S.; Gäbler, F.; Delmdahl, R. Using excimer lasers to clean CFRP prior to adhesive bonding. *Reinf. Plast.* **2013**, *57*, 43–46. [\[CrossRef\]](#)
56. Mohan, J.; Ramamoorthy, A.; Ivanković, A.; Dowling, D.; Murphy, N. Effect of an atmospheric pressure plasma treatment on the mode I fracture toughness of a co-cured composite joint. *J. Adhes.* **2014**, *90*, 733–754. [\[CrossRef\]](#)
57. Holtmannspötter, J.; Czarnecki, J.V.; Feucht, F.; Wetzel, M.; Gudladt, H.J.; Hofmann, T.; Meyer, J.C.; Niedernhuber, M. On the fabrication and automation of reliable bonded composite repairs. *J. Adhes.* **2015**, *91*, 39–70. [\[CrossRef\]](#)
58. Arenas, J.M.; Alía, C.; Narbón, J.J.; Ocaña, R.; González, C. Considerations for the industrial application of structural adhesive joints in the aluminium–composite material bonding. *Compos. Part B Eng.* **2013**, *44*, 417–423. [\[CrossRef\]](#)
59. Kanerva, M.; Sarlin, E.; Hoikkanen, M.; Rämö, K.; Saarela, O.; Vuorinen, J. Interface modification of glass fibre–polyester composite–composite joints using peel plies. *Int. J. Adhes. Adhes.* **2015**, *59*, 40–52. [\[CrossRef\]](#)
60. Buchmann, C.; Langer, S.; Filsinger, J.; Drechsler, K. Analysis of the removal of peel ply from CFRP surfaces. *Compos. Part B Eng.* **2016**, *89*, 352–361. [\[CrossRef\]](#)
61. Thull, D.; Zimmer, F.; Hofmann, T.; Holtmannspötter, J.; Koerwien, T.; Hoffmann, M. Investigation of fluorine-based release agents for structural adhesive bonding of carbon fibre reinforced plastics. *Appl. Adhes. Sci.* **2019**, *7*, 2. [\[CrossRef\]](#)
62. Rhee, K.Y.; Yang, J.H. A study on the peel and shear strength of aluminum/CFRP composites surface-treated by plasma and ion assisted reaction method. *Compos. Sci. Technol.* **2003**, *63*, 33–40. [\[CrossRef\]](#)
63. Ramaswamy, K.; O'Higgins, R.M.; Kadiyala, A.K.; McCarthy, M.A.; McCarthy, C.T. Evaluation of grit-blasting as a pre-treatment for carbon-fibre thermoplastic composite to aluminium bonded joints tested at static and dynamic loading rates. *Compos. Part B Eng.* **2020**, *185*, 107765. [\[CrossRef\]](#)
64. Prolongo, S.G.; Gude, M.R.; Del Rosario, G.; Ureña, A. Surface pretreatments for composite joints: Study of surface profile by SEM image analysis. *J. Adhes. Sci. Technol.* **2010**, *24*, 1855–1867. [\[CrossRef\]](#)
65. Schmutzler, H.; Popp, J.; Büchter, E.; Wittich, H.; Schulte, K.; Fiedler, B. Improvement of bonding strength of scarf-bonded carbon fibre/epoxy laminates by Nd: YAG laser surface activation. *Compos. Part A Appl. Sci. Manuf.* **2014**, *67*, 123–130. [\[CrossRef\]](#)
66. De Barros, S.; Kenedi, P.P.; Ferreira, S.M.; Budhe, S.; Bernardino, A.J.; Souza, L.F.G. Influence of mechanical surface treatment on fatigue life of bonded joints. *J. Adhes.* **2017**, *93*, 599–612. [\[CrossRef\]](#)
67. Brack, N.; Rider, A.N. The influence of mechanical and chemical treatments on the environmental resistance of epoxy adhesive bonds to titanium. *Int. J. Adhes. Adhes.* **2014**, *48*, 20–27. [\[CrossRef\]](#)
68. Baker, A.A.; Chester, R.J. Minimum surface treatments for adhesively bonded repairs. *Int. J. Adhes. Adhes.* **1992**, *12*, 73–78. [\[CrossRef\]](#)
69. Schubbe, J.J.; Mall, S. Investigation of a cracked thick aluminum panel repaired with a bonded composite patch. *Eng. Fract. Mech.* **1999**, *63*, 305–323. [\[CrossRef\]](#)

70. Oliveira, V.; Sharma, S.P.; De Moura, M.F.S.F.; Moreira, R.D.F.; Vilar, R. Surface treatment of CFRP composites using femtosecond laser radiation. *Opt. Lasers Eng.* **2017**, *94*, 37–43. [\[CrossRef\]](#)
71. De Freese, J.; Holtmannspötter, J.; Raschendorfer, S.; Hofmann, T. End milling of Carbon Fiber Reinforced Plastics as surface pretreatment for adhesive bonding—Effect of intralaminar damages and particle residues. *J. Adhes.* **2018**, *96*, 1122–1140. [\[CrossRef\]](#)
72. Morano, C.; Tao, R.; Alfano, M.; Lubineau, G. Effect of Mechanical Pretreatments on Damage Mechanisms and Fracture Toughness in CFRP/Epoxy Joints. *Materials* **2021**, *14*, 1512. [\[CrossRef\]](#)
73. Leone, C.; Genna, S. Effects of surface laser treatment on direct co-bonding strength of CFRP laminates. *Compos. Struct.* **2018**, *194*, 240–251. [\[CrossRef\]](#)
74. Akman, E.; Erdoğan, Y.; Bora, M.Ö.; Çoban, O.; Oztoprak, B.G.; Demir, A. Investigation of the differences between photochemical and photothermal laser ablation on the shear strength of CFRP/CFRP adhesive joints. *Int. J. Adhes. Adhes.* **2020**, *98*, 102548. [\[CrossRef\]](#)
75. Akman, E.; Erdoğan, Y.; Bora, M.Ö.; Çoban, O.; Oztoprak, B.G.; Demir, A. Investigation of accumulated laser fluence and bondline thickness effects on adhesive joint performance of CFRP composites. *Int. J. Adhes. Adhes.* **2019**, *89*, 109–116. [\[CrossRef\]](#)
76. Brune, K.; Lima, L.; Noeske, M.; Thiel, K.; Tornow, C.; Dieckhoff, S.; Hoffmann, M.; Stübing, D. Pre-bond quality assurance of CFRP surfaces using optically stimulated electron emission. In Proceedings of the 3rd International Conference of Engineering Against Failure, ICEAF, Kos, Greece, 26–28 June 2013; pp. 300–307.
77. Kumar, R.L.; Bhat, M.R.; Murthy, C.R.L. Non Destructive Evaluation of Degradation in Bond Line of Glass Fiber Reinforced Polymer Composite Adhesive Lap Joints. *Int. J. Aerosp. Innov.* **2013**, *5*, 61–72. [\[CrossRef\]](#)
78. Malinowski, P.; Wandowski, T.; Ostachowicz, W. The use of electromechanical impedance conductance signatures for detection of weak adhesive bonds of carbon fibre-reinforced polymer. *Struct. Health Monit.* **2015**, *14*, 332–344. [\[CrossRef\]](#)
79. Teixeira de Freitas, S.; Zarouchas, D.; Poulis, J.A. The use of acoustic emission and composite peel tests to detect weak adhesion in composite structures. *J. Adhes.* **2018**, *94*, 743–766. [\[CrossRef\]](#)
80. Yılmaz, B.; Jasiūnienė, E. Advanced ultrasonic NDT for weak bond detection in composite-adhesive bonded structures. *Int. J. Adhes. Adhes.* **2020**, *102*, 102675. [\[CrossRef\]](#)
81. Baek, S.J.; Kim, M.S.; An, W.J.; Choi, J.H. Defect detection of composite adhesive joints using electrical resistance method. *Compos. Struct.* **2019**, *220*, 179–184. [\[CrossRef\]](#)
82. Kwon, D.J.; Wang, Z.J.; Choi, J.Y.; Shin, S.; DeVries, K.L.; Park, J.M. Damage sensing and fracture detection of CNT paste using electrical resistance measurements. *Compos. Part B Eng.* **2016**, *90*, 386–391. [\[CrossRef\]](#)
83. An, W.J.; Kim, C.H.; Kim, T.H.; Choi, J.H. Study on strength and defect detection capability of bonded joints according to CNT content. *Compos. Struct.* **2019**, *207*, 204–212. [\[CrossRef\]](#)
84. Kumar, R.V.; Bhat, M.R.; Murthy, C.R.L. Evaluation of kissing bond in composite adhesive lap joints using digital image correlation: Preliminary studies. *Int. J. Adhes. Adhes.* **2013**, *42*, 60–68. [\[CrossRef\]](#)
85. Ashcroft, I.A.; Hughes, D.J.; Shaw, S.J. Adhesive bonding of fibre reinforced polymer composite materials. *Assem. Autom.* **2000**, *20*, 150–161. [\[CrossRef\]](#)
86. Masmanidis, I.T.; Philippidis, T.P. Progressive damage modeling of adhesively bonded lap joints. *Int. J. Adhes. Adhes.* **2015**, *59*, 53–61. [\[CrossRef\]](#)
87. Bishop, S.M.; Gilmore, R.B. *Fatigue of Bonded CFRP Joints: Fracture Mechanisms and Environmental Effects*, Adhesion 90; Plastics and Rubber Institute: Cambridge, UK, 1990.
88. Mohan, J.; Ivanković, A.; Murphy, N. Mixed-mode fracture toughness of co-cured and secondary bonded composite joints. *Eng. Fract. Mech.* **2015**, *134*, 148–167. [\[CrossRef\]](#)
89. Song, M.G.; Kweon, J.H.; Choi, J.H.; Byun, J.H.; Song, M.H.; Shin, S.J.; Lee, T.J. Effect of manufacturing methods on the shear strength of composite single-lap bonded joints. *Compos. Struct.* **2010**, *92*, 2194–2202. [\[CrossRef\]](#)
90. Mohan, J.; Ivanković, A.; Murphy, N. Mode I fracture toughness of co-cured and secondary bonded composite joints. *Int. J. Adhes. Adhes.* **2014**, *51*, 13–22. [\[CrossRef\]](#)
91. Sebastiani, G.; Pfeifer, S.; Röber, L.; Katoh, J.; Yamaguchi, Z.; Takada, S. Bonding Strength of FRP-Metal Hybrids. *Technol. Lightweight Struct.* **2019**, *3*, 1–8. [\[CrossRef\]](#)
92. Mohan, J.; Ivanković, A.; Murphy, N. Effect of prepreg storage humidity on the mixed-mode fracture toughness of a co-cured composite joint. *Compos. Part A Appl. Sci. Manuf.* **2013**, *45*, 23–34. [\[CrossRef\]](#)
93. Balzani, C.; Wagner, W.; Wilckens, D.; Degenhardt, R.; Büsing, S.; Reimerdes, H.G. Adhesive joints in composite laminates—A combined numerical/experimental estimate of critical energy release rates. *Int. J. Adhes. Adhes.* **2012**, *32*, 23–38. [\[CrossRef\]](#)
94. Hart-Smith, L.J. Designing to minimize peel stresses in adhesive-bonded joints. In *Delamination and Debonding of Materials*; ASTM International: West Conshohocken, PA, USA, 1985.
95. Reis, N.B.; Antunes, F.J.V.; Ferreira, J.A.M. Influence of superposition length on mechanical resistance of single-lap adhesive joints. *Compos. Struct.* **2005**, *67*, 125–133. [\[CrossRef\]](#)
96. Kaye, R.H.; Heller, M. Through-thickness shape optimisation of bonded repairs and lap-joints. *Int. J. Adhes. Adhes.* **2002**, *22*, 7–21. [\[CrossRef\]](#)
97. Lang, T.P.; Mallick, K. The effect of recessing on the stresses in adhesively bonded single-lap joints. *Int. J. Adhes. Adhes.* **1999**, *19*, 257–271. [\[CrossRef\]](#)

98. Tsai, M.Y.; Morton, J. The effect of a spew fillet on adhesive stress distributions in laminated composite single-lap joints. *Compos. Struct.* **1995**, *32*, 123–131. [\[CrossRef\]](#)
99. Rispler, A.R.; Tong, L.; Steven, G.P.; Wisnom, M.R. Shape optimisation of adhesive fillets. *Int. J. Adhes. Adhes.* **2000**, *20*, 221–231. [\[CrossRef\]](#)
100. Chen, I.; Wang, K.Y.; Huang, H.H. Strength and failure modes of adhesively bonded composite joints with easily fabricated nonflat interfaces. *Compos. Struct.* **2019**, *225*, 111162. [\[CrossRef\]](#)
101. Zeng, Q.G.; Sun, C.T. Novel design of a bonded lap joint. *AIAA J.* **2001**, *39*, 1991–1996. [\[CrossRef\]](#)
102. Kishore, A.N.; Prasad, N.S. An experimental study of Flat-Joggle-Flat bonded joints in composite laminates. *Int. J. Adhes. Adhes.* **2012**, *35*, 55–58. [\[CrossRef\]](#)
103. de Freitas, S.T.; Sinke, J. Adhesion properties of bonded composite-to-aluminium joints using peel tests. *J. Adhes.* **2014**, *90*, 511–525. [\[CrossRef\]](#)
104. de Freitas, S.T.; Banea, M.D.; Budhe, S.; De Barros, S. Interface adhesion assessment of composite-to-metal bonded joints under salt spray conditions using peel tests. *Compos. Struct.* **2017**, *164*, 68–75. [\[CrossRef\]](#)
105. Dadian, A.; Rahnama, S. Experimental and numerical study of optimum functionally graded Aluminum/GFRP adhesive lap shear joints using Epoxy/CTBN. *Int. J. Adhes. Adhes.* **2021**, *107*, 102854. [\[CrossRef\]](#)
106. Da Silva, L.F.; Adams, R.D. Joint strength predictions for adhesive joints to be used over a wide temperature range. *Int. J. Adhes. Adhes.* **2007**, *27*, 362–379. [\[CrossRef\]](#)
107. Akhavan-Safar, A.; Ramezani, F.; Delzendehrooy, F.; Ayatollahi, M.R.; da Silva, L.F.M. A review on bi-adhesive joints: Benefits and challenges. *Int. J. Adhes. Adhes.* **2022**, *114*, 103098. [\[CrossRef\]](#)
108. Ramezani, F.; Ayatollahi, M.R.; Akhavan-Safar, A.; Da Silva, L.F.M. A comprehensive experimental study on bi-adhesive single lap joints using DIC technique. *Int. J. Adhes. Adhes.* **2020**, *102*, 102674. [\[CrossRef\]](#)
109. Jairaja, R.; Naik, G.N. Single and dual adhesive bond strength analysis of single lap joint between dissimilar adherends. *Int. J. Adhes. Adhes.* **2019**, *92*, 142–153.
110. Arenas, J.M.; Alía, C.; Narbón, J.J.; Ocaña, R.; Recio, M.M. Considerations for application of structural adhesives for joining aluminium with compound materials in the manufacturing of competition motorcycles. In *AIP Conference Proceedings*; American Institute of Physics: New York, NY, USA, 2012; Volume 1431, pp. 959–966.
111. Machado, J.J.M.; Gamarra, R.; Marques, E.A.S.; da Silva, L.F. Numerical study of the behaviour of composite mixed adhesive joints under impact strength for the automotive industry. *Compos. Struct.* **2018**, *185*, 373–380. [\[CrossRef\]](#)
112. Stapleton, S.E.; Waas, A.M.; Arnold, S.M. Functionally graded adhesives for composite joints. *Int. J. Adhes. Adhes.* **2012**, *35*, 36–49. [\[CrossRef\]](#)
113. Da Silva, L.F.; Adams, R.D. Adhesive joints at high and low temperatures using similar and dissimilar adherends and dual adhesives. *Int. J. Adhes. Adhes.* **2007**, *27*, 216–226. [\[CrossRef\]](#)
114. Jojibabu, P.; Zhang, Y.X.; Prusty, B.G. A review of research advances in epoxy-based nanocomposites as adhesive materials. *Int. J. Adhes. Adhes.* **2020**, *96*, 102454. [\[CrossRef\]](#)
115. Al-Turaif, H.A. Effect of nano TiO₂ particle size on mechanical properties of cured epoxy resin. *Prog. Org. Coat.* **2010**, *69*, 241–246. [\[CrossRef\]](#)
116. Akpınar, I.A.; Gültekin, K.; Akpınar, S.; Akbulut, H.; Ozel, A. Experimental analysis on the single-lap joints bonded by a nanocomposite adhesives which obtained by adding nanostructures. *Compos. Part B Eng.* **2017**, *110*, 420–428. [\[CrossRef\]](#)
117. Tutunchi, A.; Kamali, R.; Kianvash, A. Adhesive strength of steel-epoxy composite joints bonded with structural acrylic adhesives filled with silica nanoparticles. *J. Adhes. Sci. Technol.* **2015**, *29*, 195–206. [\[CrossRef\]](#)
118. Pavlidou, S.; Papaspyrides, C.D. A review on polymer-layered silicate nanocomposites. *Prog. Polym. Sci.* **2008**, *33*, 1119–1198. [\[CrossRef\]](#)
119. Feng, L.; Bae, D.H. Joining STS304l sheets by using nano-adhesives. *J. Mech. Sci. Technol.* **2013**, *27*, 1943–1947. [\[CrossRef\]](#)
120. Hsiao, K.T.; Alms, J.; Advani, S.G. Use of epoxy/multiwalled carbon nanotubes as adhesives to join graphite fibre reinforced polymer composites. *Nanotechnology* **2003**, *14*, 791. [\[CrossRef\]](#)
121. Kinloch, A.J.; Lee, J.H.; Taylor, A.C.; Sprenger, S.; Eger, C.; Egan, D. Toughening structural adhesives via nano-and micro-phase inclusions. *J. Adhes.* **2003**, *79*, 867–873. [\[CrossRef\]](#)
122. Patel, S.; Bandyopadhyay, A.; Ganguly, A.; Bhowmick, A.K. Synthesis and properties of nanocomposite adhesives. *J. Adhes. Sci. Technol.* **2006**, *20*, 371–385. [\[CrossRef\]](#)
123. Park, S.W.; Lee, D.G. Strength of double lap joints bonded with carbon black reinforced adhesive under cryogenic environment. *J. Adhes. Sci. Technol.* **2009**, *23*, 619–638. [\[CrossRef\]](#)
124. Dorigato, A.; Pegoretti, A. The role of alumina nanoparticles in epoxy adhesives. *J. Nanopart. Res.* **2011**, *13*, 2429–2441. [\[CrossRef\]](#)
125. Shang, X.; Marques, E.A.S.; Machado, J.J.M.; Carbas, R.J.C.; Jiang, D.; Da Silva, L.F.M. A strategy to reduce delamination of adhesive joints with composite substrates. *Proc. Inst. Mech. Eng. Part L J. Mater. Des. Appl.* **2019**, *233*, 521–530. [\[CrossRef\]](#)
126. Meguid, S.A.; Sun, Y. On the tensile and shear strength of nano-reinforced composite interfaces. *Mater. Des.* **2004**, *25*, 289–296. [\[CrossRef\]](#)
127. Srivastava, V.K. Effect of carbon nanotubes on the strength of adhesive lap joints of C/C and C/C–SiC ceramic fibre composites. *Int. J. Adhes. Adhes.* **2011**, *31*, 486–489. [\[CrossRef\]](#)

128. Faulkner, S.D.; Kwon, Y.W.; Bartlett, S.; Rasmussen, E.A. Study of composite joint strength with carbon nanotube reinforcement. *J. Mater. Sci.* **2009**, *44*, 2858–2864. [\[CrossRef\]](#)
129. Kumar, A.; Kumar, K.; Ghosh, K.; Rath, A.; Yadav, K.L. MWCNTs toward superior strength of epoxy adhesive joint on mild steel adherent. *Compos. Part B Eng.* **2018**, *143*, 207–216. [\[CrossRef\]](#)
130. Gude, M.R.; Prolongo, S.G.; Gómez-del Río, T.; Ureña, A. Mode-I adhesive fracture energy of carbon fibre composite joints with nanoreinforced epoxy adhesives. *Int. J. Adhes. Adhes.* **2011**, *31*, 695–703. [\[CrossRef\]](#)
131. Khashaba, U.A.; Aljinaidi, A.A.; Hamed, M.A. Analysis of adhesively bonded CFRE composite scarf joints modified with MWCNTs. *Compos. Part A Appl. Sci. Manuf.* **2015**, *71*, 59–71. [\[CrossRef\]](#)
132. Zielecki, W.; Kubit, A.; Trzepieciński, T.; Narkiewicz, U.; Czech, Z. Impact of multiwall carbon nanotubes on the fatigue strength of adhesive joints. *Int. J. Adhes. Adhes.* **2017**, *73*, 16–21. [\[CrossRef\]](#)
133. Kang, M.H.; Choi, J.H.; Kwon, J.H. Fatigue life evaluation and crack detection of the adhesive joint with carbon nanotubes. *Compos. Struct.* **2014**, *108*, 417–422. [\[CrossRef\]](#)
134. Bily, M.A.; Kwon, Y.W.; Pollak, R.D. Study of composite interface fracture and crack growth monitoring using carbon nanotubes. *Appl. Compos. Mater.* **2010**, *17*, 347–362. [\[CrossRef\]](#)
135. Hua, Y.; Gu, L.; Trogon, M. Three-dimensional modeling of carbon/epoxy to titanium single-lap joints with variable adhesive recess length. *Int. J. Adhes. Adhes.* **2012**, *38*, 25–30. [\[CrossRef\]](#)
136. Moya-Sanz, E.M.; Ivañez, I.; Garcia-Castillo, S.K. Effect of the geometry in the strength of single-lap adhesive joints of composite laminates under uniaxial tensile load. *Int. J. Adhes. Adhes.* **2017**, *72*, 23–29. [\[CrossRef\]](#)
137. Ostapiuk, M.; Bienias, J. Fracture analysis and shear strength of aluminum/CFRP and GFRP adhesive joint in fiber metal laminates. *Materials* **2019**, *13*, 7. [\[CrossRef\]](#) [\[PubMed\]](#)
138. Akpinar, S. Effects of laminate carbon/epoxy composite patches on the strength of double-strap adhesive joints: Experimental and numerical analysis. *Mater. Des.* **2013**, *51*, 501–512. [\[CrossRef\]](#)
139. Hazimeh, R.; Challita, G.; Khalil, K.; Othman, R. Experimental investigation of the influence of substrates' fibers orientations on the impact response of composite double-lap joints. *Compos. Struct.* **2015**, *134*, 82–89. [\[CrossRef\]](#)
140. Purimpat, S.; Jérôme, R.; Shahram, A. Effect of fiber angle orientation on a laminated composite single-lap adhesive joint. *Adv. Compos. Mater.* **2013**, *22*, 139–149. [\[CrossRef\]](#)
141. Arteiro, A.; Catalanotti, G.; Xavier, J.; Linde, P.; Camanho, P.P. A strategy to improve the structural performance of non-crimp fabric thin-ply laminates. *Compos. Struct.* **2018**, *188*, 438–449. [\[CrossRef\]](#)
142. Ramezani, F.; Carbas, R.J.; Marques, E.A.; Ferreira, A.M.; da Silva, L.F. A study of the fracture mechanisms of hybrid carbon fiber reinforced polymer laminates reinforced by thin-ply. *Polym. Compos.* **2022**. [\[CrossRef\]](#)
143. Sih, S.; Kim, R.Y.; Kawabe, K.; Tsai, S.W. Experimental studies of thin-ply laminated composites. *Compos. Sci. Technol.* **2007**, *67*, 996–1008. [\[CrossRef\]](#)
144. Roure, T. C-PLY™, a new structural approach to multiaxials in composites: BI-ANGLE NCF. *JEC Compos.* **2011**, *68*, 53–54.
145. Amacher, R.; Cugnoni, J.; Botsis, J.; Sorensen, L.; Smith, W.; Dransfeld, C. Thin ply composites: Experimental characterization and modeling of size-effects. *Compos. Sci. Technol.* **2014**, *101*, 121–132. [\[CrossRef\]](#)
146. Köttler, B.; Karsten, J.; Körbelin, J.; Fiedler, B. CFRP thin-ply fibre metal laminates: Influences of ply thickness and metal layers on open hole tension and compression properties. *Materials* **2020**, *13*, 910. [\[CrossRef\]](#)
147. Yokozeki, T.; Kuroda, A.; Yoshimura, A.; Ogasawara, T.; Aoki, T. Damage characterization in thin-ply composite laminates under out-of-plane transverse loadings. *Compos. Struct.* **2010**, *93*, 49–57. [\[CrossRef\]](#)
148. Mania, R.J.; York, C.B. Buckling strength improvements for Fibre Metal Laminates using thin-ply tailoring. *Compos. Struct.* **2017**, *159*, 424–432. [\[CrossRef\]](#)
149. Zubillaga, L.; Turon, A.; Renart, J.; Costa, J.; Linde, P. An experimental study on matrix crack induced delamination in composite laminates. *Compos. Struct.* **2015**, *127*, 10–17. [\[CrossRef\]](#)
150. Wisnom, M.R.; Khan, B.; Hallett, S.R. Size effects in unnotched tensile strength of unidirectional and quasi-isotropic carbon/epoxy composites. *Compos. Struct.* **2008**, *84*, 21–28. [\[CrossRef\]](#)
151. Kim, R.Y.; Soni, S.R. Experimental and analytical studies on the onset of delamination in laminated composites. *J. Compos. Mater.* **1984**, *18*, 70–80. [\[CrossRef\]](#)
152. Saito, H.; Takeuchi, H.; Kimpara, I. Experimental evaluation of the damage growth restraining in 90 layer of thin-ply CFRP cross-ply laminates. *Adv. Compos. Mater.* **2012**, *21*, 57–66. [\[CrossRef\]](#)
153. Camanho, P.P.; Dávila, C.G.; Pinho, S.T.; Iannucci, L.; Robinson, P. Prediction of in situ strengths and matrix cracking in composites under transverse tension and in-plane shear. *Compos. Part A Appl. Sci. Manuf.* **2006**, *37*, 165–176. [\[CrossRef\]](#)
154. Kupski, J.; Zarouchas, D.; de Freitas, S.T. Thin-ply in adhesively bonded carbon fiber reinforced polymers. *Compos. Part B Eng.* **2020**, *184*, 107627. [\[CrossRef\]](#)
155. Carbas, R.J.; Palmares, M.P.; Da Silva, L.F. Experimental and FE study of hybrid laminates aluminium carbon-fibre joints with different lay-up configurations. *Manuf. Rev.* **2020**, *7*, 2. [\[CrossRef\]](#)
156. Ramezani, F.; Nunes, D.P.; Carbas, R.J.C.; Marques, E.A.S.; da Silva, L.F.M. The joint strength of hybrid composite joints reinforced with different laminates materials. *J. Adv. Join. Process.* **2022**, *5*, 100103. [\[CrossRef\]](#)
157. Morgado, M.A.; Carbas, R.J.C.; Marques, E.A.S.; Da Silva, L.F.M. Reinforcement of CFRP single lap joints using metal laminates. *Compos. Struct.* **2019**, *230*, 111492. [\[CrossRef\]](#)

158. Dos Santos, D.G.; Carbas, R.J.C.; Marques, E.A.S.; da Silva, L.F.M. Reinforcement of CFRP joints with fibre metal laminates and additional adhesive layers. *Compos. Part B Eng.* **2019**, *165*, 386–396. [[CrossRef](#)]
159. Carbas, R.J.C.; Marques, E.A.S.; Da Silva, L.F.M. The influence of epoxy adhesive toughness on the strength of hybrid laminate adhesive joints. *Appl. Adhes. Sci.* **2021**, *9*, 1. [[CrossRef](#)]
160. Morgado, M.A.; Carbas, R.J.C.; Dos Santos, D.G.; Da Silva, L.F.M. Strength of CFRP joints reinforced with adhesive layers. *Int. J. Adhes. Adhes.* **2020**, *97*, 102475. [[CrossRef](#)]
161. Schollerer, M.J.; Kosmann, J.; Völkerink, O.; Holzhüter, D.; Hühne, C. Surface toughening—A concept to decrease stress peaks in bonded joints. *J. Adhes.* **2019**, *95*, 495–514. [[CrossRef](#)]

Disclaimer/Publisher’s Note: The statements, opinions and data contained in all publications are solely those of the individual author(s) and contributor(s) and not of MDPI and/or the editor(s). MDPI and/or the editor(s) disclaim responsibility for any injury to people or property resulting from any ideas, methods, instructions or products referred to in the content.

Appendix B

Paper B

A study of the fracture mechanisms of hybrid carbon fiber reinforced polymer laminates reinforced by thin-ply

RESEARCH ARTICLE

Polymer
COMPOSITES

WILEY

A study of the fracture mechanisms of hybrid carbon fiber reinforced polymer laminates reinforced by thin-ply

Farin Ramezani¹ | Ricardo J. C. Carbas^{1,2} | Eduardo A. S. Marques¹ | Antonio M. Ferreira² | Lucas F. M. da Silva²

¹Instituto de Ciência e Inovação Em Engenharia Mecânica e Engenharia Industrial (INEGI), Porto, Portugal

²Departamento de Engenharia Mecânica, Faculdade de Engenharia (FEUP), Universidade Do Porto, Porto, Portugal

Correspondence

R. J. C. Carbas, Instituto de Ciência e Inovação Em Engenharia Mecânica e Engenharia Industrial (INEGI), Rua Dr. Roberto Frias, 4200-465 Porto, Portugal.

Email: rcarbas@fe.up.pt

Funding information

Fundação para a Ciência e a Tecnologia, Grant/Award Numbers: 2021.07943.BD, CEECIND/03276/2018, PTDC/EME-EME/2728/2021

Abstract

The main stress component which creates delamination in bonded single lap joints with composite adherends is the transverse tensile stress. Therefore, the following study investigates the behavior of composite laminates (reference and hybrid laminates reinforced by thin-ply) under transverse tensile loading. Texipreg HS 160T700 and NTPT-TP415 were used as the conventional carbon fiber reinforced polymer (CFRP) and thin-ply respectively. Hybrid composite laminates were studied using different amounts of thin-ply, applied through the thickness. The manufactured laminates, of unidirectionally stacked construction, were tested under transverse tensile loading. Digital image correlation was performed to investigate the average peel strain distribution for the composite and to better understand the phenomena associated to the use of hybrid laminates. Experimental results show that the reinforced hybrid composite laminates, created using thin-ply, present higher failure load compared to the reference conventional CFRP or thin-ply laminates. This was found to be due to the higher ductility enabled by the presence of thin-ply. Distributing a constant amount of thin-ply through the thickness was found to increase the laminate transverse strength, as the thin-ply laminates act as a barrier against crack propagation. A representative volume element was studied for each configuration since this numerical method brings the opportunity to investigate the studied configurations in microscale.

KEYWORDS

composites, fracture, mechanical testing

1 | INTRODUCTION

Thin-ply can be generally defined as composites with ply thicknesses below 100 μm and a ply areal weight of less than 100 g/m^2 . Thin-ply composites are rapidly gaining interest in the composite and high-performance industries (e.g., aerospace) due to the increased design flexibility they bring and the improved mechanical performance under various loading conditions. Different methods have been

used to increase composite strength or delay its delamination (e.g., reinforcing laminates using adhesives or metal laminates^[1] or glass fabric reinforcement^[2] when used as adherends in single lap joints). Moreover, studies have shown that, through the use of thin-ply, the damage location in the composite moves from the adhesive interface toward the mid-thickness of the composite adherends.^[3]

The use of carbon fiber reinforced polymers (CFRP) in various industries is steadily increasing, and a wide

range of material types is now available for the design and manufacture of high-performance composite products such as vehicle structures, sporting goods, and a variety of other consumer products.^[4,5] Modern composites usually consist of two main components. These are the matrix, which provides the cohesion of the material, and reinforcement, such as fibers, which provide the material its strength and stiffness.^[6] However, since the strength of the matrix is at least an order of magnitude lower than that of the reinforcement, composites are generally susceptible to delamination failure. Loads applied in a direction perpendicular to the reinforcement are carried solely by the low-strength matrix, resulting in delamination. This is particularly true for bonded joints of composites, where load transfer through the joint can result in significant peel loads.^[7] The growth of delamination-induced cracks under these loads can lead to rapid deterioration of the mechanical performance of the structure and cause its catastrophic failure.^[8]

A significant development in the field of composites has been the development of thin-ply laminates. Thin-ply laminates are defined as those consisting of layers less than 100 μm thick.^[9] These extremely low layer thicknesses have been made possible through the advancement and industrialization of the spread-tow process^[10] which enables the production of flat, straight plies with a dry ply thickness of only 0.02 mm. Thin-ply plies permit a higher degree of freedom in laminate design since by reducing the thickness of a single layer, the number, and orientation of layers in a laminate can be more precisely controlled and adjusted to be more load-dependent.^[11]

Thin-ply laminates are generally known for their enhanced mechanical performance, hinged on their ability to delay the onset of matrix damage, suppress transverse microcracking,^[9] and free edge delamination,^[11] under static, fatigue, and impact loadings. This can be achieved without the use of high-performance resins and/or 3D reinforcements, unlike what is typically observed for conventional composites.^[12–15] Consequently, the failure modes change from complex multi-mode failure to quasi-brittle failure, from thick- to thin-ply.^[10] Due to the larger number of layers and the associated larger number of interfaces, the shear stresses are known to be lower in thin-ply laminates.^[11] Therefore, thinner plies of composites are acknowledged to have higher in situ transverse strength,^[14] which is not only a function of laminae thickness but also of the orientation of the adjacent laminae.^[16] Furthermore, both the onset and propagation of free-edge delamination are dependent on ply thickness and also on stacking sequence.^[17] Additionally, due to the lower layer thicknesses and the resin spreading process associated with these materials, a more

homogeneous fiber distribution and generally smaller resin-rich areas are achieved.^[18] Nonetheless, the properties of the laminate can still deteriorate rapidly after damage, leading to premature failure.^[19]

Experimental data show that, in ultra-thin-ply laminates, failure occurs through direct delamination, triggered by shear forces and minor matrix cracking whereas the damage onset in laminates with thicker plies is fundamentally due to matrix cracking which then induces delamination and occurs earlier compared to laminates with thinner plies. Moreover, fiber breakage appears earlier in ultra-thin-ply laminates.^[20] On the other hand, as composite laminates often exhibit brittle failure and are vulnerable to damage accumulation, e.g. matrix cracks and delamination, interlaminar properties are considered to be the key to enhancing the performance of composite laminates.^[21] Due to superior damage and delamination resistance characteristics, thin-ply laminates have the potential to exhibit higher interlaminar shear properties^[21] and strain energy^[3] than conventional plies. Moreover, other detailed studies have investigated the effect of aging,^[22] electrical resistance^[23] and the use of hybrid thin ply composites.^[24]

Composites have been widely studied in structural joints.^[25–27] Thin-ply plies also represent a promising approach to improving the performance of adhesively bonded composite joints due to their ability to enhance the off-axis performance of composites and postpone delamination.^[3] Moreover, due to the in-situ effect,^[28] the locus of composite failure in composite bonded joints could be changed from the ply interface toward the mid thickness of the composite adherend.

Through-thickness reinforcement can effectively provide improved interlaminar strength and delamination resistance while producing a more integrated composite structure.^[29] Multiple methods of fiber architecture for through-thickness reinforcing have been practically demonstrated, such as the use of weaves or braids. However, although effective, the complexity and limited flexibility of these techniques restrict their usage. Furthermore, such methods normally require the implementation of at least one additional production step,^[30,31] increasing process costs. This process is now closely supported through the development of multiple analytical and numerical models.^[32,33]

The study seeks to study and quantify the performance of hybrid composite blocks loaded under transverse tensile stresses, analyzing the effect of reinforcing unidirectional conventional composite using thin-ply, under different configurations. In this work, “HS 160 T700” and “TP415” by NTPT are used as conventional composite and thin-ply plies, respectively.

2 | EXPERIMENTAL DETAIL

2.1 | Conventional composite

All materials used in the following study were selected to be representative of materials used in the aerospace industry. A unidirectional carbon-epoxy prepreg with ply thickness of 0.15 mm was used as the conventional, composite, with the commercial reference Texipreg HS 160T700 (Seal Spa, Legnano, Italy). The conventional composite is an orthotropic material, its elastic mechanical properties are presented in Table 1. The elastic mechanical properties of the conventional composite correspond to the orientation of a 0° ply (x , y , and z represent the fiber transverse and thickness direction respectively). The mode I interlaminar fracture toughness energy (G_{IC}) was determined by the ISO 15024 standard which specifies the procedure to define G_{IC} of carbon fiber composites manufactured from unidirectional tape.

2.2 | Thin-ply

For a thin-ply material, a unidirectional 0° oriented carbon-epoxy prepreg with a ply thickness of 0.07 mm was selected. This thin-ply has the commercial reference NTPT-TP415. The elastic orthotropic properties for this thin-ply composite are presented in Table 2, as provided by the manufacturer and the G_{IC} was determined by EN 6033 standard.

2.3 | Plate manufacturing

The manufacturing process for either the conventional or the thin-ply composite starts with a layer-by-layer

stacking of the plies. This process is continued until the desired block thickness is reached (see Figure 1). For the hybrid blocks, three configurations have been considered, using thin-ply layers placed on the outer surfaces of a central conventional composite block. Three different thickness values for the thin-ply laminates (0.16, 0.4, and 0.8 mm) were used. However, irrespectively of the thin-ply layer dimensions used, the overall thickness of all configurations is made to be the same (3.2 mm). A mold is used to ensure the uniform thickness of the plate. The mold is coated with a release agent to ensure easy removal of the finished plates. Finally, the plates were cured in a hot press at 30 bar and 130°C for 2 h as recommended by the producer.

After curing, the plates were cut to the desired dimensions ($25 \times 25 \text{ mm}^2$) and, finally, steel blocks (see Figure 2) were attached to the composite plates using the PLEXUS MA422 adhesive. This adhesive cures at room temperature after a 24 h period. The excess adhesive or resin present in these specimens after curing was carefully removed manually with the use of a file and sandpaper.

2.4 | Configurations

Specimens with conventional composite and thin-ply laminates (serving as references) were manufactured first, followed by the already mentioned hybrid blocks (with the labels CFRP+12.5%thin-ply, CFRP+25%thin-ply, and CFRP+50%thin-ply). These configurations are schematized in Figure 3. Following preliminary testing, two new configurations were considered to study the effect of distributing thin-ply layers in three and four layers through the laminated thickness. These new configurations are labeled CFRP+25%thin-ply/3 and CFRP+25%thin-ply/4 (per Figure 3).

2.5 | Scanning electron microscope studies

The cross-section of diverse specimen configurations was observed using a scanning electron Microscope (SEM). The cross-sections were polished before observation. In specimens manufactured with composite prepreg, resin-rich and fiber-rich areas are apparent (marked by a red rectangle in Figure 4). In contrast, fibers are generally better distributed in specimens manufactured using thin-ply prepreps, with smaller resin-rich and fiber-rich areas than those found for conventional composite laminates (see Figure 4). These observations are in line with the literature.^[18]

TABLE 1 Conventional composite mechanical properties^[34]

Mechanical property	Value
E_1 (MPa)	109,000
E_2 (MPa)	8819
G_{12} (MPa)	4315
G_{IC} [N/mm]	0.59

TABLE 2 Thin-ply mechanical properties based on manufacturer data

Mechanical property	Value
E_1 (MPa)	62,300
E_2 (MPa)	8900
G_{12} (MPa)	5070
G_{IC} [N/mm]	0.73

FIGURE 1 (A) Layer-by-layer stacking of the composite prepreg and (B) conventional composite plate

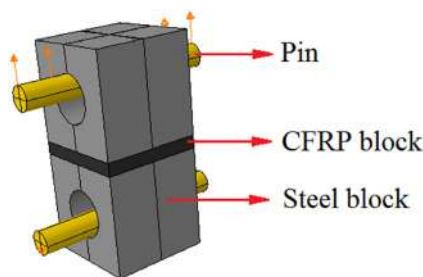


FIGURE 2 Schematic design of steel blocks attached to conventional composite blocks and loading condition

2.6 | Surface treatment

As mentioned in Section 2.3, composite blocks are attached to steel blocks, (as shown in Figure 2) to enable tensile testing. To perform this process, the surface of the composite blocks was first prepared using light sandpaper and cleaned with acetone to remove the contaminants^[35] the release agent used in the plate manufacturing step (see Section 2.3). Plasma treatment^[36,37] was then performed on the composite surfaces to increase the surface energy prior to bonding. The plasma treatment was accomplished through the use of an Arcojet PG 051 plasma device, which provides 50–60 Hz frequency. The nozzle was placed at the distance of 20 mm from the surface of the composite laminates and the treatment was applied for 5 s. The steel blocks were prepared with sand-blasting, followed by an acetone degreasing process. Figure 5 shows the plasma treatment for thin-ply blocks.

2.7 | Testing conditions

The specimens were tested using a servo-hydraulic testing machine (Instron 8801), with a load cell of 100 kN. All tests were performed under laboratory ambient conditions (room temperature of 24°C, relative humidity of 55%) and at a constant crosshead speed of 1 mm/min (quasi-static). A minimum of three repetitions were performed for each of the configurations tested.

3 | EXPERIMENTAL RESULTS

3.1 | Effect of thin-ply thickness

Figure 6 presents the experimentally obtained load-displacement curves for the reference CFRP, thin-ply, and hybrid blocks. For all configurations under testing, the highest values and failure load and failure displacement were found for the CFRP+12.5%thin-ply and CFRP+25%thin-ply configurations.

As shown in Figure 6, there is a 28% and 25.5% increase in failure load attained by the CFRP+12.5% thin-ply and CFRP+25%thin-ply respectively, compared to the reference CFRP. However, there is a 9.4% decrease in failure load found for the CFRP+50%thin-ply configuration.

Digital image correlation (DIC) was used to determine the strain field in the conventional CFRP, thin-ply, and CFRP+25%thin-ply (the configuration presenting the highest strength). The cross-section of the blocks was painted in a base white color interspersed with randomly distributed black speckles (see Figure 7A). A Nikon D5300 digital camera was used to automatically take pictures of the loaded specimens every 5 s (the first figure is captured as soon as the loading starts). Using this data, the peeling strain at the cross-section area was obtained for the mentioned configurations using Moiré analysis software. Therefore, each image (depicting the obtained strain) was related to a displacement value attained under a precise testing rate. Thus, the related load was determined. Accordingly, the engineering stress was calculated for each strain. The stresses are calculated by correlating the DIC data and the load cell values. Figure 7B shows the stress-strain curves obtained with DIC for the reference and hybrid blocks. Specimens with thin-ply were generally found to present higher peeling strain values than those found in specimens using conventional CFRP plies. Therefore, replacing conventional CFRP plies with thin-ply in the hybrid block increases the ductility and ultimately led to an increase in the failure load of the hybrid blocks.

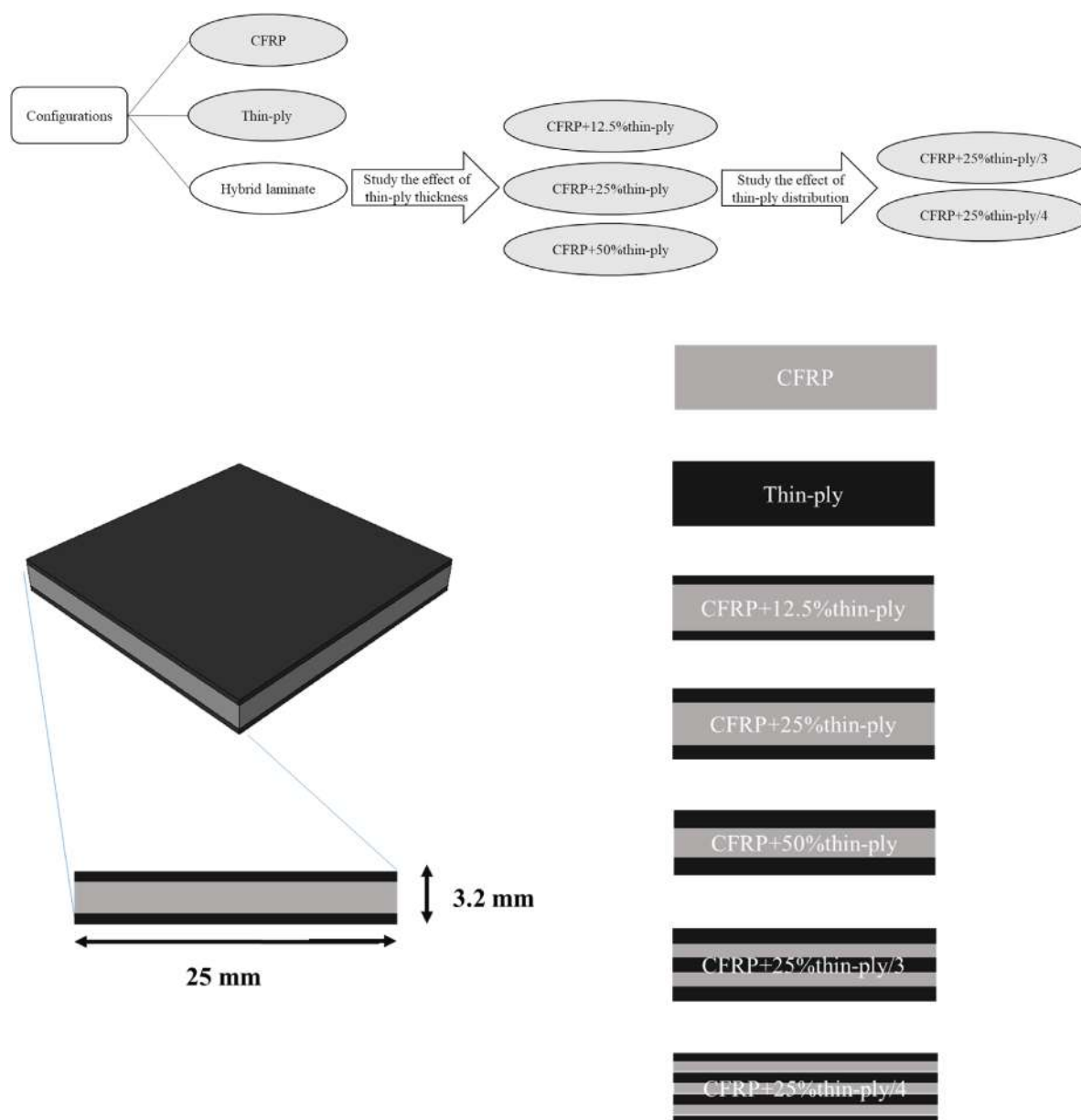


FIGURE 3 Schematic design for conventional carbon fiber reinforced polymer, thin-ply, and hybrid blocks

Moreover, since the fracture toughness (G_{IC}) of thin-ply is higher than that of conventional CFRP (as presented in Tables 1 and 2), this also explains the improved performance that the use of thin-ply brings over compared to the use of CFRP.

A high-speed camera, capable of recording at 4000 frames per second, was used to precisely determine the crack path for all configurations. In a process similar to that used for the DIC analysis, the cross-section of fibers was coated with a thin layer of white paint (see Figure 8), allowing to highlight the crack path. The red circle in Figure 8 shows an example of a crack initiation process. In the hybrid blocks, the crack initiated mainly on the

corner of the CFRP laminate and then propagated toward the interface between the CFRP and thin-ply (see Figure 8C). In some cases, after reaching the interface the crack propagates back into the CFRP (see Figure 8B,D). This shows that the thin-ply acts as an effective barrier to crack propagation, offering more uniform fiber distribution and a minimal amount of resin-rich and fiber-rich areas. This results in lowered stress concentrations and enables hybrid laminates to attain higher values of strain. This is in line with the literature review and also with the SEM micrographs presented in Figure 4. Figure 9 shows a schematic representation of the failure mechanism in the hybrid blocks described above.

FIGURE 4 SEM micrographs of (A) carbon fiber reinforced polymers and (B) thin-ply

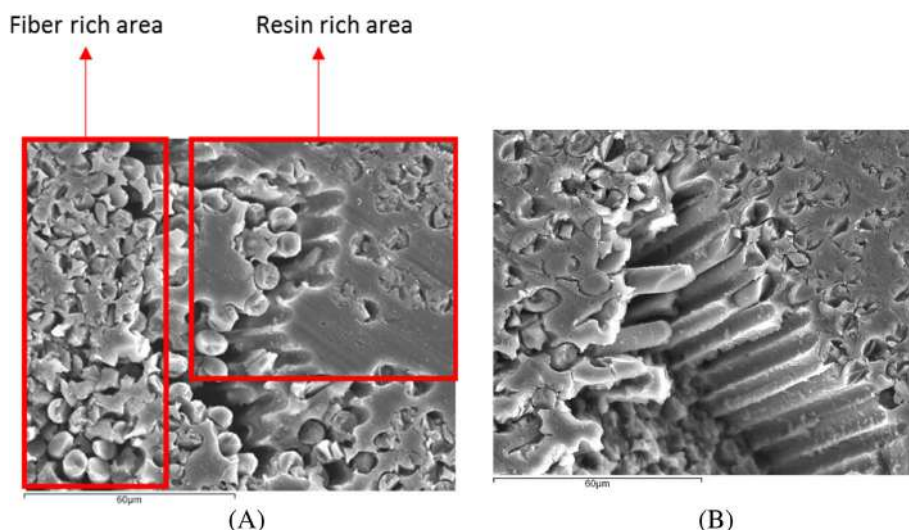


FIGURE 5 Plasma treatment for thin-ply blocks

3.2 | Effect of thin-ply distribution

Figure 10 shows the experimentally obtained load-displacement curves for CFRP+25%thin-ply/3 and CFRP+25%thin-ply/4. The failure load for CFRP+25%thin-ply/3 and CFRP+25%thin-ply/4 was found to increase by 32% and 43% respectively when compared to the reference conventional CFRP. Figures 11 and 12 shows the failure mechanism for CFRP+25%thin-ply/3 and CFRP+25%thin-ply/4, which initiate from a corner of the hybrid block in the interface, propagate through the CFRP, and then reaches the opposite interface.

Figure 13 presents a summary of the experimentally obtained results. These results suggest that replacing up to 25% of the layers of the conventional CFRP by a thin-ply layer increases composite laminate strength under transverse tensile loads. Based on the digital image correlation process performed on the conventional CFRP, Thin-ply and hybrid laminate, thin-ply appears to be a ductile material compared to the conventional CFRP. Therefore, the improvement in the failure load under

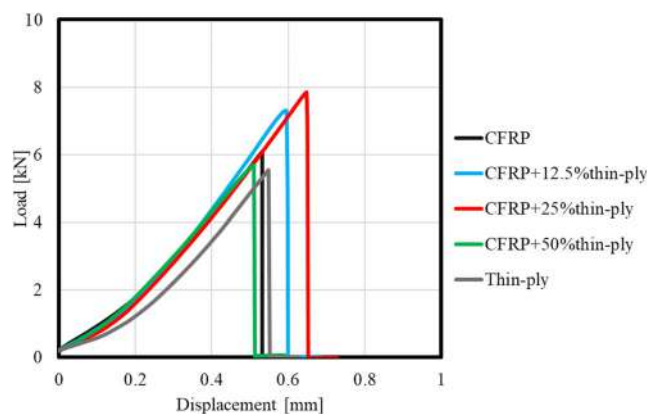


FIGURE 6 Representative experimentally obtained load-displacement curves for carbon fiber reinforced polymers, thin-ply, and hybrid blocks

transverse tensile loading is mostly attributed to an increase in the ductility of the laminate due to the presence of thin-ply in hybrid laminated. In addition, distributing a constant amount of thin-ply in three or four layers through the thickness of the composite laminate further increases the failure load. According to the SEM images of the laminates after failure, the presence of thin-ply is found to provide additional resistance against crack propagation. The reduction in the presence of resin and fiber-rich areas in the thin-ply layer can be seen in the SEM micrographs.

4 | NUMERICAL STUDY

A representative volume element (RVE) model has been created to study the mechanics and the advantages associated with the reinforcement of composite blocks with

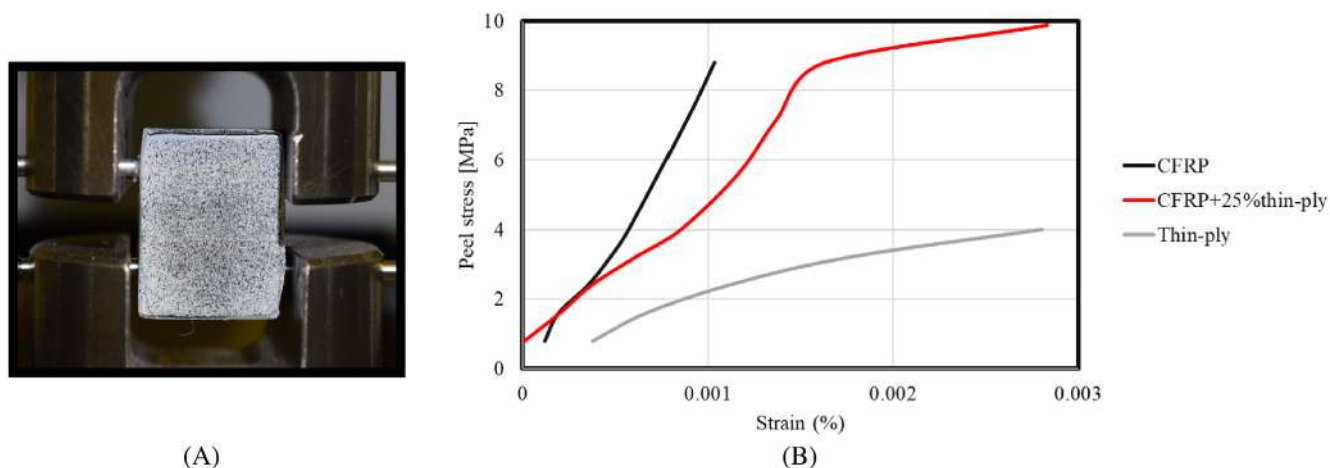


FIGURE 7 (A) Representative image captured for digital image correlation process and (B) stress-strain curve for the reference blocks ad CFRP+25%thin-ply

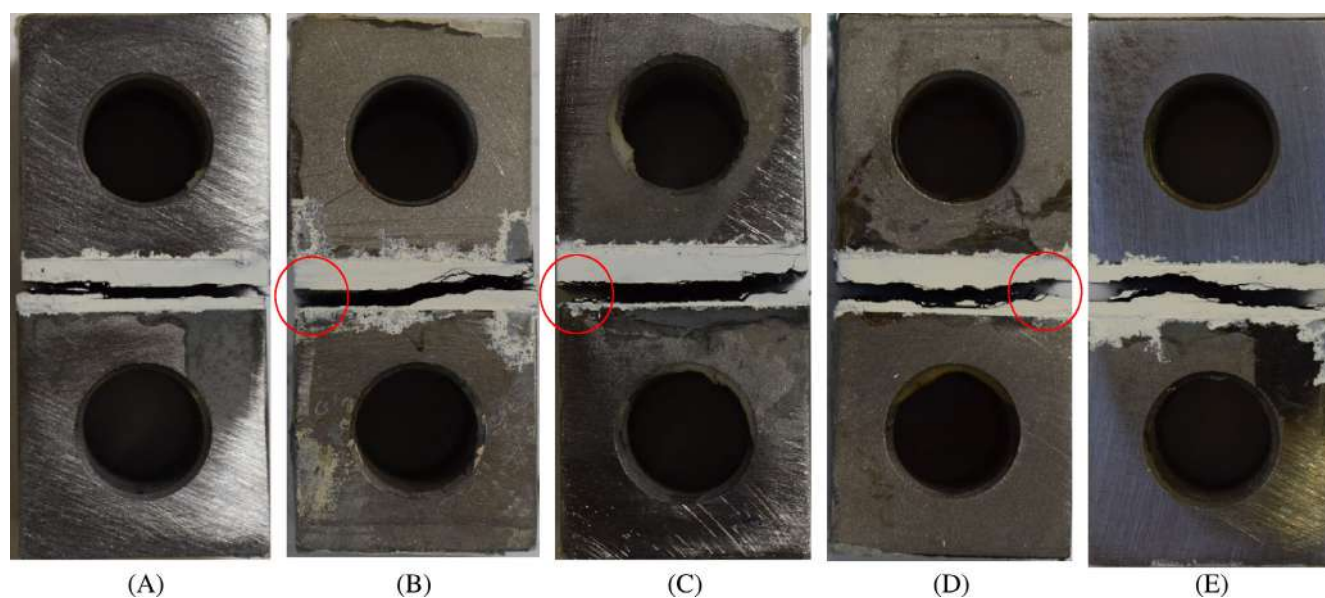


FIGURE 8 Failure mechanism for (A) carbon fiber reinforced polymer (CFRP), (B) CFRP+12.5%thin-ply, (C) CFRP+25%thin-ply, (D) CFRP+50%thin-ply and (E) thin-ply

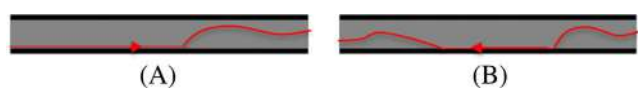


FIGURE 9 Schematic design of failure mechanism for (A) CFRP+12.5%thin-ply and CFRP+25%thin-ply and (B) CFRP+50%thin-ply

thin-ply at the micro-scale, using a representative volume element. A large 2D elastoplastic RVE model with dimensions of $1.6 \times 1.6 \text{ (mm)}^2$ was studied using the ABAQUS commercial finite element package. These dimensions were selected to permit the analysis of all configurations under study. Initially, only a small-scale

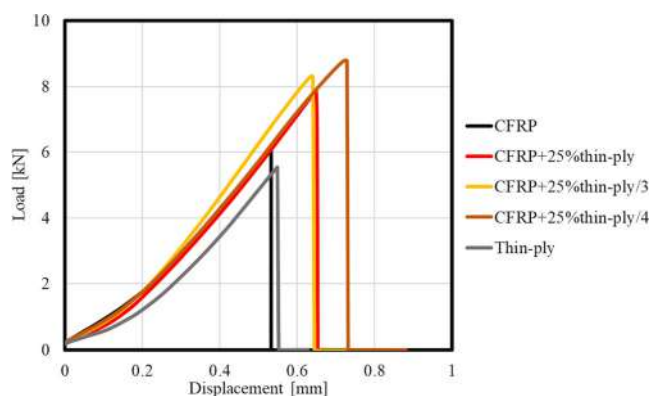


FIGURE 10 Representative experimentally obtained load-displacement curve CFRP+25%thin-ply/3 and CFRP+25%thin-ply/4

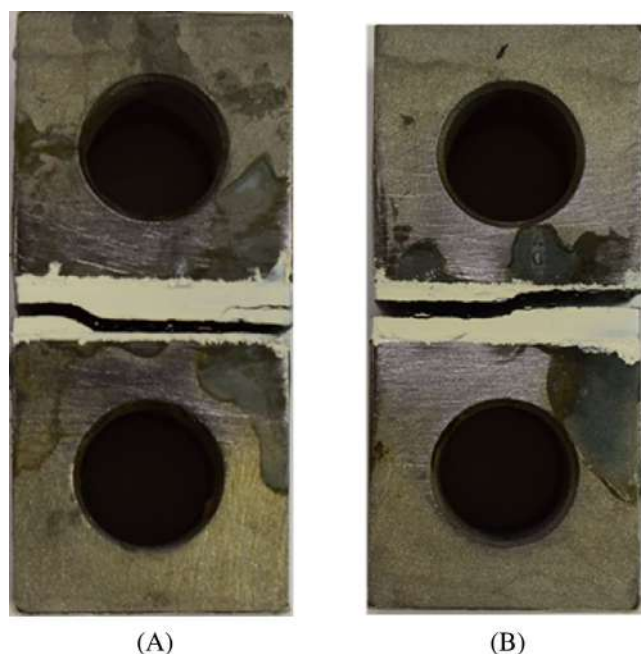


FIGURE 11 The failure mechanism for (A) CFRP+25%thin-ply/3 and (B) CFRP+25%thin-ply/4



FIGURE 12 Schematic design of failure mechanism for (A) CFRP+25%thin-ply/3 and (B) CFRP+25%thin-ply/4

RVE of CFRP and thin-ply with the dimension of $0.16 \times 0.2 \text{ (mm)}^2$ was generated (see Figure 14). The main purpose of this initial RVE was to study the distribution of fibers as close as possible to that found through SEM images (see Figure 4), allowing to reproduce the presence of resin-rich and fiber-rich areas in the model. Moreover, the number of fibers was calculated using Equation (1) in which N and D are the numbers and the diameter of the fibers respectively and L , W , and H are the length, width, and the depth of the RVE respectively. Moreover, V_f is the fiber volume fraction. A total of 291 fibers were used in these initial RVEs (see Figure 14). The properties of the fiber and matrix (for the CFRP and thin-ply) are presented in Table 3, according to manufacturer supplied data. E_f and E_m represent the Young's modulus of fiber and matrix, respectively.

$$V_f = \frac{N\pi D^2}{4LW} \quad (1)$$

Afterward, the initial RVE was simply reproduced in the main RVE for each representative configuration. Figure 15 illustrates the RVEs generated for studied

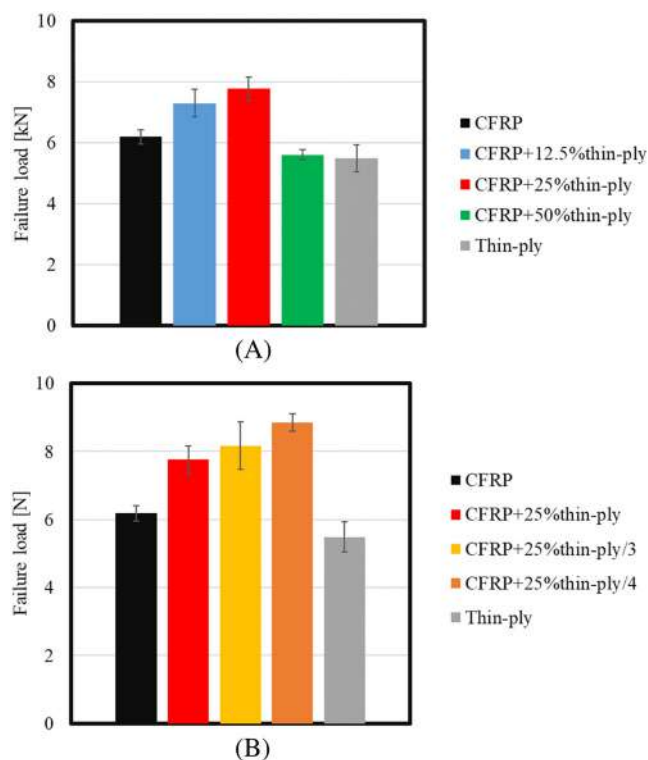


FIGURE 13 Summary of the experimental results for (A) effect of thin-ply thickness and (B) effect of thin-ply distribution

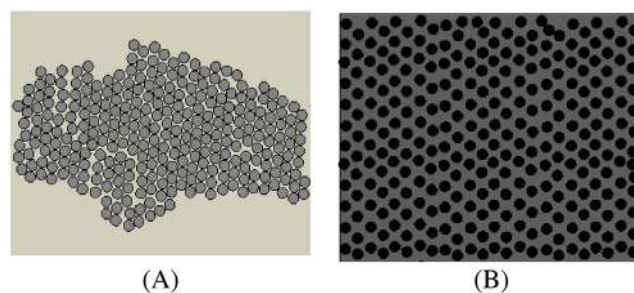


FIGURE 14 Initial representative volume element for the (A) carbon fiber reinforced polymer and (B) thin-ply

TABLE 3 Mechanical properties for the fiber and matrix

	CFRP	Thin-ply
Diameter (μm)	7	7
E_f (GPa)	230	294
E_m (GPa)	3.6	3.3
V_f	0.35	0.35
Matrix maximum strength [MPa]	148	138

Abbreviation: CFRP, carbon fiber reinforced polymer.

configurations. The same boundary conditions were considered for all RVE models (see Figure 15, CFRP), with a

maximum displacement of 0.05 mm being imposed. Two dimensional, 3-node linear plane stress triangular elements were used to mesh the model.

4.1 | Effect of thin-ply thickness

Figures 16 and 18 show the peel stress distribution for each RVE, loaded with a displacement of 0.03 and

0.05 mm, respectively. As the strength of fibers is much higher than that of the matrix, failure is always expected to occur in the matrix. Therefore, stresses in the fibers were eliminated from the results in order to better highlight the behavior of the matrix. The color scale is limited to maximum stress within the CFRP matrix (148 MPa) and any elements with stress values higher than this value are shown in a gray color. As shown in Figure 16, some elements have exceeded the matrix maximum strength in the RVE relevant to the conventional CFRP, expected to correspond to the initiation of matrix failure. It has to be mentioned that if the color scale was limited to the thin-ply matrix maximum strength (138 MPa), a larger area would be seen to exceed the matrix maximum strength in each configuration. The results for the hybrid configurations are presented at the interface of the CFRP and thin-ply. As shown, as the thin-ply thickness increases, a lower number of elements exceeds the maximum of the CFRP matrix and the CFRP+25%thin-ply configuration presents a lower level of stress when compared to other configurations. These results are in line with the experimental observations. Figure 17 shows the level of failure, which is calculated by dividing the area

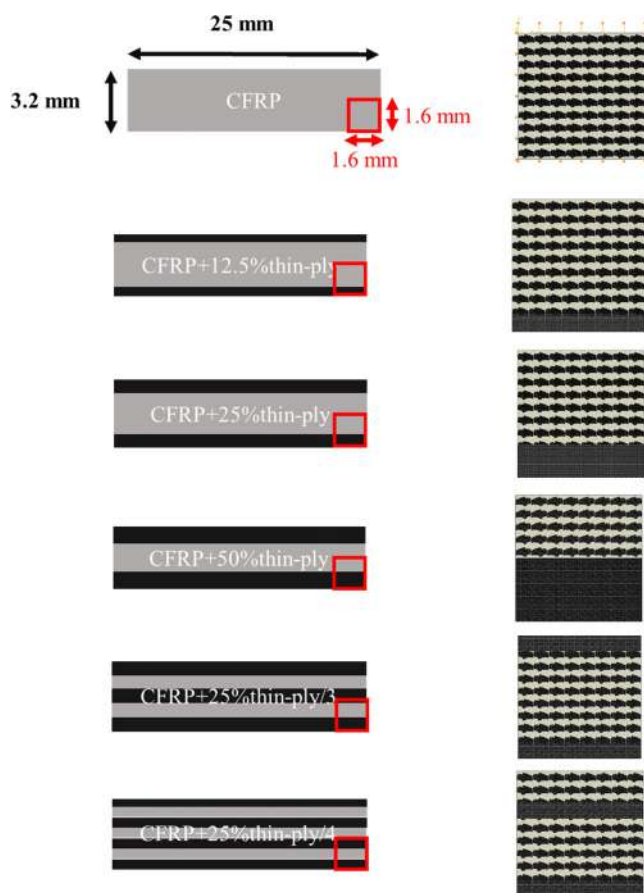


FIGURE 15 Simulated representative volume element for reference carbon fiber reinforced polymer and hybrid configurations

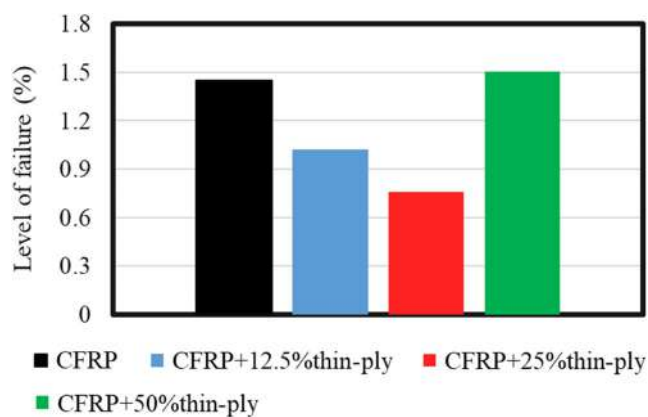


FIGURE 17 Level of failure for carbon fiber reinforced polymer and hybrid configurations

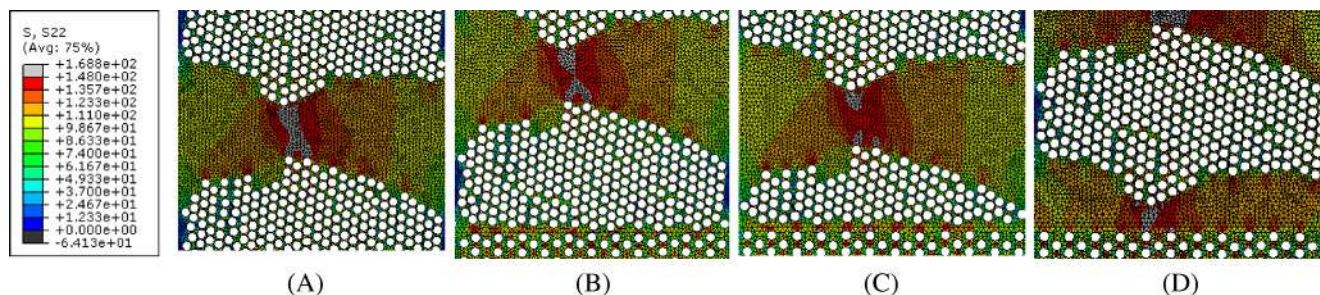


FIGURE 16 Peel stress distribution for (A) carbon fiber reinforced polymer (CFRP), (B) CFRP+12.5%thin-ply, (C) CFRP+25%thin-ply, (D) CFRP+50%thin-ply at displacement of 0.03 mm

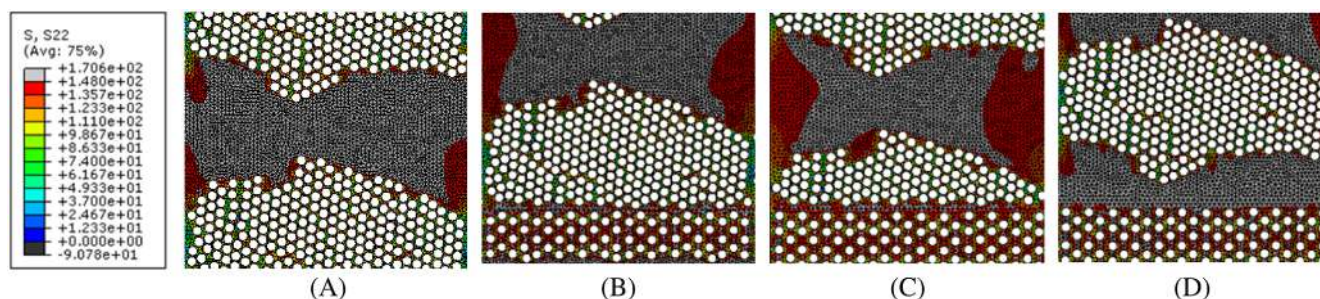


FIGURE 18 Peel stress distribution for (A) carbon fiber reinforced polymer (CFRP), (B) CFRP+12.5%thin-ply, (C) CFRP+25%thin-ply, (D) CFRP+50%thin-ply at displacement of 0.05 mm

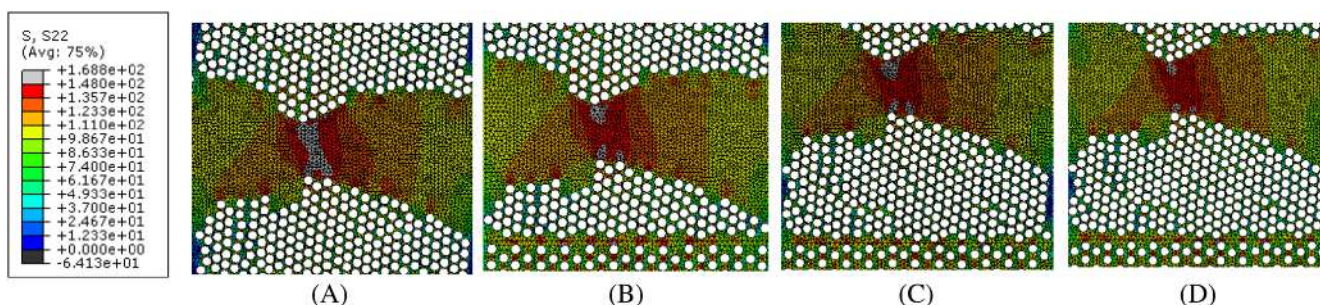


FIGURE 19 Peel stress distribution for (A) carbon fiber reinforced polymer (CFRP), (B) CFRP+25%thin-ply, (C) CFRP+25%thin-ply/3, (D) CFRP+50%thin-ply/4 at the displacement of 0.03 mm

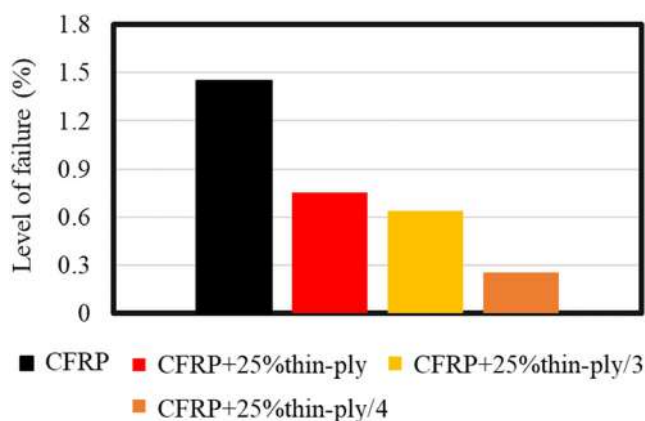


FIGURE 20 Level of failure for carbon fiber reinforced polymer and hybrid configurations

of failed elements by the total area. By replacing layers of CFRP with thin-ply in the composite laminate for 12.5 and 25% of the total laminate thickness, a now lower number of elements exceeds the maximum strength of the matrix. However, as the displacement increases up to 0.05 mm (see Figure 18), a larger number of elements will exceed the CFRP matrix maximum strength and the

difference between the configurations starts to become more apparent.

4.2 | Effect of thin-ply distribution

Figures 19 and 21 illustrate the effect of distributing a constant amount of thin-ply through the thickness of the composite laminate, presenting the peel stress distribution in each representative volume for the same imposed displacement values 0.03 and 0.05 mm, respectively. These results suggest that distributing the thin-ply through the thickness decreases the level of stress and reduces the number of elements which have exceeded the CFRP matrix maximum strength for CFRP+25%thin-ply/3 and CFRP+25%thin-ply/4. The CFRP+25%thin-ply/4 configuration remains as the configuration, which presents the lowest level of peel stress distribution. This is in line with the experimental results presented before. Figure 20 shows the level of failure, calculated by dividing the area of failed element over the total area. By distributing a constant amount of thin-ply through the thickness of a composite laminate in three and four layers, fewer elements exceed the matrix maximum

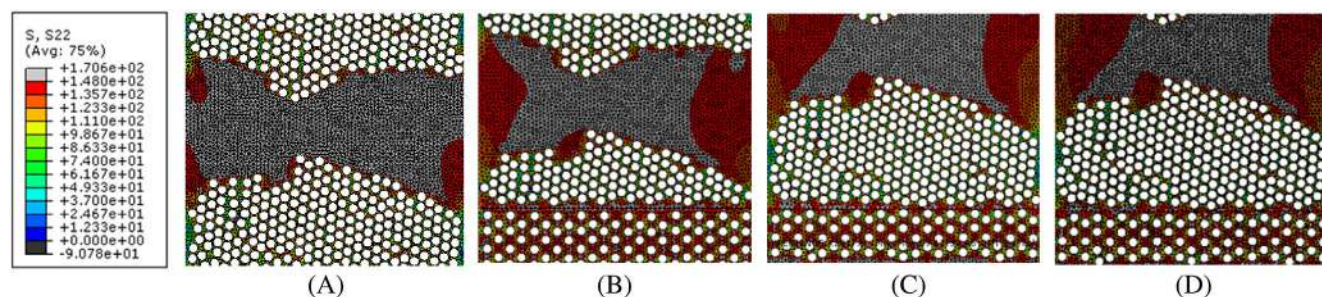


FIGURE 21 Peel stress distribution for (A) carbon fiber reinforced polymer (CFRP), (B) CFRP+25%thin-ply, (C) CFRP+25%thin-ply/3, (D) CFRP+50%thin-ply/4 at the displacement of 0.05 mm

strength. The numerical results are thus again in line with the experimental results.

5 | CONCLUSIONS

This work studied the effect of reinforcing unidirectional CFRP laminates using 0° unidirectional thin-ply. Different layup configurations, combining thin-ply and conventional CFRP plies were studied.

- Experimental results show that the hybrid composite blocks using 12.5% and 25% of thin-ply present 28% and 25.5% higher failure load (respectively) when compared to the reference CFRP. This is mainly due to higher ductility conferred to the material by the presence of thin-ply.
- Analysis of the failure mechanism shows that the thin-ply resistance to crack propagation is mainly due to the more uniform fiber distribution and less resin-rich and fiber-rich area in the thin-ply. This is in a line with the literature review and the SEM micrographs obtained within the context of this work.
- Distributing a constant amount of thin-ply through the thickness increases the failure load up to 43% (compared to the reference CFRP).
- A numerical 2D representative volume element model was created for the reference CFRP and hybrid configurations. The numerical 2D elastoplastic simulation has shown a larger number of elements exceeding the matrix maximum strength of the strength in conventional CFRP RVE when compared to the hybrid configuration.

ACKNOWLEDGMENTS

This work was supported by the Portuguese Foundation for Science and Technology (FCT) through the individual grant's CEECIND/03276/2018 and 2021.07943.BD, and the Project No. PTDC/EME-EME/2728/2021. New

approaches to improve the joint strength and reduce the delamination of composite adhesive joints.

DATA AVAILABILITY STATEMENT

Data available on request from the authors.

ORCID

Ricardo J. C. Carbas  <https://orcid.org/0000-0002-1933-0865>

REFERENCES

- [1] F. Ramezani, P. D. P. Nunes, R. J. C. Carbas, E. A. S. Marques, L. F. M. da Silva, *J. Adv. Joining Process.* **2022**, *5*, 100103.
- [2] X. Shang, E. A. S. Marques, J. J. M. Machado, R. J. C. Carbas, D. Jiang, L. F. M. Da Silva, *Proc. Inst. Mech. Eng. Part L* **2019**, *233*(3), 521.
- [3] J. Kupski, D. Zarouchas, S. T. de Freitas, *Compos. Part B* **2020**, *184*, 107627.
- [4] M. F. Ashby, D. R. Jones, *Engineering materials 1: an introduction to properties, applications and design*, Vol. 1, Elsevier, Great Britain **2012**.
- [5] B. Liu, Q. Zhang, X. Li, Y. Guo, Z. Zhang, H. Yang, Y. Yuan, *Polym. Compos.* **2021**, *42*(7), 3404.
- [6] M. A. Karataş, H. Gökkaya, *Defence Technol.* **2018**, *14*(4), 318.
- [7] W. J. Cantwell, J. Morton, *Composites* **1991**, *22*(5), 347.
- [8] K. B. Su, *Delamination resistance of stitched thermoplastic matrix composite laminates*, ASTM International, Wilmington, DE **1989**, p. 279.
- [9] A. Arteiro, G. Catalanotti, J. Xavier, P. Linde, P. P. Camanho, *Compos. Struct.* **2018**, *188*, 438.
- [10] S. Sihn, R. Y. Kim, K. Kawabe, S. W. Tsai, *Compos. Sci. Technol.* **2007**, *67*(6), 996.
- [11] B. Kötter, J. Karsten, J. Körbelin, B. Fiedler, *Materials* **2020**, *13*(4), 910.
- [12] L. Zubillaga, A. Turon, J. Renart, J. Costa, P. Linde, *Compos. Struct.* **2015**, *127*, 10.
- [13] T. Yokozeki, Y. Aoki, T. Ogasawara, *Compos. Struct.* **2008**, *82*(3), 382.
- [14] M. R. Wisnom, B. Khan, S. R. Hallett, *Compos. Struct.* **2008**, *84*(1), 21.
- [15] R. J. Mania, C. B. York, *Compos. Struct.* **2017**, *159*, 424.
- [16] D. L. Flaggs, M. H. Kural, *J. Compos. Mater.* **1982**, *16*(2), 103.

- [17] R. Y. Kim, S. R. Soni, *J. Compos. Mater.* **1984**, 18(1), 70.
- [18] R. Amacher, J. Cugnoni, J. Botsis, L. Sorensen, W. Smith, C. Dransfeld, *Compos. Sci. Technol.* **2014**, 101, 121.
- [19] G. Guillet, A. Turon, J. Costa, J. Renart, P. Linde, J. A. Mayugo, *Compos. Sci. Technol.* **2014**, 98, 44.
- [20] A. Wagih, P. Maimi, E. V. González, N. Blanco, J. S. de Aja, F. M. De La Escalera, R. Olsson, E. Alvarez, *Compos. A: Appl. Sci. Manuf.* **2016**, 87, 66.
- [21] C. Huang, M. He, Y. He, J. Xiao, J. Zhang, S. Ju, D. Jiang, *J. Compos. Mater.* **2018**, 52(17), 2375.
- [22] V. I. Petkov, R. Joffe, P. Fernberg, *Polym. Compos.* **2022**, 43(5), 2615.
- [23] J. N. Zhang, C. Y. Wang, Z. Guo, Y. G. Zhou, H. H. Wu, *Polym. Compos.* **2020**, 41(10), 4318.
- [24] A. Ichenihi, W. Li, Y. Gao, *Polym. Compos.* **2021**, 42(12), 6764.
- [25] S. Safaei, M. R. Ayatollahi, A. Akhavan-Safar, M. Moazzami, L. F. M. Da Silva, *J. Adhes.* **2021**, 97(11), 1052.
- [26] Z. Qin, K. Yang, J. Wang, L. Zhang, J. Huang, H. Peng, J. Xu, *J. Adhes.* **2021**, 97(11), 1024.
- [27] S. Akpınar, K. Demir, E. Gavali, A. F. Yetim, *J. Adhes.* **2021**, 98, 1972.
- [28] P. P. Camanho, C. G. Dávila, S. T. Pinho, L. Iannucci, P. Robinson, *Compos. A: Appl. Sci. Manuf.* **2006**, 37(2), 165.
- [29] W. S. Chan, *J. Compos. Technol. Res.* **1991**, 13(2), 91.
- [30] I. Verpoest, M. Wevers, P. De Meester, P. Declercq, *SAMPE J.* **1989**, 25(3), 51.
- [31] K. Dransfield, C. Baillie, Y. W. Mai, *Compos. Sci. Technol.* **1994**, 50(3), 305.
- [32] M. R. T. Arruda, M. Garrido, L. M. S. Castro, A. J. M. Ferreira, J. R. Correia, *Compos. Struct.* **2018**, 183, 103.
- [33] M. F. Caliri Jr., A. J. Ferreira, V. Tita, *Thin-Walled Struct.* **2021**, 163, 107648.
- [34] R. D. Campilho, M. F. S. F. De Moura, J. J. M. S. Domingues, *Compos. Sci. Technol.* **2005**, 65(13), 1948.
- [35] H. Akiyama, T. Fukata, T. Sato, S. Horiuchi, C. Sato, *J. Adhes.* **2020**, 96(15), 1311.
- [36] Y. Ohkubo, M. Shibahara, A. Nagatani, K. Honda, K. Endo, K. Yamamura, *J. Adhes.* **2020**, 96(8), 776.
- [37] R. Freund, S. Koch, H. Watschke, E. Stammen, T. Vietor, K. Dilger, *J. Adhes.* **2021**, 1, <https://doi.org/10.1080/00218464.2021.1983431>

How to cite this article: F. Ramezani, R. J. C. Carbas, E. A. S. Marques, A. M. Ferreira, L. F. M. da Silva, *Polym. Compos.* **2023**, 44(3), 1672. <https://doi.org/10.1002/pc.27196>

Paper C

**Out-of-plane tensile strength of CFRP laminates reinforced
by thin-ply under different loading rates**

Out-of-plane tensile strength of CFRP laminates reinforced by thin-ply under different loading rates

F. Ramezani¹, Ricardo J.C. Carbas^{*2}, Eduardo A.S. Marques² and Lucas F.M. da Silva²

¹Instituto de Ciência e Inovação Em Engenharia Mecânica e Engenharia Industrial (INEGI, Rua Dr. Roberto Frias, 4200-465 Porto, Portugal)

²Departamento de Engenharia Mecânica, Faculdade de Engenharia (FEUP, Universidade Do Porto, Rua Dr. Roberto Frias, 4200-465 Porto, Portugal)

(, ,)

Abstract. Delamination in composite laminates is primarily caused by transverse tensile stress. However, experimental and numerical studies have consistently shown that hybrid composite laminates, reinforced with thin-ply, exhibit greater strength under static transverse tensile loads in comparison to reference conventional composite laminates. This study focuses on analyzing the behavior of composite laminates reinforced by thin-ply, subjected to high-rate and impact transverse tensile loading. A conventional composite, Texipreg HS 160 T700, and a thin-ply, NTPPT-TP415, were selected for this investigation. Hybrid laminates were created by integrating 25% thin-ply throughout the laminate's thickness. Subsequently, unidirectionally stacked laminates were subjected to high-rate and impact transverse tensile loading.

The experimental results showed a slight increase in the transverse tensile strength of the hybrid laminate compared to the reference conventional composite under both high-rate and impact-loading conditions. To delve into the microscale behavior of these configurations, a representative volume element was analyzed using numerical methods, providing valuable insights into the studied setups.

Keywords. composite laminate; thin-ply; high-rate loading; impact loading

1. Introduction

The utilization of carbon fibre reinforced polymers (CFRP) is steadily increasing across various industries. A wide range of composites are now available for designing and manufacturing high-performance products, including vehicle structures, sporting goods, and consumer products (Ashby and Jones (2012) and Liu *et al.* 2021). Modern composites typically consist of two main components: the matrix, responsible for material cohesion, and the reinforcement, such as fibres, which provides strength and stiffness to the composite (Karatas and Gokkaya (2018)). However, due to the significantly lower strength of the matrix compared to the reinforcement, composites are prone to delamination failure. When loads are applied perpendicularly to the reinforcement, they are primarily borne by the weak matrix, leading to delamination. This susceptibility is particularly evident in bonded joints of composites, where load transfer through the joint can result in substantial peel stresses (Cantwell and Morton (1991)), induce cracks, rapidly degrade the mechanical performance of the structure, and ultimately lead to catastrophic failure (Su (1989)). Therefore, various techniques have been employed to enhance composite strength and delay delamination. For instance, laminates have been reinforced using adhesives, metallic films (Ramezani *et al.*

^{*}Corresponding author, Ph.D. Ricardo J.C. Carbas, E-mail: rcarbas@fe.up.pt

2022 and Simoes *et al.* 2022) or glass-fibre fabric reinforcement (Shang *et al.* 2019 and Ramezani *et al.* 2023a). Through-thickness reinforcement is a reliable approach to enhance interlaminar strength and delamination resistance in composite structures while promoting integration (Chan (1991)) including the utilization of weaves or braids. While these methods have proven to be effective, their complexity and limited flexibility often impose restrictions on their application. Additionally, these techniques typically involve the incorporation of an additional production step Verpoest *et al.* 1989 and Dransfield *et al.* 1994), leading to increased process costs.

An important advancement in the field of composites is the emergence of thin-ply laminates. Thin-ply laminates are characterized by layers that are less than 100 μm in thickness (Arteiro *et al.* 2018). This remarkable reduction in layer thickness has been made possible through the progress and industrialization of the spread-tow process (Sihn *et al.* 2007), which allows the production of flat, straight plies with a very thin dry ply thickness of just 0.02 mm. The use of thin-plies offers greater flexibility in laminate design. By decreasing the thickness of each individual layer, the number and orientation of layers in a laminate can be precisely controlled and adjusted to be more responsive to specific load conditions (Kotter *et al.* 2020). This increased control over laminate design enables optimization for enhanced performance and tailored mechanical properties. The larger number of layers and associated interfaces in thin-ply laminates contributes to lower shear stresses (Kotter *et al.* 2020). Consequently, thinner plies in composites are known to exhibit higher in-situ transverse strength (Wisnom *et al.* 2008), which depends not only on lamina thickness but also on the orientation of adjacent laminae (Flaggs and Kural (1982)). Moreover, the onset and propagation of free-edge delamination are influenced by ply thickness and stacking sequence (Kim and Sony (1984)). The utilization of thinner plies and the resin spreading process in thin-ply laminates contribute to a more homogeneous fibre distribution and reduced resin-rich regions (Amacher *et al.* 2014 and Ramezani *et al.* 2023b). However, it should be noted that laminate properties can still deteriorate rapidly after damage, potentially leading to premature failure (Guillamet *et al.* 2014).

Thin-ply laminates are renowned for their improved mechanical performance, as they exhibit the ability to delay matrix damage initiation, suppress transverse microcracking (Arteiro *et al.* 2018), and mitigate free edge delamination (Kotter *et al.* 2020), under static, fatigue, and impact loads. Remarkably, these enhancements can be achieved without relying on high-performance resins or 3-D reinforcements, which are typically required in conventional composites (Zubillaga *et al.* 2015, Yokozeki *et al.* 2008, and Minia and York (2017)). As a result, failure modes in thin-ply laminates shift from complex multimode failure processes to a more quasi-brittle failure mode, particularly in thinner plies (Sihn *et al.* 2007).

Experimental data indicates that in ultra-thin-ply laminates, failure predominantly occurs through direct delamination triggered by shear forces and minor matrix cracking. In contrast, laminates with thicker plies primarily experience damage onset through matrix cracking, which subsequently induces delamination and occurs earlier compared to laminates with thinner plies. Additionally, fibre breakage tends to manifest earlier in ultra-thin-ply laminates (Wagih *et al.* 2016). Considering that composite laminates often exhibit brittle failure and are susceptible to damage accumulation, such as matrix cracks and delamination, interlaminar properties play a crucial role in enhancing the overall performance of these laminates (Huang *et al.* 2018). Thin-ply laminates, with their superior resistance to damage

and delamination, have the potential to exhibit higher interlaminar shear properties (Huang *et al.* 2018) and strain energy (Kupski *et al.* 2020) compared to conventional plies.

In a previous study (Ramezani *et al.* 2023c), the authors demonstrated that the replacement of the conventional composite with optimum layers of thin-ply resulting in hybrid composite laminates could increase the transverse tensile strength of the hybrid laminate loaded statically. The hybrid (25% thin-ply) laminates were fabricated by incorporating 25% of thin-ply throughout the laminate's thickness. The current study seeks to study and quantify the performance of hybrid (25% thin-ply) laminate reinforced by thin-ply under high-rate and impact transverse tensile loading.

2. Experimental detail

2.1. Material

2.1.1 Conventional composite

The materials employed in this study were carefully chosen to accurately reflect those commonly utilized in the aerospace industry. For the conventional composite, a unidirectional carbon-epoxy prepreg with a ply thickness of 0.15 mm was selected. This prepreg, known as Texipreg HS 160 T700 (manufactured by Seal Spa, Legnano, Italy), served as the commercial reference material and has the following mechanical properties: Young's modulus ($E_1=109.0$ and $E_2=8.8$ GPa), shear modulus ($G_{12}=4.3$ and $G_{13}=3.2$ GPa), fracture energy ($G_{IC}=0.6$ and $G_{IIC}=1.2$ N/mm) (Campilho *et al.* 2005 and Machado *et al.* 2017).

2.1.2 Thin-ply

For the thin-ply material, a unidirectional 0° oriented carbon-epoxy prepreg with a ply thickness of 0.07 mm was selected. This thin-ply has the commercial reference NTPT-TP415 and the following mechanical properties: Young's modulus ($E_1=101.7$ and $E_2=5.7$ GPa), shear modulus ($G_{12}=3.0$ and $G_{13}=3.0$ GPa), fracture energy ($G_{IC}=0.7$ and $G_{IIC}=0.8$ N/mm) (Ramezani *et al.* 2023d).

2.2 Plate manufacturing

Both the reference conventional and thin-ply composite laminates have been created following a similar manufacturing process, which involves stacking the plies layer by layer. This stacking process is repeated until the desired thickness of the laminate is achieved. In the case of the hybrid (25% thin-ply) laminate, thin-ply layers are strategically positioned on the outer surfaces and central part of a conventional composite laminate. The mentioned configuration was found to present considerably higher transverse tensile strength under static loading (Ramezani *et al.* 2023c). This configuration allows for a combination of thin-ply and conventional layers, resulting in the formation of the hybrid (25% thin-ply) laminate. Hybrid (25% thin-ply) laminates were fabricated by incorporating 25% of thin-ply throughout the laminate's thickness. Fig. 1 schematically illustrates the design of the hybrid (25% thin-ply) laminate. To maintain consistency, all configurations were designed to have the same overall thickness of 3.2 mm. To ensure uniform thickness throughout the plate, a

mould was employed during the manufacturing process. The mould was appropriately coated with a release agent to facilitate the easy removal of the finished plates. Subsequently, the plates were cured in a hot press under specific conditions of 30 bar pressure and a temperature of 130°C for a duration of two hours, following the recommendations provided by the manufacturer.

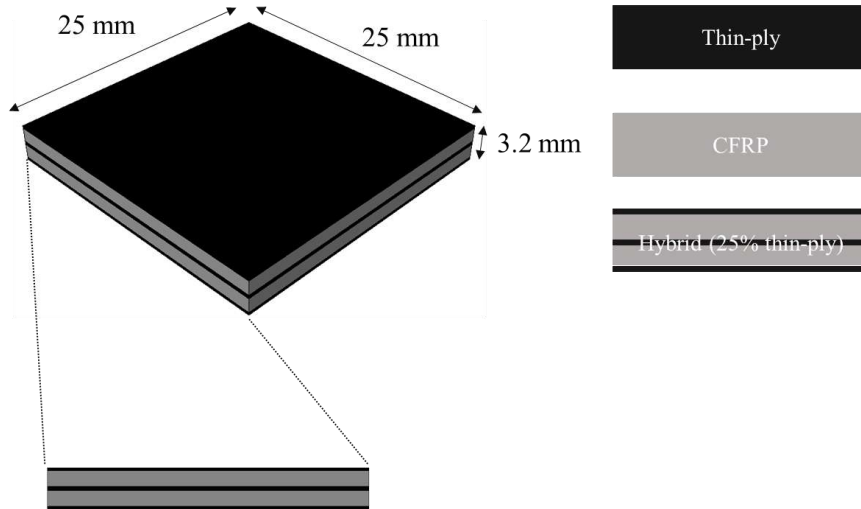


Fig. 1 Schematic design for hybrid (25% thin-ply) laminate

Following the curing process, the plates were carefully cut to the desired dimensions of (25×25 mm²). Subsequently, steel blocks, as depicted in Fig. 2, were affixed to the composite laminates using the Araldite 420 A/B adhesive. This adhesive is designed to cure at room temperature over a 24-hour period. Any excess adhesive or resin present on the specimens after curing was manually removed using a file and sandpaper, ensuring a clean and precise surface.

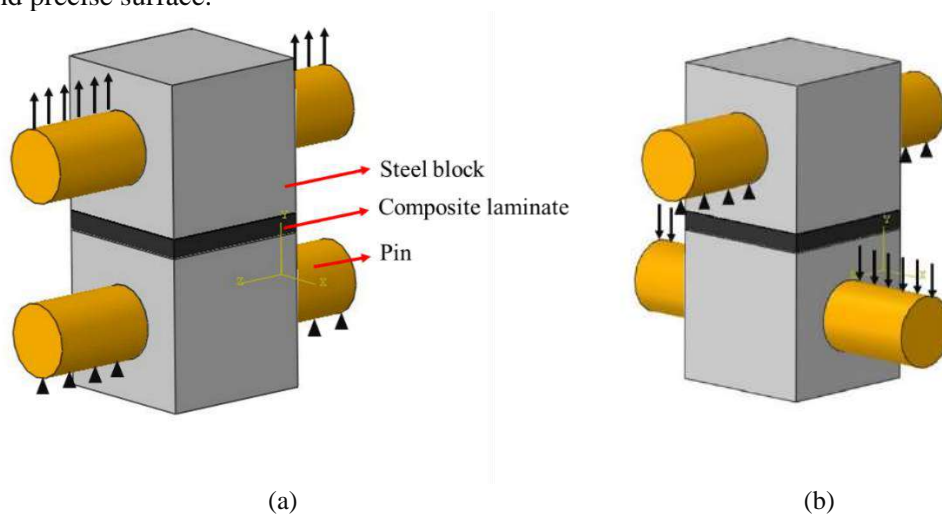


Fig. 2 Schematic design of steel blocks attached to composite laminates at (a) high-rate and (b) impact loading condition

2.3 Surface treatment

To prepare the specimens for tensile testing, the composite laminates were affixed to steel blocks, as depicted in Fig. 2. To prepare the surface of the composite laminates for bonding to the steel blocks, a light sandpaper was used to smoothen the surface, followed by cleaning with acetone to remove any contaminants (Akiyama *et al.* 2020), including the residual release agent used during the plate manufacturing step (as discussed in Section 2.2).

In order to enhance the surface energy and promote bonding, plasma treatment was conducted on the composite surfaces (Ohkubo *et al.* 2020 and Freund *et al.* 2021). This plasma treatment was carried out using an Arcojet PG 051 plasma device, operating at a frequency of 50-60 Hz. The nozzle of the device was positioned approximately 20 mm away from the surface of the composite laminates, and the treatment was applied for a duration of 5 seconds. The surface of the steel blocks was sandblasted, followed by a degreasing process using acetone to ensure the removal of any residual contaminants.

2.4 Testing conditions

The specimens were tested at two different constant crosshead rates, 0.1 and 2 m/sec. For high-rate loading, an Instron 8801 servo hydraulic testing machine equipped with a 100 kN load cell was utilized. To conduct impact tests on the specimens, an in-house developed drop-weight impact testing machine was employed (Antunes *et al.* 2019). This testing machine grips the upper part of the adherend, while leaving the lower portion free. A mass is then dropped from a specific height and impacts on the lower part of the grip. This subjects the specimen to a high-rate tension-shear loading. The impact velocity is determined by the drop height, following the principle of energy conservation. In this study, a 50 kg mass and an impact velocity of 2 m/s were chosen, resulting in an impact energy of 100 J.

All tests were carried out under laboratory ambient conditions with a room temperature of 24°C and a relative humidity of 55%. Four test repetitions were carried out for each configuration under analysis, ensuring reliable and consistent results.

3. Experimental results

Figs. 3-4 present the representative experimentally obtained load-displacement curves for the thin-ply, conventional composite, and hybrid (25% thin-ply) laminates under high-rate and impact loading, respectively. For both loading conditions, it was observed that the reference thin-ply configuration exhibited the lowest transverse tensile strength when compared to other configurations. However, an interesting finding was that the reference thin-ply laminate demonstrated a significant increase in displacement at the point of failure under impact loading, in comparison to the reference conventional composite. This suggests that while the transverse tensile strength may be lower for the reference thin-ply configuration, it possesses a greater ability to deform and absorb energy during impact events, leading to larger displacements before failure occurs. It also emphasizes the potential benefits of thin-ply laminates in terms of impact resistance and deformation capability, despite their lower transverse tensile strength compared to conventional composites. Furthermore, this provides an explanation for the ductile behaviour of the thin-ply over that of the conventional composite (Ramezani *et al.* 2023c). Moreover, it was observed that the

reference conventional composite and the hybrid (25% thin-ply) laminate exhibited similar strength characteristics under 0.1 m/sec loading conditions. However, when subjected to impact loading, the hybrid (25% thin-ply) laminate demonstrated higher transverse tensile strength and displacement at the point of failure in comparison to the reference conventional composite. These findings suggest that the inclusion of thin-ply layers in the hybrid (25% thin-ply) laminate contributes to improved performance and enhanced resistance to transverse tensile forces during impact loading.

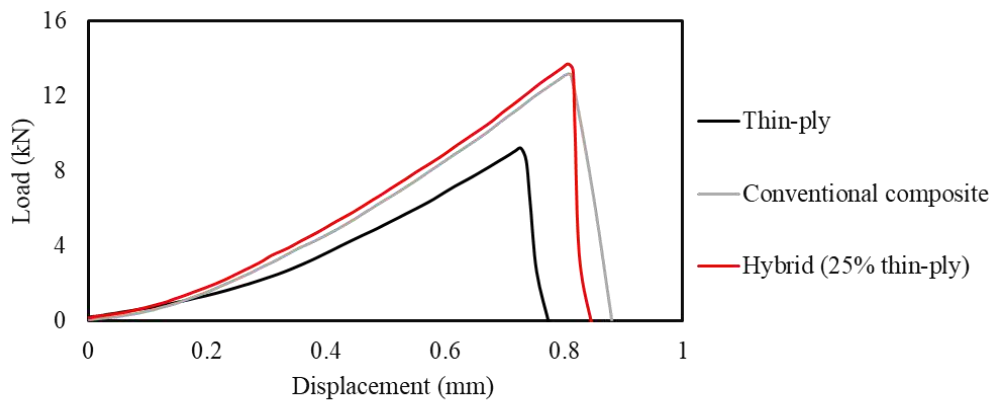


Fig. 3 Representative experimentally obtained load-displacement curves for thin-ply, conventional composite, and hybrid (25% thin-ply) laminates, loading under 0.1 m/sec

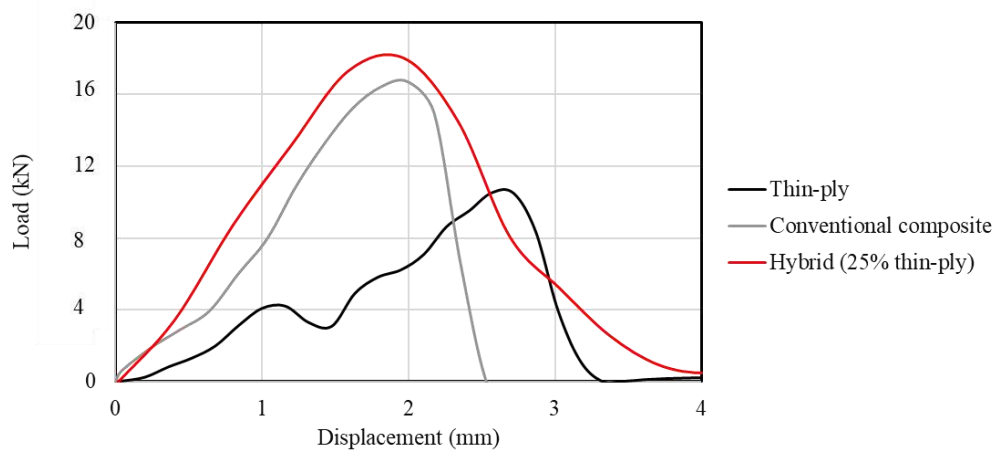


Fig. 4 Representative experimentally obtained load-displacement curves for thin-ply, conventional composite, and hybrid (25% thin-ply) laminates under impact loading (2 m/sec)

Fig. 5-6 presents the specimens after failure, illustrating the crack path through the thickness for the reference thin-ply, conventional composite, and the hybrid (25% thin-ply) laminates under high-rate and impact loading respectively. Under both high-rate and impact

loading conditions, the crack propagation through the thickness is more prominent in the reference conventional composite and thin-ply laminates.

However, in the case of hybrid (25% thin-ply) laminate, the crack initiation primarily occurs in the conventional composite and then propagates towards the interface between the conventional composite and the thin-ply. In certain cases, after reaching the interface, the crack propagates back into the conventional composite. This observation highlights the thin-ply resistance against crack propagation and its effective role of as a barrier to crack propagation, promoting a more uniform distribution of fibres and minimizing the presence of resin-rich and fibre-rich areas. Consequently, stress concentrations are reduced, and the hybrid (25% thin-ply) laminates can sustain load levels.

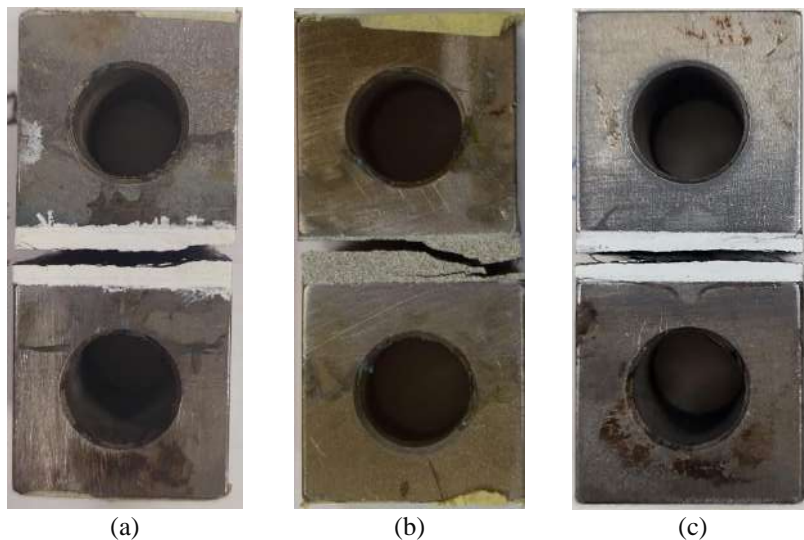


Fig. 5 Failure mechanism for (a) thin-ply, (b) conventional composite and (c) hybrid (25% thin-ply) laminates under high-rate loading

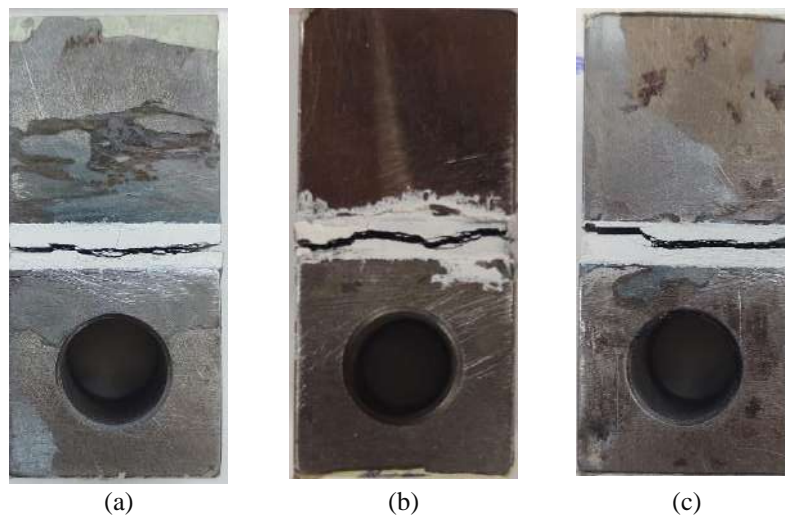


Fig. 6 Failure mechanism for (a) thin-ply, (b) conventional composite and (c) hybrid (25% thin-ply) laminates under impact loading

The examination of failure surfaces in both the reference conventional composite and the hybrid laminates, featuring a 25% thin ply content, was conducted utilizing a ZEISS AXIOPHOT microscope. Based on the microscopic images from the failure surface of the conventional composite and hybrid (25% thin-ply) laminate depicted in Fig. 7, the failure surface of the reference conventional composite revealed the presence of numerous instances of fiber breakages (Liu *et al.* 2012) fibre pull-outs (Okoli and Smith (1998)) and fibre matrix debonding. In contrast, these specific failure mechanisms were significantly less common on the failure surface of the hybrid joint, as demonstrated in this analysis.

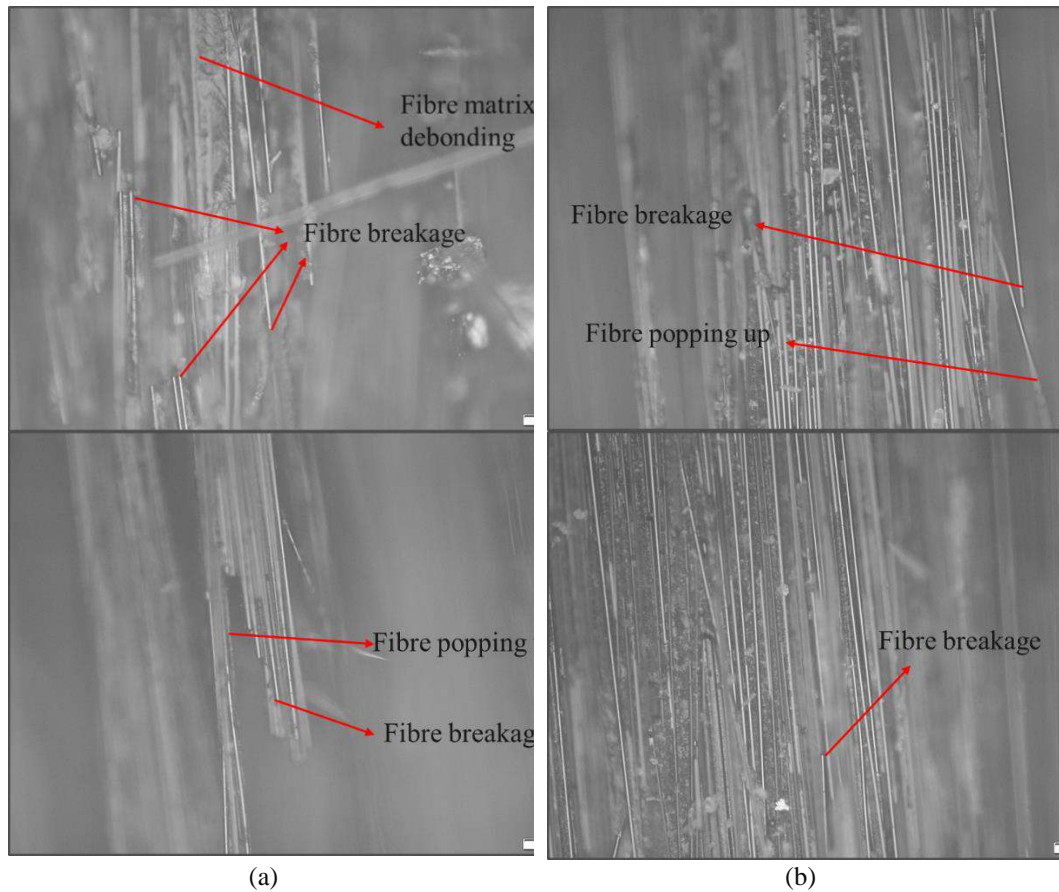


Fig. 7 Microscopic images of (a) conventional composite and (b) hybrid (25% thin ply) laminates

4. Numerical study

To investigate the mechanical behaviour and better understand the advantages of reinforcing composite laminates with thin-ply at the micro-scale, a representative volume element (RVE) model was developed. The RVE model employed a large 2-D elastoplastic analysis and was created using the ABAQUS commercial finite element package. The

dimensions of the RVE model were set at $1.60 \times 1.60 \text{ mm}^2$ to ensure the analysis could encompass all configurations under study.

Initially, a smaller-scale RVE model of the conventional composite and thin-ply was generated with dimensions of $0.20 \times 0.20 \text{ mm}^2$ (see Fig. 8). This smaller-scale RVE model was designed to closely replicate the fibre distribution observed in scanning electron microscopy (SEM) images (Ramezani *et al.* 2023c). By doing so, the model aimed to accurately capture the presence of resin-rich and fibre-rich areas.

The purpose of this RVE analysis was to gain insights into the distribution of fibres within the composite material, mirroring the real-world characteristics observed through SEM images. This enabled the model to reproduce the resin-rich and fibre-rich regions, thus providing a more realistic representation of the material properties and behaviour at the micro-scale. In the numerical models, the following material properties were assigned to the matrix and fibres which are based on the information provided by the supplier. For the conventional composite, the fibre Young's modulus (E_f)= 230 GPa, matrix Young's modulus (E_m)= 3.6 GPa and the matrix maximum strength (σ)=148 MPa and for the thin-ply, the fibre Young's modulus (E_f)= 294 GPa, matrix Young's modulus (E_m)= 3.3 GPa and the matrix maximum strength (σ)=138 MPa was reported. The fibre diameter (D) and the fibre volume fraction (V_f) for both conventional composite and thin-ply was reported 7 (μm) and 0.35 respectively. A total of 293 fibres were used in these initial RVEs (see Fig. 8).

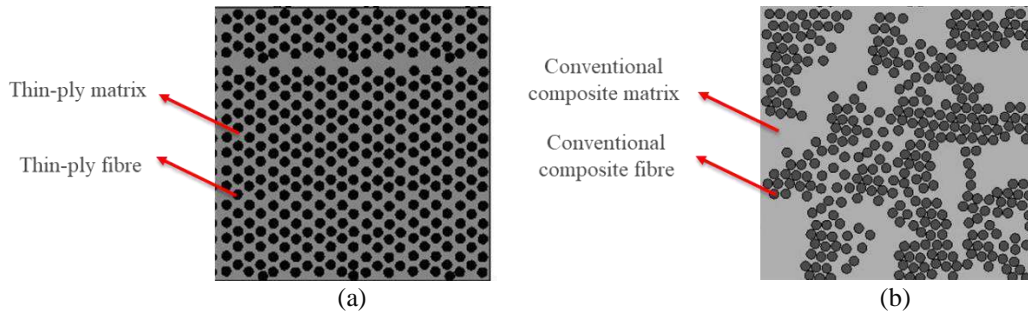


Fig. 8 Initial RVE for the (a) thin-ply and (b) conventional composite

Afterwards, the initial representative volume element (RVE) was replicated in the main RVE for the thin-ply, conventional composite and the hybrid (25% thin-ply) configuration. Fig. 9 provides an illustration of the RVEs generated for these configurations. The same boundary conditions were applied to all RVE models, as shown in Fig. 9. A displacement of 0.04 mm with an amplitude of 4×10^{-4} and 2×10^{-5} was imposed to the top edge to mimic the dynamic high-rate and impact loading conditions respectively. Two-dimensional, 3-node linear plane stress triangular elements were utilized to discretize the model and create the mesh.

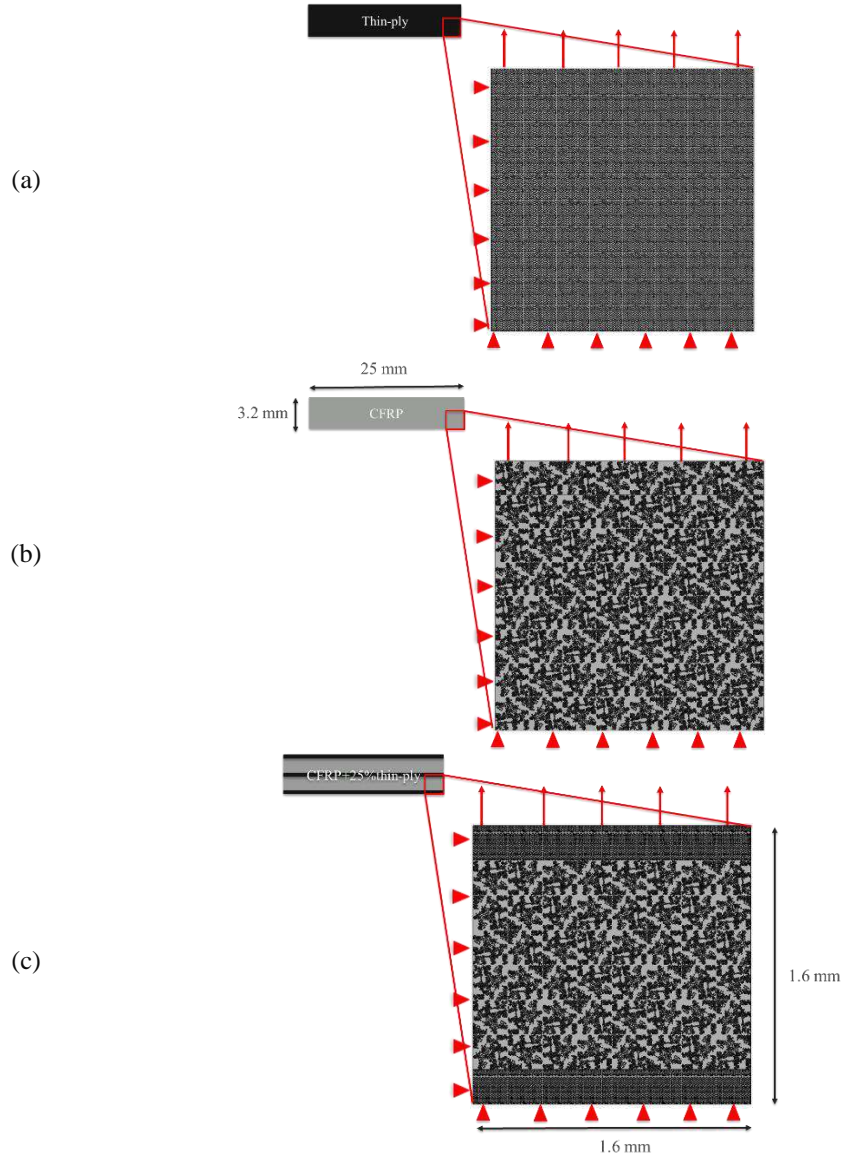
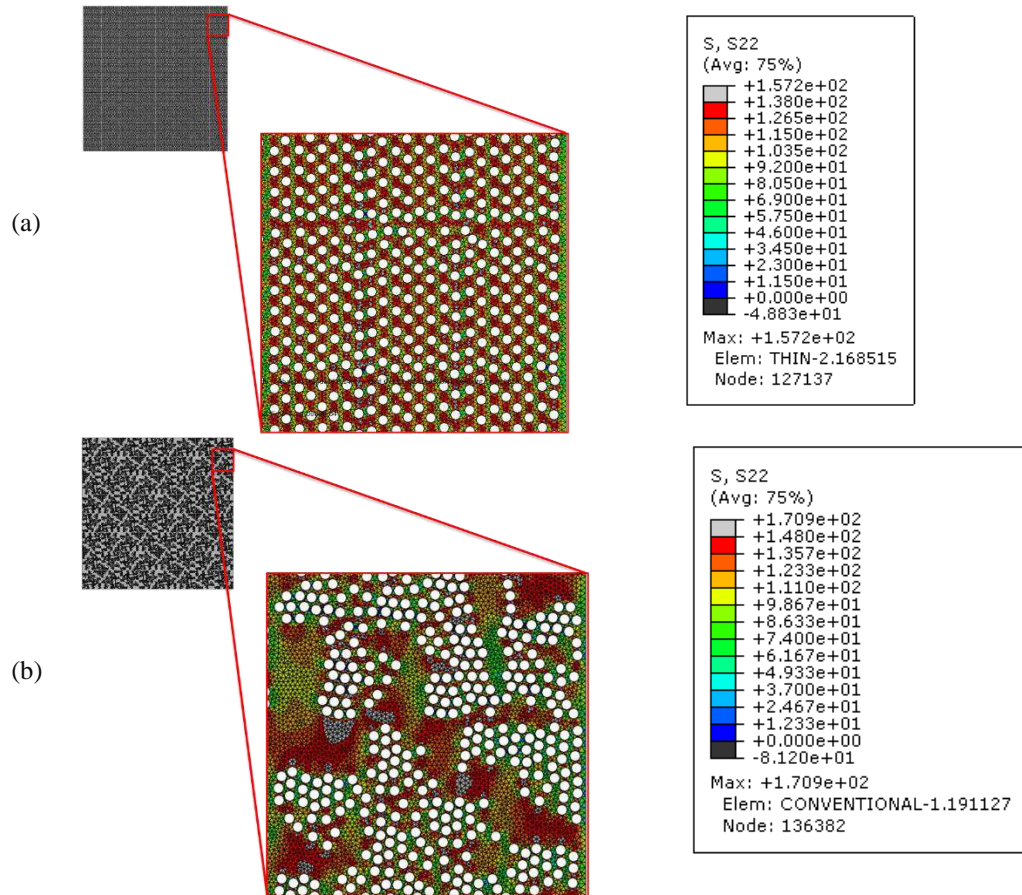


Fig. 9 Simulated RVE for (a) thin-ply, (b) conventional composite and (c) hybrid (25% thin-ply) configurations

Figs. 10-11 display the distribution of peel stress within each representative volume element (RVE) when subjected to a displacement of 0.04 mm under high-rate and impact loading, respectively. To focus on the behaviour of the matrix, the stress values in the fibres, which can withstand significantly higher stresses, were omitted from the results. The colour scale is limited to the maximum stress within the matrix of the conventional composite (148 MPa), and any elements with stress values exceeding this limit are shown in grey.

In Figs. 10-11, it can be observed that some elements in the RVE corresponding to the conventional composite have surpassed the maximum strength of the matrix, indicating the initiation of matrix failure. It should be noted that if the colour scale were limited to the maximum strength of the thin-ply matrix (138 MPa), a larger area would exceed the matrix

strength in each configuration. The results for the hybrid (25% thin-ply) configuration are taken at the interface between the conventional composite and the thin-ply since the interface was shown to be crucial. Therefore, the same location was used to display the result of the peel stress distribution for the thin-ply and the conventional composite laminates. In the case of the hybrid (25% thin-ply) model, a lower level of stress and a smaller number of elements exceeding the conventional composite matrix maximum strength compared to the conventional composite model for both high rate and impact loading. These results are consistent with the experimental observations.



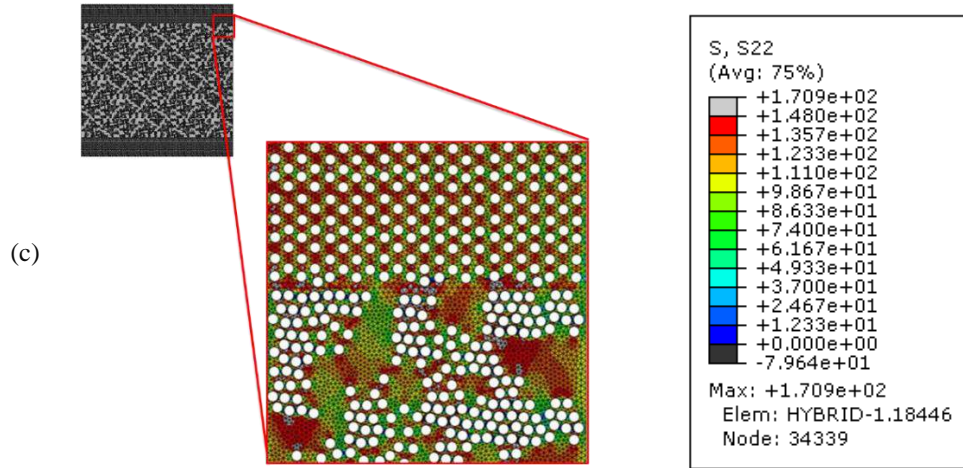
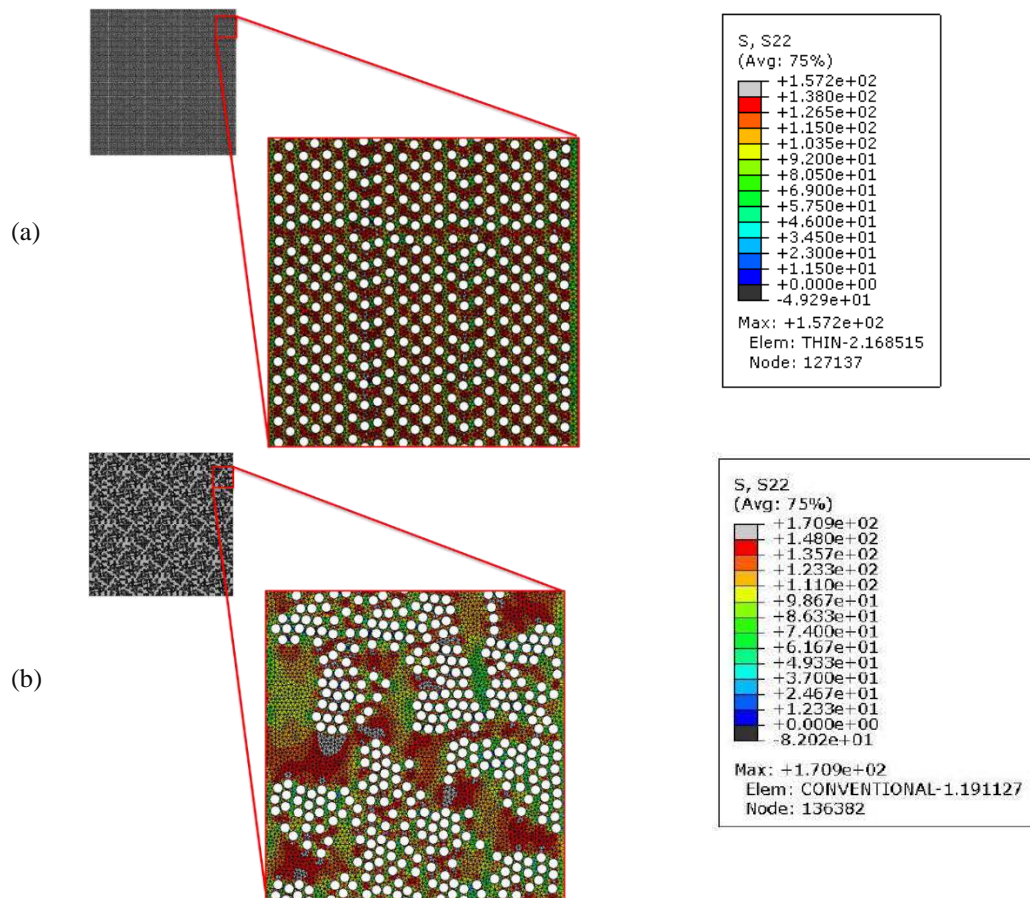


Fig. 10 Peel stress distribution for (a) thin-ply, (b) conventional composite, (c) hybrid (25% thin-ply) configuration at displacement of 0.04 mm under high-rate loading



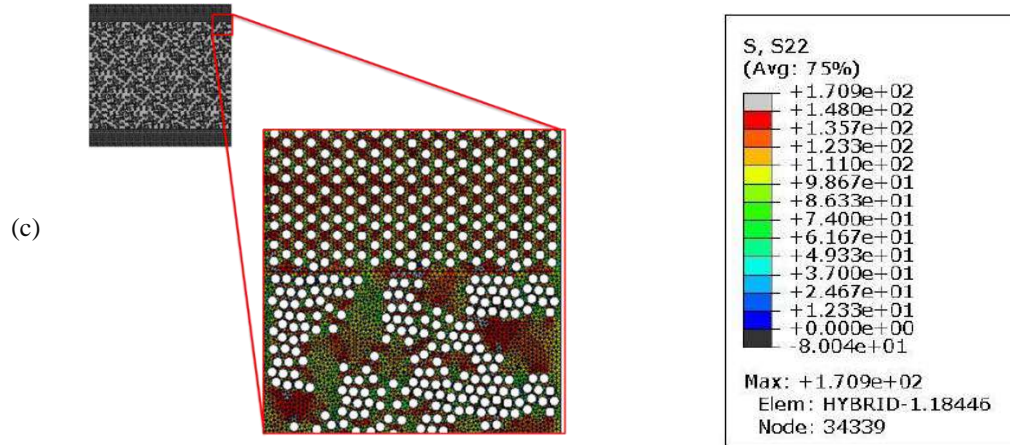


Fig. 11 Peel stress distribution for (a) thin-ply, (b) conventional composite, (c) hybrid (25% thin-ply) configuration at displacement of 0.04 mm under impact loading

Fig. 12 shows the level of failure, which is calculated by dividing the area of failed elements (grey elements) by the total area (Ramezani *et al.* 2023c). It should be noted that the total area under analysis was common to all numerical models. This ratio was precisely quantified using the IC-Measure software and the obtained results have shown that the hybrid (25% thin-ply) laminates present a lower level of failure for both the high-rate and the impact loading condition.

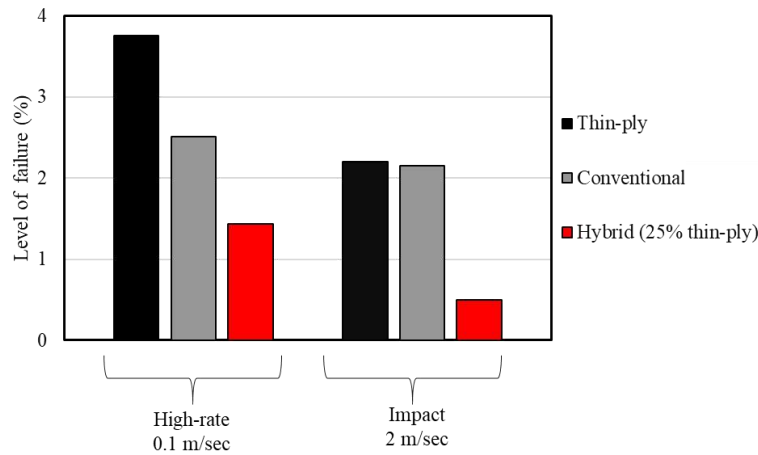


Fig. 12 Level of failure for the thin-ply, conventional composite and hybrid (25% thin-ply) configurations under high-rate and impact loading

5. Discussion

Fig. 13 provides a comprehensive summary of the experimental results obtained in this study. The findings indicate that replacing a portion of the conventional composite layers with thin-ply layers, up to a 25% content, enhances the strength of the composite laminate under transverse tensile loads. Earlier studies indicate that thin-ply materials demonstrate a more ductile behavior and are relatively weaker than conventional composites. However, conventional composite laminates, while stiffer, have a higher likelihood of experiencing

premature failure due to their inherent characteristics. Therefore, the observed increase in failure load under transverse tensile loading can primarily be attributed to the improved ductility of the laminate, resulting from the incorporation of thin-ply layers in hybrid (25% thin-ply) laminates.

SEM images support these conclusions by revealing a reduction in the presence of resin and fibre-rich regions within the thin-ply layer. Indeed, the crack propagation through the thickness is evident in the reference conventional composite and thin-ply laminates. This suggests that these configurations are more susceptible to crack propagation and do not exhibit strong resistance against crack propagation. The ease of crack propagation in these laminates can be attributed to factors such as stress concentrations, resin-rich and fibre-rich regions, and possibly lower interlaminar shear strength. However, the crack path through the thickness for the thin-ply is more even compared to the more unstable crack path through the thickness in the conventional composite laminate. This can be attributed to the more uniform fibre distribution in thin-ply laminate. The uniform fibre distribution in thin-ply laminates is achieved due to the thinner individual plies and the resin spreading process associated with these materials. This results in a more homogeneous distribution of fibres throughout the laminate, reducing the presence of resin-rich and fibre-rich areas. Therefore, the more uniform fibre distribution in thin-ply laminates plays a significant role in promoting more even crack paths through the thickness, contributing to their enhanced mechanical properties compared to conventional composite laminates.

On the other hand, the hybrid (25% thin-ply) laminate shows a different behaviour, with the crack being restricted mainly to the interface between the conventional composite and thin-ply. This indicates that the presence of the thin-ply layer acts as a barrier to crack propagation, effectively impeding the crack from propagating through the thickness. The improved crack resistance in the hybrid (25% thin-ply) laminate can be attributed to a more uniform fibre distribution, reduced resin-rich and fibre-rich areas, and possibly enhanced interfacial bonding between the conventional composite and thin-ply layers. Overall, the crack propagation behaviour observed in the different laminates highlights the advantages of the hybrid (25% thin-ply) configuration in terms of improved crack resistance and reduced susceptibility to crack propagation through the thickness. The schematic representation in Figs. 14-15 illustrates the proposed failure mechanism in the reference thin-ply, conventional composite, and hybrid (25% thin-ply) laminates under high-rate and impact loading respectively, as described above. Although thin-ply materials exhibit a more ductile behavior, they offer advantages in terms of enhanced resistance against certain failure modes, which can contribute to improved overall performance and durability in specific applications.

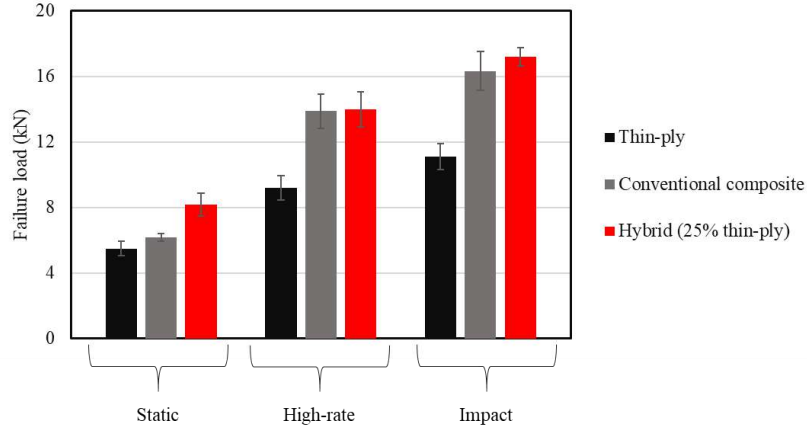


Fig. 13 Summary of the experimental results for thin-ply, conventional composite, and hybrid (25% thin-ply) laminates under static (Ramezani *et al.* 2023c), high-rate and impact loading

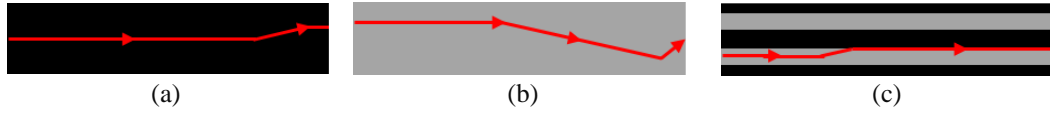


Fig. 14 Schematic design of failure mechanism for (a) thin-ply, (b) conventional composite and (c) hybrid (25% thin-ply) laminates under high-rate loading

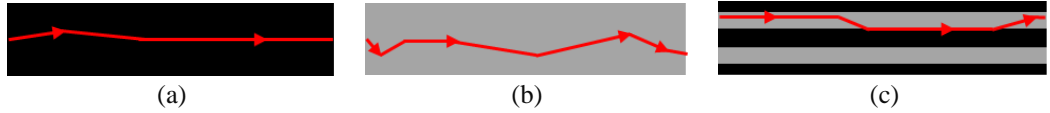


Fig. 15 Schematic design of failure mechanism for (a) thin-ply, (b) conventional composite and (c) hybrid (25% thin-ply) laminates under impact loading

The numerical model used in the previous study by the authors (Ramezani *et al.* 2023c) for the hybrid (25% thin-ply) configuration under static loading was replicated to enable a direct comparison with the numerical results obtained under high-rate and impact loading conditions. Fig. 16 depicts the peel stress distribution of the hybrid (25% thin-ply) under static loading at the displacement of 0.04 mm. The level of failure obtained was then compared with the ones obtained under high rate and impact loading as shown in Fig. 17(a). As observed, the level of failure decreases as the loading speed transitions from static to high-rate and from high-rate to impact loading. This observation is corroborated by the experimentally obtained failure loads presented in Fig. 17(b) demonstrating an increase in the failure load as the loading condition shifts from static loading to high-rate and from high-rate to impact loading.

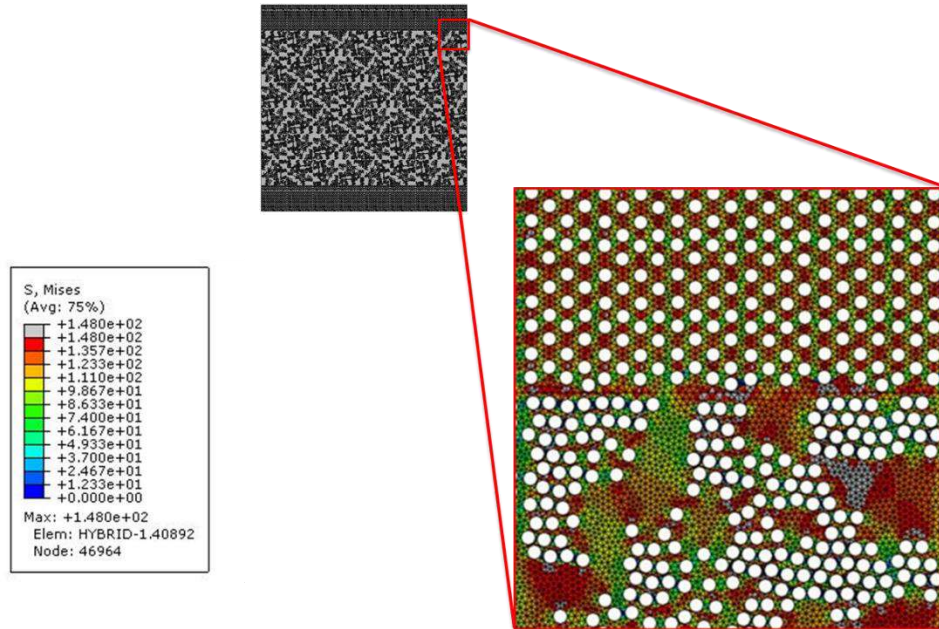


Fig. 16 Peel stress distribution for the hybrid (25% thin-ply) configuration at displacement of 0.04 mm under static loading

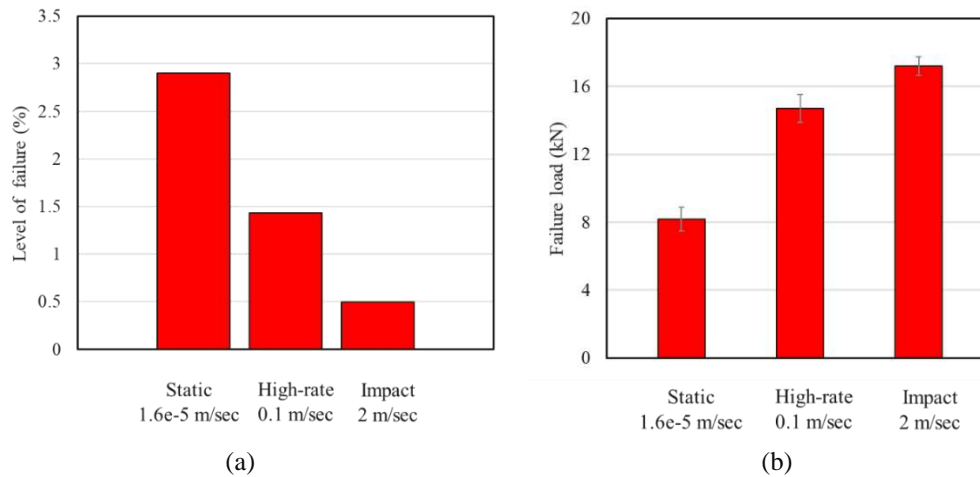


Fig. 17 (a) Level of failure and (b) experimentally obtained failure load for the hybrid (25% thin-ply) configuration under static, high-rate and impact loading

6. Conclusions

This work studied the effect of reinforcing unidirectional conventional composite laminates using thin-ply under high-rate and impact transverse tensile loading.

- Experimental findings indicate that the hybrid (25% thin-ply) composite laminates exhibit a 25.5% higher failure load under static loading and a 5% higher failure load under impact loading, compared to the reference conventional composite laminate. This enhanced strength can be primarily attributed to the increased ductility resulting from the presence of

thin-ply. However, both the conventional composite and hybrid (25% thin-ply) laminates demonstrate similar strength under high-rate loading conditions.

- In the hybrid (25% thin-ply) laminates, the thin-ply layers act as a barrier against crack propagation for both high-rate and impact loading. Consequently, the crack is predominantly confined to the interface between the conventional composite and thin-ply layers. Analysis of the failure mechanism reveals that the thin-ply layers effectively impede crack propagation, primarily due to their more uniform fibre distribution and reduced presence of resin-rich and fibre-rich areas.

- Numerical simulations using a 2D representative volume element model were conducted for the reference conventional composite and hybrid (25% thin-ply) configurations under both high-rate and impact loading. The results indicate that the conventional composite model exhibits a larger number of elements surpassing the maximum strength of the matrix (which have failed) compared to the hybrid (25% thin-ply) model.

- The numerical model for the hybrid (25% thin-ply) was replicated under static loading and compared to the ones under high-rate and impact loading. The results illustrated a decrease in failure level as the loading speed transitions from static to high-rate and from high-rate to impact loading which is consistent with the experimental observations.

Acknowledgments

The authors gratefully acknowledge the Portuguese Foundation for Science and Technology (FCT) for supporting the work presented here, through the individual grant's CEECIND/03276/2018 and 2021.07943.BD, and the Project No. PTDC/EME-EME/2728/2021 'New approaches to improve the joint strength and reduce the delamination of composite adhesive joints.

Reference

- Akiyama, H., Fukata, T., Sato, T., Horiuchi, S. and Sato, C. (2020) "Influence of surface contaminants on the adhesion strength of structural adhesives with aluminium", *Adhesion*, **96**(15), 1311-1325. <https://doi.org/10.1080/00218464.2019.1598393>.
- Amacher, R., Cugnoni, J., Botsis, J., Sorensen, L., Smith, W. and Dransfeld, C. (2014), "Thin ply composites: Experimental characterization and modeling of size-effects", *Composites Science and Technology*, **101**, 121-132. <https://doi.org/10.1016/j.compscitech.2014.06.027>.
- Antunes, D.P.C., Lopes, A.M., Moreira da Silva, C.M.S., da Silva, L.F.M., Nunes, P.D.P., Marques, E.A.S. and Carbas, R.J.C. (2019), "Development of a drop weight machine for adhesive joint testing", *Testing and Evaluation*, **49**(3), 20190147. <http://dx.doi.org/10.1520/jte20190147>.

- Arteiro, A., Catalanotti, G., Xavier, J., Linde, P. and Camanho, P.P. (2018), "A strategy to improve the structural performance of non-crimp fabric thin-ply laminates", *Composite Structures*, **188**, 438-449. <https://doi.org/10.1016/j.compstruct.2017.11.072>.
- Ashby, M.F. and Jones, D.R. (2012), *Engineering Materials 1: An Introduction to Properties, Applications and Design*, Elsevier, Amsterdam, Netherlands.
- Campilho, R.D., De Moura, M.F.S.F. and Domingues, J.J.M.S. (2005), "Modelling single and double-lap repairs on composite materials". *Composites Science and Technology*, **65**(13), 1948-1958. <https://doi.org/10.1016/j.compscitech.2005.04.007>.
- Cantwell, W.J. and Morton, J. (1991), "The impact resistance of composite materials—a review", *Composites*, **22**(5) 347-362. [https://doi.org/10.1016/0010-4361\(91\)90549-V](https://doi.org/10.1016/0010-4361(91)90549-V).
- Chan, W.S. (1991) "Design approaches for edge delamination resistance in laminated composites", *Composites Technology and Research*, **13**(2), 91-96. <https://doi.org/10.1520/CTR10212J>.
- Dransfield, K., Baillie, C. and Mai, Y.W. (1994), "Improving the delamination resistance of CFRP by stitching—a review", *Composites Science and Technology*, **50**(3), 305-317. [https://doi.org/10.1016/0266-3538\(94\)90019-1](https://doi.org/10.1016/0266-3538(94)90019-1).
- Flaggs, D.L. and Kural, M.H. (1982), "Experimental determination of the in situ transverse lamina strength in graphite/epoxy laminates", *Composite Materials*, **16**(2), 103-116. <https://doi.org/10.1177/002199838201600203>.
- Freund, R., Koch, S., Watschke, H., Stammen, E., Vietor, T. and Dilger, K. (2021) "Utilization of additively manufactured lattice structures for increasing adhesive bonding using material extrusion", *Adhesion*, 1-22. <https://doi.org/10.1080/00218464.2021.1983431>.
- Guillamet, G., Turon, A., Costa, J., Renart, J., Linde, P. and Mayugo, J.A. (2014), "Damage occurrence at edges of non-crimp-fabric thin-ply laminates under off-axis uniaxial loading", *Composites Science and Technology*, **98**, 44-50. <https://doi.org/10.1016/j.compscitech.2014.04.014>.
- Huang, C., He, M., He, Y., Xiao, J., Zhang, J., Ju, S. and Jiang, D. (2018), "Exploration relation between interlaminar shear properties of thin-ply laminates under short-beam bending and meso-structures", *Composite Materials*, **52**(17), 2375-2386. <https://doi.org/10.1177/0021998317745586>.
- Karataş, M.A. and Gökkaya, H. (2018), "A review on machinability of carbon fiber reinforced polymer (CFRP) and glass fiber reinforced polymer (GFRP) composite materials", *Defence Technology*, **14**(4), 318-326. <https://doi.org/10.1016/j.dt.2018.02.001>.
- Kim, R.Y. and Soni, S.R. (1984), "Experimental and analytical studies on the onset of delamination in laminated composites", *Composite Materials*, **18**(1), 70-80. <https://doi.org/10.1177/002199838401800106>.
- Kötter, B., Karsten, J., Körbelin, J. and Fiedler, B. (2020), "CFRP thin-ply fibre metal laminates: Influences of ply thickness and metal layers on open hole tension and compression properties", *Materials*, **13**(4), 910. <https://doi.org/10.3390/ma13040910>.

- Kupski, J., Zarouchas, D. and de Freitas, S.T. (2020), "Thin-ply in adhesively bonded carbon fiber reinforced polymers", *Composites Part B: Engineering*, **184**, 107627. <https://doi.org/10.1016/j.compositesb.2019.107627>.
- Liu, B., Zhang, Q., Li, X., Guo, Y., Zhang, Z., Yang, H. and Yuan, Y. (2021), "Potential advantage of thin-ply on the composite bolster of a bogie for a high-speed electric multiple unit", *Polymer Composites*, **42**(7), 3404-3417. <https://doi.org/10.1002/pc.26067>.
- Liu, P.F., Chu, J.K., Liu, Y.L. and Zheng, J.Y. (2012), "A study on the failure mechanisms of carbon fiber/epoxy composite laminates using acoustic emission", *Materials & Design*, **37**, pp.228-235. <https://doi.org/10.1016/j.matdes.2011.12.015>.
- Machado, J.J.M., Marques, E.A.S., Campilho, R.D.S.G. and da Silva, L.F. (2017), "Mode I fracture toughness of CFRP as a function of temperature and strain rate". *Composite Materials*, **51**(23), 3315-3326. <https://doi.org/10.1177/0021998316682309>.
- Mania, R.J. and York, C.B. (2017), "Buckling strength improvements for Fibre Metal Laminates using thin-ply tailoring", *Composite Structures*, **159**, 424-432. <https://doi.org/10.1016/j.compstruct.2016.09.097>.
- Okoli, O.I. and Smith, G.F. (1998) "Failure modes of fibre reinforced composites: The effects of strain rate and fibre content". *Materials Science*, **33**, 5415-5422. <https://doi.org/10.1023/a:1004406618845>.
- Ohkubo, Y., Shibahara, M., Nagatani, A., Honda, K., Endo, K. and Yamamura, K. (2020), "Comparison between adhesion properties of adhesive bonding and adhesive-free adhesion for heat-assisted plasma-treated polytetrafluoroethylene (PTFE)", *Adhesion*, **96**(8), 776-796. <https://doi.org/10.1080/00218464.2018.1512859>.
- Ramezani, F., Simões, B.D., Carbas, R.J., Marques, E.A. and da Silva, L.F. (2023a), "Developments in laminate modification of adhesively bonded composite joints", *Materials*, **16**(2), 568. <https://doi.org/10.3390/ma16020568>.
- Ramezani, F., Carbas, R.J., Marques, E.A. and da Silva, L.F. (2023b), "Study of hybrid composite joints with thin-ply-reinforced adherends", *Materials*, **16**(11), 4002. <https://doi.org/10.3390/ma16114002>.
- Ramezani, F., Carbas, R.J., Marques, E.A., Ferreira, A.M. and da Silva, L.F. (2023c), "A study of the fracture mechanisms of hybrid carbon fiber reinforced polymer laminates reinforced by thin-ply", *Polymer Composites*, **44**(3), 1672-1683. <https://doi.org/10.1002/pc.27196>.
- Ramezani, F., Carbas, R., Marques, E.A.S., Ferreira, A.M. and da Silva, L.F.M. (2023d), "Study on out-of-plane tensile strength of angle-ply reinforced hybrid CFRP laminates using thin-ply" *Mechanics of Advanced Materials and Structures*, 1-14. <https://doi.org/10.1080/15376494.2023.2165742>.
- Ramezani, F., Nunes, P.D.P., Carbas, R.J.C., Marques, E.A.S. and da Silva, L.F.M. (2022), "The joint strength of hybrid composite joints reinforced with different laminates materials", *Advanced Joining Processes*, **5**, 100103. <https://doi.org/10.1016/j.jajp.2022.100103>.
- Shang, X., Marques, E.A.S., Machado, J.J.M., Carbas, R.J.C., Jiang, D. and Da Silva, L.F.M. (2019), "A strategy to reduce delamination of adhesive joints with composite substrates", *Proceedings of*

the Institution of Mechanical Engineers, Part L: Journal of Materials: Design and Applications, **233**(3), 521-530. <https://doi.org/10.1177/14644207188057>.

Sihn, S., Kim, R.Y., Kawabe, K. and Tsai, S.W. (2007), "Experimental studies of thin-ply laminated composites", *Composites Science and Technology*, **67**(6), 996-1008. <https://doi.org/10.1016/j.compscitech.2006.06.008>.

Simões, B.D., Nunes, P.D., Ramezani, F., Carbas, R.J., Marques, E.A. and da Silva, L.F. (2022), "Experimental and numerical study of thermal residual stresses on multimaterial adherends in single-lap joints", *Materials*, **15**(23), 8541. <https://doi.org/10.3390/ma15238541>.

Su, K.B. (1989), *Delamination Resistance of Stitched Thermoplastic Matrix Composite Laminates*, ASTM International, Conshohocken, PA, USA.

Verpoest, I., Wevers, M., De Meester, P. and Declercq, P. (1989), "2.5 D-and 3D-fabrics for delamination resistant composite laminates and sandwich structures". *Sampe*, **25**(3), 51-56.

Wagih, A., Maimí, P., González, E.V., Blanco, N., de Aja, J.S., De La Escalera, F.M., Olsson, R. and Alvarez, E. (2016), "Damage sequence in thin-ply composite laminates under out-of-plane loading", *Composites Part A: Applied Science and Manufacturing*, **87**, 66-77. <https://doi.org/10.1016/j.compositesa.2016.04.010>.

Wisnom, M.R., Khan, B. and Hallett, S.R. (2008), "Size effects in unnotched tensile strength of unidirectional and quasi-isotropic carbon/epoxy composites", *Composite Structures*, **84**(1), 21-28. <https://doi.org/10.1016/j.compstruct.2007.06.002>.

Yokozeki, T., Aoki, Y. and Ogasawara, T. (2008), "Experimental characterization of strength and damage resistance properties of thin-ply carbon fiber/toughened epoxy laminates", *Composite Structures*, **82**(3), 382-389. <https://doi.org/10.1016/j.compstruct.2007.01.015>.

Zubillaga, L., Turon, A., Renart, J., Costa, J. and Linde, P. (2015), "An experimental study on matrix crack induced delamination in composite laminates", *Composite Structures*, **127**, 10-17. <https://doi.org/10.1016/j.compstruct.2015.02.077>.

Appendix D

Paper D

Study on out-of-plane tensile strength of angle-ply reinforced hybrid CFRP laminates using thin-ply

Study on out-of-plane tensile strength of angle-ply reinforced hybrid CFRP laminates using thin-ply

F. Ramezani^a, R. Carbas^a , E. A. S. Marques^a , A. M. Ferreira^b , and L. F. M. da Silva^b 

^aInstituto de Ciência e Inovação Em Engenharia Mecânica e Engenharia Industrial (INEGI), Porto, Portugal; ^bDepartamento de Engenharia Mecânica, Faculdade de Engenharia (FEUP), Universidade Do Porto, Porto, Portugal

ABSTRACT

Thin-ply composites are generally defined as composites with ply thicknesses below 100 μm . These materials are rapidly gaining interest for high-performance applications, for example, the aerospace sector. Many practical techniques have been proposed to prevent delamination and improve the strength of composite laminates. A recent study has shown that the delamination could be postponed by replacing layers of CFRP with thin-ply in a unidirectional composite laminate, a configuration known as hybrid laminates reinforced with thin-ply. Since fiber orientation is known to be one of the most important parameters in composite laminate design, this study investigates the effect of oriented layers of thin-ply or both thin-ply and conventional CFRP in a hybrid laminate under out-of-plane tensile loading. A numerical Representative Volume Element (RVE) model for CFRP and thin-ply was generated, considering the unidirectional [0], cross-ply [45/−45], and [0/90] in order to better understand the effect of angle-ply hybrid composite laminates. Experimental results show that angle-ply composite laminates present higher failure load under out-of-plane tensile loading compared to the unidirectional ones. This can be attributed to the fact that an initiated crack is faced with a significantly more complex crack path in an angle-ply laminate to advance in the through-the-thickness direction.

ARTICLE HISTORY

Received 17 November 2022
Accepted 3 January 2023

KEYWORDS

Composite laminates; Thin-ply; Angle-ply laminates

1. Introduction



The use of carbon fiber reinforced polymer (CFRP) materials in different industries is continuously increasing [1–4]. Thin-ply laminates are defined as laminates composed using plies with a thickness of less than 100 μm [5]. These layer thicknesses are available through the spread-tow process [6] which produces flat and straight plies with a dry ply thickness as low as 0.02 mm [7]. With an improved spreading process, small layer thicknesses and more homogeneous fiber are achieved [8].

By reducing the thickness of the single layer, the quantity of the individual layers and therefore the degrees of freedom in the orientation are increased [9]. This results in a larger number of interfaces in thin-ply laminates, lowering the shear stresses [9, 10]. Moreover, thin-ply laminates are known for their ability to delay the onset of the matrix damage mechanisms and suppress out-of-plane microcracking [5] and free edge delamination [9, 11] for static, fatigue, and impact loadings. Due to their superior damage and delamination resistance properties, thin-ply laminates could exhibit higher interlaminar shear properties [12] and strain energy [13] compared to conventional plies. Thin plies can also represent a favorable approach to improve the performance of adhesively bonded CFRP due to their ability to enhance the off-axis performance of composites and postpone

delamination [13]. Moreover, due to the in situ effect [14] the location of composite failure could be changed from the ply interface toward the mid-thickness of the composite adherend.

Delamination in a composite laminate can lead to rapid deterioration of the mechanical properties and may cause catastrophic failure of the composite structure [15, 16]. Once the damage is initiated, laminate properties may deteriorate, leading to premature failure [17, 18]. Accordingly, multiple studies have investigated methods for composite laminate modification to delay delamination as the use of Fiber Metal Laminate (FML) [19], composite laminates with toughened layers [20], using Z-pins [21, 22], 3D weaving [23], stitching [24], braiding [25], or using additional thermoplastic inter-ply [26], etc.

In the case of composite laminates, the effect of the stacking sequence has been widely studied [27, 28]. Ultimately, an optimum stacking sequence is dependent on the specimen configuration, material properties, and the load being transferred to the composite laminate. Ozel et al. [29] studied the effect of the stacking sequence in a single lap composite/composite joint considering [0]₁₆, [0/90]₈, [45/−45]₈, and [0/45/−45/90]₄. In this case, the stacking sequence of [0/45/−45/90]₄ presented the highest strength. This is while when they [29] changed one of the adherend to aluminum (composite/aluminum joint), the

CONTACT R. J. C. Carbas  rcarbas@fe.up.pt  Instituto de Ciência e Inovação Em Engenharia Mecânica e Engenharia Industrial (INEGI), Rua Dr. Roberto Frias, 4200-465, Porto, Portugal.

© 2023 The Author(s). Published with license by Taylor & Francis Group, LLC

This is an Open Access article distributed under the terms of the Creative Commons Attribution License (<http://creativecommons.org/licenses/by/4.0/>), which permits unrestricted use, distribution, and reproduction in any medium, provided the original work is properly cited. The terms on which this article has been published allow the posting of the Accepted Manuscript in a repository by the author(s) or with their consent.

optimum stacking sequence of the adherend changed to $[0]_{16}$. Akpinar [30] studied five different orientations ($[0]_{16}$, $[90]_{16}$, $[0/90]_8$, $[45/-45]_8$, $[0/45/-45/90]_4$) in a double strap joint under tensile loading. The authors [30] found out that the joints with the composite patches of $[0]_{16}$ presented the highest failure load.

It has been mentioned that, in the case of single lap joints, failure load seems to be directly correlated to the distance of the ply at 0° to the adhesive layer. Since the 0° layer is known to be the location of the final failure, it can be assumed that its distance from the adhesive layer hinders the crack propagation process and thus increases the joint strength [31]. However, in the case of double lap joints under impact loading [32] joints having substrates with fibers oriented parallel to the loading direction (unidirectional 0°) were found to present the highest shear strength.

A previous study by the authors [33] has shown that replacing layers of conventional composite in a unidirectional laminate with layers of thin-ply can postpone the delamination and increase the strength under out-of-plane tensile loading. In the first stage of the study, the effect of the thin-ply thickness in a specific hybrid laminate was studied. It was found that the use of 25% thin-ply per total thickness of the laminate presents the highest laminate strength under out-of-plane tensile loading (representing the optimum amount). In a second stage, the effect of distributing the optimum amount through the thickness was investigated. Figure 1a shows the studied configuration for

unidirectional reference CFRP, thin-ply, and the optimum hybrid laminate configuration. Figure 1b illustrates the experimental results obtained.

The current article investigates the effect of using angle-ply layers in hybrid composite laminates under out-of-plane tensile loading, both numerically and experimentally. The HS 160 T700 by CIT and TP415 by NTPT are used as conventional CFRP and thin-ply, respectively. An experimental study was performed by testing reference angle-ply CFRP and thin-ply configurations. Afterwards, a RVE model was carried out to better understand the effect of angle-ply layers in both CFRP and thin-ply configurations. The experimental results showed that angle-ply composite laminates present higher performance load under out-of-plane tensile loading when compared to the unidirectional configurations.

2. Experimental details

2.1. Conventional CFRP

The materials used in the studied configurations were chosen to be as representative as possible of a final application in

Table 1. CFRP mechanical properties [34].

Mechanical property	Value
E_1 (MPa)	109,000
E_2 (MPa)	8819
G_{12} (MPa)	4315
G_{IC} (N/mm)	0.59

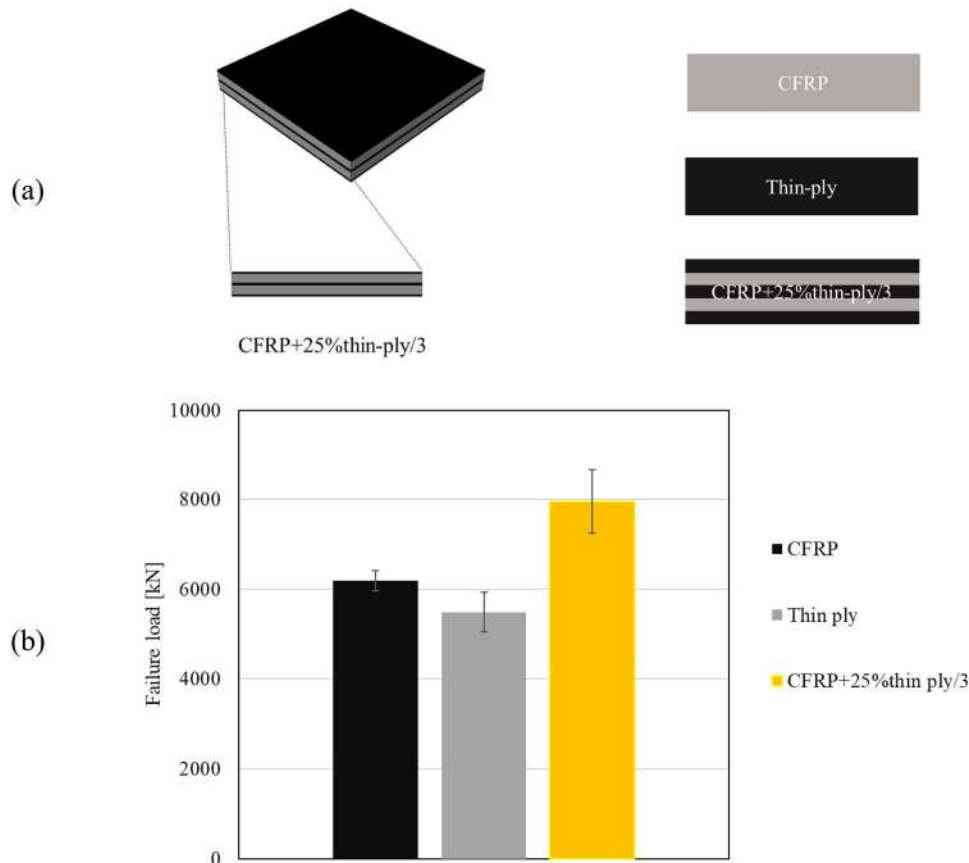


Figure 1. (a) Schematic design for conventional CFRP, thin-ply, and hybrid laminate and (b) summary of the experimental results for unidirectional reference CFRP, thin-ply, and hybrid laminate. Adopted from [33].

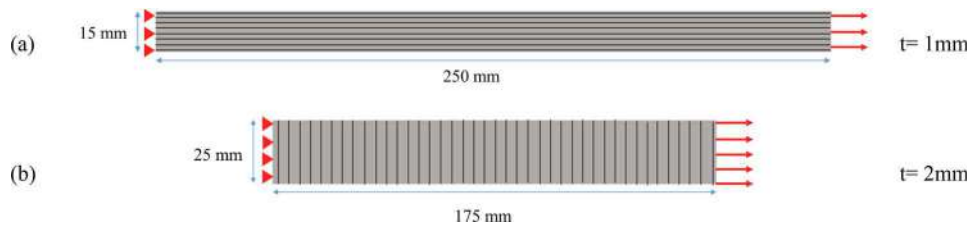


Figure 2. Schematic design of (a) 0° and (b) 90° tensile test specimens.

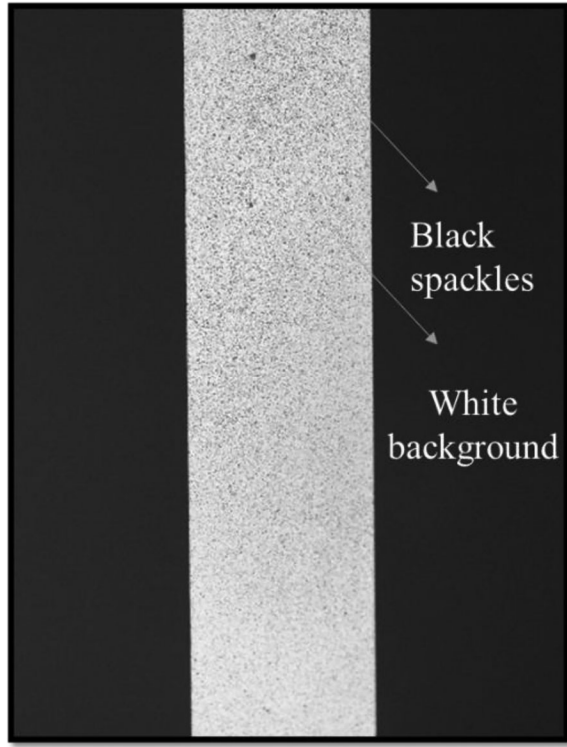


Figure 3. Figure captured for DIC process from 90° specimen while testing.

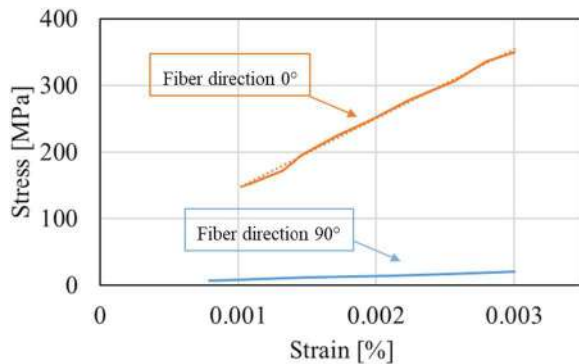


Figure 4. Representative stress-strain curve obtained from the 90° and 0° tensile test.

the aerospace sector. Thus, a unidirectional prepreg carbon-epoxy composite with ply thickness of 0.15 mm was selected, with the commercial reference Texipreg HS 160 T700 (Seal Spa, Legnano, Italy). This is an orthotropic material, whose mechanical properties are presented in Table 1. The elastic mechanical properties of the CFRP correspond to the orientation of a 0° CFRP ply (1 and 2 are defined as fiber and out-of-plane direction)

2.2. Thin-ply

Unidirectional 0° oriented carbon-epoxy prepreg composite with ply thickness of 0.07 mm was selected, with the commercial reference NTPT-TP415. The elastic orthotropic properties for this thin-ply were characterized using a servo-hydraulic testing machine (Instron 8801), with a load cell of 100 kN and following appropriate testing standards.

2.2.1. Tensile test 0° and 90°

The tensile test in order to obtain E_1 and E_2 is performed using ASTM D 3039/D 3039 M standard. Figure 2 presents the schematic design for specimens used for (a) Longitudinal and (b) Out-of-plane tensile test. Mentioned t in Figure 2 represents the thickness of the specimen. A quasi-static test (2 mm/min) was performed according to the mentioned standard.

Digital image correlation was performed in order to obtain the strain using an open-source Moire software in order to measure contour of deformation, strain on the composite material. The specimens were painted with white spray and speckled with white ink dots (see Figure 3). This is necessary to support the DIC analysis, based on the correlation of a set of neighboring points considered in pictures captured before and after loading [20]. Figure 4 shows the representative stress-strain curve obtained for the specimens with 0 and 90 fiber direction.

2.2.2. Shear test

Different standards have been used to perform the shear test for composite unidirectional materials. In this case, the

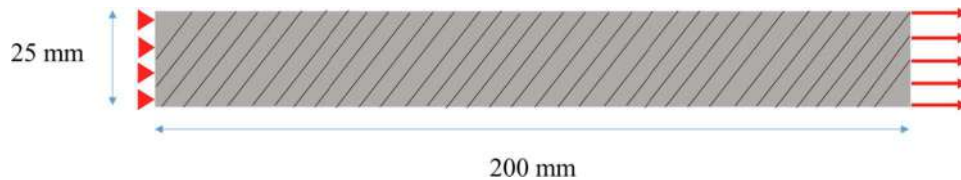


Figure 5. Schematic design of specimens for shear test.

ASTM D 3518/D 3518M standard was used in order to obtain G_{12} . A plate with lay up of $[45/-45]_{6s}$ was manufactured. Figure 5 shows a schematic design for the manufactured specimen. A quasi-static test (2 mm/min) was performed according to the mentioned standard.

Digital image correlation was performed in order to obtain the strain using an open-source Moire software for data processing. Figure 6 shows the stress-strain curve obtained for the specimens. Figure 7 shows the samples after failure.

2.2.3. DCB test

In this case, the D 5528-01 standard was used to obtain mode I fracture energy (G_{IC}). Figure 8 shows the schematic design of the specimens manufactured for DCB test. Steel blocks were attached to the DCB specimens. A Teflon layer was used to create a precrack in the DCB specimen, which is shown by as green line in Figure 8.

The specimens are attached to steel blocks, as shown in Figure 8, allowing testing in a universal testing machine. The surface of laminates was abraded smoothly using sandpaper and then cleaned with acetone, since release agent was used in the plate manufacturing step in order to prevent the

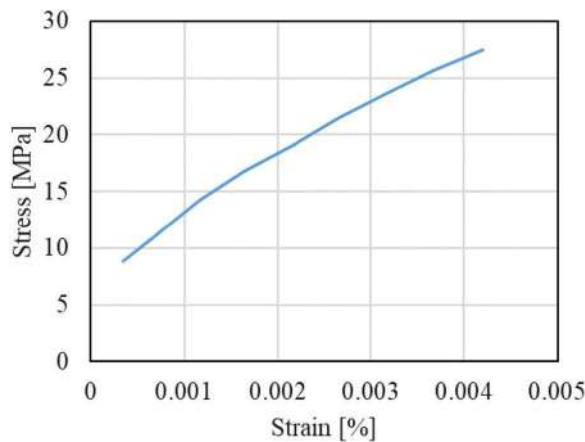


Figure 6. Representative stress-strain curve obtained from shear test.

adhesion between the plates and the mold. Moreover, plasma treatment was performed on the composite surfaces. Furthermore, it has to be mentioned that the steel blocks were sandblasted and then washed with acetone.

CBBM [35] method is used in order to obtain G_{IC} and Figure 9 shows the representative R-curve obtained using the CBBM method. The DCB specimen testing and its failure morphology are shown in Figure 10. Table 2 shows a summary of mechanical property characterization for NTPT-TP415 thin-ply

2.3. Plate manufacturing

The manufacturing process of the reference CFRP or thin-ply starts with the layer-by-layer stacking of the CFRP prepreg, until the desired block thickness is attained. It should be mentioned that the overall thickness of the laminates is set to 3.2 mm. A mold is used to ensure the thickness of the manufactured plates and release agent is used to ensure easy separation of the plate and the mold after curing. Finally, the plates were cured in a hot plate press under 30 bar of pressure and 130 °C for 2 h as recommended by the producer.

After curing, the plates were cut to the desired dimensions (25 × 25 mm²). Steel cubes (see Figure 11) were then

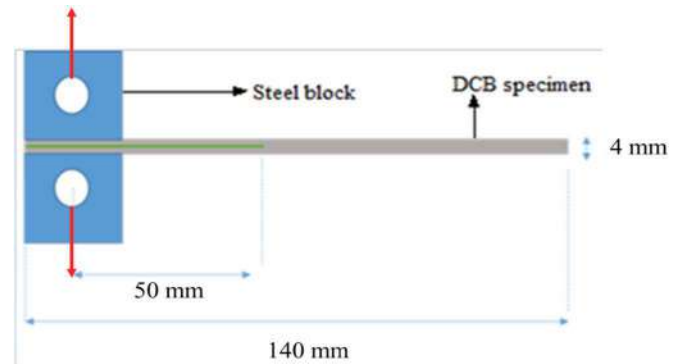


Figure 8. Schematic design of the specimens manufactured for DCB test.

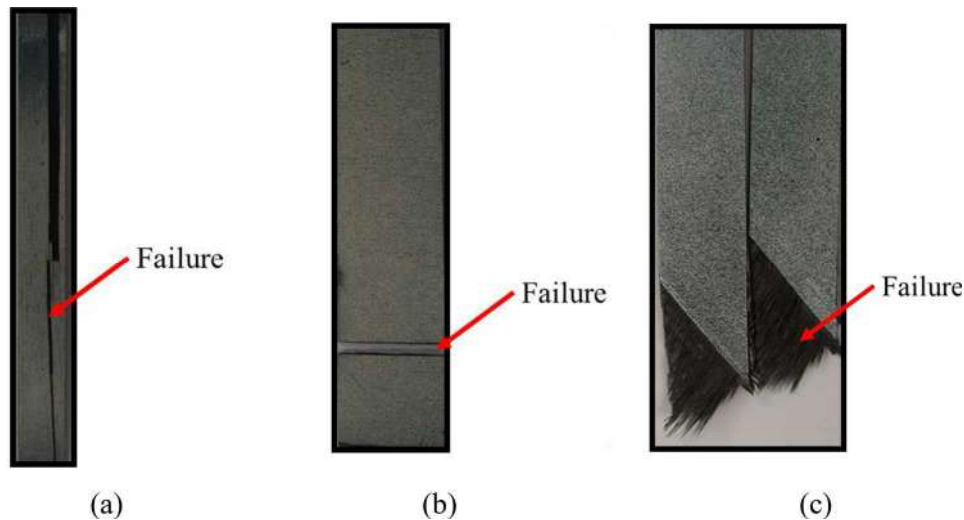


Figure 7. (a) 0° tensile test, (b) 90° tensile test and (c) shear test after failure.

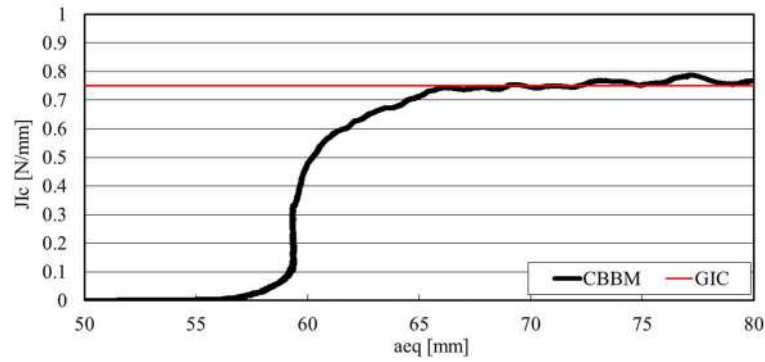


Figure 9. Representative R-curve obtained for DCB specimen using CBBM method.

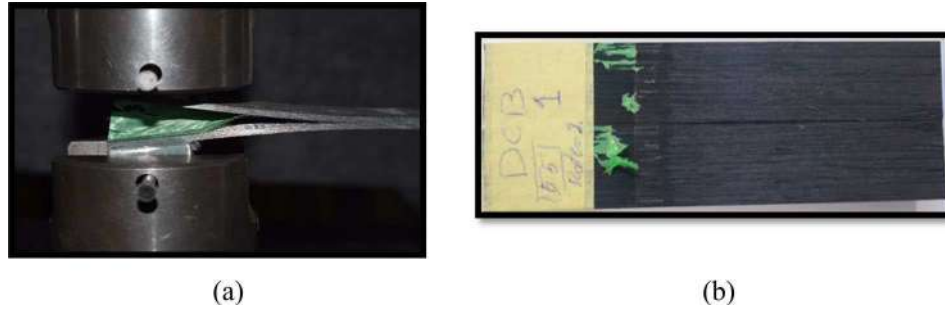


Figure 10. DCB specimen (a) while testing and (b) after failure.

Table 2. Thin-ply mechanical properties.

Mechanical property	Value
E_1 (MPa)	101,720
E_2 (MPa)	5680
G_{12} (MPa)	3030
G_{IC} (N/mm)	0.76

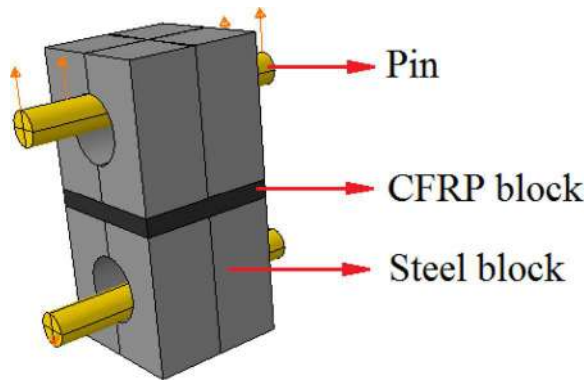


Figure 11. Schematic design of steel blocks attached to conventional CFRP laminates and loading condition.

attached to blocks, using the PLEXUS MA422 adhesive, which cures in room temperature after 24 h. The adhesive overflow was removed from the outer surface of the blocks using sandpaper.

2.4. Configurations

Based on the results previously obtained by the authors [33], the CFRP + 25%thin-ply/3 configuration was

considered for this study. For the first stage of the study, in a hybrid block, the conventional CFRP was kept uni-directional (0°) and thin-ply layers were oriented at $[45/-45]_n$ and $[0/90]_n$ seeking symmetry of the final laminate (see Figure 12a, b). Moreover, the reference angle-ply thin-ply laminates ($[0/90]_{ns}$ and $[45/-45]_{ns}$) were also examined.

For the second stage, both the thin-ply layers and the conventional CFRP layers were oriented at $[45/-45]_n$ and $[0/90]_n$ seeking symmetry of the final laminate (see Figure 12c, d). Moreover, the reference-oriented CFRP laminate ($[0/90]_{ns}$ and $[45/-45]_{ns}$) was studied. The results for the reference unidirectional CFRP, thin-ply, and hybrid laminate (CFRP + 25% thin-ply/3) were obtained in a previous study [33].

2.5. Scanning electron microscope studies

The cross-section of blocks with polished surfaces was observed using a Scanning Electron Microscope (SEM). In specimens manufactured with CFRP prepreg, resin-rich, and fiber-rich area is apparent (marked by red rectangle in Figure 13a). On the other hand, the fibers are well distributed in specimens manufactured using thin-ply prepreps. Therefore, less resin-rich and fiber-rich area is observed, when compared to the conventional CFRP (see Figure 13) which is in line with the literature review [8].

2.6. Surface treatment

As mentioned in Section 2.3, composite blocks have to be attached to steel blocks, (as shown in Figure 11) in order to

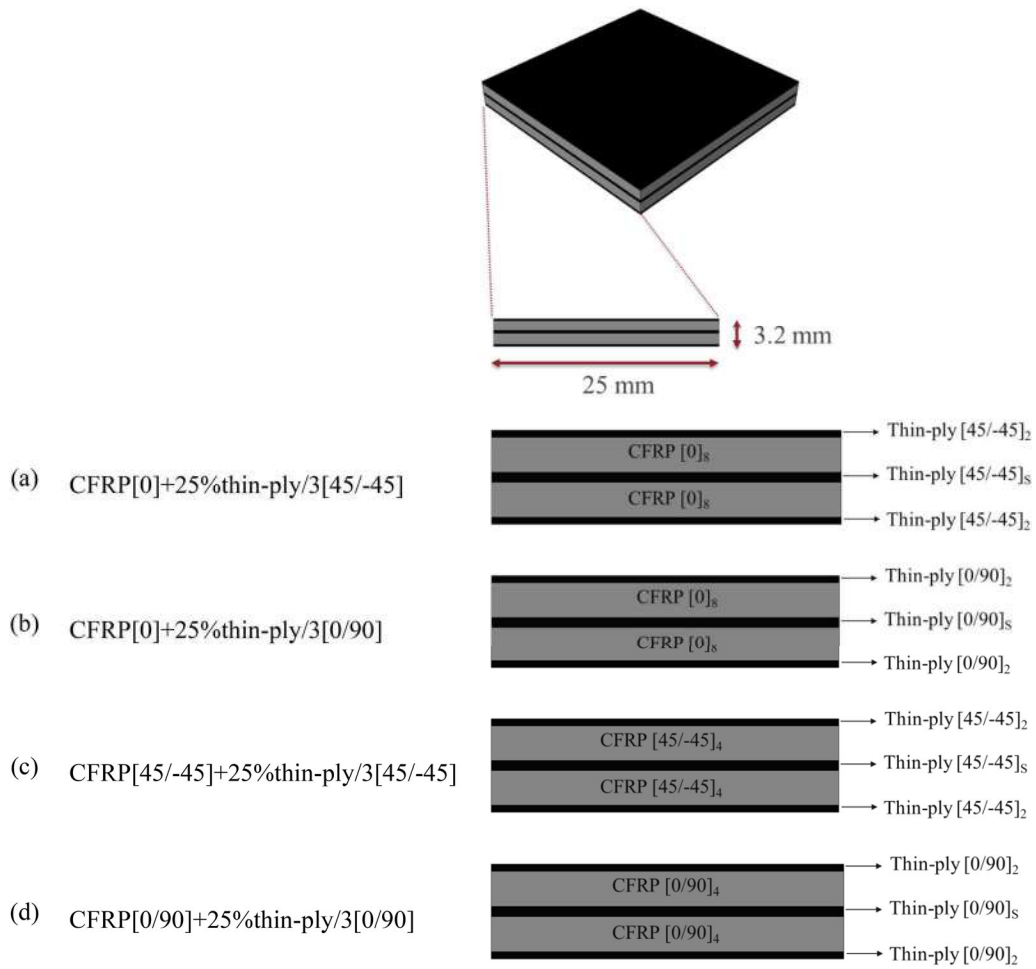


Figure 12. Schematic design of the studied hybrid laminates with oriented plies.

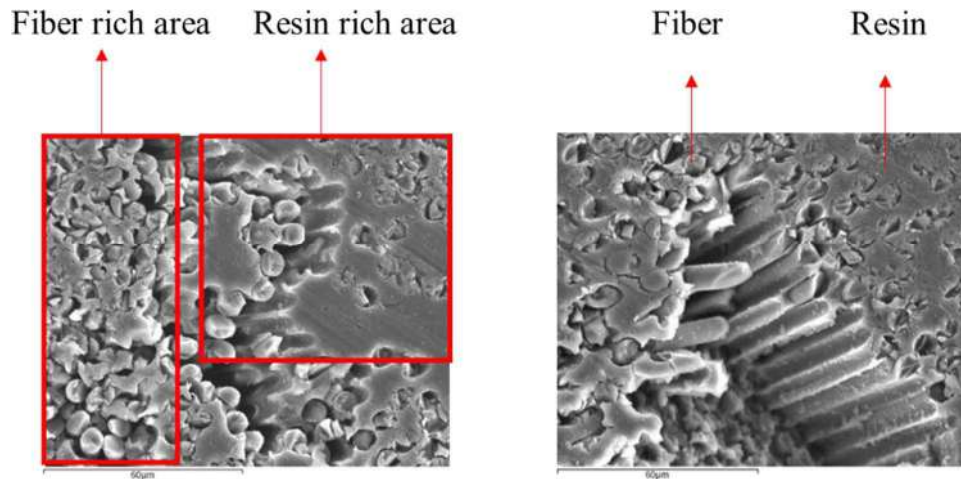


Figure 13. SEM micrographs of (a) CFRP and (b) thin-ply.

allow for assembly in the testing machine. Initially, the surface of the CFRP blocks was abraded using sandpaper. Afterwards, the blocks were cleaned with acetone, removing any release agent remaining from the plate manufacturing step (see Section 2.3). Finally, a plasma treatment was performed on composite surfaces. The steel blocks were sand-blasted followed by cleaning with acetone.

2.7. Testing condition

The SLJs were tested using an Instron 8801 servo-hydraulic testing machine with a load cell of 100 kN, at a constant crosshead speed of 1 mm/min (quasi-static). All tests were performed under laboratory ambient conditions (room temperature of 24 °C, relative humidity of 55%). A minimum of three repetitions were made for each configuration tested.

3. Experimental results

3.1. CFRP

The manufactured blocks were tested as described in Section 2.7. Figure 14a shows the representative load–displacement curve obtained for unidirectional and angle-ply CFRP laminates, tested under out-of-plane tensile loading. Experimental results illustrate that angle-ply laminates present higher strength compared to the unidirectional ones. According to the literature [31], higher strength in the angle-ply blocks may be due to the more complex through the thickness crack path these materials exhibit, especially when compared to the crack paths of the unidirectional configurations. Overall, this results in a higher failure load (see Figure 14b) and this was clearly observed in the experimentally obtained failure mechanism. As seen in Figure 15, an initiated crack in the laminate

can easily propagate through the thickness in the unidirectional laminate. The crack path is expected to be more complex in angle-ply layers if the crack is moving through the thickness, which requires higher fracture energy. Therefore, as seen in Figure 14b, the crack will actually be forced to propagate between two plies in the angle-ply layers.

3.2. Thin-ply

Unidirectional and angle-ply thin-ply laminates were also manufactured and tested. The representative load–displacement curves registered under out-of-plane tensile loads are presented in Figure 16a. According to the experimental results, the angle-ply laminates present higher strength compared to the unidirectional ones. The explanation presented in Section 3.1 is also applicable. Moreover, Figure 16b

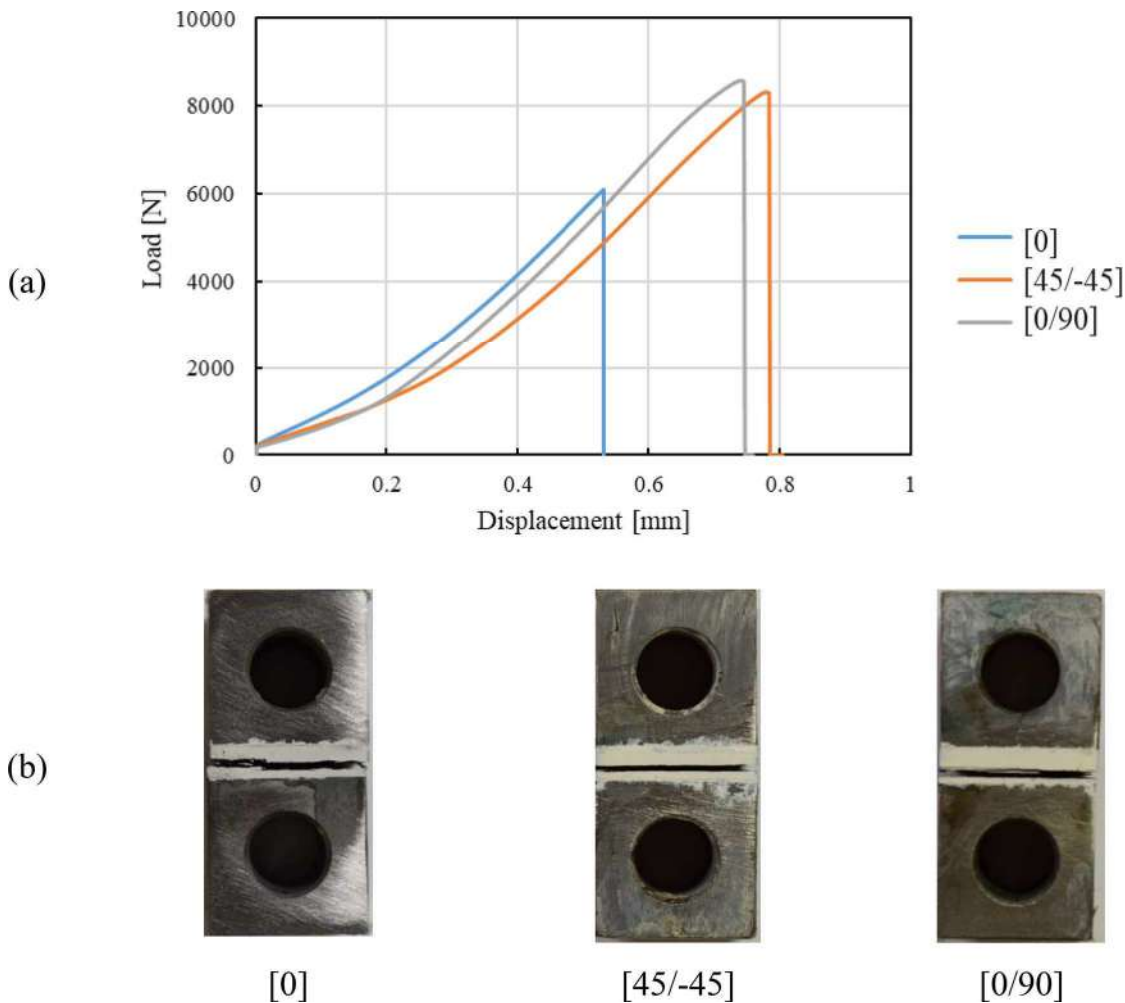


Figure 14. (a) Representative load–displacement curve and (b) failure mechanism for reference unidirectional and angle-ply CFRP laminates.

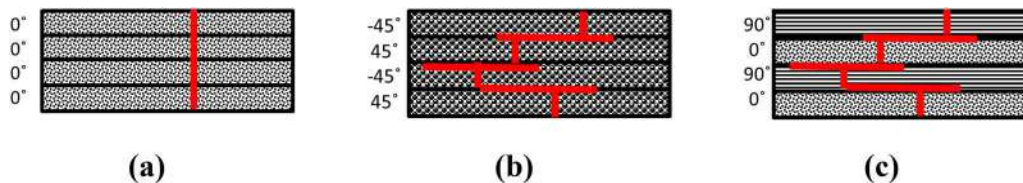


Figure 15. Expected through-the-thickness crack path in unidirectional and angle-ply laminates.

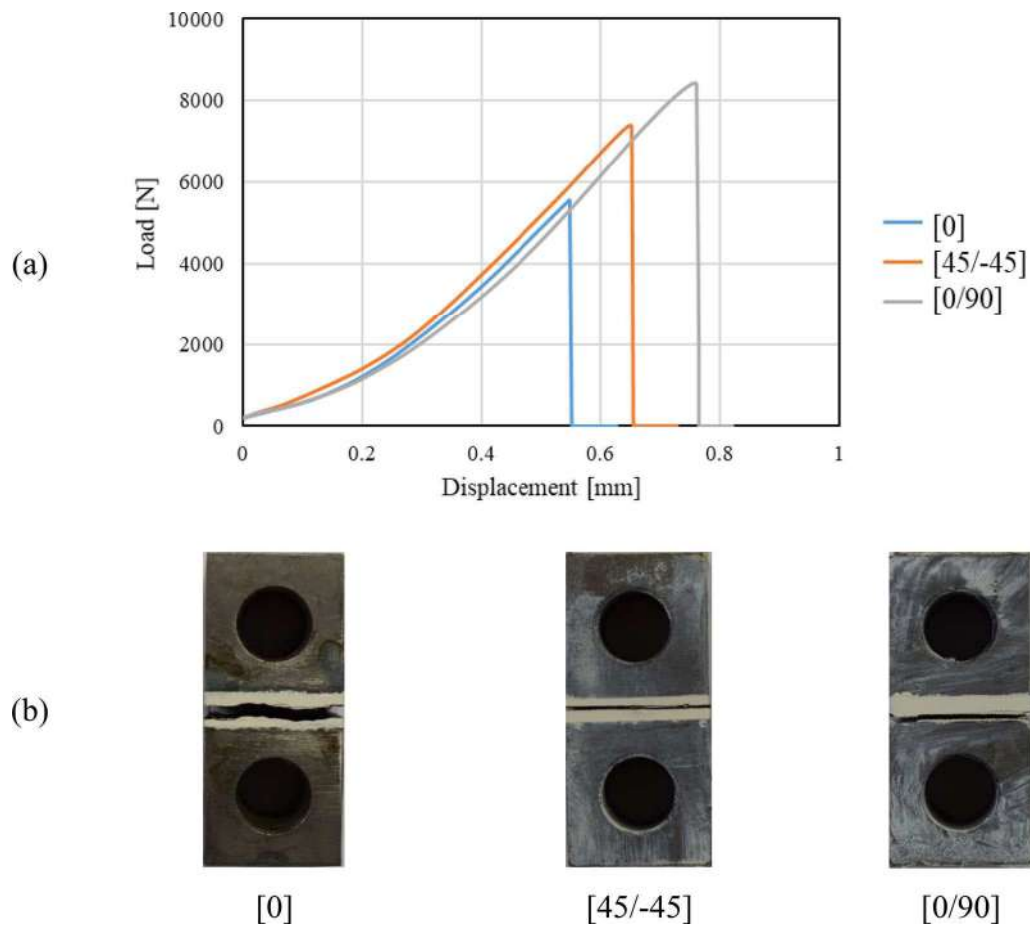


Figure 16. (a) Representative load–displacement curve and (b) failure mechanism for reference unidirectional and angle-ply thin-ply laminates.

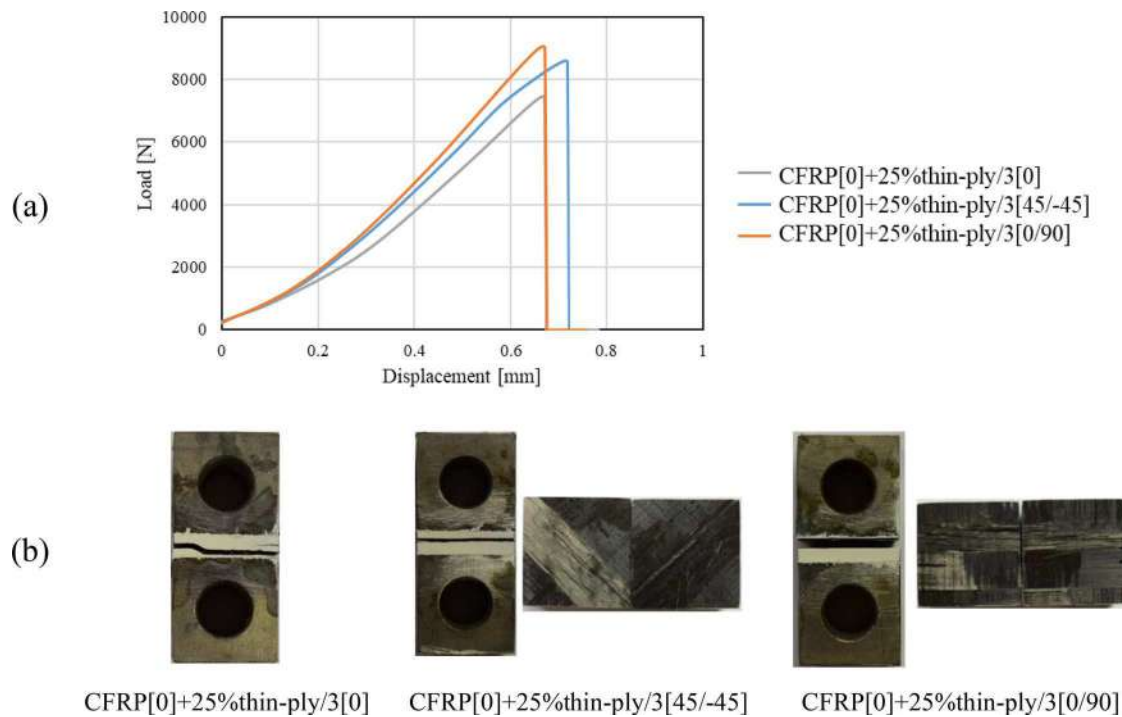


Figure 17. (a) Representative load–displacement curve and (b) failure mechanism for hybrid laminate with unidirectional CFRP and oriented thin-ply.

presents the failure mechanism for the unidirectional and angle-ply thin-ply laminates. As seen in Figure 16b, in a unidirectional laminate the crack can easily propagate through the

thickness of the laminate while in an angle-ply configuration the crack path progression through the thickness is more restricted, leading to its propagation between two layers.

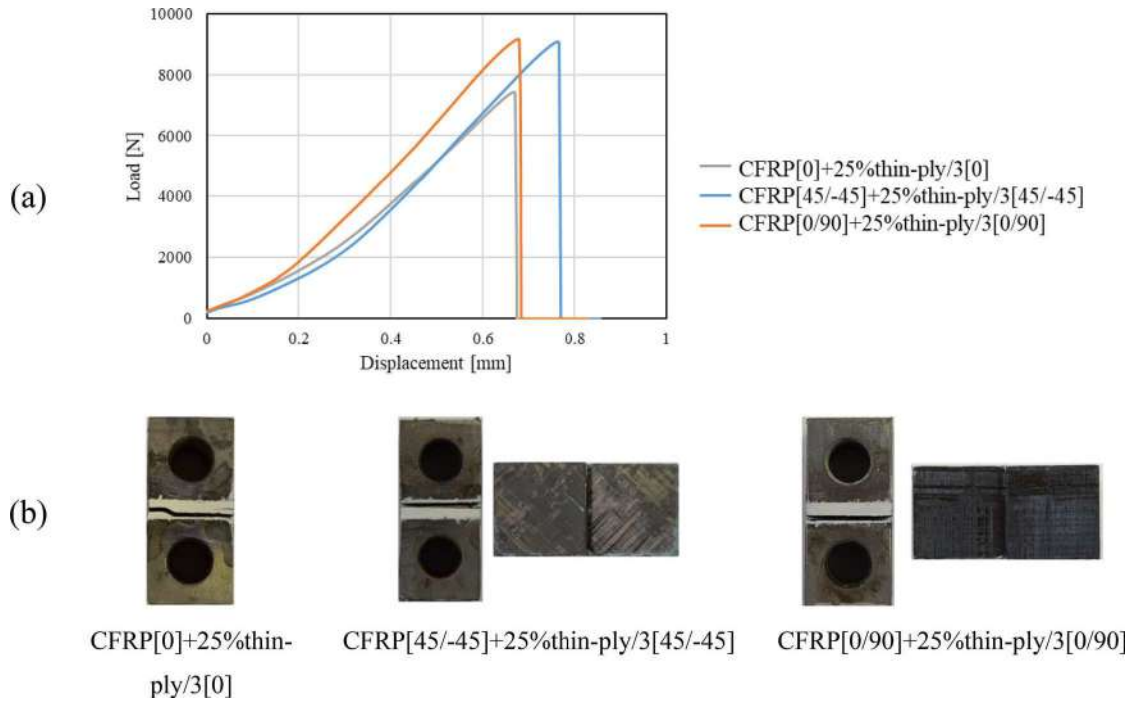


Figure 18. (a) Representative load–displacement curve and (b) failure mechanism for hybrid laminate with oriented CFRP and thin-ply.

3.3. Hybrid laminate with unidirectional CFRP and oriented thin-ply

The hybrid laminate configurations presented in Section 2.4 were tested and the resulting load–displacement curves are shown in Figure 17a. Generally, hybrid configurations with the unidirectional CFRP and angle-ply thin-ply layers were found to present higher failure loads when compared to the unidirectional laminate (CFRP[0] + 25%thin-ply/3[0]). This is acceptable due to the increase in the failure load in angle-ply thin-ply laminate loaded under out-of-plane tension loading (see Section 3.2). Figure 17b presents the failure mechanism for the mentioned unidirectional and angle-ply hybrid laminate. As seen in Figure 17b, the crack could easily propagate through the thickness in unidirectional hybrid laminate. In contrast, the crack progression through the thickness is more complex in an angle-ply laminate, which forces failure to occur between plies.

3.4. Hybrid laminate with oriented CFRP and thin-ply

Figure 18a shows the representative load–displacement curves obtained for hybrid configurations with oriented CFRP and thin-ply layers. As presented in Sections 3.1 and 3.2, the reference angle-ply CFRP and thin-ply laminates present higher failure load than the corresponding unidirectional reference laminates. This explains the increase in the failure load in a hybrid laminate with angle-ply CFRP and thin-ply. Figure 18b presents the failure mechanism for the hybrid blocks with unidirectional and angle-ply CFRP and thin-ply. As seen in Figure 18b, a crack could easily propagate through the thickness in unidirectional hybrid laminate.

Table 3. Geometrical and mechanical properties for the fiber and matrix.

	CFRP	Thin-ply
Diameter (μm)	7	7
E fiber (GPa)	230	294
E matrix (GPa)	3.6	3.3
V_f	0.35	0.35
Matrix maximum strength (MPa)	148	138

4. Numerical study

A representative volume element (RVE) model is employed to better understand the advantages associated with angle-ply laminates in micro-scale. The RVE was modeled using the ABAQUS commercial software. Following the result of the SEM micrographs presented in Section 2.5, the model was designed to account for the difference in fiber distribution between the CFRP and the thin-ply (fiber clustering in CFRP RVE and relatively uniform fiber distribution for the thin-ply). Moreover, the number of the fiber was calculated using Eq. (1) in which N and D are the number and the diameter of the fibers, respectively, and L , W , and H are the length, width and the depth of the RVE, respectively. Moreover, V_f is the volume fraction. The properties of the used fiber and matrix for the CFRP and thin-ply presented in Table 3 are provided by the manufacturer.

$$V_f = \frac{NID^2}{4LW} \quad (1)$$

4.1. CFRP

A 3D elastoplastic RVE model with dimensions of $100 \times 100 \times 100 \text{ } (\mu\text{m})^3$ was studied to partially model two plies of CFRP. Therefore, fiber directions of [0], [45/–45],

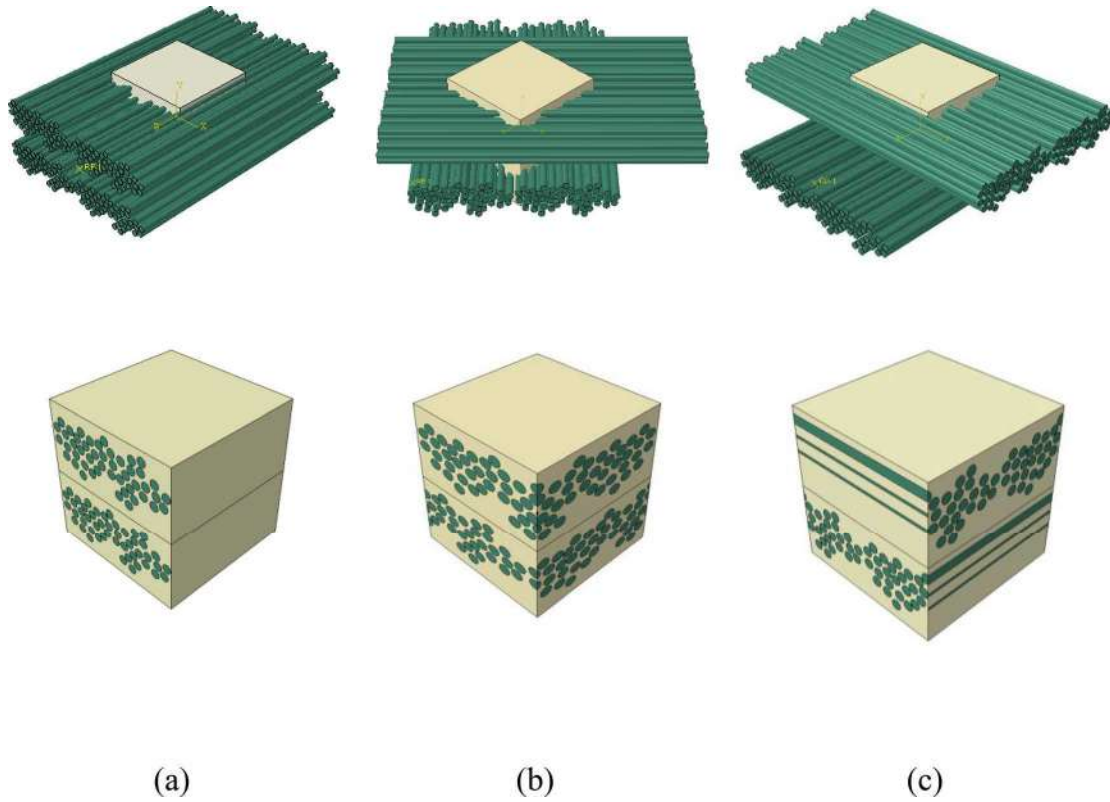


Figure 19. RVE models for (a) unidirectional [0] and angle plied (b) [45/-45] (c) [0/90] CFRP.

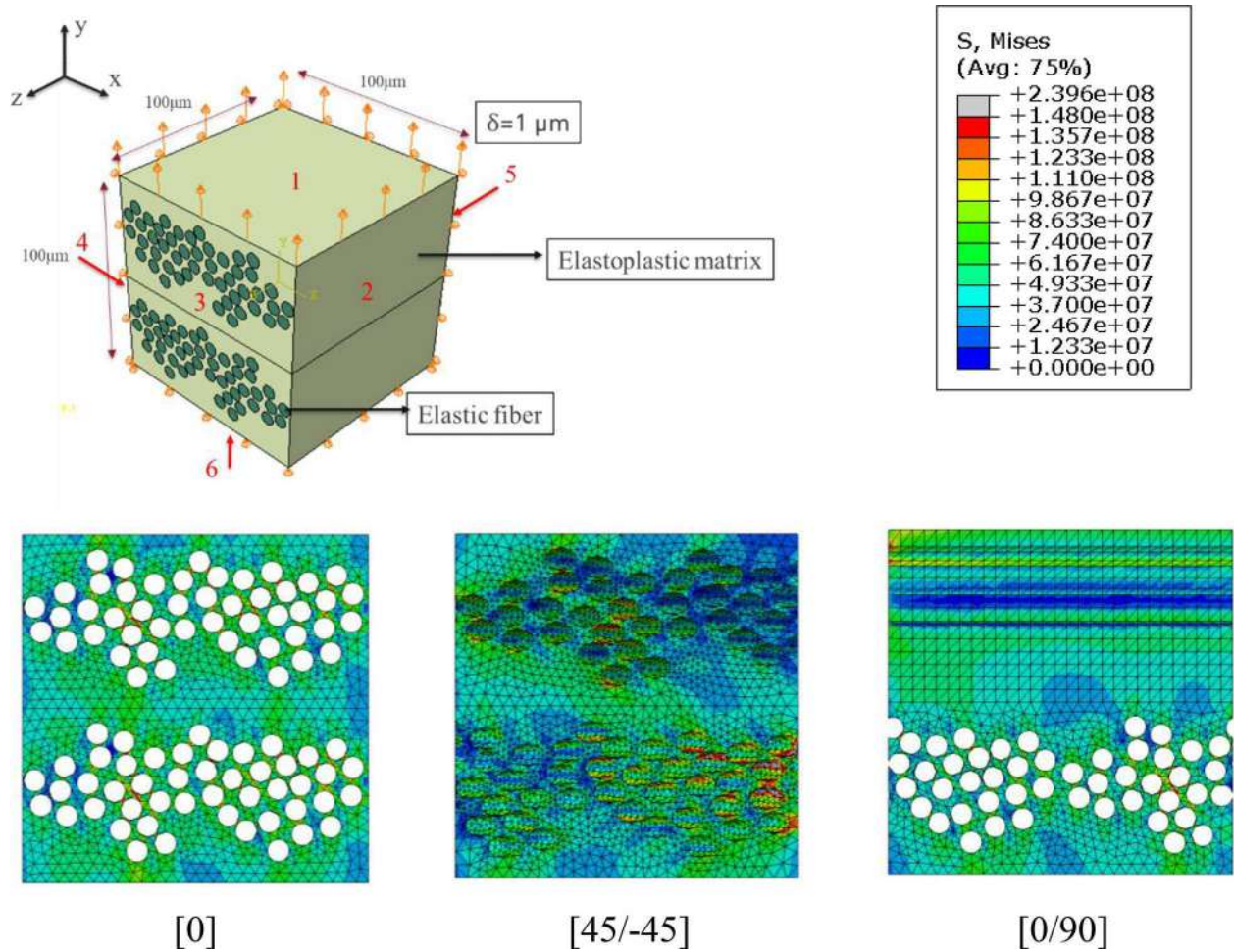


Figure 20. Von Mises stress distribution for unidirectional and angle-ply CFRP RVE on plane number 5.

and $[0/90]$ were considered (see Figure 19). According to Table 3, and Eq. (1) the number of fibers was calculated considering the before mentioned RVEs dimensions. Moreover, fiber clustering is also considered for CFRP RVE models (according to the SEM micrograph data shown in Section 2.5). The boundary condition applied is shown in Figure 20. An out-of-plane displacement of $1\mu\text{m}$ was applied to plane number 1 (in y direction) to fulfill the out-of-plane tensile loading and the other plane perpendicular to the y -axis (plane number 6), was fixed in the mentioned direction. Both planes perpendicular to the x - and z -axis (in this case plane numbers 4 and 5) were fixed in related perpendicular directions (x and z , respectively). The boundary conditions were equally applied for all configurations under study.

The critical plane in each RVE should be determined, which is expected to be a plane transverse to the

displacement direction. The planes were evaluated for each configuration and the critical plane was determined as plane number 5 for all configurations. Figure 20 shows the Von Mises equivalent stress distribution for CFRP RVE with the ply orientation of $[0]$, $[45/-45]$, and $[0/90]$ on plane number 5. The color bar was restricted to 148 MPa which corresponds to the CFRP matrix maximum strength. Therefore, the elements with stress value higher than 148 MPa (shown by grey color) are known as failed elements. An open-source software (IC Measure) was used in order to obtain the area of failed elements. The level of failure is the defined as the area of failed elements divided by the total area of the RVE. Figure 21 presents the level of failure described above. According to Figure 21, since the unidirectional RVE shows a lower level of failure, it is expected for the angle-plyed laminates to present higher strength compared to the unidirectional ones, with the $[0/90]$ configuration expected to present the highest strength (the $[0/90]$ configuration shows the lowest level of failure).

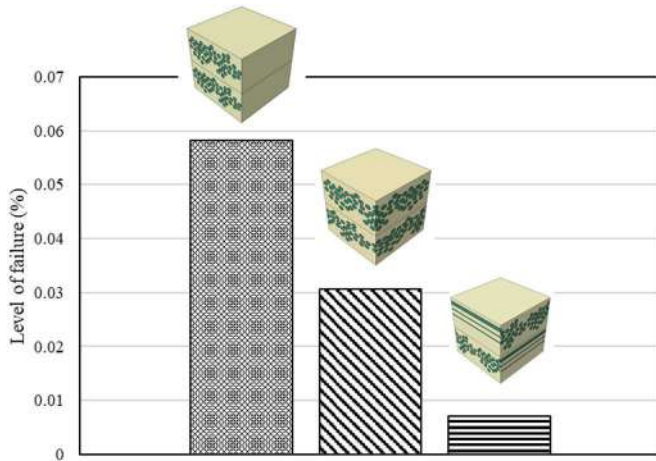


Figure 21. Level of failure obtained for unidirectional and angle-plyed CFRP RVE on plane number 5.

4.2. Thin-ply

The same approach mentioned in Section 4.1 was used for RVEs with the thin-ply configuration, as shown in Figure 22. Considering Figures 19 and 22, an attempt was made to implement the difference in fiber distribution between CFRP and thin-ply (considering relatively uniform fiber distribution in thin-ply RVE models compared to the models presented in Section 4.1). Consequently, RVEs with the fiber direction of $[0]$, $[45/-45]$, and $[0/90]$ were considered (see Figure 22). The boundary condition is the same as mentioned in Section 4.1.

The critical plane in each RVE should be determined, which is expected to be a plane transverse to the displacement direction. Planes were evaluated for each configuration and the critical plane was determined to be plane number 5

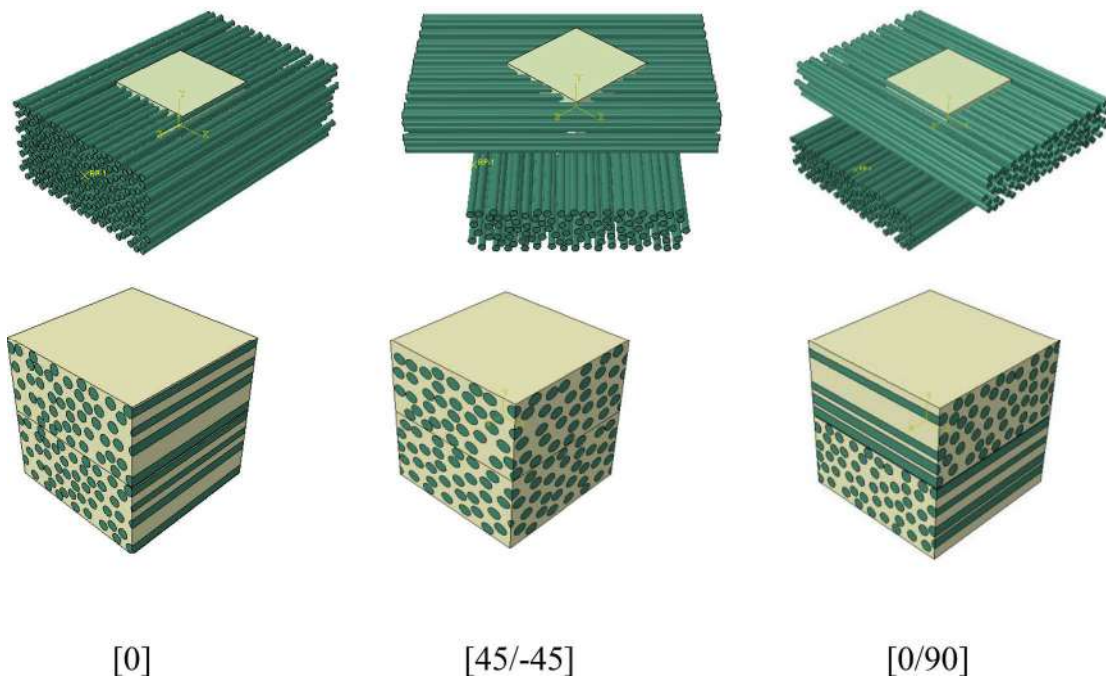


Figure 22. RVE models for (a) unidirectional $[0]$ and angle plyed (b) $[45/-45]$ (c) $[0/90]$ thin-ply.

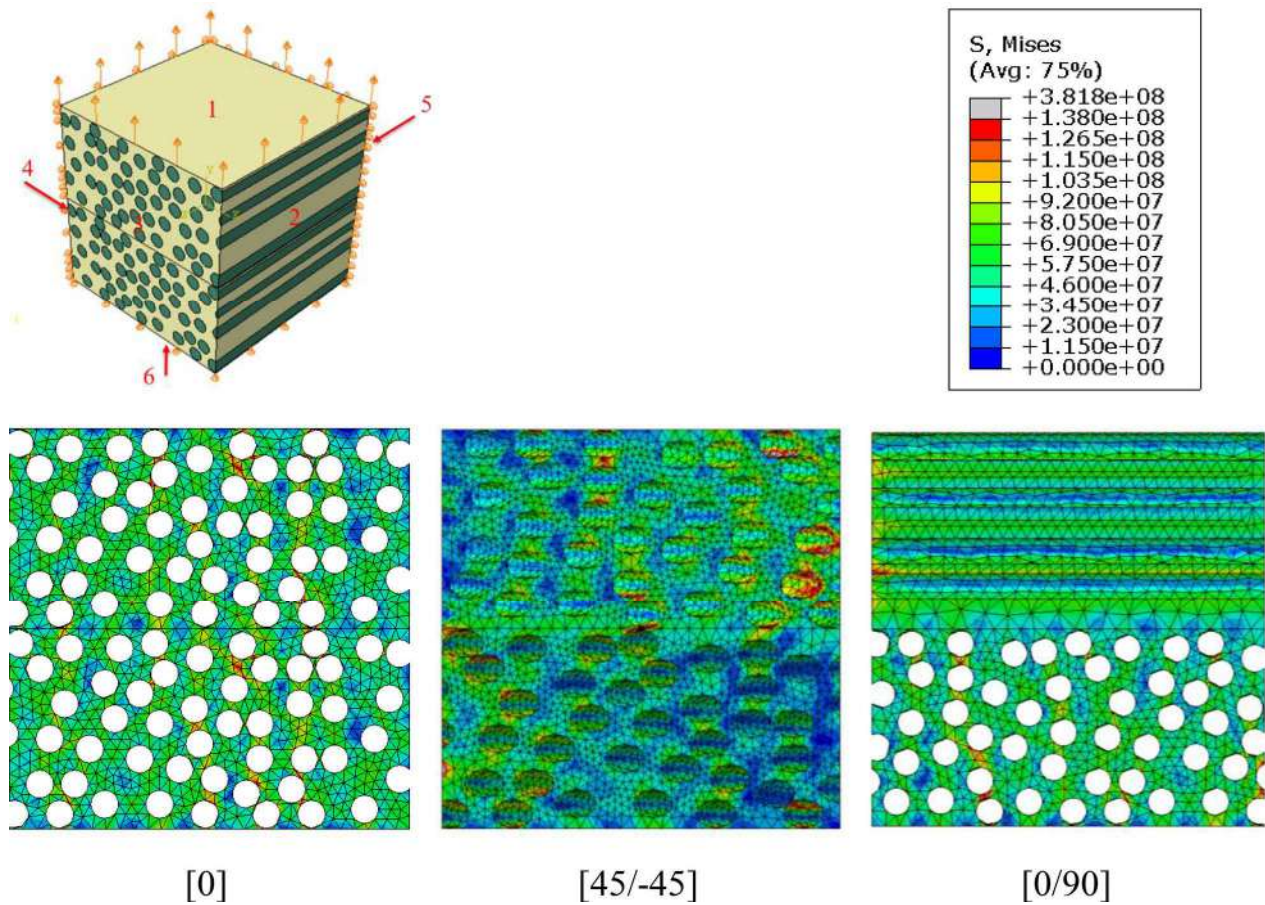


Figure 23. Von Mises stress distribution for unidirectional and angle-ply thin-ply RVE on plane number 5.

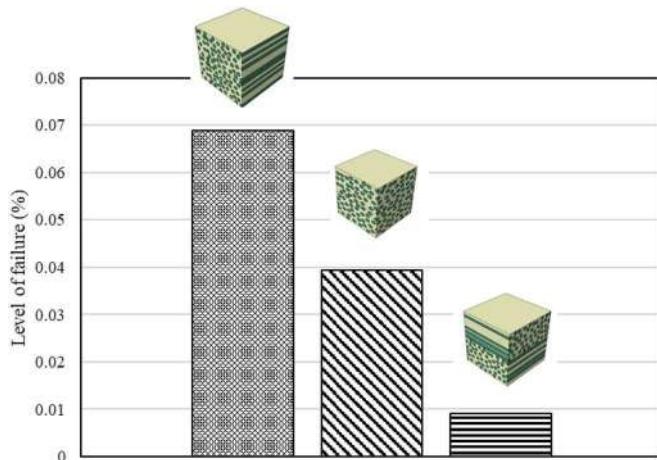


Figure 24. Level of failure obtained for unidirectional and angle-ply thin-ply RVE on plane number 5.

for all configurations. Figure 23 shows the Von Mises equivalent stress distribution for thin-ply RVE with the ply orientation of [0], [45/−45], and [0/90] on plane number 5. The color bar was restricted to 138 MPa which corresponds to the maximum strength of the thin-ply matrix. Therefore, the elements with stress value higher than 138 MPa (shown in grey color) are known as failed elements. The level of failure as defined in Section 4.1 was then obtained and presented in Figure 24. According to Figure 24, as the unidirectional RVE is presenting higher level of failure. It is

expectable for laminates with angle-ply layers to present higher strength compared to the unidirectional ones, with the [0/90] configuration expected to present the highest strength (the [0/90] configuration shows the lowest level of failure).

5. Discussion

Figure 25 presents a summary of experimentally obtained failure loads for the unidirectional and angle-ply laminates. Generally, the experimental study showed that hybrid laminates present higher strength compared to the reference conventional CFRP and composite. Moreover, angle-ply conventional CFRP and thin-ply laminates present higher strength compared to the unidirectional ones for both [45/−45]_{ns} and [0/90]_{ns} configurations. Therefore, an angle-ply hybrid composite laminate (unidirectional CFRP with angle-ply thin-ply or angle-ply CFRP and thin-ply) presents higher failure load than unidirectional hybrid laminates (see Figure 25). A comparison between Figure 25a and b shows that the failure load obtained for angle-ply hybrid laminates with oriented CFRP and thin-ply is slightly higher than that exhibited by configurations with unidirectional CFRP and angle-ply thin-ply. This is mainly due to a more complex through the thickness crack path. Experimental results also show that the angle-ply laminates with [0/90]_{ns} stacking sequence present higher strength for

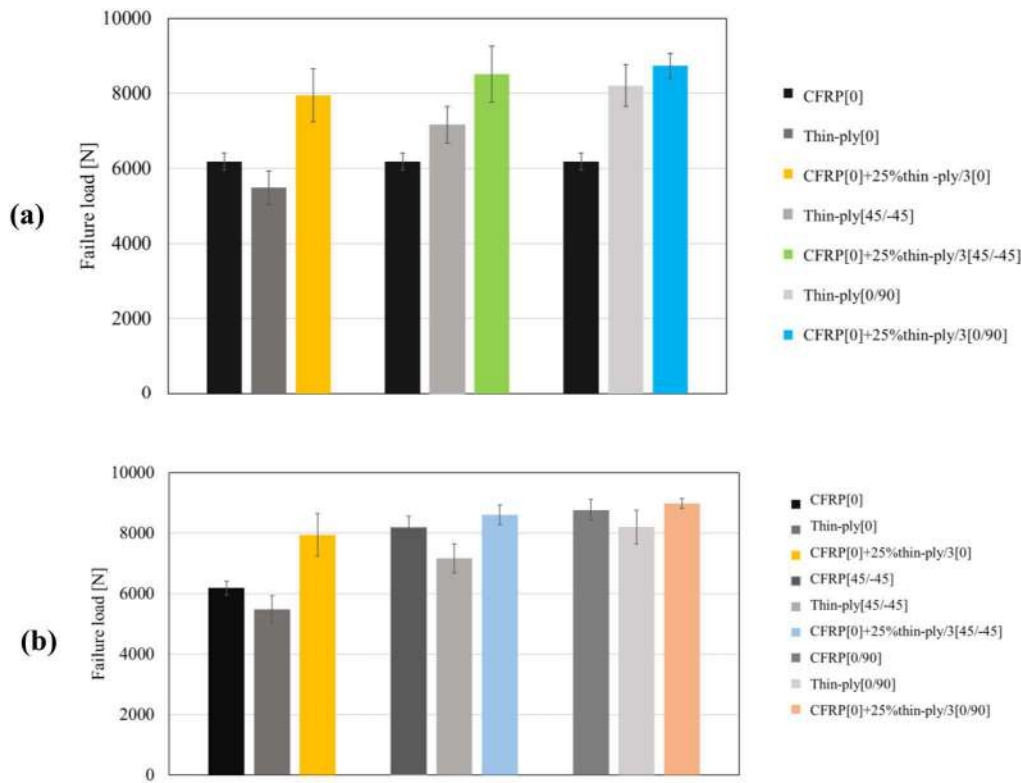


Figure 25. Average failure load for laminates with (a) unidirectional CFRP and oriented thin-ply and (b) oriented CFRP and thin-ply.

all configurations. A microscale numerical study shows that in the case of $[0/90]_{ns}$ stacking sequence, the matrix failure is delayed compared to the $[45/-45]_{ns}$ configuration.

6. Conclusion

This study investigated the effect of introducing angled ply layers in a composite laminate, approaching the problem from numerical and experimental perspectives. Two stacking sequences of $[45/-45]_{ns}$ and $[0/90]_{ns}$ were considered for the manufacture of reference CFRP and thin-ply-based laminates. A hybrid laminate configuration was also studied experimentally. A numerical elastoplastic RVE model was generated for the CFRP and thin-ply with unidirectional and angle-plyed fibers. Based on the obtained results, it can be concluded that:

1. A numerical analysis indicated that angle-plyed CFRP and thin-ply laminates experience a lower level of failure under out-of-plane tensile loading, and therefore the matrix failure process is delayed. Accordingly, angle-plyed laminates are expected to present higher strength compared to the unidirectional ones.
2. According to the same numerical study, the stacking sequence of $[0/90]$ presents a lower level of failure compared to $[45/-45]$ for both CFRP and thin-ply configurations.
3. Experimental results confirm that using angled plyed laminates in the reference or hybrid laminate increases the failure load under out-of-plane tensile loading. This is because the through the thickness crack path is more

complex in angle-plyed laminate than unidirectional laminates. This is a line with the literature review.

4. According to experimental result, hybrid laminates reinforced with thin-plyes and with the stacking sequence of $[0/90]_{ns}$ present the highest strength under out-of-plane tensile loads.

Funding

The authors gratefully acknowledge the Portuguese Foundation for Science and Technology (FCT) for supporting the work presented here, through the individual grants CEECIND/02752/2018, CEECIND/03276/2018 and 2021.07943.BD, and the Project No. PTDC/EME-EME/2728/2021 'New approaches to improve the joint strength and reduce the delamination of composite adhesive joints'.

ORCID

R. Carbas <http://orcid.org/0000-0002-1933-0865>
 E. A. S. Marques <http://orcid.org/0000-0002-2750-8184>
 A. M. Ferreira <http://orcid.org/0000-0003-4043-9838>
 L. F. M. da Silva <http://orcid.org/0000-0003-3272-4591>

References

- [1] M. F. Ashby, and D. R. H. Jones, Chapter 1-engineering materials and their properties. In: Engineering Materials, Elsevier, vol. 1, 2012. <https://doi.org/10.1016/B978-0-08-096665-6.00001-5>
- [2] P. Sahu, and M. K. Gupta, A review on the properties of natural fibres and its bio-composites: Effect of alkali treatment, Proc. Inst. Mech. Eng. Part L J. Mater. Design Appl., vol. 234, no. 1, pp. 198–217, 2020. DOI: 10.1177/1464420719875163.
- [3] M. Zhou, W. Gu, G. Wang, J. Zheng, C. Pei, F. Fan and G. Ji, Sustainable wood-based composites for microwave absorption and

- electromagnetic interference shielding, *J. Mater. Chem. A*, vol. 8, no. 46, pp. 24267–24283, 2020. DOI: [10.1039/D0TA08372K](https://doi.org/10.1039/D0TA08372K).
- [4] M. K. Budzik, M. Wolfahrt, P. Reis, M. Kozłowski, J. Sena-Cruz, L. Papadakis, M. Nasr Saleh, K.V. Machalicka, S.T. de Freitas and A.P. Vassilopoulos, Testing mechanical performance of adhesively bonded composite joints in engineering applications: an overview, *J. Adhesion*, vol. 98, no. 14, pp. 2133–2209, 2022. DOI: [10.1080/00218464.2021.1953479](https://doi.org/10.1080/00218464.2021.1953479).
 - [5] A. Arteiro, G. Catalanotti, J. Xavier, P. Linde, and P. P. Camanho, A strategy to improve the structural performance of non-crimp fabric thin-ply laminates, *Compos. Struct.*, vol. 188, pp. 438–449, 2018. DOI: [10.1016/j.compstruct.2017.11.072](https://doi.org/10.1016/j.compstruct.2017.11.072).
 - [6] S. Sihm, R. Y. Kim, K. Kawabe, and S. W. Tsai, Experimental studies of thin-ply laminated composites, *Compos. Sci. Technol.*, vol. 67, no. 6, pp. 996–1008, 2007. DOI: [10.1016/j.compscitech.2006.06.008](https://doi.org/10.1016/j.compscitech.2006.06.008).
 - [7] T. Roure, C-PLY™, a new structural approach to multiaxials in composites: BI-ANGLE NCF, *JEC Compos.*, no. 68, pp. 53–54, 2011.
 - [8] R. Amacher, J. Cugnoni, J. Botsis, L. Sorensen, W. Smith, and C. Dransfeld, Thin ply composites: Experimental characterization and modeling of size-effects, *Compos. Sci. Technol.*, vol. 101, pp. 121–132, 2014. DOI: [10.1016/j.compscitech.2014.06.027](https://doi.org/10.1016/j.compscitech.2014.06.027).
 - [9] B. Kötter, J. Karsten, J. Körbelin, and B. Fiedler, CFRP thin-ply fibre metal laminates: Influences of ply thickness and metal layers on open hole tension and compression properties, *Materials*, vol. 13, no. 4, pp. 910, 2020. DOI: [10.3390/ma13040910](https://doi.org/10.3390/ma13040910).
 - [10] M. R. Wisnom, B. Khan, and S. R. Hallett, Size effects in unnotched tensile strength of unidirectional and quasi-isotropic carbon/epoxy composites, *Compos. Struct.*, vol. 84, no. 1, pp. 21–28, 2008. DOI: [10.1016/j.compstruct.2007.06.002](https://doi.org/10.1016/j.compstruct.2007.06.002).
 - [11] R. Y. Kim, and S. R. Soni, Experimental and analytical studies on the onset of delamination in laminated composites, *J. Compos. Mater.*, vol. 18, no. 1, pp. 70–80, 1984. DOI: [10.1177/002199838401800106](https://doi.org/10.1177/002199838401800106).
 - [12] C. Huang, M. He, Y. He, J. Xiao, J. Zhang, S. Ju, and D. Jiang, Exploration relation between interlaminar shear properties of thin-ply laminates under short-beam bending and meso-structures, *J. Compos. Mater.*, vol. 52, no. 17, pp. 2375–2386, 2018. DOI: [10.1177/0021998317745586](https://doi.org/10.1177/0021998317745586).
 - [13] J. Kupski, D. Zarouchas, and S. T. de Freitas, Thin-ply in adhesively bonded carbon fiber reinforced polymers, *Compos. B: Engin.*, vol. 184, pp. 107627, 2020. DOI: [10.1016/j.compositesb.2019.107627](https://doi.org/10.1016/j.compositesb.2019.107627).
 - [14] P. P. Camanho, C. G. Dávila, S. T. Pinho, L. Iannucci, and P. Robinson, Prediction of in situ strengths and matrix cracking in composites under transverse tension and in-plane shear, *Compos. A: Appl. Sci. Manuf.*, vol. 37, no. 2, pp. 165–176, 2006. DOI: [10.1016/j.compositesa.2005.04.023](https://doi.org/10.1016/j.compositesa.2005.04.023).
 - [15] K. B. Su, Delamination resistance of stitched thermoplastic matrix composite laminates. In G. M. Nawaz (ed.), *Advances in thermoplastic matrix composite materials*, ASTM American Society of Testing and Materials STP 1044, Philadelphia; 1989. pp. 270–300.
 - [16] X. Zhou, J. Li, C. Qu, W. Bu, Z. Liu, Y. Fan and G. Bao, Bending behavior of hybrid sandwich composite structures containing 3D printed PLA lattice cores and magnesium alloy face sheets, *J. Adhesion*, vol. 98, no. 11, pp. 1713–1731, 2022. DOI: [10.1080/00218464.2021.1939015](https://doi.org/10.1080/00218464.2021.1939015).
 - [17] G. Guillet, A. Turon, J. Costa, J. Renart, P. Linde, and J. A. Mayugo, Damage occurrence at edges of non-crimp-fabric thin-ply laminates under off-axis uniaxial loading, *Compos. Sci. Technol.*, vol. 98, pp. 44–50, 2014. DOI: [10.1016/j.compscitech.2014.04.014](https://doi.org/10.1016/j.compscitech.2014.04.014).
 - [18] K. Tserpes, A. Barroso-Caro, P.A. Carraro, V.C. Beber, I. Floros, W. Gamon, M. Kozłowski, F. Santandrea, M. Shahverdi, D. Skejić, C. Bedon and V. Rajčić, A review on failure theories and simulation models for adhesive joints, *J. Adhesion*, vol. 98, no. 12, pp. 1855–1915, 2022. DOI: [10.1080/00218464.2021.1941903](https://doi.org/10.1080/00218464.2021.1941903).
 - [19] B. D. Simões, P. D. Nunes, F. Ramezani, R. J. Carbas, E. A. Marques, and L. F. da Silva, Experimental and numerical study of thermal residual stresses on multimaterial adherends in single-lap joints, *Materials*, vol. 15, no. 23, pp. 8541, 2022. DOI: [10.3390/ma15238541](https://doi.org/10.3390/ma15238541).
 - [20] F. Ramezani, P. D. P. Nunes, R. J. C. Carbas, E. A. S. Marques, and L. F. M. da Silva, The joint strength of hybrid composite joints reinforced with different laminates materials, *J. Adv. Joining Process.*, vol. 5, pp. 100103, 2022. DOI: [10.1016/j.jajp.2022.100103](https://doi.org/10.1016/j.jajp.2022.100103).
 - [21] K. D. Potter, F. J. Guild, H. J. Harvey, M. R. Wisnom, and R. D. Adams, Understanding and control of adhesive crack propagation in bonded joints between carbon fibre composite adherends I. Experimental, *Int. J. Adhes. Adhes.*, vol. 21, no. 6, pp. 435–443, 2001. DOI: [10.1016/S0143-7496\(01\)00020-3](https://doi.org/10.1016/S0143-7496(01)00020-3).
 - [22] A. P. Mouritz, Review of z-pinned composite laminates, *Compos. A: Appl. Sci. Manuf.*, vol. 38, no. 12, pp. 2383–2397, 2007. DOI: [10.1016/j.compositesa.2007.08.016](https://doi.org/10.1016/j.compositesa.2007.08.016).
 - [23] F. K. Ko, Three-dimensional fabrics for composites. In: TW Chou and FK Ko (eds) *Textile Structural Composites*, Elsevier, Amsterdam; 1989. pp.129–171
 - [24] J. W. Sawyer, Effect of stitching on the strength of bonded composite single lap joints, *AIAA J.*, vol. 23, no. 11, pp. 1744–1748, 1985. DOI: [10.2514/3.9160](https://doi.org/10.2514/3.9160).
 - [25] W. S. Chan, Design approaches for edge delamination resistance in laminated composites, *J. Compos. Technol. Res.*, vol. 13, no. 2, pp. 91–96, 1991.
 - [26] L. Hader-Kregl, G. M. Wallner, C. Kralovec, and C. Eyßell, Effect of inter-ply on the short beam shear delamination of steel/composite hybrid laminates, *J. Adhes.*, vol. 95, no. 12, pp. 1088–1100, 2019. DOI: [10.1080/00218464.2018.1474460](https://doi.org/10.1080/00218464.2018.1474460).
 - [27] A. Sadeghi, R. Mahshid, M. Heidari-Rarani, and L. Lessard, Effect of lamina fiber orientation interfaced with semi-flexible adhesive layer on strength and failure mode of composite single-lap joints, *Int. J. Adhes. Adhes.*, vol. 118, pp. 103232, 2022. DOI: [10.1016/j.ijadhadh.2022.103232](https://doi.org/10.1016/j.ijadhadh.2022.103232).
 - [28] H. Greife, M. W. Kandula, and K. Dilger, Influence of the fibre orientation on the lap shear strength and fracture behaviour of adhesively bonded composite metal joints at high strain rates, *Int. J. Adhes. Adhes.*, vol. 97, pp. 102486, 2020. DOI: [10.1016/j.ijadhadh.2019.102486](https://doi.org/10.1016/j.ijadhadh.2019.102486).
 - [29] A. Ozel, B. Yazici, S. Akpınar, M. D. Aydin, and Ş. Temiz, A study on the strength of adhesively bonded joints with different adherends, *Compos. B: Eng.*, vol. 62, pp. 167–174, 2014. DOI: [10.1016/j.compositesb.2014.03.001](https://doi.org/10.1016/j.compositesb.2014.03.001).
 - [30] S. Akpınar, Effects of laminate carbon/epoxy composite patches on the strength of double-strap adhesive joints: experimental and numerical analysis, *Mater. Design.*, vol. 51, pp. 501–512, 2013. DOI: [10.1016/j.matdes.2013.04.037](https://doi.org/10.1016/j.matdes.2013.04.037).
 - [31] S. Purimpat, R. Jérôme, and A. Shahram, Effect of fiber angle orientation on a laminated composite single-lap adhesive joint, *Adv. Compos. Mater.*, vol. 22, no. 3, pp. 139–149, 2013. DOI: [10.1080/09243046.2013.782805](https://doi.org/10.1080/09243046.2013.782805).
 - [32] R. Hazimeh, G. Challita, K. Khalil, and R. Othman, Experimental investigation of the influence of substrates' fibers orientations on the impact response of composite double-lap joints, *Compos. Struct.*, vol. 134, pp. 82–89, 2015. DOI: [10.1016/j.compstruct.2015.08.040](https://doi.org/10.1016/j.compstruct.2015.08.040).
 - [33] F. Ramezani, R. J. Carbas, E. A. Marques, A. M. Ferreira, and L. F. da Silva, A study of the fracture mechanisms of hybrid carbon fiber reinforced polymer laminates reinforced by thin-ply, *Polym. Compos.* <https://doi.org/10.1002/pc.27196>
 - [34] R. D. Campilho, M. F. S. F. De Moura, and J. J. M. S. Domingues, Modelling single and double-lap repairs on composite materials, *Compos. Sci. Technol.*, vol. 65, no. 13, pp. 1948–1958, 2005. DOI: [10.1016/j.compscitech.2005.04.007](https://doi.org/10.1016/j.compscitech.2005.04.007).
 - [35] M. F. S. F. De Moura, R. D. S. G. Campilho, and J. P. M. Gonçalves, Crack equivalent concept applied to the fracture characterization of bonded joints under pure mode I loading, *Compos. Sci. Technol.*, vol. 68, no. 10–11, pp. 2224–2230, 2008. DOI: [10.1016/j.compscitech.2008.04.003](https://doi.org/10.1016/j.compscitech.2008.04.003).



Appendix E

Paper E

Study of Hybrid Composite Joints with Thin-Ply-Reinforced Adherends

Article

Study of Hybrid Composite Joints with Thin-Ply-Reinforced Adherends

Farin Ramezani ¹, Ricardo J. C. Carbas ^{1,2,*} , Eduardo A. S. Marques ² and Lucas F. M. da Silva ² 

¹ Instituto de Ciência e Inovação Em Engenharia Mecânica e Engenharia Industrial (INEGI), Rua Dr. Roberto Frias, 4200-465 Porto, Portugal

² Departamento de Engenharia Mecânica, Faculdade de Engenharia (FEUP), Universidade Do Porto, Rua Dr. Roberto Frias, 4200-465 Porto, Portugal

* Correspondence: rcarbas@fe.up.pt

Abstract: It has been demonstrated that a possible solution to reducing delamination in a unidirectional composite laminate lies in the replacement of conventional carbon-fibre-reinforced polymer layers with optimized thin-ply layers, thus creating hybrid laminates. This leads to an increase in the transverse tensile strength of the hybrid composite laminate. This study investigates the performance of a hybrid composite laminate reinforced by thin plies used as adherends in bonded single lap joints. Two different composites with the commercial references Texipreg HS 160 T700 and NTPT-TP415 were used as the conventional composite and thin-ply material, respectively. Three configurations were considered in this study: two reference single lap joints with a conventional composite or thin ply used as the adherends and a hybrid single lap. The joints were quasi-statically loaded and recorded with a high-speed camera, allowing for the determination of damage initiation sites. Numerical models of the joints were also created, allowing for a better understanding of the underlying failure mechanisms and the identification of the damage initiation sites. The results show a significant increase in tensile strength for the hybrid joints compared to the conventional ones as a result of changes in the damage initiation sites and the level of delamination present in the joint.

Keywords: composite joints; thin ply; single lap joints



Citation: Ramezani, F.; Carbas, R.J.C.; Marques, E.A.S.; da Silva, L.F.M. Study of Hybrid Composite Joints with Thin-Ply-Reinforced Adherends. *Materials* **2023**, *16*, 4002. <https://doi.org/10.3390/ma16114002>

Academic Editor: Alessandro Pirondi

Received: 31 March 2023

Revised: 13 April 2023

Accepted: 21 April 2023

Published: 26 May 2023



Copyright: © 2023 by the authors. Licensee MDPI, Basel, Switzerland. This article is an open access article distributed under the terms and conditions of the Creative Commons Attribution (CC BY) license (<https://creativecommons.org/licenses/by/4.0/>).

1. Introduction

Composites usually consist of two main components known as the matrix, which provides the cohesion of the material, and the reinforcement, such as fibres, which provides the material with its strength and stiffness [1]. The use of carbon-fibre-reinforced polymer (CFRP) materials in multiple industrial applications is continuously increasing [2–7], leading to the use of a vast range of composite materials for the design and manufacture of high-performance composite products such as vehicle structures, sporting goods, etc. [2,8]. However, since the strength of the matrix is at least an order of magnitude lower than the strength of the reinforcement, the loads applied in a perpendicular direction to the reinforcement are almost exclusively carried by the low-strength matrix. This results in the onset of delamination, which can lead to the rapid degradation of the mechanical performance of the structure and cause premature failure [9–12]. Accordingly, multiple studies have investigated methods for adhesive layer modification [13,14] or composite laminate modification to delay delamination in a composite joint [15–17], such as the use of fibre metal laminates (FML), composite laminates with toughened layers [18,19], glass fabric reinforcement [20], the use of Z-pins [21,22], 3D weaving [23], stitching [23], braiding [24], or even the adoption of additional thermoplastic inter-ply [25]. However, the significant complexity of these techniques often restricts their usage. Furthermore, such methods normally require the implementation of at least one additional production step [26,27] and thus increase the costs associated to the production process.

Recent advancements in composite manufacturing techniques have led to the development of spread-tow technology [28], which results in flat and straight plies with a more homogeneous fibre distribution and smaller resin-rich regions [29,30]. In this case, a dry ply thickness as low as 0.02 mm can be achieved. Generally, plies with a thickness below 100 μm are known as thin plies [31]. By reducing the thickness of a single layer, the number of possible total layers and therefore the degrees of freedom in design are increased [32]. This also results in a larger number of interfaces in thin-ply laminates, lowering the shear stresses [32,33]. Moreover, thin-ply laminates are known for their ability to delay the onset of the matrix damage mechanisms and suppress transverse microcracking [31] and free edge delamination [32,34] for static, fatigue, and impact loadings. Due to their superior damage and delamination resistance, thin-ply laminates could exhibit higher interlaminar shear properties [35] and strain energy [36] compared to conventional plies. Therefore, thinner composite plies are acknowledged to have higher in situ transverse strength [33]. Nonetheless, the properties of the laminate can still rapidly deteriorate after the onset of damage, leading to premature structural failure [11]. Thin plies are now seen as a promising approach to improve the performance of adhesively bonded CFRP, mainly due to their ability to enhance the off-axis performance of composites and postpone delamination [36]. Moreover, studies have shown that through the use of thin plies in a structural joint, the damage location in the composite moves from the adhesive interface towards the mid-thickness of the composite adherends [36], mainly due to the in situ effect [37]. Through-thickness reinforcement can effectively provide improved interlaminar strength and delamination resistance while producing a more integrated composite structure [38].

A previous study by the authors [39] showed that replacing layers of a conventional composite in a unidirectional laminate with layers of thin ply can increase the composite's strength under transverse tensile loading. The authors postulate that this is due to the increase in laminate ductility, which could postpone the delamination under transverse tensile loads. Moreover, experimental observation clearly demonstrated that the presence of thin plies acts as a barrier against crack propagation. It was shown that the use of 25% (corresponding to the optimum amount) thin ply per total thickness of the laminate (12.5% on each top) increased the transverse tensile strength considerably. Figure 1a shows the studied configuration for a reference conventional composite: thin ply and the optimum hybrid laminate. Figure 1b illustrates the experimentally obtained failure loads for the mentioned configurations.

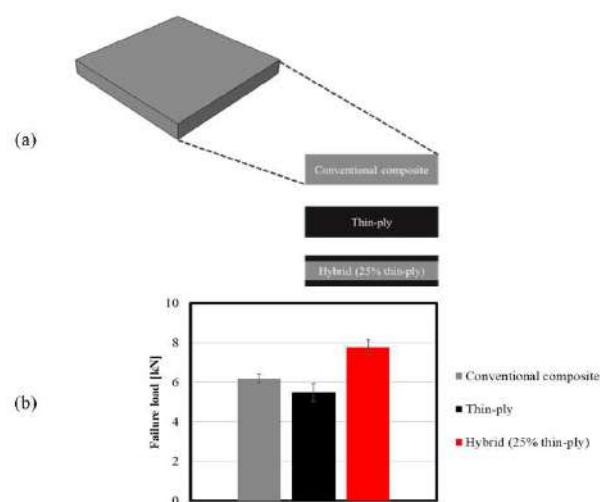


Figure 1. (a) Schematic design for conventional composite, thin-ply, and hybrid (25% thin ply) laminates and (b) summary of the experimentally obtained failure load for unidirectional reference conventional composite, thin-ply, and hybrid (25% thin ply) laminates. Adopted from [39].

The current study seeks to further investigate this topic, quantifying the performance of a hybrid composite single lap joint and analysing the effect of reinforcing the unidirectional conventional composite adherend using thin ply. In this work, “HS 160 T700” and “NTPT-TP415” are used as a conventional composite and thin-ply material, respectively. The tests were recorded using a high-speed camera to determine the location of damage initiation. Afterwards, the failure surface of specimens was analysed and measured via image analysis, allowing for an accurate estimation of the delaminated area. It was found that the use of hybrid single lap joints reinforced with thin-ply layers results in a considerable increase in the joint strength compared to the reference conventional composite joint. Numerical models were also created via cohesive zone modelling, allowing for the accurately replication and description of the experimentally determined failure processes.

2. Experimental Details

2.1. Adhesive

The adhesive used in this work was an epoxy structural adhesive, supplied in film form, with the commercial reference Scotch Weld AF 163-2k (3M, Saint Paul, MN, USA) [40]. The adhesive was cured following the manufacturer’s recommendations at 130 °C for 2 h. The mechanical properties of the AF 163-2k adhesive are presented in Table 1.

Table 1. Main mechanical properties of “AF 163-2k” [41].

Mechanical Property	Value
Young’s modulus [MPa]	1521.87
Shear modulus [MPa]	563.67
Tensile strength [MPa]	46.93
Shear strength [MPa]	46.93
G_{IC} [N/mm]	4.05
G_{IIC} [N/mm]	9.77

2.2. Adherend

2.2.1. Conventional Composite

The materials used in the studied configurations were chosen to be representative of a possible application within the aerospace sector. Accordingly, a unidirectional prepreg carbon–epoxy composite with a ply thickness of 0.15mm was selected, with the commercial reference Texipreg HS 160 T700 (Seal Spa, Legnano, Italy). This is an orthotropic material whose mechanical properties are presented in Table 2. The elastic mechanical properties of the conventional composite correspond to the orientation of a 0° composite ply (1 and 2 are defined as the fibre and transverse directions). Moreover, the cohesive properties of the conventional composite’s resin are presented separately in Table 3.

Table 2. Conventional composite mechanical properties [42].

Mechanical Property	Value
E_1 [MPa]	109,000
E_2 [MPa]	8819
G_{12} [MPa]	4315
G_{23} [MPa]	3200
ν_{12}	0.34
ν_{23}	0.38

Table 3. Cohesive properties of conventional composite [43].

Property	Value
Tensile strength [MPa]	25
Shear strength [MPa]	13.5
G_{IC} [N/mm]	0.33
G_{IIC} [N/mm]	0.79

2.2.2. Thin-Ply

A unidirectional, 0° oriented carbon–epoxy prepreg composite with a ply thickness of 0.075 mm was selected for use in this work, serving as the thin-ply material. This material has the commercial reference NTPT-TP415 (North thin ply technology, Zory, Poland). The elastic orthotropic and cohesive properties for the thin ply, characterised by the authors in a previous work [44], are presented in Tables 4 and 5, respectively.

Table 4. Thin ply mechanical properties [44].

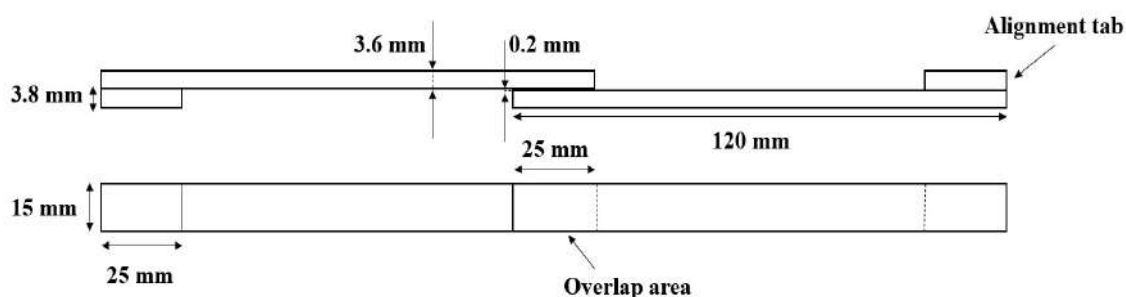
Mechanical Property	Value
E_1 [MPa]	101,720
E_2 [MPa]	5680
G_{12} [MPa]	3030
G_{23} [MPa]	3030
ν_{12}	0.38
ν_{23}	0.04

Table 5. Cohesive properties of the thin ply [44].

Property	Value
Tensile strength [MPa]	35
Shear strength [MPa]	32
G_{IC} [N/mm]	0.76
G_{IIC} [N/mm]	0.83

2.3. Single Lap Joint Manufacturing

Single lap joints (SLJs) were manufactured with the geometry shown in Figure 2. The width for all specimens under consideration was set at 15 mm.

**Figure 2.** Single lap joint geometry.

The manufacturing process for the reference conventional composite and thin-ply adherends began with a layer-by-layer stacking of the conventional composite and thin-ply prepregs respectively, until the desired adherend thickness was attained (3.6 mm). In this case, 24 and 48 layers of conventional composite and thin-ply prepreg were used, respectively. For the hybrid (25% thin ply) adherends, 6 plies of conventional composite were replaced by 12 plies of thin ply on the adherend tops (6 layers of thin ply on each adherend top). The joints were then bonded by applying an additional layer of adhesive between the adherends. A mould was used to ensure the thickness of the adherends and

adhesive. A mould-release agent was used to ensure easy debonding of the specimen from the mould after curing. It was observed that the curing sequence, i.e., curing the adhesive and substrate composite plies in one cure (co-curing) or in two separate cures, had no significant effect on the mechanical properties of the joint for the AF163-2k adhesive. Therefore, a one-step curing manufacturing method was preferred to simultaneously reducing manufacturing time and energy usage. Accordingly, the joint was co-cured at 130 °C for two hours, following the manufacturer's recommended procedure. A schematic design of the reference conventional composite, thin-ply, and hybrid (25% thin-ply) single lap joints are shown in Figure 3.

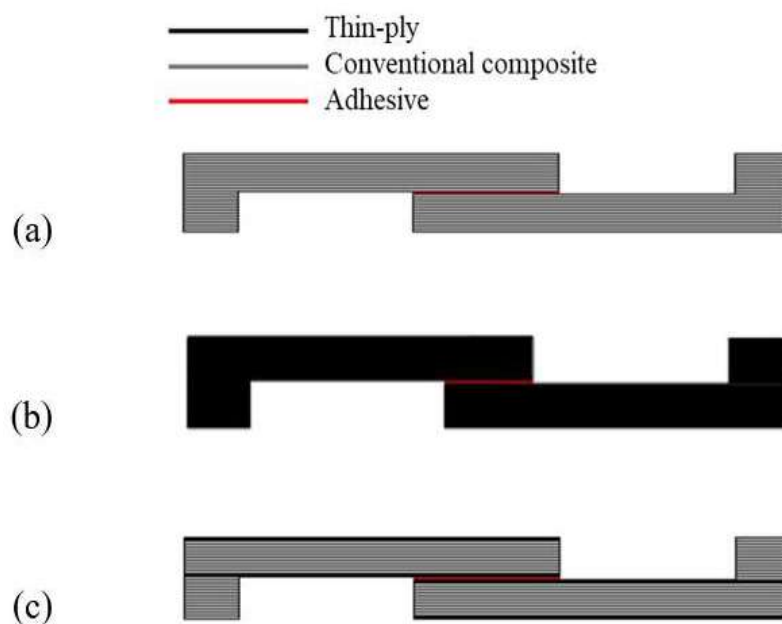


Figure 3. Schematic design of (a) conventional composite, (b) thin-ply, and (c) hybrid (25% thin-ply) joints.

2.4. Testing Condition

The SLJs were tested using an Instron 8801 servo hydraulic testing machine with a load cell of 100 kN and at a constant crosshead speed of 1 mm/min. All tests were performed under laboratory ambient conditions (room temperature of 24 °C, relative humidity of 55%). Four repetitions were performed for each configuration under analysis.

3. Experimental Results

3.1. Load–Displacement Curve

Figure 4 shows representative, experimentally obtained load–displacement curves for the studied configurations. The hybrid (25% thin ply) joint presented the highest failure load, with an increase in joint strength of approximately 90% compared to the reference conventional composite configuration.

3.2. Damage Initiation

A high-speed camera was used to record the specimens under load, seeking to determine whether the damage initiation occurred first in the adhesive layer or within the adherend. A Chronos 1.4 high speed camera was used, recording at 5000 frames per second. Figure 5 presents the images at damage initiation for each configuration. The adhesive and adherend boundaries were roughly defined by correlating the known specimen's dimensions and the equivalent image pixels. As can be seen in Figure 5, in the reference conventional composite and the thin-ply, damage initiation occurred in the composite

adherend. In contrast, for the hybrid (25% thin ply) joint, the damage initiation occurred in the adhesive layer.

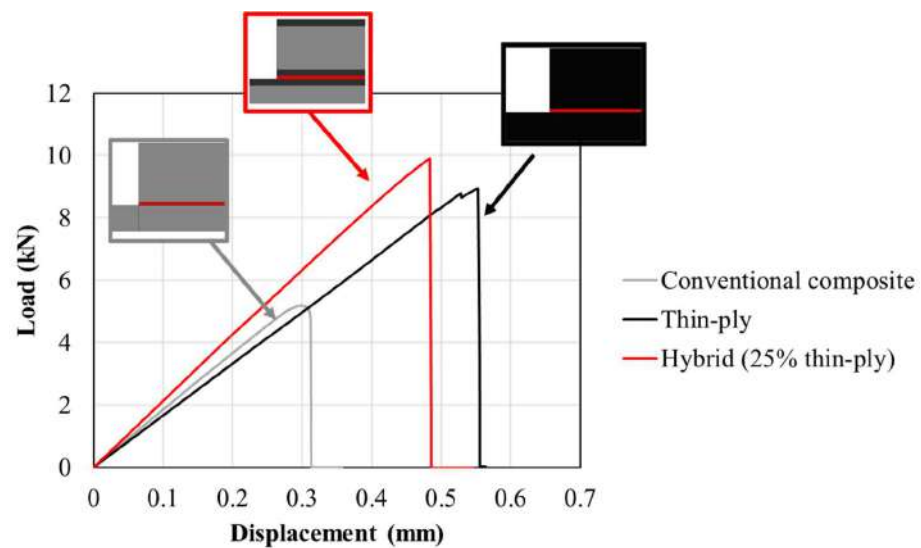


Figure 4. Representative load–displacement curves for reference conventional composite, thin-ply, and hybrid (25% thin ply) joints.

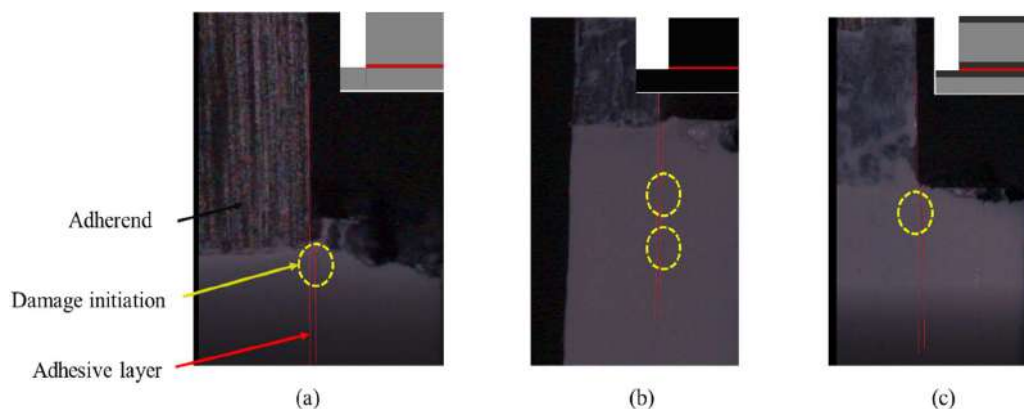


Figure 5. Damage initiation for (a) conventional composite, (b) thin-ply, and (c) hybrid (25% thin ply) joints.

3.3. Delamination

Digital images of the failure surface were analysed in order to obtain the delamination ratio for each configuration. The open-source software IC Measure was used to calculate the delamination area for each joint. The delamination ratio is defined as the delamination area divided by the total bonded area, as presented in Equation (1). It should be noted that the total bonded area was constant and equal to 375 mm² for all configurations. Figure 6 provides representative images of the failure surface for all configurations. The representative delamination area from Figure 6 and the average delamination area are presented in Table 6. The reference conventional composite joint shown in Figure 6 presents delamination of about 51%, while the hybrid (25% thin ply) configuration presents delamination of about 29%. In contrast, around 80% of the total area was observed to have suffered delamination in the reference thin-ply joint.

$$\text{Delamination ratio (\%)} = \frac{\text{Delamination area}}{\text{Total bonded area}} \quad (1)$$

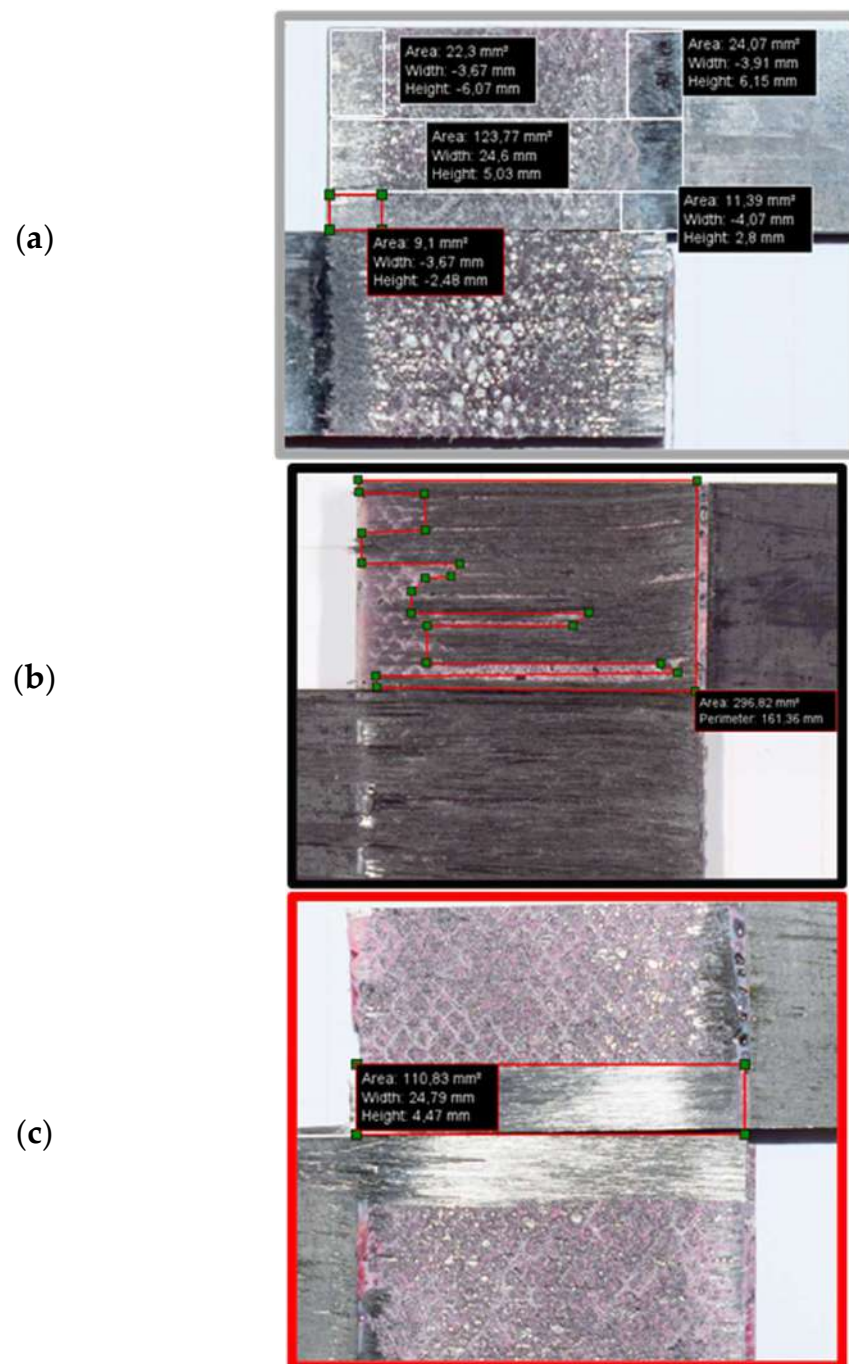


Figure 6. Representative images of failure surface of (a) reference conventional composite, (b) thin-ply, and (c) hybrid (25% thin ply) joints.

Table 6. Representative and average delamination area.

Configuration	Representative [mm ²]	Average [mm ²]
Conventional composite	190.52	210.00 ± 32.75
Thin-ply	296.82	332.07 ± 39.65
Hybrid (25% thin ply)	110.83	128.20 ± 36.92

3.4. Microscopic Images

The failure surfaces of the reference conventional composite and hybrid (25% thin ply) joint were analysed using a ZEISS AXIOPHOT microscope. According to the microscopic images presented in Figure 7, multiple fibre breakages [45] and fibre pull-outs [46] were observed on the failure surface of the reference conventional composite failure surface. These failure mechanisms were not observed in the failure surface of the hybrid (25% thin ply) joint under analysis.

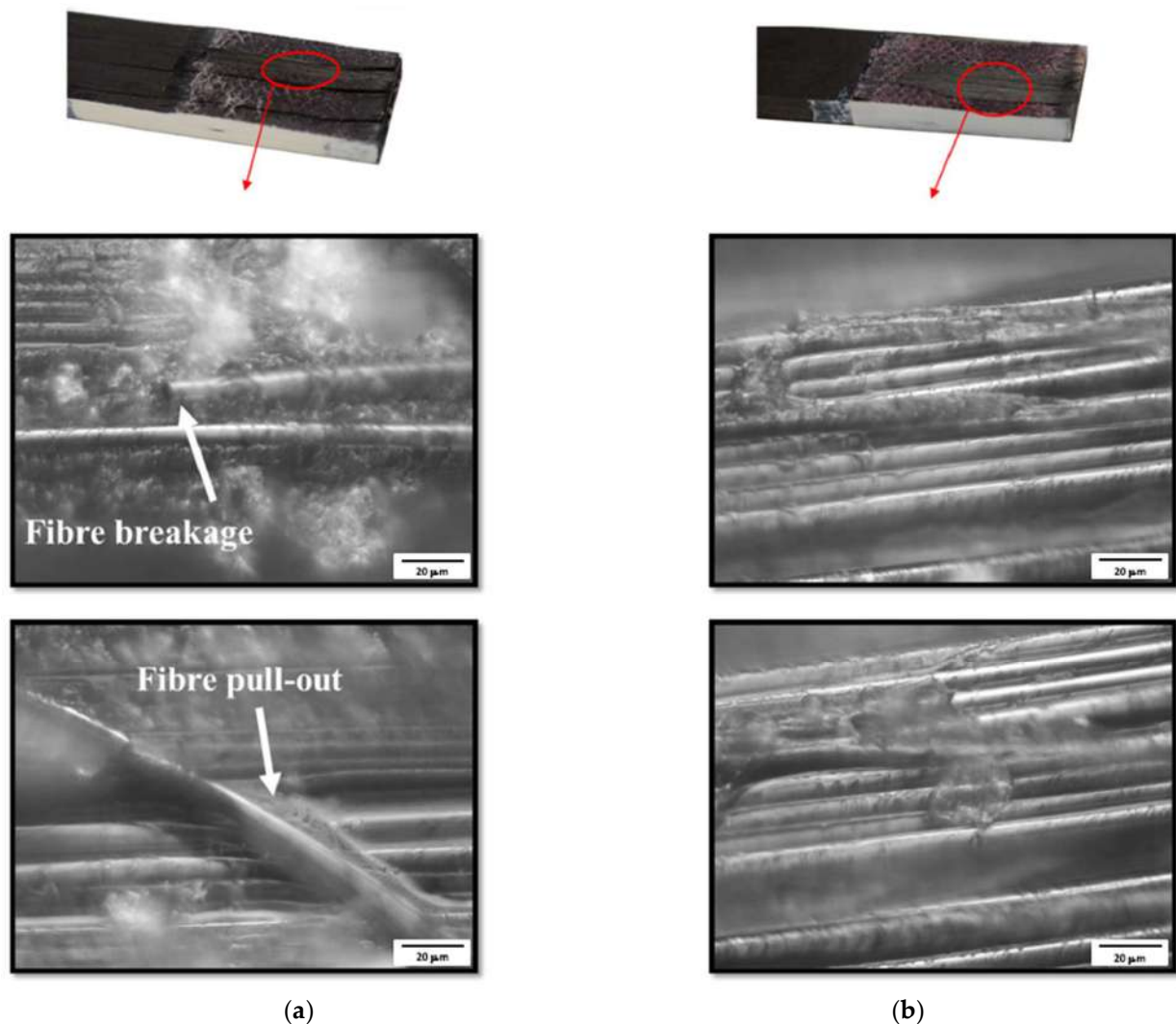


Figure 7. Microscopic images of (a) conventional composite and (b) hybrid (25% thin ply) joints.

4. Numerical Study

4.1. Load–Displacement Curve

A two-dimensional statically loaded model was used to simplify the problem under analysis and reduce the computational time. Boundary conditions were defined as shown in Figure 8. The left end of the joint was fixed while a displacement was applied in the right end to replicate the testing fixtures. A cohesive zone model (CZM) was used to model the adhesive behaviour, employing four node elements: cohesive quadrilateral elements. Non-linear geometrical effects were included. Solid cohesive elements following triangular traction separation laws were applied to the adhesive layers of the model to simulate damage evolution (damage initiation and propagation). Cohesive behaviour was specified directly in terms of a traction–separation law, which has been shown to be suitable to represent delamination in composite laminates [47]. Therefore, a similar

CZM was introduced into the composite material (conventional composite or thin-ply) to model delamination due to the experimental failure mode obtained. These interlaminar cohesive element layers were placed in between elastic homogeneous sections (see Figure 9) and effectively simulated the possible debonding between the plies of composite. The CZM layers were placed at a distance of 0.15, 0.37, and 0.13 mm from the interface of the adherend and adhesive layer for the conventional composite, thin-ply, and hybrid (25% thin ply) joints, respectively. This distance roughly corresponded to the experimentally measured distance of the delamination plane from the adhesive layer. The thickness of the cohesive layer matched the thickness of one equivalent composite ply (0.075 mm for thin ply and 0.15 mm for the conventional composite).

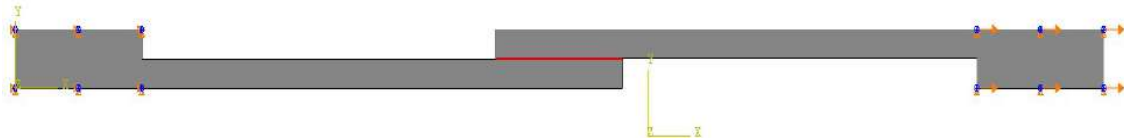


Figure 8. Boundary condition of simulated single lap joint.

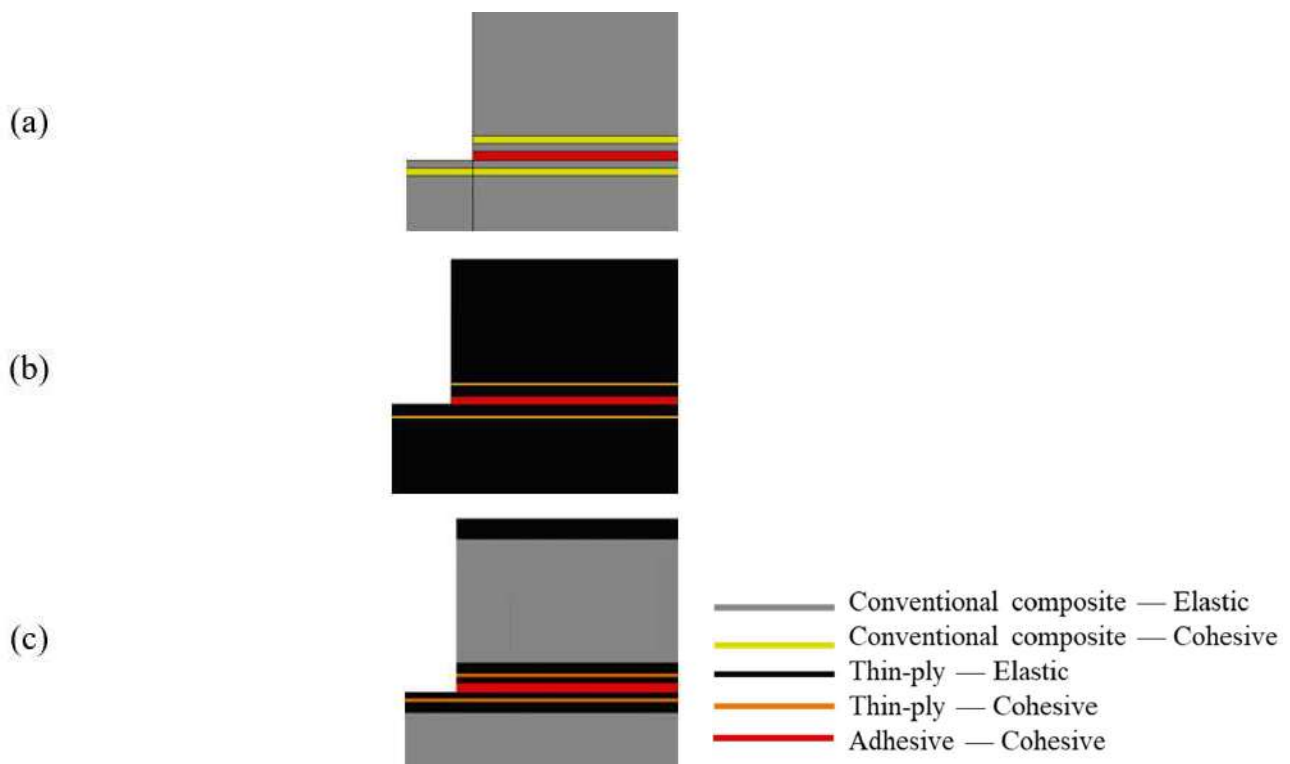


Figure 9. Assigned mechanical properties for (a) conventional composite, (b) thin-ply, and (c) hybrid (25% thin ply) joints.

Double and single biased mesh distributions were considered in the x direction (see Figure 10) for the bondline and the adherends, respectively. The minimum and maximum sizes for the mesh were considered 0.2 and 0.5 mm respectively. However, a uniform mesh distribution with the size of 0.5 mm was considered for the end tabs (in the x direction). Moreover, a uniform distribution through the mesh thickness (y direction) was considered for all models with a mesh size of 0.2 mm. Figure 10 illustrates the mesh distribution mentioned above. As a result, around 15,000 elements were generated for each numerical model. Figure 11 presents the numerical load–displacement curves obtained for all configurations. As shown, the numerical results are in good agreement with the experimentally obtained load–displacement curves.

4.2. Damage

The same model was used to determine the damage initiation and its propagation mode for each configuration under analysis. According to the numerical results presented in Figure 12, the damage for the reference conventional composite and thin-ply joint initiated in the composite (conventional composite and thin-ply joints, respectively). For the hybrid (25% thin ply) joint, damage initiation occurred in the adhesive layer. The loads at damage initiation for the mentioned configurations were 3.6, 6.9, and 7.3 kN, respectively. It should be noted that the damage generated in the configurations at the equivalent numerically obtained failure loads illustrates that delamination is expected to be the final failure mode for all configurations under analysis (see Figure 13).

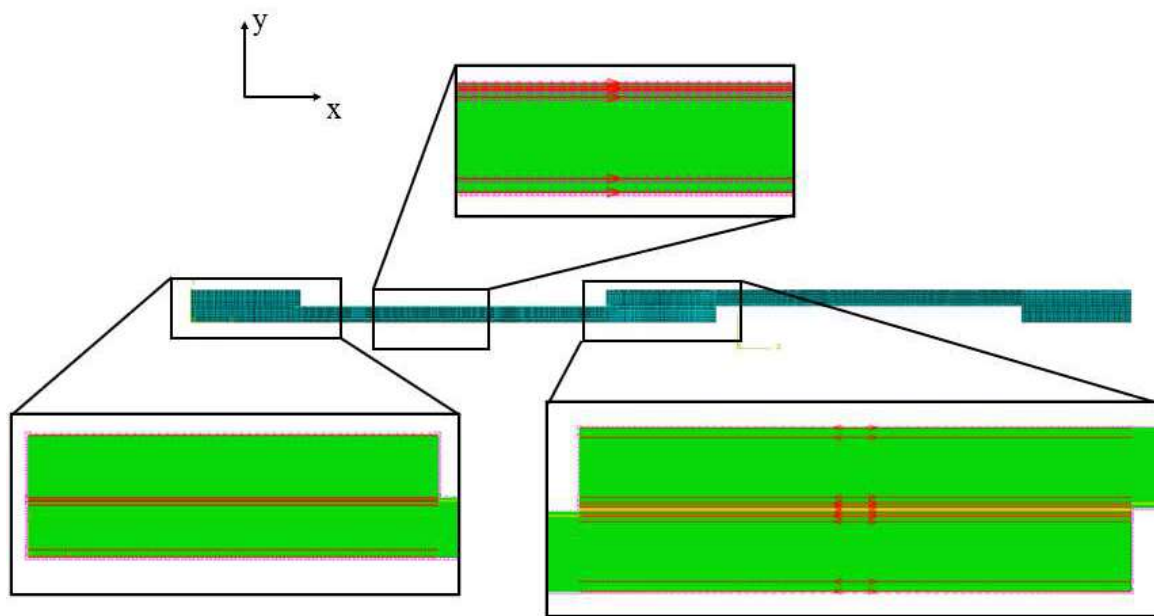


Figure 10. Mesh distribution for numerical models.

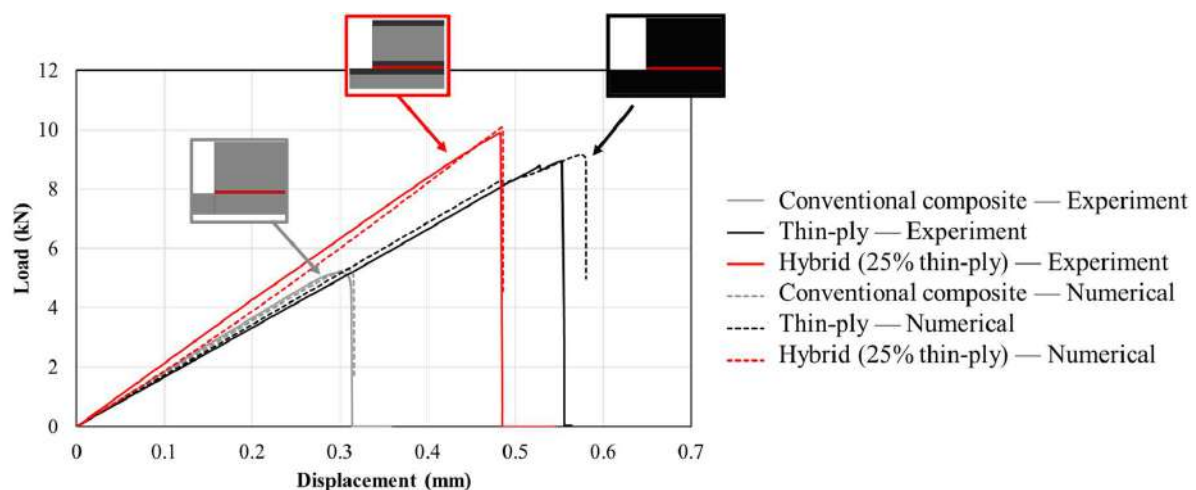


Figure 11. Comparison of numerically obtained load–displacement curves for conventional composite, thin-ply, and hybrid (25% thin ply) joints with the representative experimental results.

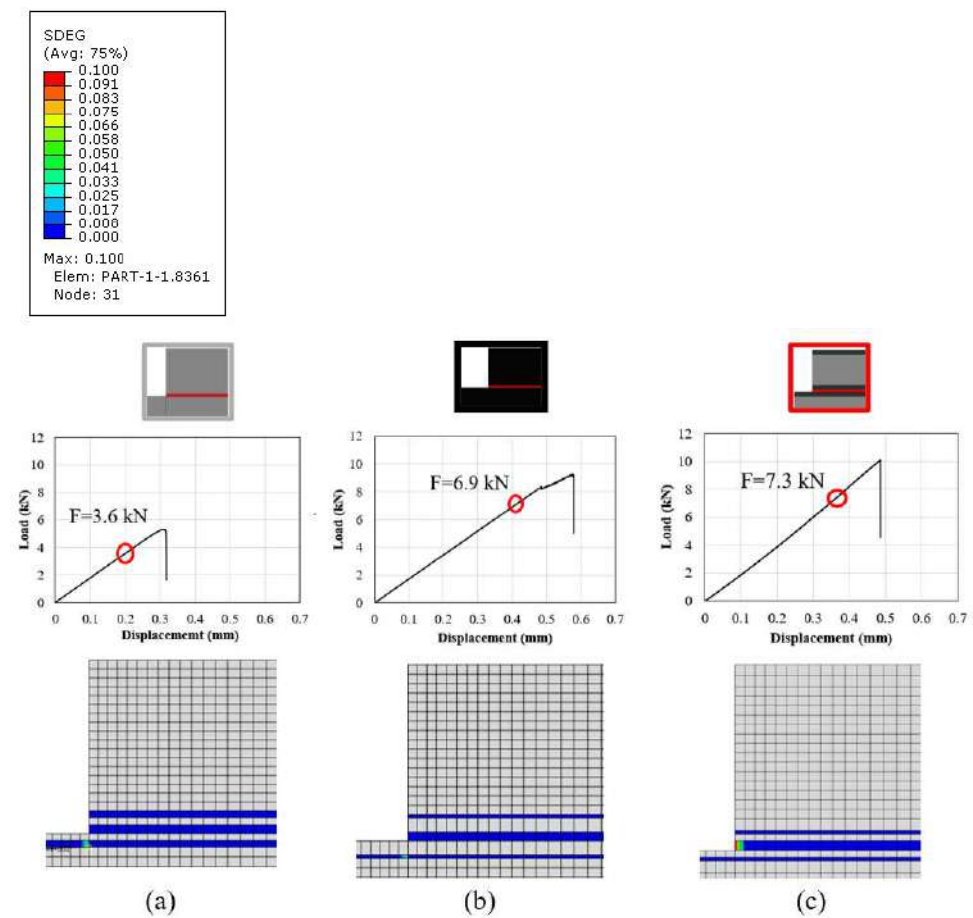


Figure 12. SDEG at damage initiation for (a) conventional composite, (b) thin-ply and (c) hybrid (25% thin ply) joints (equivalent loads for each configuration are 3.6, 6.9, and 7.3 kN, respectively).

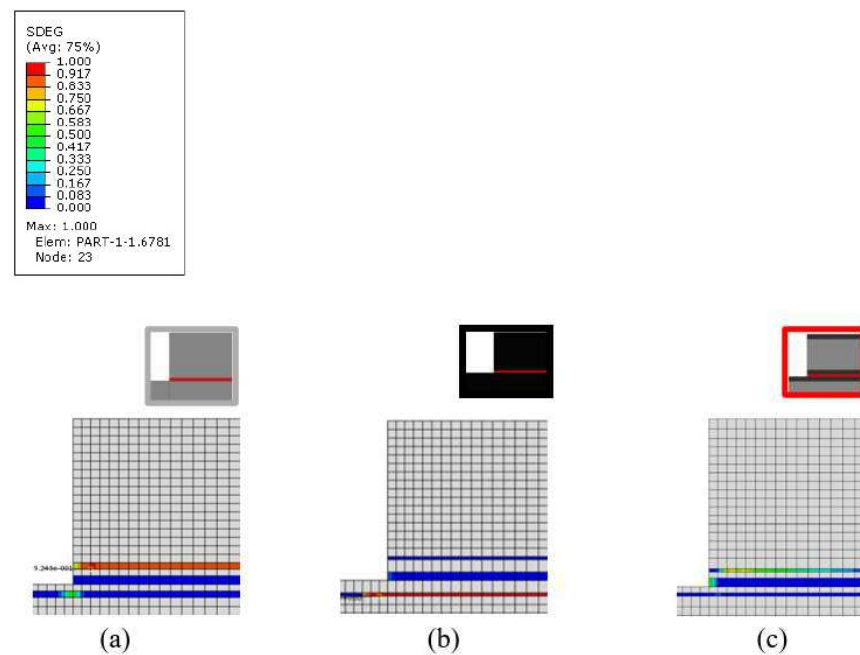


Figure 13. SDEG at failure load for (a) conventional composite, (b) thin-ply and (c) hybrid (25% thin ply) joints (equivalent loads for each configuration are 5.4, 9.2, and 10.0 kN, respectively).

5. Discussion

The use of hybrid, adhesively bonded composite joints reinforced with thin plies increases the tensile strength compared to that of reference joints manufactured using only a conventional composite. Figure 14 presents the average failure load obtained for the reference conventional composites, thin-ply, and hybrid (25% thin ply) single lap joints. An increase of about 90% in the failure load was obtained for the hybrid (25% thin ply) joints. Although similar failure loads were obtained for the hybrid (25% thin ply) and reference thin-ply joint, it must be mentioned that the manufacturing process for a hybrid (25% thin ply) joint costs less and is less time-consuming compared to the process of manufacturing the reference thin-ply joint. Moreover, experimental observation illustrates that the delamination ratio decreases considerably while using hybrid composite joints reinforced with thin-ply compared to the reference conventional composite and thin-ply single lap joint. The average delamination ratio obtained for this configuration can be found in Figure 15. According to the numerical and experimental study, the damage initiation location depends on the joint configuration. Damage first occurs in the adherend in the reference conventional composite and thin ply, but it initiates in the adhesive layer for the hybrid (25% thin ply) joint. The initiated damage propagates as a combination of delamination and cohesive failure for all configurations, but a lower level of delamination was obtained for the hybrid joint. A schematic representation of the mentioned failure mechanism could be found in Figure 16.

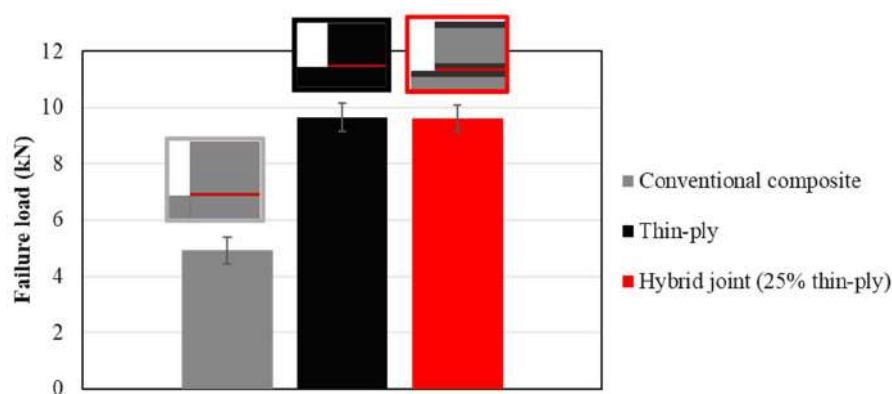


Figure 14. Average failure loads obtained experimentally for reference conventional composite, thin-ply, and hybrid (25% thin ply) joints.

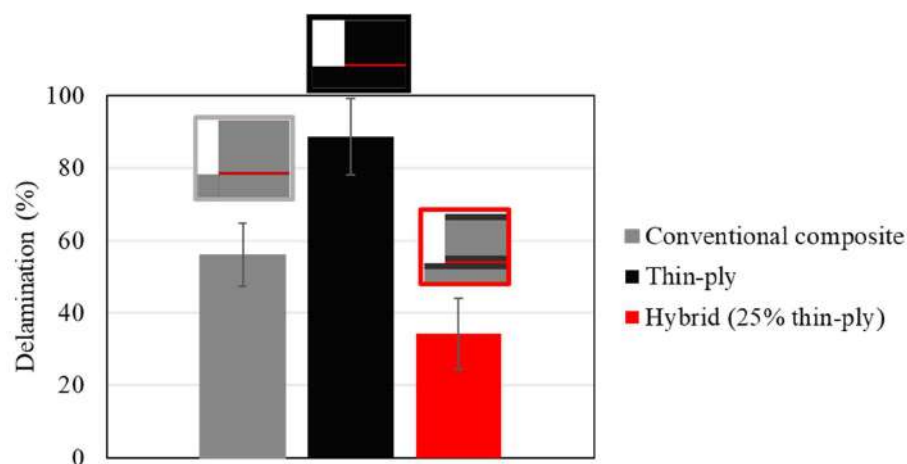


Figure 15. Average delamination ratios for reference conventional composite, thin-ply, and hybrid (25% thin ply) joints.

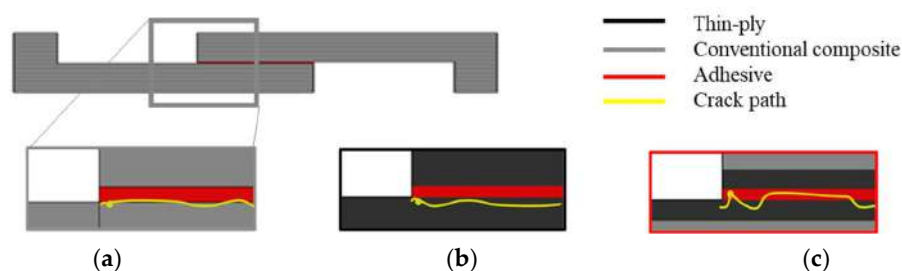


Figure 16. Schematic representation of the failure mechanism for (a) reference conventional composite, (b) thin-ply, and (c) hybrid (25% thin ply) joints.

6. Conclusions

This study investigated the mechanical performance of composite single lap joints using toughened adherends reinforced with thin plies. A numerical and experimental study was performed accordingly. The main conclusions drawn from this work are as follows:

- An increase of approximately 90% in the failure load was found for the hybrid joint reinforced with thin ply when compared to the reference conventional composite joint.
- According to the experimental observation, damage initiation occurs in the adherend for the reference conventional composite and thin-ply joint, while for the hybrid (25% thin ply) joint, damage initiation occurs in the adhesive layer.
- Damage propagates as a combination of delamination and cohesive failure for all configurations. However, a more limited amount of delamination was obtained for the hybrid joint.
- Microscopic images of the bond line allowed for the identification of multiple fibre breakages and fibre pull-outs on the failure surface of the reference conventional composite configuration. In contrast, the fibres were still intact and well-aligned in the failure surface of the hybrid joint.
- The configurations under analysis were modelled numerically, and a good agreement was obtained between the numerical and experimental results, allowing for a precise representation of the damage initiation and failure processes.

Author Contributions: Investigation, F.R.; Writing—original draft, F.R.; Writing—review & editing, R.J.C.C., E.A.S.M. and L.F.M.d.S.; Supervision, R.J.C.C., E.A.S.M. and L.F.M.d.S. All authors have read and agreed to the published version of the manuscript.

Funding: The authors gratefully acknowledge the Portuguese Foundation for Science and Technology (FCT) for supporting the work presented here through the individual grants CEECIND/03276/2018 and 2021.07943.BD and Project No. PTDC/EME-EME/2728/2021, “New approaches to improve the joint strength and reduce the delamination of composite adhesive joints”.

Institutional Review Board Statement: Not applicable.

Informed Consent Statement: Not applicable.

Data Availability Statement: Not applicable.

Conflicts of Interest: The authors declare no conflict of interest.

References

1. Karataş, M.A.; Gökkaya, H. A review on machinability of carbon fiber reinforced polymer (CFRP) and glass fiber reinforced polymer (GFRP) composite materials. *Def. Technol.* **2018**, *14*, 318–326. [\[CrossRef\]](#)
2. Ashby, M.F.; Jones, D.R. *Engineering Materials 1: An Introduction to Properties, Applications and Design*; Elsevier: Amsterdam, The Netherlands, 2011; Volume 1.
3. Sahu, P.; Gupta, M.K. A review on the properties of natural fibres and its bio-composites: Effect of alkali treatment. *Proc. Inst. Mech. Eng. Part L J. Mater. Des. Appl.* **2020**, *234*, 198–217. [\[CrossRef\]](#)
4. Zhou, M.; Gu, W.; Wang, G.; Zheng, J.; Pei, C.; Fan, F.; Ji, G. Sustainable wood-based composites for microwave absorption and electromagnetic interference shielding. *J. Mater. Chem. A* **2020**, *8*, 24267–24283. [\[CrossRef\]](#)

5. Budzik, M.K.; Wolfahrt, M.; Reis, P.; Kozłowski, M.; Sena-Cruz, J.; Papadakis, L.; Nasr Saleh, M.; Machalicka, K.V.; Teixeira de Freitas, S.; Vassilopoulos, A.P. Testing mechanical performance of adhesively bonded composite joints in engineering applications: An overview. *J. Adhes.* **2022**, *98*, 2133–2209. [\[CrossRef\]](#)
6. Nassiraei, H.; Rezadoost, P. Static capacity of tubular X-joints reinforced with fiber reinforced polymer subjected to compressive load. *Eng. Struct.* **2021**, *236*, 112041. [\[CrossRef\]](#)
7. Nassiraei, H.; Rezadoost, P. Local joint flexibility of tubular T/Y-joints retrofitted with GFRP under in-plane bending moment. *Mar. Struct.* **2021**, *77*, 102936. [\[CrossRef\]](#)
8. Liu, B.; Zhang, Q.; Li, X.; Guo, Y.; Zhang, Z.; Yang, H.; Yuan, Y. Potential advantage of thin-ply on the composite bolster of a bogie for a high-speed electric multiple unit. *Polym. Compos.* **2021**, *42*, 3404–3417. [\[CrossRef\]](#)
9. Su, K.B. *Delamination Resistance of Stitched Thermoplastic Matrix Composite Laminates*; ASTM International: Conshohocken, PA, USA, 1989; pp. 279–300.
10. Zhou, X.; Li, J.; Qu, C.; Bu, W.; Liu, Z.; Fan, Y.; Bao, G. Bending behavior of hybrid sandwich composite structures containing 3D printed PLA lattice cores and magnesium alloy face sheets. *J. Adhes.* **2022**, *98*, 1713–1731. [\[CrossRef\]](#)
11. Guillaumet, G.; Turon, A.; Costa, J.; Renart, J.; Linde, P.; Mayugo, J.A. Damage occurrence at edges of non-crimp-fabric thin-ply laminates under off-axis uniaxial loading. *Compos. Sci. Technol.* **2014**, *98*, 44–50. [\[CrossRef\]](#)
12. Tserpes, K.; Barroso-Caro, A.; Carraro, P.A.; Beber, V.C.; Floros, I.; Gamon, W.; Kozłowski, M.; Santandrea, F.; Shahverdi, M.; Skejić, D.; et al. A review on failure theories and simulation models for adhesive joints. *J. Adhes.* **2021**, *98*, 1855–1915. [\[CrossRef\]](#)
13. Sam-Daliri, O.; Farahani, M.; Araei, A. Condition monitoring of crack extension in the reinforced adhesive joint by carbon nanotubes. *Weld. Technol. Rev.* **2020**, *91*, 7–15. [\[CrossRef\]](#)
14. Ghabezi, P.; Farahani, M. Trapezoidal traction–separation laws in mode II fracture in nano-composite and nano-adhesive joints. *J. Reinf. Plast. Compos.* **2018**, *37*, 780–794. [\[CrossRef\]](#)
15. Ramezani, F.; Simões, B.D.; Carbas, R.J.; Marques, E.A.; da Silva, L.F. Developments in Laminate Modification of Adhesively Bonded Composite Joints. *Materials* **2023**, *16*, 568. [\[CrossRef\]](#)
16. Akhavan-Safar, A.; Ramezani, F.; Delzendehrooy, F.; Ayatollahi, M.R.; da Silva, L.F.M. A review on bi-adhesive joints: Benefits and challenges. *Int. J. Adhes. Adhes.* **2022**, *114*, 103098. [\[CrossRef\]](#)
17. Qin, Z.; Yang, K.; Wang, J.; Zhang, L.; Huang, J.; Peng, H.; Xu, J. The effects of geometrical dimensions on the failure of composite-to-composite adhesively bonded joints. *J. Adhes.* **2021**, *97*, 1024–1051. [\[CrossRef\]](#)
18. Ramezani, F.; Nunes, P.D.P.; Carbas, R.J.C.; Marques, E.A.S.; da Silva, L.F.M. The joint strength of hybrid composite joints reinforced with different laminates materials. *J. Adv. Join. Process.* **2022**, *5*, 100103. [\[CrossRef\]](#)
19. Simões, B.D.; Nunes, P.D.; Ramezani, F.; Carbas, R.J.; Marques, E.A.; da Silva, L.F. Experimental and Numerical Study of Thermal Residual Stresses on Multimaterial Adherends in Single-Lap Joints. *Materials* **2022**, *15*, 8541. [\[CrossRef\]](#)
20. Shang, X.; Marques, E.A.S.; Machado, J.J.M.; Carbas, R.J.C.; Jiang, D.; Da Silva, L.F.M. A strategy to reduce delamination of adhesive joints with composite substrates. *Proc. Inst. Mech. Eng. Part L J. Mater. Des. Appl.* **2019**, *233*, 521–530. [\[CrossRef\]](#)
21. Potter, K.D.; Guild, F.J.; Harvey, H.J.; Wisnom, M.R.; Adams, R.D. Understanding and control of adhesive crack propagation in bonded joints between carbon fibre composite adherends I. Experimental. *Int. J. Adhes. Adhes.* **2001**, *21*, 435–443. [\[CrossRef\]](#)
22. Mouritz, A.P. Review of z-pinned composite laminates. *Compos. Part A Appl. Sci. Manuf.* **2007**, *38*, 2383–2397. [\[CrossRef\]](#)
23. Ko, F.K.; Chou, T.W. *Textile Structural Composites*, 6th ed.; Composite Materials Series; Elsevier Science: Amsterdam, The Netherlands, 1989; Volume 3.
24. Sawyer, J.W. Effect of stitching on the strength of bonded composite single lap joints. *AIAA J.* **1985**, *23*, 1744–1748. [\[CrossRef\]](#)
25. Hader-Kregl, L.; Wallner, G.M.; Kralovec, C.; Eyßell, C. Effect of inter-ply on the short beam shear delamination of steel/composite hybrid laminates. *J. Adhes.* **2019**, *95*, 1088–1100. [\[CrossRef\]](#)
26. Verpoest, I.; Wevers, M.; De Meester, P.; Declercq, P. 2.5 D-fabrics and 3D-fabrics for delamination resistant composite laminates and sandwich structures. *Sampe J.* **1989**, *25*, 51–56.
27. Dransfield, K.; Baillie, C.; Mai, Y.W. Improving the delamination resistance of CFRP by stitching—A review. *Compos. Sci. Technol.* **1994**, *50*, 305–317. [\[CrossRef\]](#)
28. Sih, S.; Kim, R.Y.; Kawabe, K.; Tsai, S.W. Experimental studies of thin-ply laminated composites. *Compos. Sci. Technol.* **2007**, *67*, 996–1008. [\[CrossRef\]](#)
29. Amacher, R.; Cugnoni, J.; Botsis, J.; Sorensen, L.; Smith, W.; Dransfeld, C. Thin ply composites: Experimental characterization and modeling of size-effects. *Compos. Sci. Technol.* **2014**, *101*, 121–132. [\[CrossRef\]](#)
30. Roure, T. C-PLY™, a new structural approach to multiaxials in composites: BI-ANGLE NCF. *JEC Compos.* **2011**, *68*, 53–55.
31. Arteiro, A.; Catalanotti, G.; Xavier, J.; Linde, P.; Camanho, P.P. A strategy to improve the structural performance of non-crimp fabric thin-ply laminates. *Compos. Struct.* **2018**, *188*, 438–449. [\[CrossRef\]](#)
32. Kötter, B.; Karsten, J.; Körbelin, J.; Fiedler, B. CFRP thin-ply fibre metal laminates: Influences of ply thickness and metal layers on open hole tension and compression properties. *Materials* **2020**, *13*, 910. [\[CrossRef\]](#)
33. Wisnom, M.R.; Khan, B.; Hallett, S.R. Size effects in unnotched tensile strength of unidirectional and quasi-isotropic carbon/epoxy composites. *Compos. Struct.* **2008**, *84*, 21–28. [\[CrossRef\]](#)
34. Kim, R.Y.; Soni, S.R. Experimental and analytical studies on the onset of delamination in laminated composites. *J. Compos. Mater.* **1984**, *18*, 70–80. [\[CrossRef\]](#)

35. Huang, C.; He, M.; He, Y.; Xiao, J.; Zhang, J.; Ju, S.; Jiang, D. Exploration relation between interlaminar shear properties of thin-ply laminates under short-beam bending and meso-structures. *J. Compos. Mater.* **2018**, *52*, 2375–2386. [[CrossRef](#)]
36. Kupski, J.; Zarouchas, D.; de Freitas, S.T. Thin-ply in adhesively bonded carbon fiber reinforced polymers. *Compos. Part B Eng.* **2020**, *184*, 107627. [[CrossRef](#)]
37. Camanho, P.P.; Dávila, C.G.; Pinho, S.T.; Iannucci, L.; Robinson, P. Prediction of in situ strengths and matrix cracking in composites under transverse tension and in-plane shear. *Compos. Part A Appl. Sci. Manuf.* **2006**, *37*, 165–176. [[CrossRef](#)]
38. Chan, W.S. Design approaches for edge delamination resistance in laminated composites. *J. Compos. Technol. Res.* **1991**, *13*, 91–96.
39. Ramezani, F.; Carbas, R.J.; Marques, E.A.; Ferreira, A.M.; da Silva, L.F. A study of the fracture mechanisms of hybrid carbon fiber reinforced polymer laminates reinforced by thin-ply. *Polym. Compos.* **2023**, *44*, 1672–1683. [[CrossRef](#)]
40. 3M. *3m Scotch-Weld Structural Adhesive Lm Af 163-2k Technical Datasheet*; Technical Report; 3M: St. Paul, MN, USA, 2009.
41. Morgado, M.A.; Carbas, R.J.C.; Dos Santos, D.G.; Da Silva, L.F.M. Strength of CFRP joints reinforced with adhesive layers. *Int. J. Adhes. Adhes.* **2020**, *97*, 102475. [[CrossRef](#)]
42. Campilho, R.D.; De Moura, M.F.S.F.; Domingues, J.J.M.S. Modelling single and double-lap repairs on composite materials. *Compos. Sci. Technol.* **2005**, *65*, 1948–1958. [[CrossRef](#)]
43. Machado, J.J.M.; Marques, E.A.S.; Campilho, R.D.S.G.; da Silva, L.F. Mode I fracture toughness of CFRP as a function of temperature and strain rate. *J. Compos. Mater.* **2017**, *51*, 3315–3326. [[CrossRef](#)]
44. Ramezani, F.; Carbas, R.; Marques, E.A.S.; Ferreira, A.M.; da Silva, L.F.M. Study on out-of-plane tensile strength of angle-ply reinforced hybrid CFRP laminates using thin-ply. *Mech. Adv. Mater. Struct.* **2023**, 1–14. [[CrossRef](#)]
45. Liu, P.F.; Chu, J.K.; Liu, Y.L.; Zheng, J.Y. A study on the failure mechanisms of carbon fiber/epoxy composite laminates using acoustic emission. *Mater. Des.* **2012**, *37*, 228–235. [[CrossRef](#)]
46. Okoli, O.I.; Smith, G.F. Failure modes of fibre reinforced composites: The effects of strain rate and fibre content. *J. Mater. Sci.* **1998**, *33*, 5415–5422. [[CrossRef](#)]
47. Ghabezi, P.; Farahani, M. A cohesive model with a multi-stage softening behavior to predict fracture in nano composite joints. *Eng. Fract. Mech.* **2019**, *219*, 106611. [[CrossRef](#)]

Disclaimer/Publisher's Note: The statements, opinions and data contained in all publications are solely those of the individual author(s) and contributor(s) and not of MDPI and/or the editor(s). MDPI and/or the editor(s) disclaim responsibility for any injury to people or property resulting from any ideas, methods, instructions or products referred to in the content.

Appendix F

Paper F

Study of Hybrid Composite Joints with Thin-ply-reinforced Adherends under High-rate and Impact Loadings



Shahid Chamran
University of Ahvaz

Journal of Applied and Computational Mechanics



Research Paper

Study of Hybrid Composite Joints with Thin-ply-reinforced Adherends under High-rate and Impact Loadings

Farin Ramezani¹, Ricardo J.C. Carbas^{1,2}, Eduardo A.S. Marques², Lucas F.M. da Silva²

¹ Instituto de Ciência e Inovação Em Engenharia Mecânica e Engenharia Industrial (INEGI), Rua Dr. Roberto Frias, 4200-465 Porto, Portugal, Email: farinramezani@gmail.com

² Departamento de Engenharia Mecânica, Faculdade de Engenharia (FEUP), Universidade Do Porto, Rua Dr. Roberto Frias, 4200-465 Porto, Portugal, Email: rcarbas@fe.up.pt (R.J.C.C.); emarques@fe.up.pt (E.A.S.M.); lucas@fe.up.pt (L.F.M.S.)

Received July 04 2023; Revised October 31 2023; Accepted for publication October 31 2023.

Corresponding author: R.J.C. Carbas (rcarbas@fe.up.pt)

© 2023 Published by Shahid Chamran University of Ahvaz

Abstract. This research aims to examine the tensile strength of a hybrid composite laminate reinforced by thin-ply when used as an adherend in bonded single lap joints subjected to high-rate and impact loading. Two different composites, namely Texpreg HS 160 T700 and NTPT-TP415, are employed as the conventional and thin-ply composites, respectively. The study considers three configurations: a conventional composite, a thin-ply, and a hybrid single lap joint. Numerical models of the configurations are developed to provide insight into failure mechanisms and the initiation of damage. The results indicate a significant increase in tensile strength for the hybrid joints over the conventional and thin-ply joints, due to the mitigation of stress concentrations. Overall, this study demonstrates the potential of hybrid laminates for improving the performance of composite joints under high-rate loading and impact conditions.

Keywords: Composite joints, thin-ply, single lap joints, high-rate loading, impact loading.

1. Introduction

In composites, two primary components are involved: the matrix and the reinforcement. The matrix offers the material cohesion, while the reinforcement, usually in fibre form, provides strength and stiffness [1]. The utilization of carbon fibre-reinforced polymer (CFRP) materials is experiencing continuous growth [2-6] in various industries, including those manufacturing vehicle structures, sporting goods, etc [7]. However, despite their numerous benefits, bonding composites faces a critical issue, arising from the likelihood of the presence of defects in the adhesive layer, taking the form of voids or debonding [8, 9]. Generally, studies have shown that the presence of an imperfection such as a void or a debond in the overlap region will cause an increase in the value of interfacial shear stress in the regions close to the imperfection. This increase depends on the length and, especially, location of the defect [10, 11]. On the other hand, the significant disparity between the strength of the reinforcement and the matrix means that the loads applied perpendicularly to the reinforcement are predominantly borne solely by the low-strength matrix, resulting in the development of matrix cracks and subsequent delamination. Delamination can cause rapid degradation in the mechanical performance of the structure and lead to premature failure [12-16]. Several research studies have explored methods to modify joints in order to mitigate delamination in adhesively bonded composite joints [17-29]. However, the implementation of these methods usually necessitates at least one extra production step, which, in turn, leads to increased production costs. Moreover, the intricate nature of these techniques often constrains their practical application [30, 31].

The spread-tow technique has emerged as a result of recent advances in composite manufacturing technology [32] which results in plies with a more homogeneous fibre distribution and smaller resin-rich regions [33], allowing achieve a dry ply thickness as low as 0.02 mm. Typically, plies with a thickness of less than 100 μm are referred to as thin-ply [34]. Reducing the thickness of an individual layer expands the number of feasible layers, increasing the degrees of freedom in design [35], while it also results in a larger number of interfaces in thin-ply laminates, lowering the shear stresses [35, 36]. Furthermore, thin-ply laminates are recognized for their capacity to postpone the initiation of matrix damage mechanisms, suppress transverse microcracking [32] and free edge delamination [35, 37] for static, fatigue, and impact loadings. Due to their exceptional resistance to damage and delamination, thin-ply laminates could potentially display elevated interlaminar shear properties [38] and strain energy [39] compared to conventional plies. Consequently, thinner composite plies are recognized to possess superior in situ transverse strength [36]. Use of thin-ply is currently regarded as a promising strategy to enhance the performance of adhesively bonded CFRP structures, primarily because of the capability to improve the off-axis properties of composites and delay the onset of delamination [39]. Additionally, research has indicated that the incorporation of thin-ply in a structural joint results in a shift of the damage location in the composite from the adhesive interface towards the mid-thickness of the adherends [39], mainly due to the in-situ effect [40].



In a previous study conducted by the authors [41], it was demonstrated that substituting conventional composite layers with thin-ply layers in the adherends of a single lap joint can significantly enhance the strength of the composite joint, as well as improve the failure mode (by reducing delamination) under static loads. The authors attribute this change to the improved ductility of the laminate, which can delay delamination [42]. Moreover, experimental observation clearly demonstrated that the presence of thin-ply acts as a barrier against crack propagation.

In summary, the study aims to investigate the performance of a hybrid (25% thin-ply) composite single lap joint reinforced with thin-ply layers under high-rate and impact loads. Two types of materials were considered to create the hybrid (25% thin-ply) joint: a conventional composite (HS 160 T700) and a thin-ply material (NTPT-TP415). Numerical models were also created using cohesive zone modelling to accurately replicate the experimentally determined failure processes.

2. Experimental Details

2.1. Adhesive

The adhesive used in this work was an epoxy structural adhesive, supplied in film form, with the commercial reference Scotch Weld AF 163-2k (3M, Saint Paul, Minnesota, USA) and the following properties: Young's modulus (E)=1.5 GPa, shear modulus (G)=0.6 GPa, tensile strength (σ)=46.9 MPa, shear strength (τ)=46.8 MPa, fracture energy (G_{IC} = 4.05 and G_{IIC} =9.77 N/mm) [43]. Morgado et al. [43] characterized the mechanical properties of AF 163-2k is under quasi-static (1 mm/min) and impact loading conditions (3 m/s). The mechanical properties at high-rate (0.1 m/s) and impact loading (2 m/sec) were calculated using a linear extrapolation. The adhesive was cured following the manufacturer's recommendations, at 130°C for 2 hours.

2.2. Adherend

2.2.1. Conventional Composite

The materials used in the studied configurations were selected in order to be representative of a possible application within the aerospace sector. Accordingly, a unidirectional prepreg carbon-epoxy composite with a ply thickness of 0.15 mm was selected, with the commercial reference "Texipreg HS 160 T700" (Seal Spa, Legnano, Italy) and the following properties: Young's modulus (E_1 =109.0 and E_2 =8.8 GPa), shear modulus (G_{12} =4.3 and G_{13} =3.2 GPa), fracture energy (G_{IC} = 0.6 and G_{IIC} =1.2 N/mm) [44, 45]. Morgado et al. [46] presented the mechanical properties of the cured prepreg under static (1mm/min) and impact loading conditions (3 m/s). The mechanical properties at high-rate (0.1 m/s) and impact loading (2 m/sec) were calculated using a linear extrapolation.

2.2.2. Thin-Ply

A unidirectional 0° oriented carbon-epoxy prepreg composite with a ply thickness of 0.075mm was selected for use in this work, serving as the thin-ply material. This material has the commercial reference "NTPT-TP415" (North thin-ply technology, Poland) and the following properties: Young's modulus (E_1 =101.7 and E_2 =5.7 GPa), shear modulus (G_{12} =3.0 and G_{13} =3.0 GPa), fracture energy (G_{IC} = 0.7 and G_{IIC} =0.8 N/mm) [47]. The mechanical properties at high-rate (0.1 m/s) and impact loading (2 m/sec) were calculated using a linear extrapolation.

2.3. Single Lap Joint Manufacturing

The manufacturing process for the single lap joints involved layer-by-layer stacking of conventional composite and thin-ply prepreps to achieve the desired adherend thickness of 3.6mm. The reference conventional composite adherends consisted of 24 layers, while the thin-ply adherends consisted of 48 layers. For the hybrid adherends (25% thin-ply), 6 plies of conventional composite were replaced by 12 plies of thin-ply on the adherend tops (6 layers of thin-ply on each adherend top), resulting in a 25% thin-ply composition. An additional layer of adhesive was then applied between the adherends. A mould was used to ensure the thickness of the adherends and adhesive. To facilitate easy detachment of the specimens from the mould after curing, a release agent was applied. The effect of curing sequence on the mechanical properties of the joint was investigated by comparing the performance of joints where the composite and the adhesive were cured together (co-cured) with the joints where curing occurred separately. It was found that, for the AF163-2k adhesive used in this study, the curing sequence had no significant impact on the mechanical properties of the joint. As a result, a one-step curing process was selected as the preferred method of manufacturing, allowing for a reduction in both the manufacturing time and energy consumption. The joint was cured at 130°C for 2 hours following the manufacturer's recommended procedure. Single lap joints (SLJs) were manufactured with the geometry shown in Fig. 1.

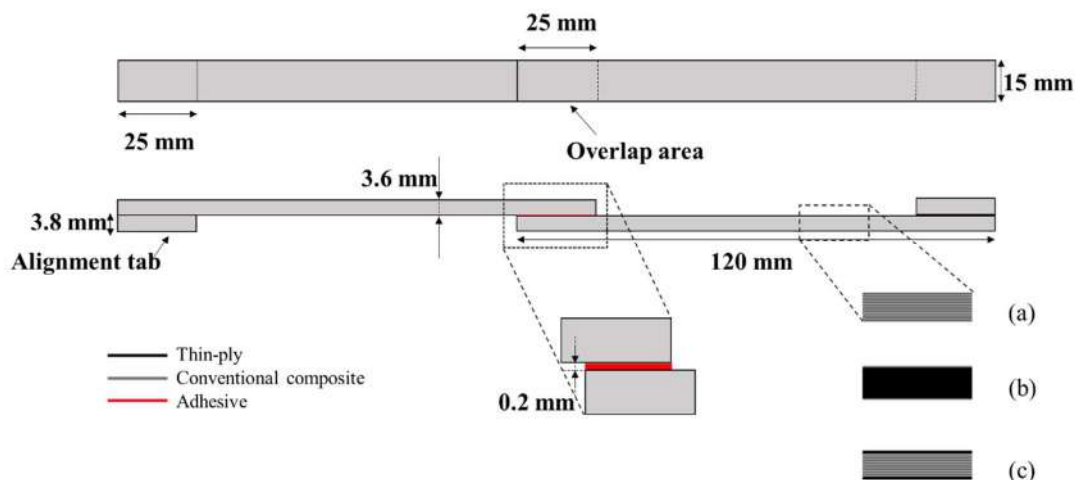


Fig. 1. Schematic design of single lap joint with (a) conventional composite, (b) thin-ply and, (c) hybrid (25% thin-ply) adherends.



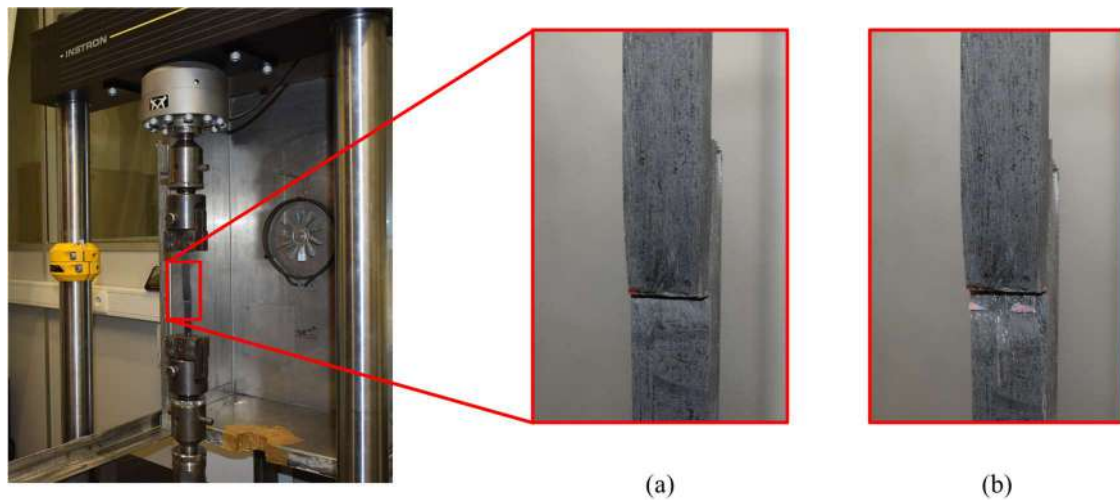


Fig. 2. (a) Intact, (b) failed specimen in servo hydraulic testing machine.

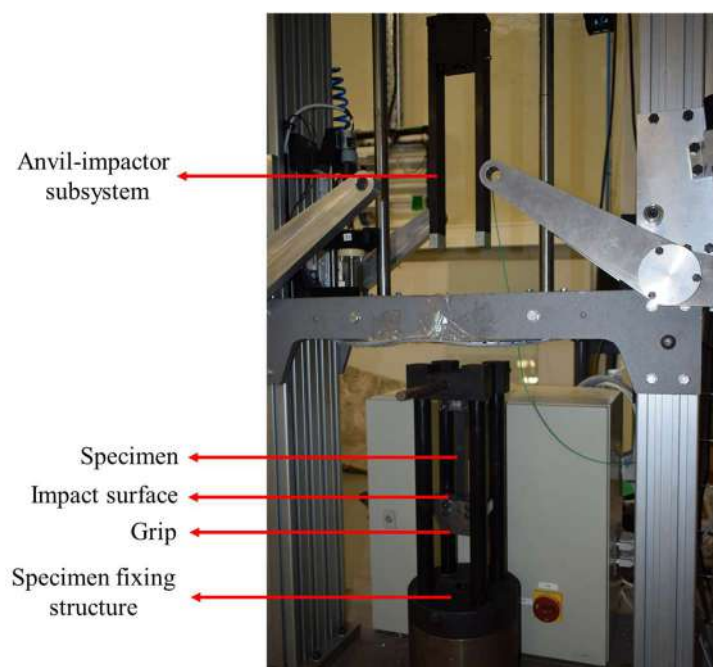


Fig. 3. Drop weight machine.

2.4. Testing Condition

The SLJs were tested at two different constant crosshead speeds of 0.1 and 2 m/sec known as the high-rate and impact loading condition. An Instron 8801 servo hydraulic testing machine with a load cell of 100 kN for the high-rate loading. Figure 2 provides an image of the intact and damaged specimen in the servo hydraulic testing machine. An in-house developed drop-weight testing machine was used to carry out impact tests on the specimens [48]. This machine grips the upper part adherend, leaving the lower portion free. A mass is then dropped from a specific height, causing an impact on the lower part of the grip and loading the specimen in tension-shear. The impact velocity is determined by the drop height, which follows the principle of energy conservation. For the impact tests in this study, a 50 kg mass and an impact velocity of 2 m/s were chosen, resulting in an impact energy of 100 J. Figure 3 presents an image of an intact specimen in the drop weight testing machine. It has to be mentioned that the rising time of the impactor from the stationary station was about three seconds, considering the speed, mass, and stationary state mentioned above. All tests were performed under laboratory ambient conditions (room temperature of 24°C, relative humidity of 55%). Four repetitions were performed for each configuration under analysis.

3. Experimental Result

3.1. High-Rate Loading

Figure 4 illustrates representative experimentally obtained load-displacement curves for the studied configurations under high-rate loading. The hybrid (25% thin-ply) joint presented the highest failure load, with around an 25% increase in joint strength compared to the reference conventional composite configuration. Figure 5 provides representative images of the failure surface for all configurations. As seen, delamination is the dominant failure mode observed in all tested composite single lap joint configurations.



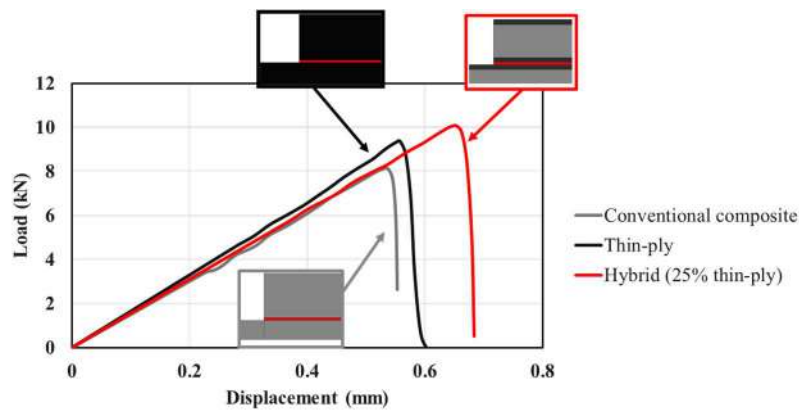


Fig. 4. Representative load-displacement curves for reference conventional composite, thin-ply and hybrid (25% thin-ply) joint under high-rate loading.

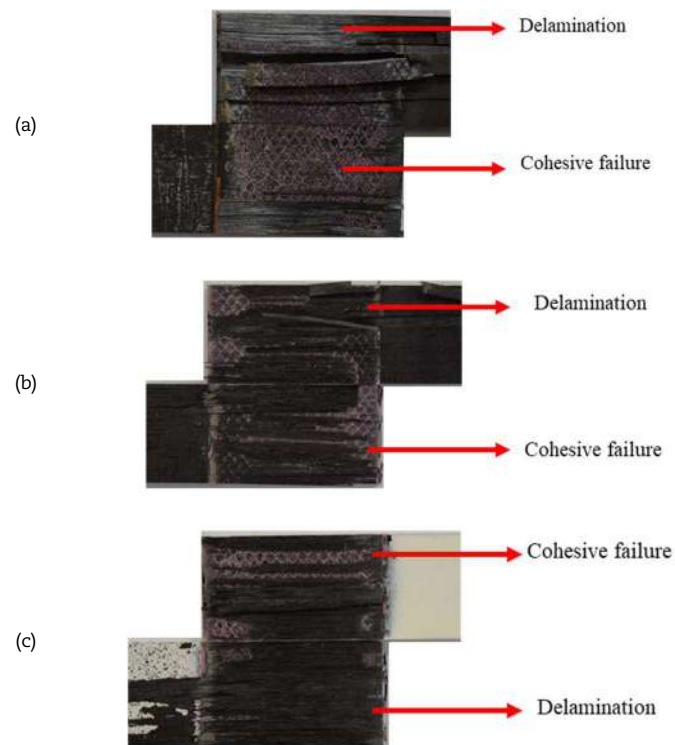


Fig. 5. Representative images of failure surface of (a) reference conventional composite, (b) thin-ply and, (c) hybrid (25% thin-ply) joint under high-rate loading.

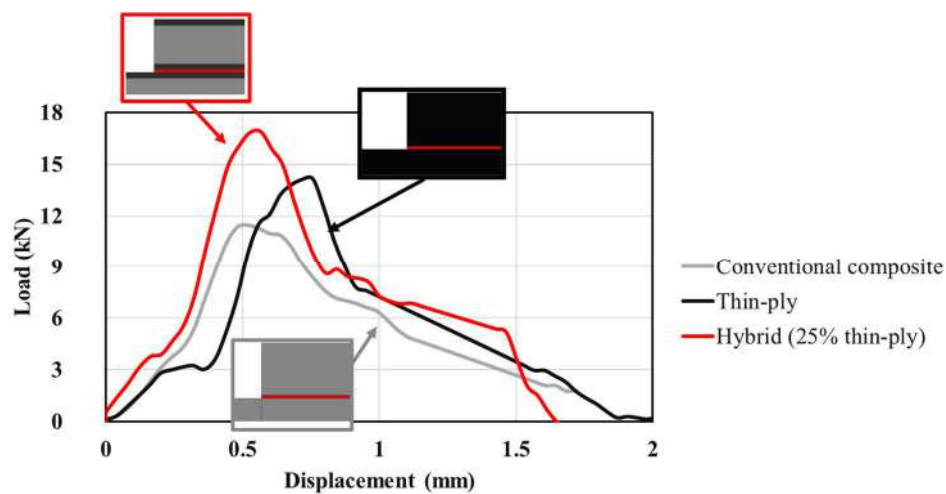


Fig. 6. Representative load-displacement curves for reference conventional composite, thin-ply and hybrid (25% thin-ply) joint under impact loading.



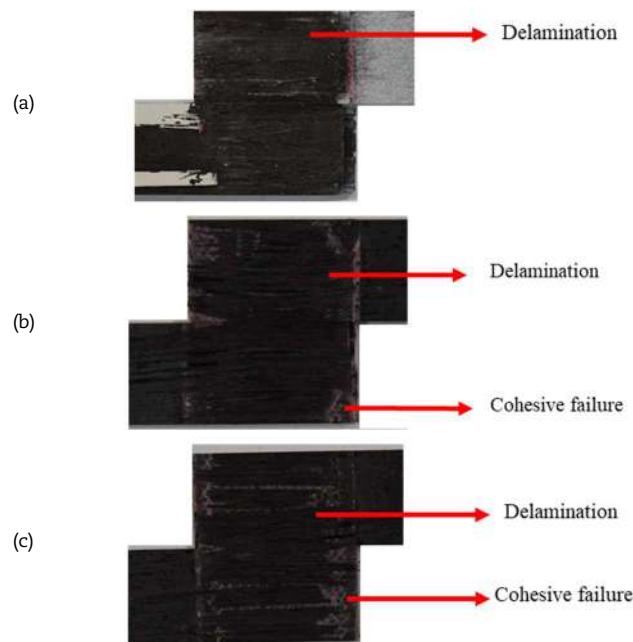


Fig. 7. Representative images of failure surface of (a) reference conventional composite, (b) thin-ply and, (c) hybrid (25% thin-ply) joint under impact loading.

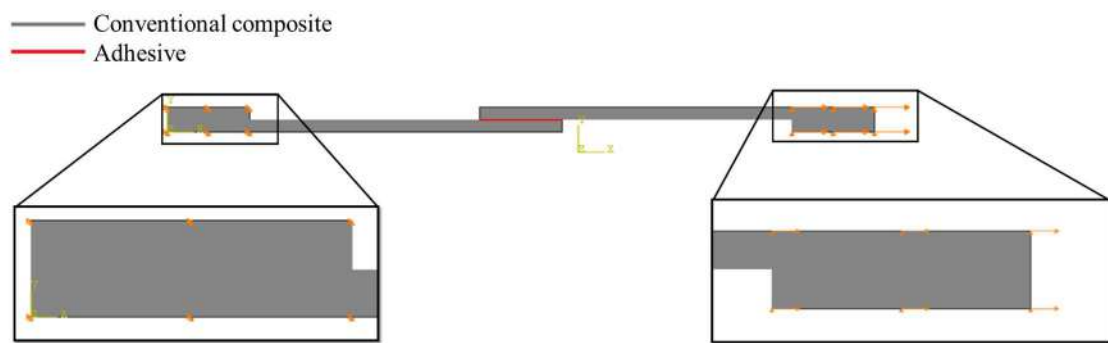


Fig. 8. Boundary condition of simulated conventional composite single lap joint.

3.2. Impact Loading

Figure 6 provides representative load-displacement curves for the configurations tested experimentally under impact loading. The hybrid (25% thin-ply) joint presented the highest failure load, with around an 50% increase in joint strength compared to the reference conventional composite configuration. Figure 7 provides representative images of the failure surface for all configurations. For the reference joints with conventional composite full delamination was observed. In contrast, for reference joints with thin-ply and the hybrid (25% thin-ply) joints, partial cohesive failure was also observed in addition to the most dominant delamination failure mode.

4. Numerical Study

For high-rate and impact loading, a 2D explicit and 3D implicit dynamically loaded model was employed, using the Abaqus/CAE 6.14-2 commercial finite element package respectively. The boundary conditions were established as depicted in Fig. 8, where the left end of the joint was fixed and an amplitude of displacement was applied to the right end to mimic the dynamic loading conditions. A displacement of 1 and 2 mm was applied to the numerical models as described above for high-rate and impact loading respectively. The mention displacement was chosen based on experimental results in order to make sure the failure occurred. In order to simulate the high-rate and impact loading an amplitude of 0.01 and 0.001 was applied to the numerical models, respectively.

To model the behaviour of the adhesive and simulate damage evolution, a cohesive zone model (CZM) was employed, using four node cohesive quadrilateral elements. Non-linear geometrical effects were considered, and solid cohesive elements were used to represent damage evolution (damage initiation and propagation), following a traction-separation law. CZM was also introduced into the composite material to model delamination, and the interlaminar cohesive element layers (conventional composite or thin-ply) were placed between elastic homogeneous sections [49].

The mechanical properties assigned to these numerical models are shown in Fig. 9, with CZM layers placed at different distances for high-rate loading and impact loading. The distance from the interface of the adherend and adhesive layer varied depending on the joint configuration and loading type. The CZM layers were placed at a distance of 0.17, 0.15, and 0.28 mm from the interface of the adherend and adhesive layer for the conventional composite, thin-ply, and hybrid (25% thin-ply) joints under high-rate loading, respectively. Similarly, for impact loading, CZM layers were placed at a distance of 0.20, 0.30, and 0.45 mm from the interface of the adherend and adhesive layer for the mentioned configurations. This distance roughly corresponded to the experimentally measured distance of the delamination plane from the adhesive layer. The thickness of the cohesive layer matched the thickness of one equivalent composite ply (0.075 mm for thin-ply and 0.15 mm for the conventional composite).



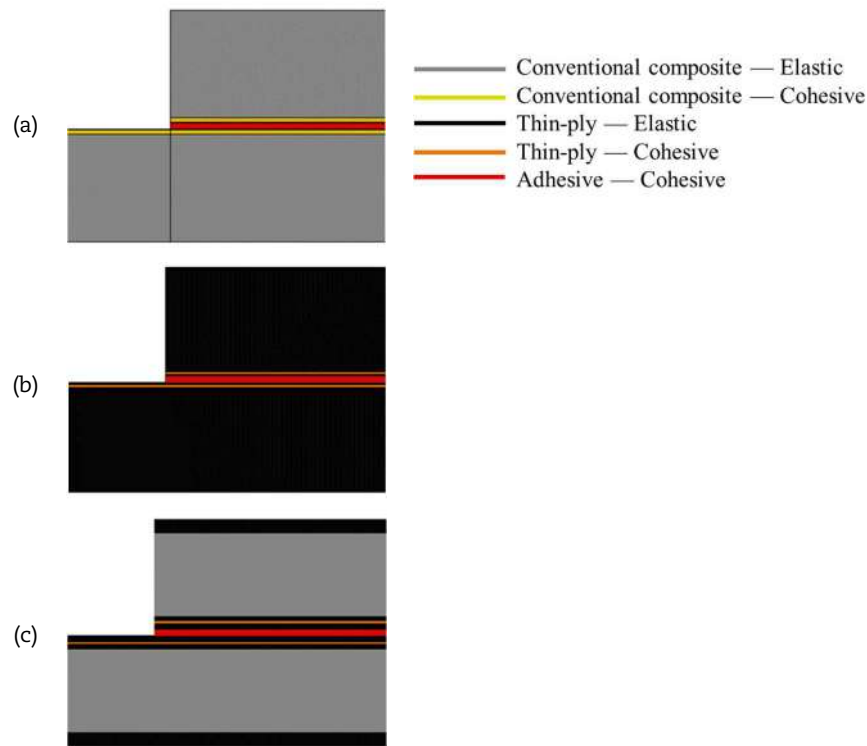


Fig. 9. Assigned mechanical properties for (a) conventional composite, (b) thin-ply, and (c) hybrid (25% thin-ply) joints for high-rate loading.

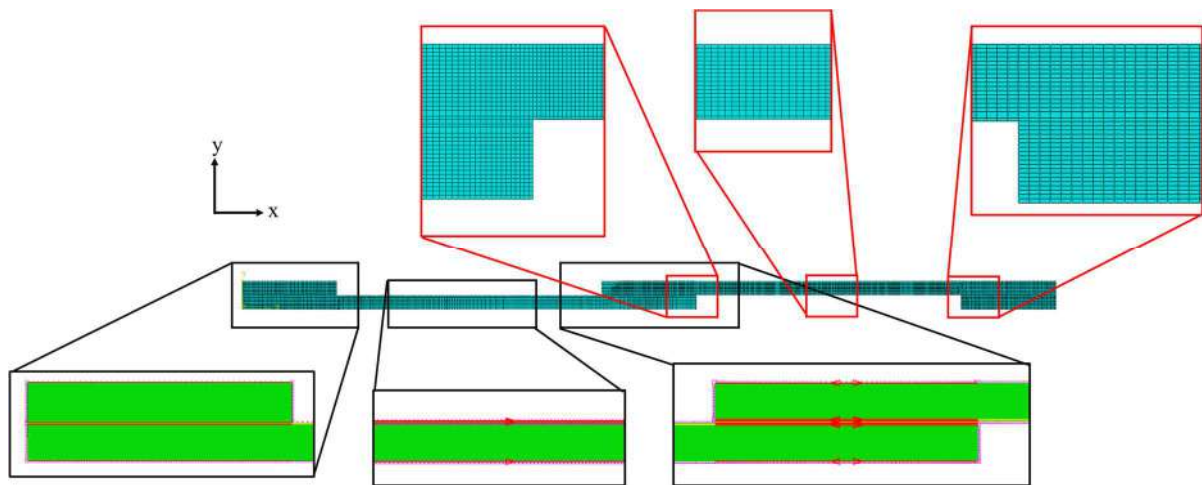


Fig. 10. Mesh distributions for single-lap joint.

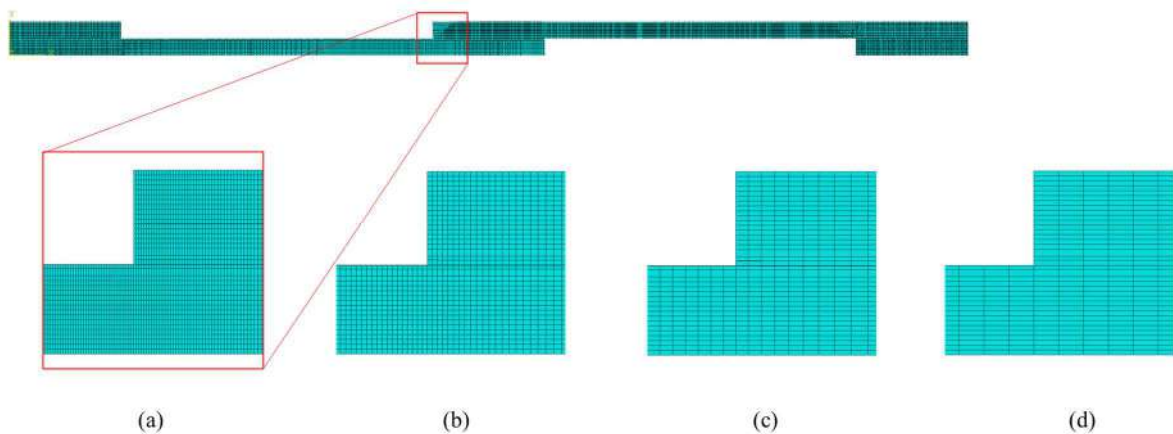


Fig. 11. Mesh distributions for single-lap joints with minimum and maximum mesh size of (a) 0.1 and 0.2 mm, (b) 0.2 and 0.5 mm, (c) 0.5 and 1 mm and (d) 1 mm, respectively.



Additionally, a mesh convergency study was performed for the reference conventional composite single lap joint under high-rate loading in order to study the effect of mesh size on the numerically obtained failure load. The mesh size in the thickness direction (y direction-see Fig. 10) is restricted to the thickness of the cohesive layer. This is because a cohesive model zone analysis allows the use of only a row of cohesive elements in the cohesive layer. Therefore, elements size of 0.2 mm (thickness of the cohesive layer) was considered for the thickness direction. However, the effect of mesh size in the x direction was studied. Double and single biased mesh distributions were considered in the x direction (see Fig. 10) for the bondline and the adherends, respectively. Accordingly, the minimum mesh size of 0.1, 0.2, 0.5 and 1 mm was considered to study the effect of mesh size on the numerical result. The detailed mesh size was presented in Fig. 11. According to the results presented in Fig. 12, the minimum mesh size of 0.2 could validate the finite element findings for the purpose of comparison with the experimental results additional to minimizing the computational cost of the numerical models. Consequently, the minimum and maximum sizes for the mesh were considered 0.2 and 0.5 mm respectively for the bondline and the adherends. End tabs were meshed uniformly with a size of 0.5 mm in the x direction, and the mesh was uniform through the thickness (y direction) with a size of 0.2 mm for all components. The same mesh size was used for all numerical models. The resulting mesh consisted of approximately 15,000 elements for 2D models and 75,000 elements for 3D models.

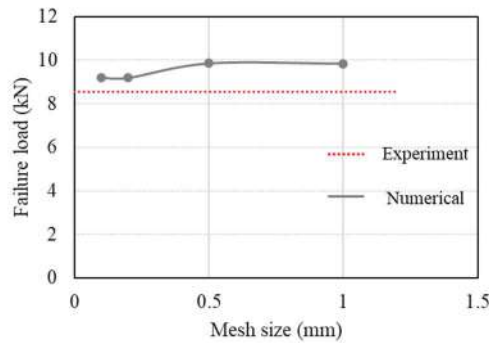


Fig. 12. Effect of mesh size on the numerically obtained failure load in comparison with the experimentally obtained result for the reference conventional composite single lap joint under high-rate loading.

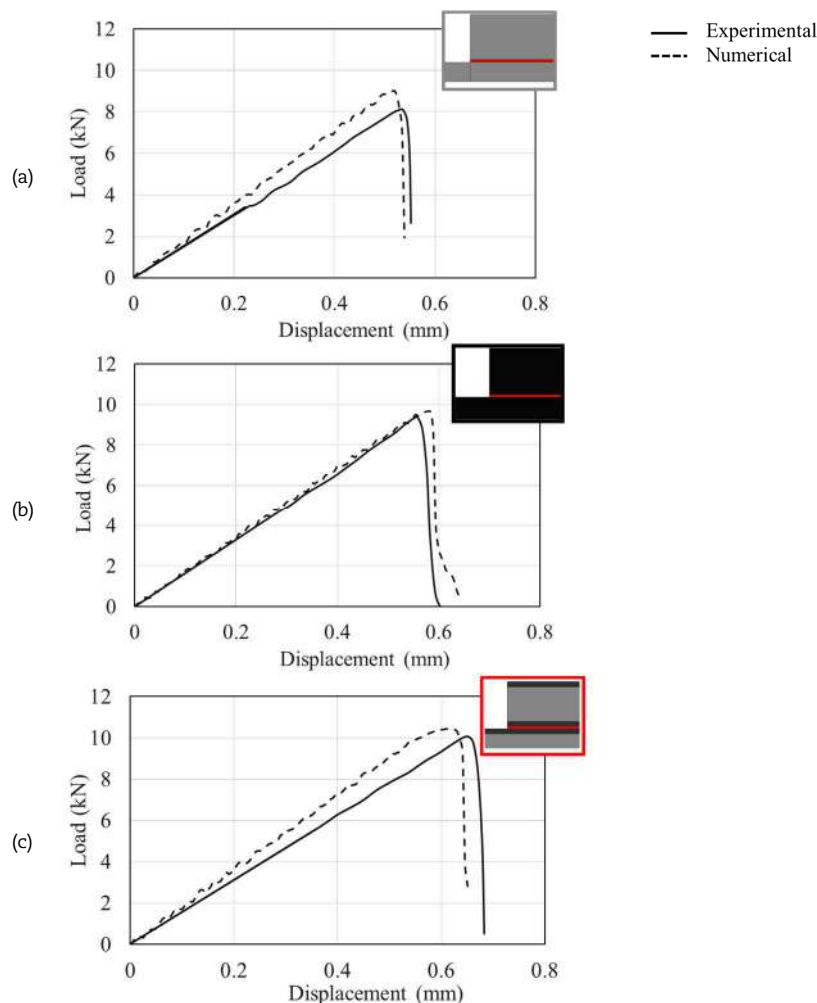


Fig. 13. Comparison of numerically obtained load-displacement curves for (a) conventional composite, (b) thin-ply and, (c) hybrid (25% thin-ply) joint with the representative experimental results under high-rate loading.



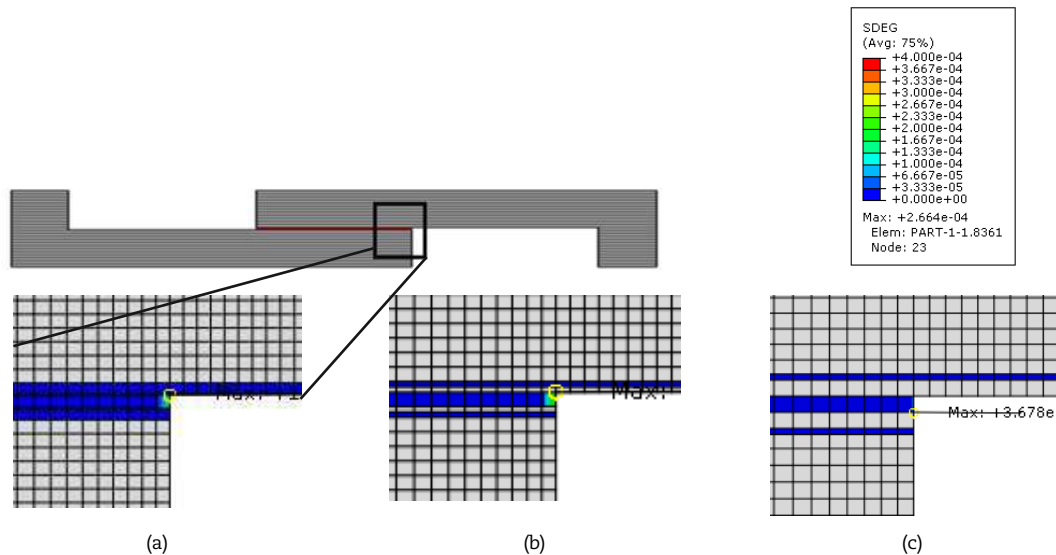


Fig. 14. SDEG at damage initiation for (a) conventional composite, (b) thin-ply and (c) hybrid (25% thin-ply) joint under high-rate loading (equivalent load for each configuration is 6.8, 6.9, and 7.0 kN, respectively).

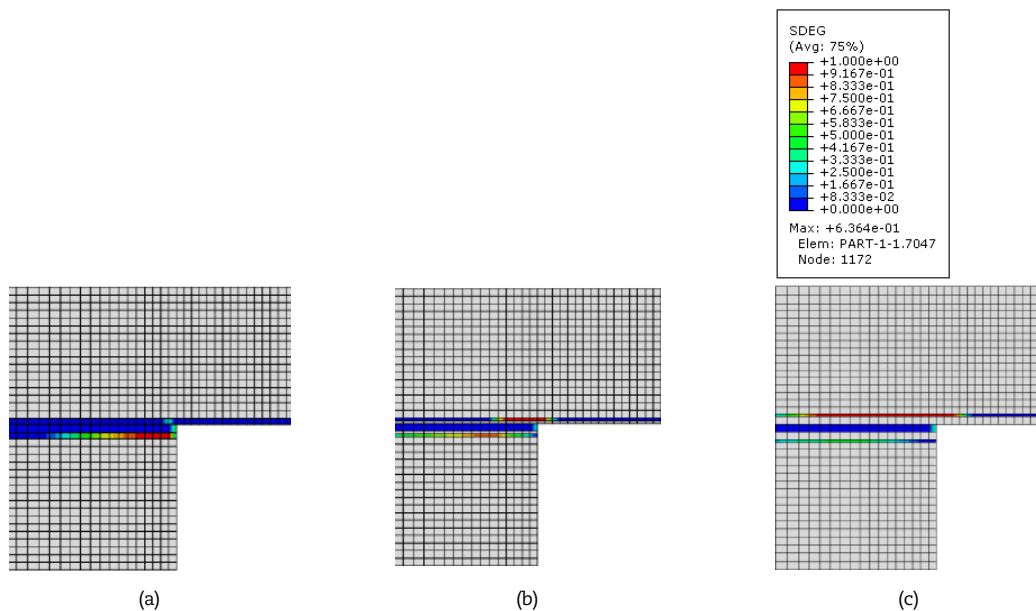


Fig. 15. SDEG at corresponding failure load for (a) conventional composite, (b) thin-ply and (c) hybrid (25% thin-ply) joint under high-rate loading.

4.1. High-Rate Loading

The load-displacement curves obtained numerically for all configurations under high-rate loading are presented in Fig. 13. As seen, there is a good match between the numerical and the experimentally obtained load-displacement curves. Figure 14 illustrates the damage initiation for each configuration. The presented area is shown within by the black square in single lap joint. The equivalent load for damage initiation (load in which damage initiation occurs) for the reference conventional composite, reference thin-ply and the hybrid (25% thin-ply) single lap joints was 6.8, 6.9, and 7.0 kN respectively. It should be mentioned that the damage initiation occurs at a higher level of load for the hybrid (25% thin-ply) compared to the both conventional composite and thin-ply reference single lap joint. Additionally, as seen in Fig. 14, the stiffness degradation was more objective in the both conventional composite and thin-ply reference single lap joint compared to the hybrid (25% thin-ply). However, damage initiation was shown to occur in the adhesive layer for all configurations. Figure 15 illustrates the damage state for all configurations at their corresponding failure load. As seen, the final failure mode is known to be delamination for all configurations which is in line with the experimentally obtained result.

4.2. Impact-Loading

The numerical load-displacement curves, obtained for all configurations under impact loading, are presented in Fig. 16 and compared with the equivalent experimentally obtained load-displacement for each configuration. Figure 17 illustrates the damage initiation for each configuration. The presented area is shown within the black square in the single lap joint. The equivalent load of damage initiation for the reference conventional composite, reference thin-ply and the hybrid (25% thin-ply) single lap joints were 6.7, 5.3, and 5.6 kN respectively which was cited in the adhesive layer. However, the final failure was illustrated as delamination as seen in Fig. 18.



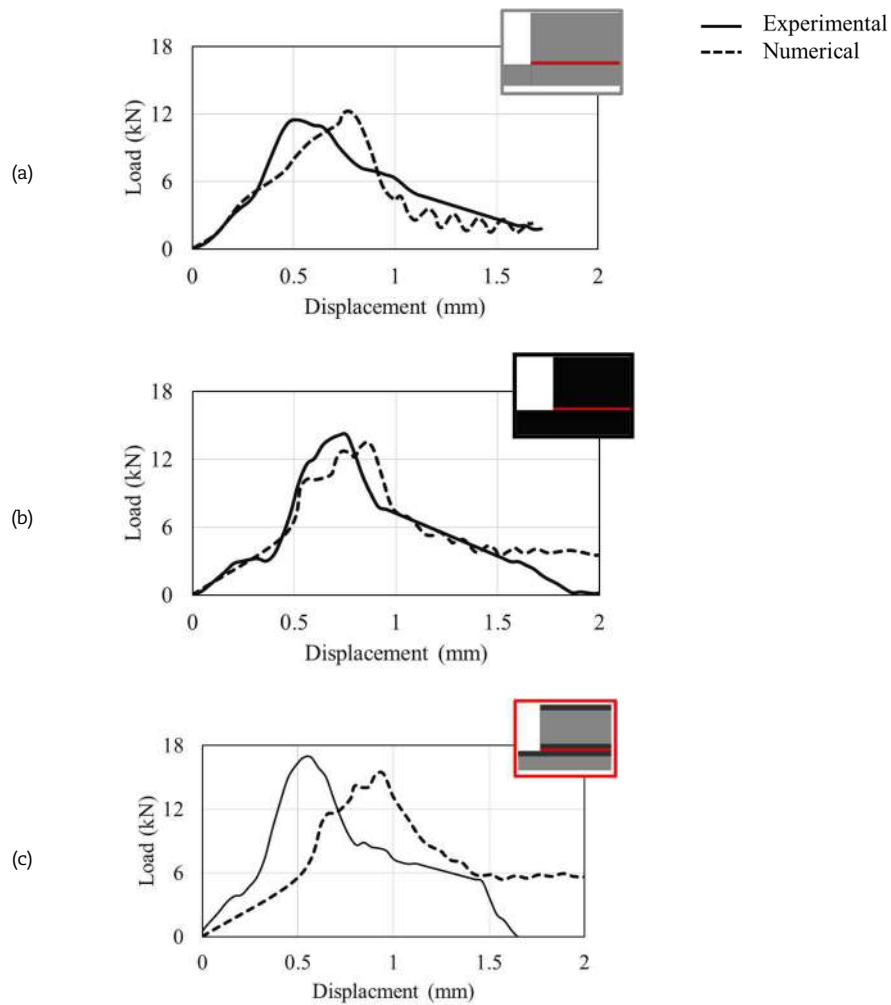


Fig. 16. Comparison of numerically obtained load-displacement curves for (a) conventional composite, (b) thin-ply and, (c) hybrid (25% thin-ply) joint with the representative experimental results under impact loading.

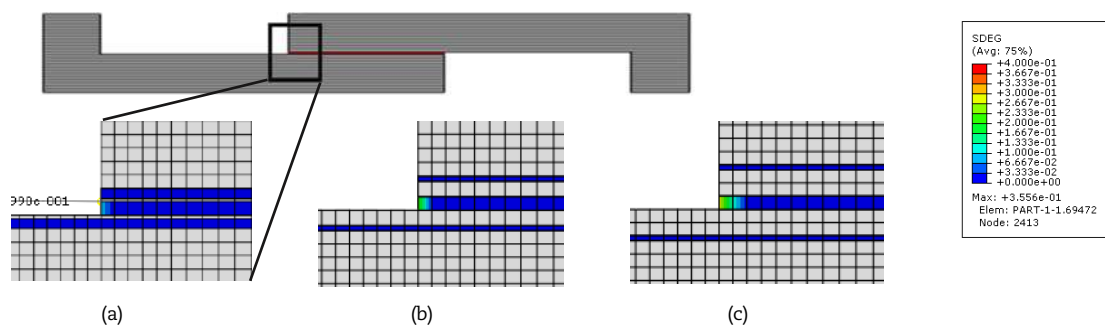


Fig. 17. SDEG at damage initiation for (a) conventional composite, (b) thin-ply and (c) hybrid (25% thin-ply) joint under impact loading (equivalent load for each configuration is 6.7, 5.3 and 5.6 kN, respectively).

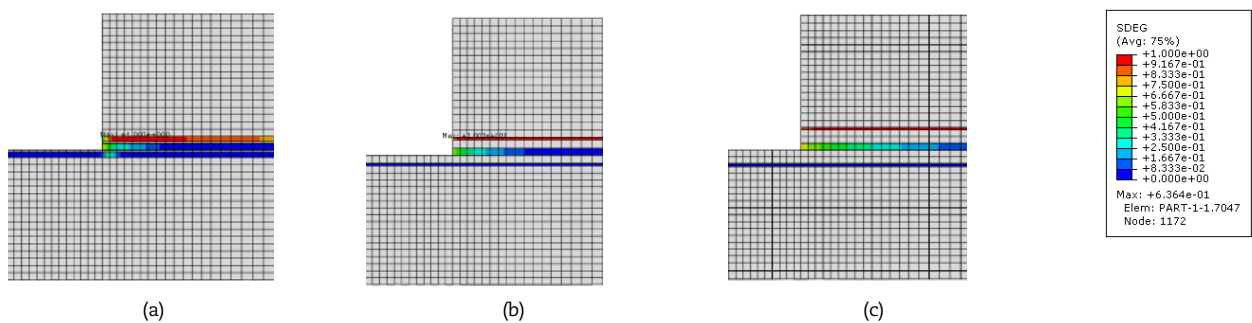


Fig. 18. SDEG at corresponding failure load for (a) conventional composite, (b) thin-ply and (c) hybrid (25% thin-ply) joint under impact loading.



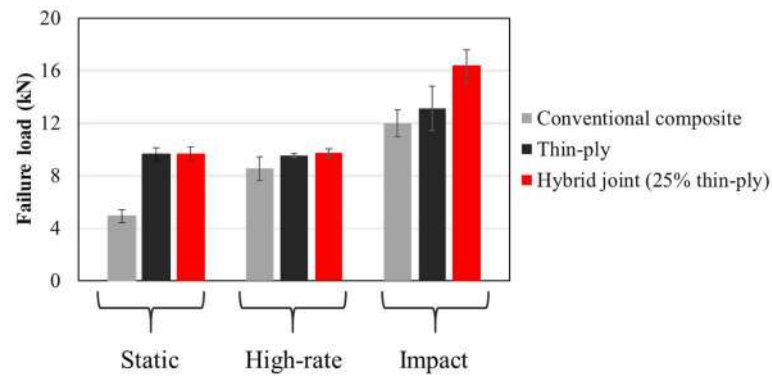


Fig. 19. Comparison of the experimentally obtained failure load for conventional composite, thin-ply and hybrid (25% thin-ply) single lap joint under high-rate and impact loading with ones obtained statically loaded.

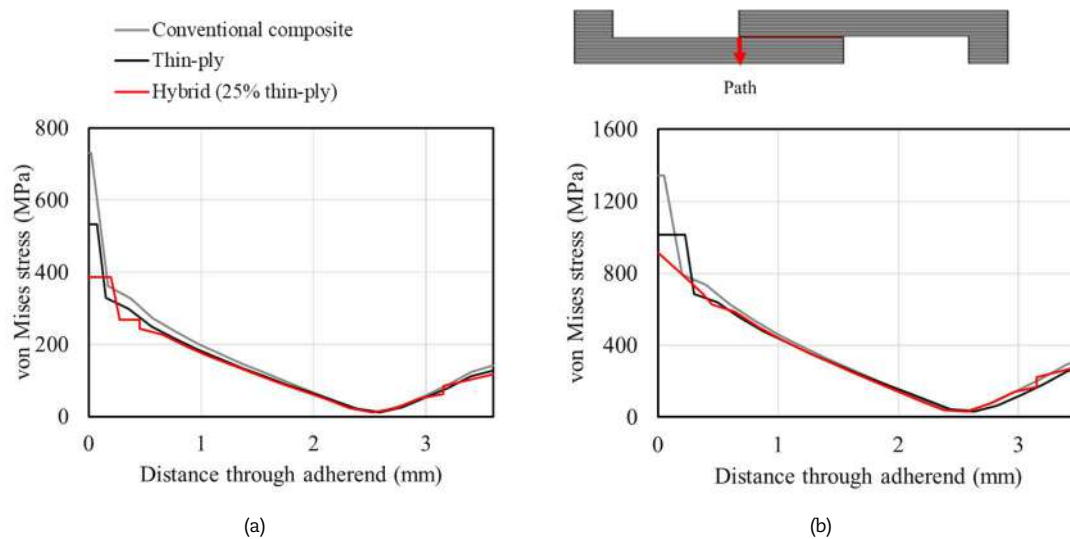


Fig. 20. von Mises stress distribution through the adherend thickness (a) under high-rate loading at 5 kN and (b) under impact loading at 11.5 kN.

5. Discussion

The use of hybrid (25% thin-ply) composite joints reinforcement with thin-ply has demonstrated a remarkable enhancement in the tensile strength of up to 90%, compared to conventional composite joints under static loading conditions. This study conducted an investigation of the performance of hybrid joints incorporating 25% thin-ply under high-rate and impact loading. Figure 19, illustrate the average failure load of conventional composite joints, thin-ply joints, and hybrid (25% thin-ply) single lap joints under static, high-rate, and impact loading conditions. These findings suggest that hybrid (25% thin-ply) single lap joints exhibit superior tensile strength not only under static loading but also under high-rate and impact loading conditions compared to conventional composite joints. This is mainly due to higher ductility conferred to the material by the presence of thin-ply [42]. Thin-ply materials are also known to have higher resistance to crack propagation which is mainly know to be due to the more uniform fibre distribution and less resin-rich and fibre-rich area in the thin-ply [42]. In the previous study [41], it was shown that for hybrid (25% thin-ply) single lap joints more limited amount of delamination was obtained compared to the reference ones under static loading. As seen in Fig 19 the thin-ply and hybrid (25% thin-ply) display almost the same strength under both static and high-rate loading (about 10 kN). This is while a considerable increase was observed in the joint strength for the reference thin-ply when increasing the cross-head speed up to 2 m/sec. It could be concluded that thin-ply materials preform even better under impact loading. Therefor when combining thin-ply with the conventional composite which is known to have more brittle behavior compared to the thin-ply (higher strength but premature failure is expected for the conventional composite), tensile resistance of the hybrid composite joint could be increased compared to both reference conventional composite and thin-ply single lap joints. However, it should be noted that the manufacturing process for the former is less expensive and time-consuming. In addition, all configurations have shown delamination to be the dominant failure mode, both under high-rate and impact loads. The numerical analysis and study revealed that damage initiation takes place in the adhesive layer and propagates through the adherend as delamination, which aligns with the experimental observations.

Since delamination is the predominant failure mode across all configurations, the equivalent von Mises stress was analysed through the adherend thickness at 5 and 11.5 kN for the high-rate and impact models respectively in order to gain a deeper understanding of the mechanism responsible for the increased tensile strength of hybrid (25% thin-ply) single lap joints. The path for which the von Mises stress was obtained was shown in Fig. 20. As depicted in Fig. 20, the composite adherends of thin-ply and hybrid (25% thin-ply) joints were found to experience lower levels of equivalent von Mises stress at a constant load level during high-rate and impact loading compared to the reference conventional composite single-lap joint. This could be explained by the ductile behavior of the thin-ply composite compared to the conventional one [42] which induces a lower level of stress to the adherends. This study highlights that hybrid (25% thin-ply) composite joints have the potential to be an effective solution for increasing structural integrity under different loading conditions.



6. Conclusion

The performance of hybrid (25% thin-ply) composite single lap joints under high-rate and impact loading was studied and compared to the static response. Overall, hybrid (25% thin-ply) composite joints were found to be a promising solution for enhancing the structural strength. In conclusion, it was observed that:

- The use of hybrid (25% thin-ply) composite joints reinforced with thin-ply exhibit higher tensile strength than conventional composite joints under all loading conditions.
- Delamination is the dominant failure mode across all configurations for high-rate and impact loads.
- The developed numerical models, using cohesive zone modelling, were found to be in a good agreement with the experimental results for both high-rate and impact conditions.
- Numerical analysis revealed that the damage initiates in the adhesive layer and propagates in the composite adherends as delamination which is in line with the experimental observation.
- The analysis of equivalent von Mises stress through the adherend thickness at a constant load revealed that hybrid (25% thin-ply) joints experience lower stress levels during high-rate and impact loading.

Author Contributions

Investigation, F. Ramezani; Writing—original draft, F. Ramezani; Writing—review & editing, R.J.C. Carbas, E.A.S. Marques and L.F.M. da Silva; Supervision, R.J.C. Carbas, E.A.S. Marques, and L.F.M. da Silva.

Acknowledgments

The authors gratefully acknowledge the Portuguese Foundation for Science and Technology (FCT) for supporting the work presented.

Conflict of Interest

The authors declared no potential conflicts of interest concerning the research, authorship, and publication of this article.

Funding

The authors gratefully acknowledge the Portuguese Foundation for Science and Technology (FCT) for supporting the work presented here through the individual grants CEECIND/03276/2018 and 2021.07943.BD and Project No. PTDC/EME-EME/2728/2021, “New approaches to improve the joint strength and reduce the delamination of composite adhesive joints”.

Data Availability Statements

Not Applicable.


References


- [1] Karatas, M.A. and Gökkaya, H., A review on machinability of carbon fiber reinforced polymer (CFRP) and glass fiber reinforced polymer (GFRP) composite materials, *Defence Technology*, 14(4), 2018, 318-326.
- [2] Sahu, P. and Gupta, M.K., A review on the properties of natural fibres and its bio-composites: Effect of alkali treatment, *Proceedings of the Institution of Mechanical Engineers, Part L: Journal of Materials: Design and Applications*, 234(1), 2020, 198-217.
- [3] Zhou, M., Gu, W., Wang, G., Zheng, J., Pei, C., Fan, F. and Ji, G., Sustainable wood-based composites for microwave absorption and electromagnetic interference shielding, *Journal of Materials Chemistry A*, 8(46), 2020, 24267-24283.
- [4] Budzik, M.K., Wolfahrt, M., Reis, P., Kozłowski, M., Sena-Cruz, J., Papadakis, L., Nasr Saleh, M., Machalicka, K.V., Teixeira de Freitas, S. and Vassilopoulos, A.P., Testing mechanical performance of adhesively bonded composite joints in engineering applications: An overview, *The Journal of Adhesion*, 98(14), 2022, 2133-2209.
- [5] Nassiraei, H. and Rezadoost, P., Static capacity of tubular X-joints reinforced with fiber reinforced polymer subjected to compressive load, *Engineering Structures*, 236, 2021, 112041.
- [6] Nassiraei, H. and Rezadoost, P., Local joint flexibility of tubular T/Y-joints retrofitted with GFRP under in-plane bending moment, *Marine Structures*, 77, 2021, 102936.
- [7] Liu, B., Zhang, Q., Li, X., Guo, Y., Zhang, Z., Yang, H. and Yuan, Y., Potential advantage of thin-ply on the composite bolster of a bogie for a high-speed electric multiple unit, *Polymer Composites*, 42(7), 2021, 3404-3417.
- [8] Shishesaz, M., Ghamarian, A.H. and Moradi, S., Stress distribution in laminated composite tubular joints with damaged adhesive layer under torsion, *The Journal of Adhesion*, 99(6), 2023, 930-971.
- [9] Zou, G.P. and Taheri, F., Stress analysis of adhesively bonded sandwich pipe joints subjected to torsional loading, *International Journal of Solids and Structures*, 43(20), 2006, 5953-5968.
- [10] Shishesaz, M. and Tehrani, S., The effects of circumferential voids or debonds on stress distribution in tubular adhesive joints under torsion, *The Journal of Adhesion*, 96, 2020, 1396-1430.
- [11] Shishesaz, M. and Tehrani, S., Interfacial shear stress distribution in the adhesively bonded tubular joints under tension with a circumferential void or debond, *Journal of Adhesion Science and Technology*, 34(11), 2020, 1172-1205.
- [12] Zhou, X., Li, J., Qu, C., Bu, W., Liu, Z., Fan, Y. and Bao, G., Bending behavior of hybrid sandwich composite structures containing 3D printed PLA lattice cores and magnesium alloy face sheets, *The Journal of Adhesion*, 98(11), 2022, 1713-1731.
- [13] Guillaumat, G., Turon, A., Costa, J., Renart, J., Linde, P. and Mayugo, J.A., Damage occurrence at edges of non-crimp-fabric thin-ply laminates under off-axis uniaxial loading, *Composites Science and Technology*, 98, 2014, 44-50.
- [14] Tserpes, K., Barroso-Caro, A., Carraro, P.A., Beber, V.C., Floros, I., Gamon, W., Kozłowski, M., Santandrea, F., Shahverdi, M., Skejic, D. and Bedon, C., A review on failure theories and simulation models for adhesive joints, *The Journal of Adhesion*, 98(12), 2022, 1855-1915.
- [15] Esmaeel, R.A. and Taheri, F., Stress analysis of tubular adhesive joints with delaminated adherend, *Journal of Adhesion Science and Technology*, 23(13-14), 2009, 1827-1844.
- [16] Esmaeel, R.A. and Taheri, F., Influence of adherend's delamination on the response of single lap and socket tubular adhesively bonded joints subjected to torsion, *Composite Structures*, 93(7), 2011, 1765-1774.
- [17] Sam-Daliri, O., Farahani, M. and Araei, A., Condition monitoring of crack extension in the reinforced adhesive joint by carbon nanotubes, *Welding Technology Review*, 91(12), 2019, 7-15.
- [18] Ghabeei, P. and Farahani, M., Trapezoidal traction-separation laws in mode II fracture in nano-composite and nano-adhesive joints, *Journal of Reinforced Plastics and Composites*, 37(11), 2018, 780-794.




- [19] Ramezani, F., Simões, B.D., Carbas, R.J., Marques, E.A. and da Silva, L.F.M., Developments in Laminate Modification of Adhesively Bonded Composite Joints, *Materials*, 16(2), 2023, 568.
- [20] Akhavan-Safar, A., Ramezani, F., Delzendehrooy, F., Ayatollahi, M.R. and Da Silva, L.F.M., A review on bi-adhesive joints: Benefits and challenges, *International Journal of Adhesion and Adhesives*, 114, 2022, 103098.
- [21] Qin, Z., Yang, K., Wang, J., Zhang, L., Huang, J., Peng, H. and Xu, J., The effects of geometrical dimensions on the failure of composite-to-composite adhesively bonded joints, *The Journal of Adhesion*, 97(11), 2021, 1024-1051.
- [22] Ramezani, F., Nunes, P.D.P., Carbas, R.J.C., Marques, E.A.S. and da Silva, L.F.M., The joint strength of hybrid composite joints reinforced with different laminates materials, *Journal of Advanced Joining Processes*, 5, 2022, 100103.
- [23] Simões, B.D., Nunes, P.D., Ramezani, F., Carbas, R.J., Marques, E.A. and da Silva, L.F.M., Experimental and numerical study of thermal residual stresses on multimaterial adherends in single-lap joints, *Materials*, 15(23), 2022, 8541.
- [24] Shang, X., Marques, E.A.S., Machado, J.J.M., Carbas, R.J.C., Jiang, D. and Da Silva, L.F.M., A strategy to reduce delamination of adhesive joints with composite substrates, *Proceedings of the Institution of Mechanical Engineers, Part L: Journal of Materials: Design and Applications*, 233(3), 2019, 521-530.
- [25] Potter, K.D., Guild, F.J., Harvey, H.J., Wisnom, M.R. and Adams, R.D., Understanding and control of adhesive crack propagation in bonded joints between carbon fibre composite adherends I, Experimental, *International Journal of Adhesion and Adhesives*, 21(6), 2001, 435-443.
- [26] Mouritz, A.P., Review of z-pinned composite laminates, *Composites Part A*, 38(12), 2007, 2383-2397.
- [27] Ko, F.K. and Wan, L.Y., *Textile structural composites: from 3-D to 1-D fiber architecture. The structural integrity of carbon fiber composites: Fifty years of progress and achievement of the science, development, and applications*, Springer, 2017.
- [28] Sawyer, J.W., Effect of stitching on the strength of bonded composite single lap joints, *AIAA Journal*, 23(11), 1985, 1744-1748.
- [29] Hader-Kregl, L., Wallner, G.M., Kralovec, C. and Eyßell, C., Effect of inter-ply on the short beam shear delamination of steel/composite hybrid laminates, *The Journal of Adhesion*, 95(12), 2019, 1088-1100.
- [30] Verpoest, I., Wevers, M., De Meester, P. and Declercq, P., 2.5 D-fabrics and 3D-fabrics for delamination resistant composite laminates and sandwich structures, *Sampe Journal*, 25(3), 1989, 51-56.
- [31] Dransfield, K., Baillie, C. and Mai, Y.W., Improving the delamination resistance of CFRP by stitching—a review, *Composites Science and Technology*, 50(3), 1994, 305-317.
- [32] Sihm, S., Kim, R.Y., Kawabe, K. and Tsai, S.W., Experimental studies of thin-ply laminated composites, *Composites Science and Technology*, 67(6), 2007, 996-1008.
- [33] Amacher, R., Cugnoni, J., Botsis, J., Sorensen, L., Smith, W. and Dransfeld, C., Thin ply composites: Experimental characterization and modeling of size-effects, *Composites Science and Technology*, 101, 2014, 121-132.
- [34] Arteiro, A., Catalanotti, G., Xavier, J., Linde, P. and Camanho, P.P., A strategy to improve the structural performance of non-crimp fabric thin-ply laminates, *Composite Structures*, 188, 2018, 438-449.
- [35] Kötter, B., Karsten, J., Körbelin, J. and Fiedler, B., CFRP thin-ply fibre metal laminates: Influences of ply thickness and metal layers on open hole tension and compression properties, *Materials*, 13(4), 2020, 910.
- [36] Wisnom, M.R., Khan, B. and Hallett, S.R., Size effects in unnotched tensile strength of unidirectional and quasi-isotropic carbon/epoxy composites, *Composite Structures*, 84(1), 2008, 21-28.
- [37] Kim, R.Y. and Soni, S.R., Experimental and analytical studies on the onset of delamination in laminated composites, *Journal of Composite Materials*, 18(1), 1984, 70-80.
- [38] Huang, C., He, M., He, Y., Xiao, J., Zhang, J., Ju, S. and Jiang, D., Exploration relation between interlaminar shear properties of thin-ply laminates under short-beam bending and meso-structures, *Journal of Composite Materials*, 52(17), 2018, 2375-2386.
- [39] Kupski, J., Zarouchas, D. and de Freitas, S.T., Thin-ply in adhesively bonded carbon fiber reinforced polymers, *Composites Part B: Engineering*, 184, 2020, 107627.
- [40] Camanho, P.P., Dávila, C.G., Pinho, S.T., Iannucci, L. and Robinson, P., Prediction of in situ strengths and matrix cracking in composites under transverse tension and in-plane shear, *Composites Part A: Applied Science and Manufacturing*, 37(2), 2006, 165-176.
- [41] Ramezani, F., Carbas, R.J., Marques, E.A. and da Silva, L.F.M., Study of Hybrid Composite Joints with Thin-Ply-Reinforced Adherends, *Materials*, 16(11), 2023, 4002.
- [42] Ramezani, F., Carbas, R.J., Marques, E.A., Ferreira, A.M. and da Silva, L.F.M., A study of the fracture mechanisms of hybrid carbon fiber reinforced polymer laminates reinforced by thin-ply, *Polymer Composites*, 44(3), 2023, 1672-1683.
- [43] Morgado, M.A., Carbas, R.J.C., Dos Santos, D.G. and Da Silva, L.F.M., Strength of CFRP joints reinforced with adhesive layers, *International Journal of Adhesion and Adhesives*, 97, 2020, 102475.
- [44] Campilho, R.D., De Moura, M.F.S.F. and Domingues, J.J.M.S., Modelling single and double-lap repairs on composite materials, *Composites Science and Technology*, 65(13), 2005, 1948-1958.
- [45] Machado, J.J.M., Marques, E.A.S., Campilho, R.D.S.G. and da Silva, L.F.M., Mode I fracture toughness of CFRP as a function of temperature and strain rate, *Journal of Composite Materials*, 51(23), 2017, 3315-3326.
- [46] Morgado, M.A., Carbas, R.J.C., Marques, E.A.S. and Da Silva, L.F.M., Reinforcement of CFRP single lap joints using metal laminates, *Composite Structures*, 230, 2019, 111492.
- [47] Ramezani, F., Carbas, R., Marques, E.A.S., Ferreira, A.M. and da Silva, L.F.M., Study on out-of-plane tensile strength of angle-ply reinforced hybrid CFRP laminates using thin-ply, *Mechanics of Advanced Materials and Structures*, 2023, 1-14.
- [48] Antunes, D.P.C., Lopes, A.M., Moreira da Silva, C.M.S., da Silva, L.F.M., Nunes, P.D.P., Marques, E.A.S. and Carbas, R. J. C., Development of a Drop Weight Machine for Adhesive Joint Testing, *Journal of Testing and Evaluation*, 49(3), 2021, 1651-1673.
- [49] Ghabezi, P. and Farahani, M., A cohesive model with a multi-stage softening behavior to predict fracture in nano composite joints, *Engineering Fracture Mechanics*, 219, 2019, 106611.

ORCID iD

Farin Ramezani  <https://orcid.org/0000-0003-3447-8515>

Ricardo J.C. Carbas  <https://orcid.org/0000-0002-1933-0865>

Eduardo A.S. Marques  <https://orcid.org/0000-0002-2750-8184>

Lucas F.M. da Silva  <https://orcid.org/0000-0003-3272-4591>



© 2023 Shahid Chamran University of Ahvaz, Ahvaz, Iran. This article is an open access article distributed under the terms and conditions of the Creative Commons Attribution-NonCommercial 4.0 International (CC BY-NC 4.0 license) (<http://creativecommons.org/licenses/by-nc/4.0/>).

How to cite this article: Ramezani F., Carbas R.J.C., Marques E.A.S., da Silva L.F.M. Study of Hybrid Composite Joints with Thin-ply-reinforced Adherends under High-rate and Impact Loadings, *J. Appl. Comput. Mech.*, 10(2), 2024, 260–271. <https://doi.org/10.22055/jacm.2023.44216.4181>

Publisher's Note Shahid Chamran University of Ahvaz remains neutral with regard to jurisdictional claims in published maps and institutional affiliations.



Appendix G

Paper G

Investigation of Adherend Thickness in Thin-Ply Hybrid Laminates

Investigation of Adherend Thickness in Thin-Ply Hybrid Laminates

Farin Ramezani¹, João C. M. Salazar², Ricardo J. C. Carbas^{1,2}, Eduardo A. S. Marques²,
Lucas F. M. da Silva²

¹Institute of Science and Innovation in Mechanical and Industrial Engineering, Rua Dr Roberto Frias, 4200-465 PORTO, Portugal.

²Department of Mechanical Engineering, Faculty of Engineering, University of Porto, Rua Dr Roberto Frias, 4200-465 PORTO, Portugal.

Abstract

The use of composite materials has been continuously increasing, hinged on its multiple advantages such as their high strength-to-weight ratio. However, this type of material is known for its anisotropic properties that may lead to premature failure of the composite laminate, stemming from the delamination of the adherend in an adhesively bonded composite joint. This study aims to study the effect of adherend thickness in uni-directional (UD) hybrid composite single lap joints reinforced by thin-ply and investigate the joint strength and failure mode. Tensile tests were carried out to evaluate the parameters mentioned experimentally, and numerical models were developed to reproduce the joint behavior. Experimental results show that adherend thickness has a minor effect on the joint strength in hybrid composite joints reinforced by thin-ply. However, a considerable change in the failure mode was observed.

Keywords:

Adhesive bonding, Cohesive zone modeling, Thin-ply, Single lap joints, Hybrid composite laminates.

1. Introduction

The utilization of composite materials within the field of mechanical engineering, particularly in the production of automotive, aeronautical, and aerospace components and structures, has exhibited a consistent upward trajectory in recent times [1]. This upward trajectory is projected to persist, primarily due to the inherent advantages offered by these materials, including enhanced performance characteristics and their ability to maintain a lightweight profile when compared to traditional metallic materials [2, 3]. These attributes align well with the pressing need for increased efficiency and reduced weight, both of which are pivotal in curbing energy consumption in aircraft and automobile operations.

Composite materials are widely acknowledged for their distinct structural properties, characterized by their anisotropic mechanical behavior. These materials exhibit varying degrees of strength in different directions, with one orientation typically demonstrating significant strength while other orientations may exhibit lower strength and even brittleness. Among the frequently employed composite materials in this field, carbon fiber-reinforced plastic (CFRP) stands out. When subjected to loads perpendicular to the fiber direction, CFRP is known to exhibit a specific response - delamination, a phenomenon in which the layers within the composite begin to separate. This delamination can lead to premature failure of the composite structure [4]. Numerous research endeavors have explored techniques aimed at modifying joints to mitigate delamination in adhesively bonded composite joints [5-8]. However, the incorporation of these techniques often necessitates an additional production step, resulting in increased production costs. Moreover, the intricate nature of these methods often limits their practical application [9, 10].

In recent times, the introduction of advanced spread tow techniques has ushered in the production of thinner plies with a more uniform fiber distribution and reduced resin-rich regions, which deviates from conventional methods [11]. This results in plies characterized by a more homogenous fiber distribution and smaller resin-rich regions [11], allowing for the achievement of a remarkably thin ply thickness, as low as 0.02 mm. Generally, plies with a thickness of less than 100 μm are referred to as thin-ply [12]. The reduction in the thickness of individual layers significantly increases the number of potential layers within a given plate thickness, thereby expanding the design possibilities [13]. Additionally, it results in a greater number of interfaces in thin-ply laminates, which, in turn, reduces shear stresses [13, 14]. Furthermore, thin-ply laminates are renowned for

their ability to postpone the initiation of matrix damage mechanisms, suppress transverse microcracking[14] and minimize free edge delamination [13, 15] under static, fatigue, and impact loads. Due to their exceptional resistance to damage and delamination, thin-ply laminates have the potential to exhibit elevated interlaminar shear properties [16] and strain energy [17] in comparison to conventional plies. Consequently, thinner composite plies are recognized for their superior in situ transverse strength [14].

In a previous study conducted by the authors [18], it was demonstrated that substituting conventional composite layers with thin-ply layers in the adherends of a single lap joint can significantly enhance the strength of the composite joint, as well as improve the failure mode (by reducing delamination) under static loads. The authors attribute this change to the improved ductility of the laminate, which can delay delamination [19]. Moreover, experimental observation clearly demonstrated that the presence of thin-ply acts as a barrier against crack propagation.

The present study delves into the influence of adherend thickness in hybrid single lap joints (SLJs) reinforced with thin-ply layers. In order to gain a deeper insight into how adherend thickness impacts the strength and failure characteristics of hybrid single lap joints strengthened with thin-ply materials, a series of experimental tests were conducted. Specifically, hybrid single lap joints, where 25% of the total adherend thickness was composed of thin-ply material, referred to as "hybrid (25% thin-ply) [18]," were fabricated and examined. The adherend thicknesses considered for these joints were 3.0 mm, 3.6 mm, and 4.0 mm. The experimental results indicate that the thickness of the adherend has a limited impact on the overall strength of hybrid composite joints reinforced with thin-ply. However, a noteworthy change in the failure mode was readily apparent.

2. Experimental Details

2.1. Adhesive

The adhesive utilized in this study was an epoxy structural adhesive, provided in film form, under the commercial designation Scotch Weld AF 163-2k (3M, Saint Paul, Minnesota, USA), possessing the following material properties: Young's modulus (E) of 1.5 GPa, shear modulus (G) of 0.6 GPa, tensile strength (σ) of 46.9 MPa, shear strength

(τ) of 46.8 MPa, and fracture energy ($G_{IC} = 4.05$ and $G_{IIC} = 9.77$ N/mm) [20]. The curing process for the adhesive adhered to the manufacturer's recommendations, involving heating at 130°C for a duration of 2 hours.

2.2. Adherend

2.2.1. Conventional Composite

The selection of materials for the configurations under investigation was undertaken with great care to ensure their suitability for possible aerospace applications. Accordingly, a unidirectional prepreg carbon-epoxy composite featuring a ply thickness of 0.15 mm was meticulously chosen, bearing the commercial designation "Texipreg HS 160 T700" (Seal Spa, Legnano, Italy). This material boasts the following crucial properties: Young's modulus ($E_1 = 109.0$ and $E_2 = 8.8$ GPa), shear modulus ($G_{12} = 4.3$ and $G_{13} = 3.2$ GPa), and fracture energy ($G_{IC} = 0.6$ and $G_{IIC} = 1.2$ N/mm) [21, 22]. These selections were made with the primary objective of aligning the study with potential applications within the aerospace sector.

2.2.2. Thin-Ply

In the context of this investigation, a carefully chosen thin-ply material was employed, specifically a unidirectional carbon-epoxy prepreg composite with a ply thickness of 0.075mm, oriented at 0°. This particular material is denoted by the commercial reference "NTPT-TP415" and is sourced from North Thin-Ply Technology, Poland. It possesses the following material properties: Young's modulus ($E_1 = 101.7$ and $E_2 = 5.7$ GPa), shear modulus ($G_{12} = 3.0$ and $G_{13} = 3.0$ GPa), and fracture energy ($G_{IC} = 0.7$ and $G_{IIC} = 0.8$ N/mm) [23]. The choice of this material aligns seamlessly with the research objectives and its potential applications.

2.3. Single Lap Joint Manufacturing

The fabrication process for creating the single lap joints involved a meticulous layer-by-layer assembly, combining both traditional composite and thin-ply prepregs to achieve the desired thickness of the adherends. In the case of the hybrid single lap joint, which incorporated 25% thin-ply material and had an adherend thickness of 3.6 mm, 18 plies of conventional composite were combined with 12 plies of thin-ply material on the adherend tops (equivalent to 6 layers of thin-ply on each adherend top, as depicted in Fig 1). This

combination resulted in a composite composition consisting of 25% thin-ply material. To facilitate bonding, an additional layer of adhesive was applied between the adherends. The single lap joints (SLJs) were manufactured according to the geometry illustrated in Fig 2.



Fig 1. Scheme design of hybrid (25% thin-ply) single lap joint

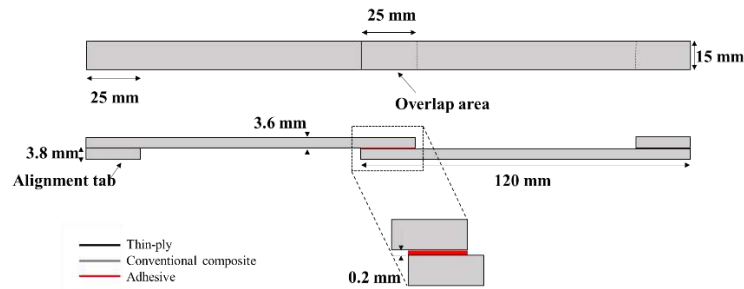


Fig 2. Schematic design of the manufactured specimens

A mold was employed to ensure the thickness of the adherends and adhesive, and to enable easy removal of the specimens from the mold after curing, a release agent was applied. Fig 3 shows the manufactured specimens before the curing process. The study also investigated the effect of the curing sequence on the mechanical properties of the joints by comparing joints where the composite and adhesive were cured simultaneously (co-cured) with joints where these components were cured separately. The results indicated that, in the case of the AF163-2k adhesive used in this study, the curing sequence did not significantly influence the mechanical properties of the joints. Consequently, a one-step curing process was adopted as the preferred manufacturing method, offering benefits such as reduced production time and energy consumption. The joint assemblies were cured at 130°C for a duration of two hours, following the manufacturer's recommended procedure.

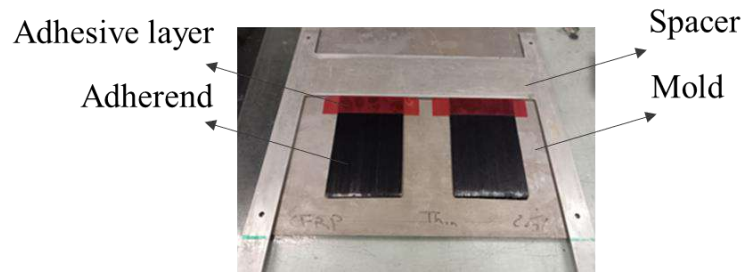


Fig 3. Manufactured specimens before the curing process

2.4. Testing Condition

The single lap joints (SLJs) underwent testing in an Instron 8801 servo hydraulic testing machine, equipped with a 100 kN load cell. The tests were conducted at a constant crosshead speed of 1 mm/min. It's important to note that all tests were carried out under controlled laboratory environmental conditions, with a room temperature of 24°C and a relative humidity of 55%. For each configuration under analysis, the testing process was repeated four times to ensure data consistency and reliability. Fig 4 presents the intact and damaged specimen in testing machine.

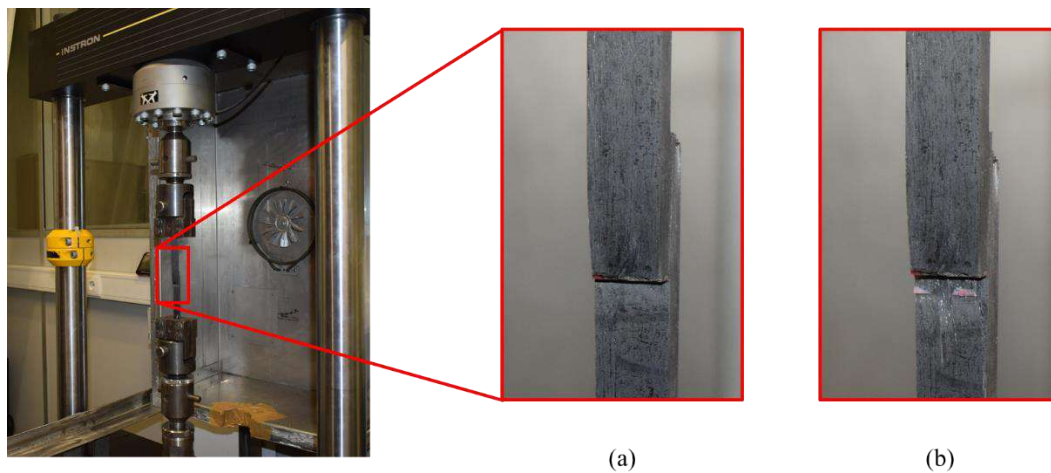


Fig 4. (a) Intact, (b) failed specimen in testing machine

3. Numerical details

Numerical models employing the finite element method and utilizing Abaqus software were created to simulate the behavior of the configurations under investigation. To streamline the problem and minimize computational time, two-dimensional (2D) static load models were generated. The boundary conditions were set up as illustrated in Fig 5, with the left end of the joint being fixed, while a displacement was applied to the right end to replicate the loading conditions. Specifically, a displacement of 1 mm was imposed on the numerical models, a value determined based on experimental findings to ensure the occurrence of failure.

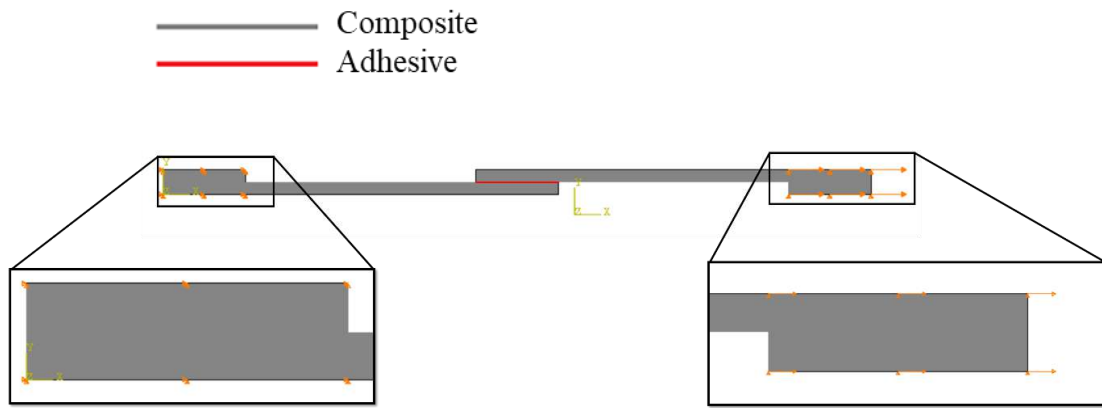


Fig 5. Boundary condition of simulated single lap joints

To model the adhesive behavior, cohesive zone modeling (CZM) was employed, utilizing four-node elements (cohesive quadrilateral elements). The simulation also took into account nonlinear geometric effects. Solid cohesive elements, governed by traction-separation laws, were applied to the adhesive layer in all models to replicate the evolution of damage, including its initiation and propagation.

Cohesive behavior was precisely defined using a traction-separation law, which has been demonstrated to effectively represent delamination in composite laminates. A similar CZM based approach was incorporated into the composite materials, whether they were conventional or thin-ply composites, to simulate delamination consistent with the experimental failure mode observed (refer to Fig 6).

The CZM layers were positioned at specific distances from the adherend-adhesive interface, depending on the thickness of the adherends (3.0, 3.6, or 4.0 mm). These

distances approximately matched the experimentally measured position of the delamination plane from the adhesive layer. Notably, the thickness of the cohesive layer corresponded to that of a single equivalent composite ply (0.075 mm for thin-ply and 0.15 mm for the conventional composite).

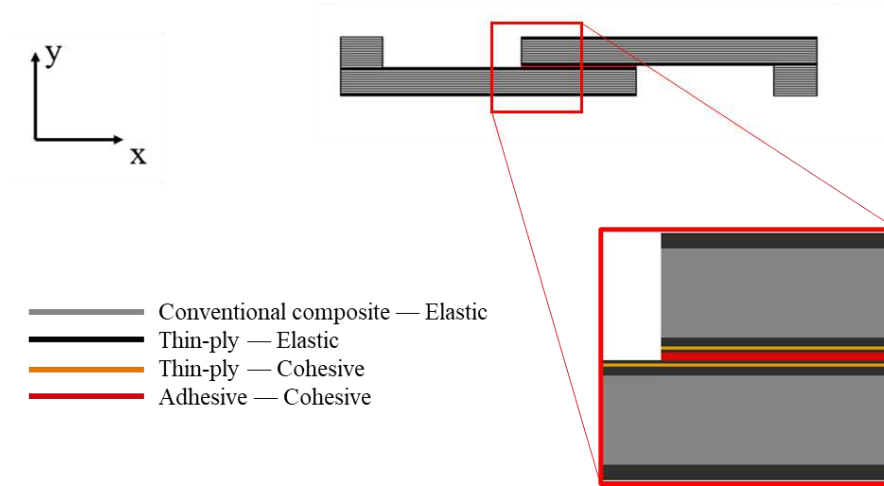


Fig 6. Representative experimentally obtained load-displacement curves for

A biased mesh distribution was applied to all the models, with a more refined mesh located near the edges of the overlap, with less detail near the extreme ends of both adherends, making the model lighter to process. Double and single biased meshed were applied in the x direction to the bondline and the adherend respectively, with seed size ranging from 0.2 mm to 0.5 mm (see Fig 7). On the extreme ends of the adherends and the end tabs, a mesh with 0.5 mm was implemented mm in the x direction. The mesh was uniform through the thickness (y direction) with a size of 0.2 mm for all configurations. The resulting mesh consisted of approximately 15,000 elements.

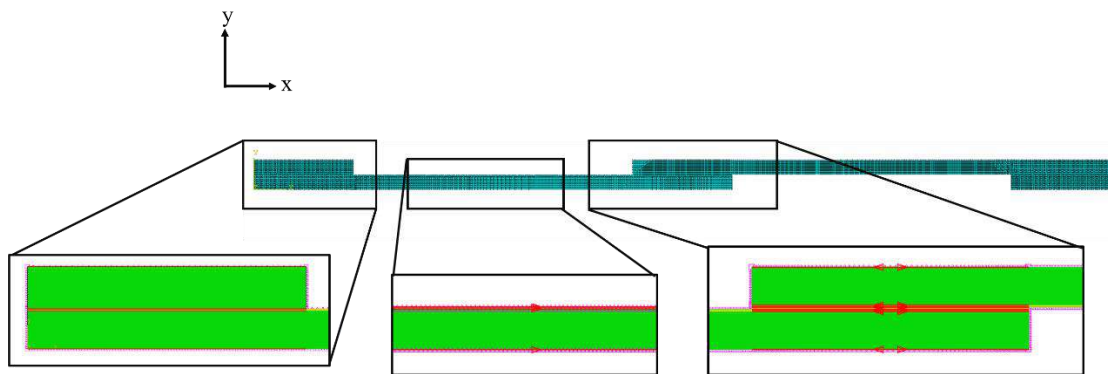
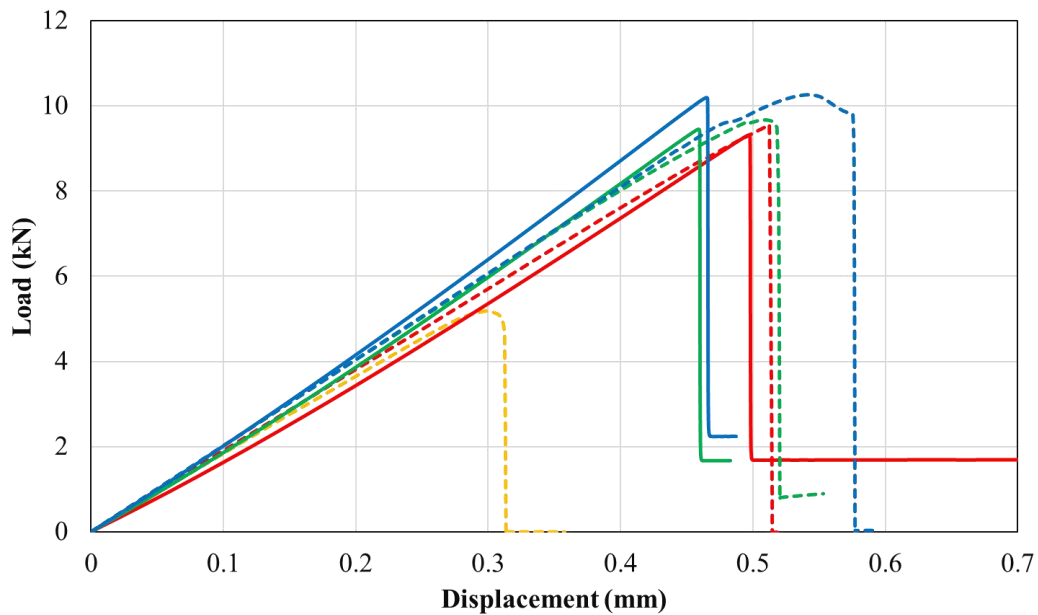


Fig 7. Mesh distributions for single lap joint

4. Results

Manufactured specimens were submitted to uniaxial tensile tests. Fig 8 and 9 presents a representative experimentally obtained load-displacement curve and obtained failure mode for the mentioned configurations respectively. The results of the experiments reveal that the increase of the adherend thickness results in a venial increase in the joint strength of the hybrid composite joints that have been enhanced with thin-ply reinforcement. Nevertheless, a significant modification in the failure mode was observed. The failure mode changes from a full delamination failure surface of the composite joint with 3.0 mm adhered thickness to partial delamination when increased up to 4.0 mm. Fig 8 also presents the numerically obtained load-displacement curve for the mentioned configurations. As seen the increase in the adherend thickness from 3 to 3.6 mm does not affect the tensile strength of the composite joint, this is while the increase of the adhered thickness from 3.6 mm to 4 mm of the hybrid (25% thin-ply) composite single lap joint leads to a slight increase in the tensile strength of the composite joint.



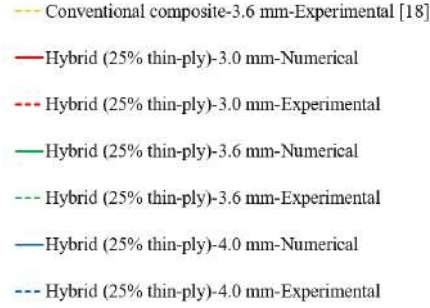


Fig 8. Representative experimentally obtained load-displacement curve for reference conventional composite, hybrid (25% thin-ply) single lap joint with 3.0, 3.6, and 4.0 mm adherend thickness and related numerical models

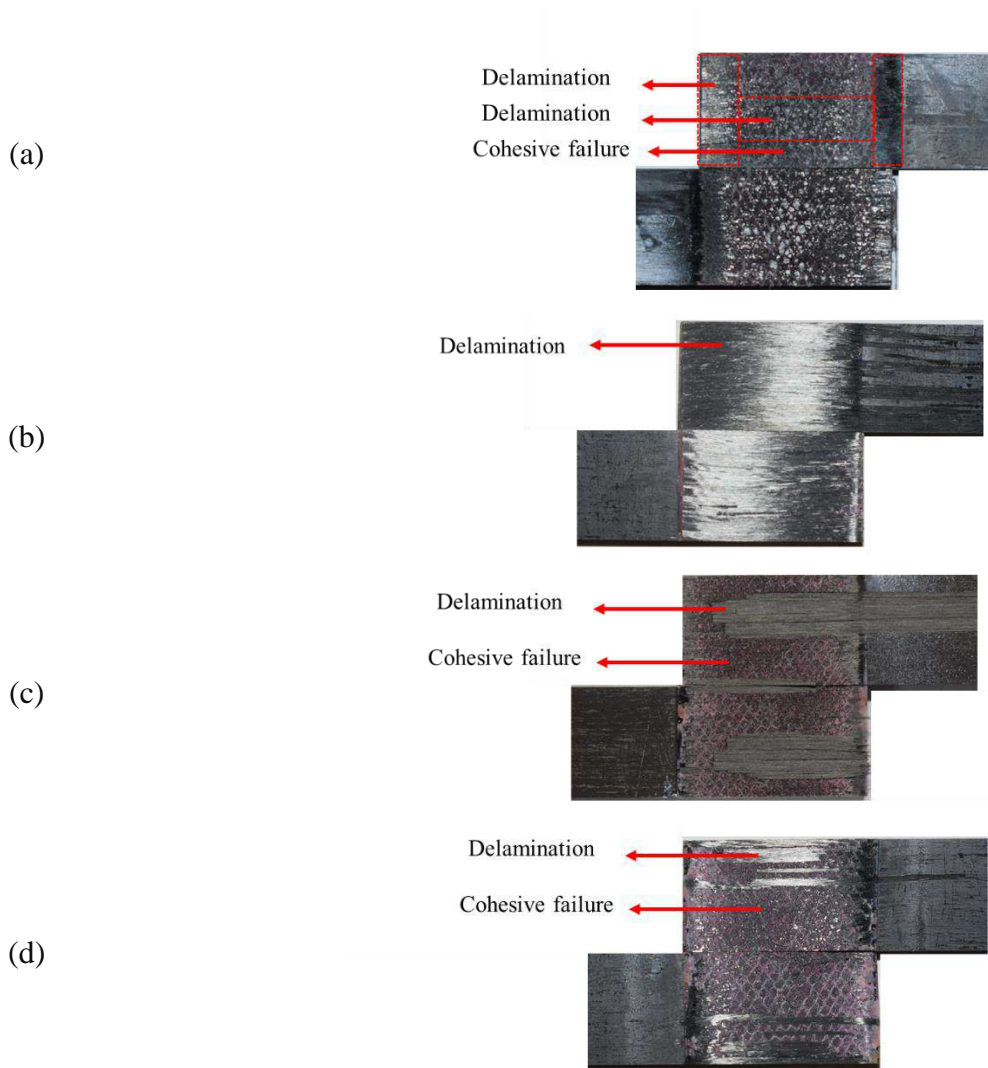


Fig 9. Failure surface of (a) reference conventional composite with the adherend thickness of 3.6 mm [18] and hybrid (25% thin-ply) single lap joint with (b) 3.0, (c) 3.6 and (d) 4.0 mm adherend thickness

Fig 10 presents a comparison between the numerical and experimentally obtained results. As seen, the numerical and experimentally obtained results are in a good agreement. The experimental result obtained by the authors in the previous study was presented [18]. As seen the use of hybrid (25% thin-ply) single lap joints could increase the failure load up to 90% (in the case of 3.6 mm adherend thickness). This is known to be due to the improved ductility of the laminate, which can delay delamination [19]. Moreover, experimental observation clearly demonstrated that the presence of thin-ply acts as a barrier against crack propagation therefore improve the failure mode (by reducing delamination) under static loads [18]. However, adherend thickness has a negligible effect on the joint strength in hybrid composite joints reinforced by thin-ply. This is while a considerable change in the failure mode was observed changing from fully delaminated failure surface (from 3.0 mm adherend thickness) to partial delamination when increased up to 4.0 mm.

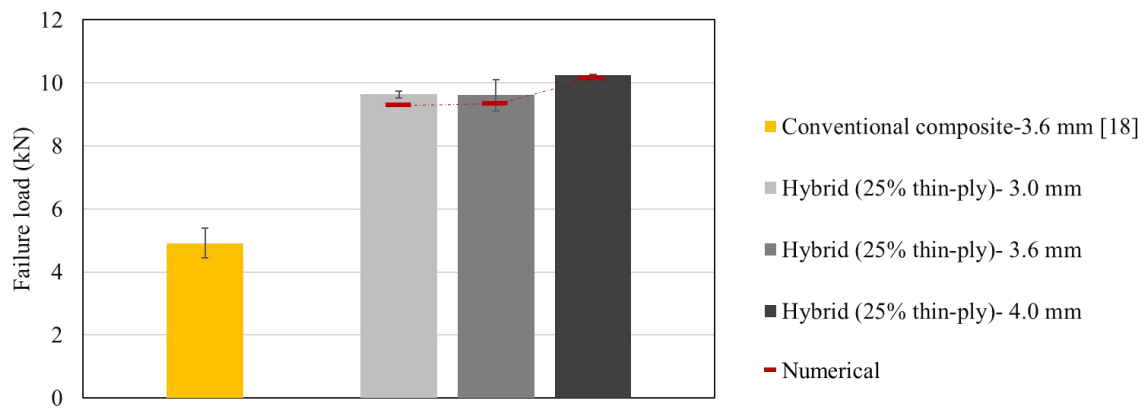


Fig 10. Average experimentally obtained failure load for hybrid (25% thin-ply) single lap joint with 3.0, 3.6, and 4.0 mm adherend thickness in comparison with the equivalent numerical result

5. Conclusion

This study examines the influence of adherend thickness on the performance of hybrid composite single lap joints strengthened with thin-ply reinforcement. Three different adherend thicknesses were considered and the manufactured specimen was conducted to tensile test. From the experimentally obtained results and the numerical models produced the main conclusions are:

- A marginal rise in the failure load was noted when the adherend thickness was increased in the hybrid composite joint reinforced with thin-ply.
- A notable alteration in the failure mode was clearly evident, changing the failure mode from full delamination to partial delamination.
- Numerical models employing finite element methods were generated to replicate the behavior of the configurations. Cohesive zone modeling was used to model the failure in the adhesive layer and delamination in the composite adherends. The numerical models show good agreement with the experimentally obtained results.

Author Contributions

Investigation, F. Ramezani, João C. M. Salazar; Writing—original draft, F. Ramezani; Writing—review & editing, R.J.C. Carbas, E.A.S. Marques and L.F.M. da Silva; Supervision, R.J.C. Carbas, E.A.S. Marques, and L.F.M. da Silva.

Acknowledgments

The authors gratefully acknowledge the Portuguese Foundation for Science and Technology (FCT) for supporting the work presented.

Conflict of Interest

Not Applicable

Funding


The authors gratefully acknowledge the Portuguese Foundation for Science and Technology (FCT) for supporting the work presented here through the individual grants CEECIND/03276/2018 and 2021.07943.BD and Project No. PTDC/EME-


EME/2728/2021, “New approaches to improve the joint strength and reduce the delamination of composite adhesive joints”.

Data Availability Statements

Not Applicable

ORCID iD

Farin Ramezani  <https://orcid.org/0000-0003-3447-8515>

Ricardo J. C. Carbas  <https://orcid.org/0000-0002-1933-0865>

Eduardo A. S. Marques  <https://orcid.org/0000-0002-2750-8184>

Lucas F. M. da Silva  <https://orcid.org/0000-0003-3272-4591>

References

- [1] Sahu, P., Gupta, M.: A review on the properties of natural fibres and its bio-composites: Effect of alkali treatment. *Proc. Inst. Mech. Eng. L: J. Mater.: Des. Appl.* 234, 198–217 (2020). <https://doi.org/10.1177/1464420719875163>
- [2] Zhou, M., Gu, W., Wang, G., Zheng, J., Pei, C., Fan, F., Ji, G.: Sustainable wood-based composites for microwave absorption and electromagnetic interference shielding. *J. Mater. Chem. A* 8, 24267–24283 (2020). <https://doi.org/10.1039/d0ta08372k>
- [3] Budzik, M.K., Wolfahrt, M., Reis, P., Kozłowski, M., Sena-Cruz, J., Papadakis, L., Nasr Saleh, M., Machalicka, K.V., Teixeira de Freitas, S., Vassilopoulos, A.P.: Testing mechanical performance of adhesively bonded composite joints in engineering applications: an overview. *J Adhes.* 98, 2133–2209 (2022). <https://doi.org/10.1080/00218464.2021.1953479>
- [4] Zhou, X., Li, J., Qu, C., Bu, W., Liu, Z., Fan, Y., Bao, G.: Bending behavior of hybrid sandwich composite structures containing 3D printed PLA lattice cores and magnesium alloy face sheets. *J Adhes.* 98, 1713–1731 (2022). <https://doi.org/10.1080/00218464.2021.1939015>

- [5] Ramezani, F., Simões, B.D., Carbas, R.J.C., Marques, E.A.S., da Silva, L.F.M.: Developments in Laminate Modification of Adhesively Bonded Composite Joints. *J. Mater.* 16, 568 (2023). <https://doi.org/10.3390/ma16020568>
- [6] Akhavan-Safar, A., Ramezani, F., Delzendehrooy, F., Ayatollahi, M.R., da Silva, L.F.M.: A review on bi-adhesive joints: Benefits and challenges. *Int. J. Adhes.* 114, 103098 (2022). <https://doi.org/10.1016/j.ijadhadh.2022.103098>
- [7] Ramezani, F., Nunes, P.D.P., Carbas, R.J.C., Marques, E.A.S., da Silva, L.F.M.: The joint strength of hybrid composite joints reinforced with different laminates materials. *J. Adv. Join. Process.* 5, 100103 (2022). <https://doi.org/10.1016/j.jaip.2022.100103>
- [8] Zhou, X., Li, J., Qu, C., Bu, W., Liu, Z., Fan, Y., Bao, G.: Bending behavior of hybrid sandwich composite structures containing 3D printed PLA lattice cores and magnesium alloy face sheets. *J. Adhes.* 98, 1713–1731 (2022). <https://doi.org/10.1080/00218464.2021.1939015>
- [9] Verpoest, I., Wevers, M., de Meester, P.: 3D-Fabrics for Composite Sandwich Structures. 535–541 (1989). https://doi.org/10.1007/978-94-009-1123-9_74
- [10] Dransfield, K., Baillie, C., Mai, Y.-W.: Improving the delamination resistance of CFRP by stitching—a review. *Compos Sci Technol.* 50, 305–317 (1994). [https://doi.org/10.1016/0266-3538\(94\)90019-1](https://doi.org/10.1016/0266-3538(94)90019-1)
- [11] Amacher, R., Cugnoni, J., Botsis, J., Sorensen, L., Smith, W., Dransfeld, C.: Thin ply composites: Experimental characterization and modeling of size-effects. *Compos Sci Technol.* 101, 121–132 (2014). <https://doi.org/10.1016/j.compscitech.2014.06.027>
- [12] Arteiro, A., Catalanotti, G., Xavier, J., Linde, P., Camanho, P.P.: A strategy to improve the structural performance of non-crimp fabric thin-ply laminates. *Compos. Struct.* 188, 438–449 (2018). <https://doi.org/10.1016/j.compstruct.2017.11.072>
- [13] Kötter, B., Karsten, J., Körbelin, J., Fiedler, B.: CFRP Thin-Ply Fibre Metal Laminates: Influences of Ply Thickness and Metal Layers on Open Hole Tension and Compression Properties. *J. Mater.* 13, 910 (2020). <https://doi.org/10.3390/ma13040910>
- [14] Wisnom, M.R., Khan, B., Hallett, S.R.: Size effects in unnotched tensile strength of unidirectional and quasi-isotropic carbon/epoxy composites. *Compos. Struct.* 84, 21–28 (2008). <https://doi.org/10.1016/j.compstruct.2007.06.002>

- [15] Kim, R.Y., Soni, S.R.: Experimental and Analytical Studies On the Onset of Delamination in Laminated Composites. *J. Compos. Mater.* 18, 70–80 (1984). <https://doi.org/10.1177/002199838401800106>
- [16] Huang, C., He, M., He, Y., Xiao, J., Zhang, J., Ju, S., Jiang, D.: Exploration relation between interlaminar shear properties of thin-ply laminates under short-beam bending and meso-structures. *J. Compos. Mater.* 52, 2375–2386 (2018). <https://doi.org/10.1177/0021998317745586>
- [17] Kupski, J., Zarouchas, D., Teixeira de Freitas, S.: Thin-ply in adhesively bonded carbon fiber reinforced polymers. *Compos. B. Eng.* 184, 107627 (2020). <https://doi.org/10.1016/j.compositesb.2019.107627>
- [18] Ramezani, F., Carbas, R.J.C., Marques, E.A.S., da Silva, L.F.M.: Study of Hybrid Composite Joints with Thin-Ply-Reinforced Adherends. *J. Mater.* 16, 4002 (2023)(a). <https://doi.org/10.3390/ma16114002>
- [19] Ramezani, F., Carbas, R.J.C., Marques, E.A.S., Ferreira, A.M., da Silva, L.F.M.: A study of the fracture mechanisms of hybrid carbon fiber reinforced polymer laminates reinforced by thin-ply. *Polym. Compos.* 44, 1672–1683 (2023)(a). <https://doi.org/10.1002/pc.27196>
- [20] Morgado, M.A., Carbas, R.J.C., Santos, D.G. dos, da Silva, L.F.M.: Strength of CFRP joints reinforced with adhesive layers. *Int. J. Adhes* 97, 102475 (2020). <https://doi.org/10.1016/j.ijadhadh.2019.102475>
- [21] Campilho, R.D.S.G., de Moura, M.F.S.F., Domingues, J.J.M.S.: Modelling single and double-lap repairs on composite materials. *Compos Sci Technol.* 65, 1948–1958 (2005). <https://doi.org/10.1016/j.compscitech.2005.04.007>
- [22] Machado, J., Marques, E., Campilho, R., da Silva, L.F.: Mode I fracture toughness of CFRP as a function of temperature and strain rate. *J. Compos. Mater.* 51, 3315–3326 (2017). <https://doi.org/10.1177/0021998316682309>
- [23] Ramezani, F., Carbas, R., Marques, E.A.S., Ferreira, A.M., da Silva, L.F.M.: Study on out-of-plane tensile strength of angle-ply reinforced hybrid CFRP laminates using thin-ply. *Mech. Adv. Mater. Struct.* 1–14 (2023)(a). <https://doi.org/10.1080/15376494.2023.2165742>

